THE RHODIUM/PHOSPHINE CATALYSED DOUBLE CARBONYLATION OF DIIODOMETHANE

William Scott Weston

A Thesis Submitted for the Degree of PhD
at the
University of St Andrews

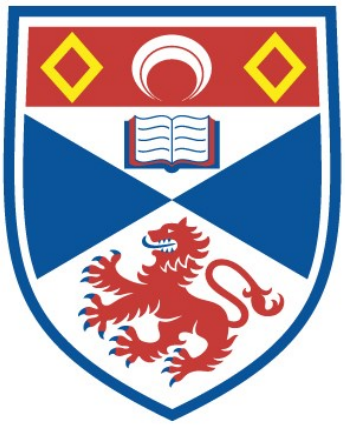

1997

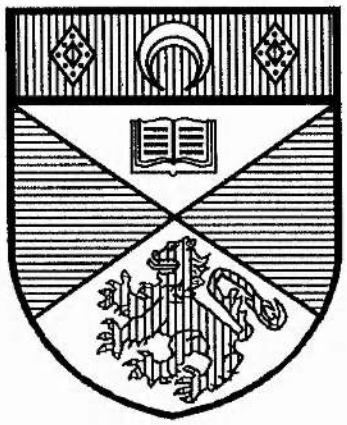

The Rhodium / Phosphine Catalysed Double Carbonylation of Diiodomethane

a thesis presented by
William Scott Weston

to the

University of St. Andrews

in application for
The Degree of Doctor of Philosophy

September 1996

DECLARATIONS

I, William Scott Weston, hereby certify that this thesis, which is approximately 46,100 words in length, has been written by me, that it is the record of work carried out by me and that it has not been submitted in any previous application for a higher degree.

Signed ..... Date 26th September 1996

I was admitted as a research student in October 1992 and as a candidate for the degree of Ph.D in October 1993; the higher study for which this is a record was carried out in the University of St. Andrews between 1992 and 1996.

Signed . ..... Date 26th September 1996

I hereby certify that the candidate has fulfilled the conditions of the Resolution and Regulations appropriate for the degree of Ph.D in the University of St. Andrews and that the candidate is qualified to submit this thesis in application for that degree

Signature of Supervisor

Date 26th September 1996

In submitting this thesis to the University of St. Andrews I understand that I am giving permission for it to be made available for use in accordance with the regulations of the University Library for the time being in force, subject to any copyright vested in the work not being affected thereby. I also understand that the title and abstract will be published, and that a copy of the work may be made and supplied to any bona fide library or research worker.

Signed . ..... Date 26th September 1996

"There is a theory which states that if ever anyone discovers exactly
what the Universe is for and why it is here, it will instantly
disappear and be replaced by something even more bizarre
and inexplicable.

There is another theory which states
that this has already happened."

(The Restaurant at the End of the Universe - Douglas Adams)

ACKNOWLEDGEMENTS

"For the foolishness of God is wiser than man's wisdom,
and the weakness of God is stronger than man's strength."

1 Corinthians 1: vs.25

I would like to thank Professor David Cole-Hamilton for all his guidance, support and ideas over the last four years. A man of honour and a chemist of high renown.

I should like to convey my thanks to all the technical staff of the chemistry department whose assistance I have appreciated. I would single out Peter Pogorzelec, Melanja Smith, Jim Rennie and Jim Bews all of whom went 'that extra mile' on my behalf: Peter for his experimental advice; Melanja for always allowing me more NMR that I deserved even after I had made several attempts destroy her NMR machine; Jim Rennie for persisting with the HP-NMR cell until it would spin; Jim Bews for enabling computers to save my time instead of wasting it.

I have enjoyed the help and camaraderie of the many members of the Cole-Hamilton group over the last four years. Those of special note were; Dr Mike Simpson who taught me vital schlenk techniques, Dr Charles Lindall who tried to teach me grammar (not bad for an Aussie), Jo Rankin and Marc Payne for helpful discussions and Dr Colin (Flower of Scotland) Grubb who taught me the local lingo (ya ken?) and helped me integrate into the Scottish culture. I should like to thank Dr Yuri Andreev, Dr Atilla Bényei and Dr Laurent Salles for their assistance with the translation of foreign patents and papers and Dr Graham Turner for checking the final draft of my thesis for typo's. My thanks also go to Prof. Willie Keim and his group at RWTH for being so helpful during my three weeks of ultra-high pressure autoclave work in their labs in Aachen.

I am indebted to The Russell Trust for a grant which funded my trip to RWTH in Aachen and BP who assisted with the funding which allowed me to attend the 9th International Symposium on Homogeneous Catalysis in Jerusalem. My thanks also go to the University of St. Andrews for the 'Junior Teaching Fellowship' which enabled me to carry the research which has led to this thesis.

Finally I would like to offer my sincere thanks to my fiancée, Helen, who proof read my thesis and by agreeing to marry me on the 26th October provided me with the best possible incentive to submit my thesis on time.

TABLE OF CONTENTS

Chapter Three - Synthetic and Mechanistic Studies - Steps and Species within the Catalytic Cycle

Chapter Four - Synthetic and Mechanistic Studies - Decomposition Products and Pathways

ABBREVIATIONS

Bu .....n-butyl
^{t}Bu.....tertiary-butyl
d .....doublet
DBU.....1,8-diazabicyclo[5.4.0]undec-7-ene
DEM.....diethylmalonate
dippp .....bis-(diisopropyl-phosphino)propane
DMA .....dimethylacetamide
DME.....dimethoxyethane
DMF.....N,N-dimethylformamide
DMM.....dimethylmalonate
dmpe .....bis-(dimethyl-phosphino)ethane
dppe.....bis-(dipropyl-phosphino)ethane
dppp.....bis-(dipropyl-phosphino)propane
Et .....ethyl
GC.....gas chromatograph
GCMS .....gas chromatography mass spectroscopy
HP.....high pressure
IR.....infra red
m.....multiplet
Me .....methyl
NMR .....nuclear magnetic resonance spectroscopy
OAc.....acyl
pCO .....partial pressure of carbon monoxide gas
^{i}Pr .....iso-propyl
q .....quartet
s.....singlet
t.....triplet
THF.....tetrahydafuran
TON.....turn over number
VT .....variable temperature

Abstract

The use of the catalyst precursors rhodium acetate [$Rh_2(OAc)_4$], carbon monoxide and triethyl phosphine in an alcoholic solvent forms a catalytic species capable of the double carbonylation of diiodomethane. When this reaction is carried out in ethanol, the major products are diethylmalonate (DEM) and ethyl iodide.

$$CH_2I_2 + 2CO + 2EtOH \xrightarrow{[Rh_2(OAc)_4] / PEt_3 / CO} CH_2(COOEt)_2 + 2HI$$

The ethyl iodide is formed by the reaction of EtOH with HI, presumably forming equal amounts of water. The other, minor, products of this reaction were diethoxymethane ($CH_2(OEt)_2$), ethyl propanoate ($CH_3CH_2CO_2Et$) with a trace of ethyl acetate (CH_3CO_2Et). The diethoxymethane is formed by the ethanolysis of the substrate and the ethyl propanoate may be from the carbonylation of ethyl iodide formed in situ. The source of the ethyl acetate has been shown to be ketene, a metal complex thereof being shown to be the singly carbonylated intermediate between diiodomethane and DEM. Possibly the most notable feature of this catalytic reaction is that it occurs in the absence of added base. A review of all the double carbonylation reactions reported to date reveals this catalytic system to be unique in this respect (see chapter one). It is the solvent, EtOH, which acts as the sink for HI in this system and this accounts for the high yields of EtI.

A thorough study of the mechanism of this reaction has led to the proposal of the mechanistic cycle shown overleaf in figure A. The most salient feature of this mechanism is the proposal of a metallo ketene intermediate. Evidence for the involvement of a metallo ketene complex in this reaction comes from the study of the attempted synthesis of the iodoacyl intermediate **3d** and a deuterium labelling study (see chapter three).

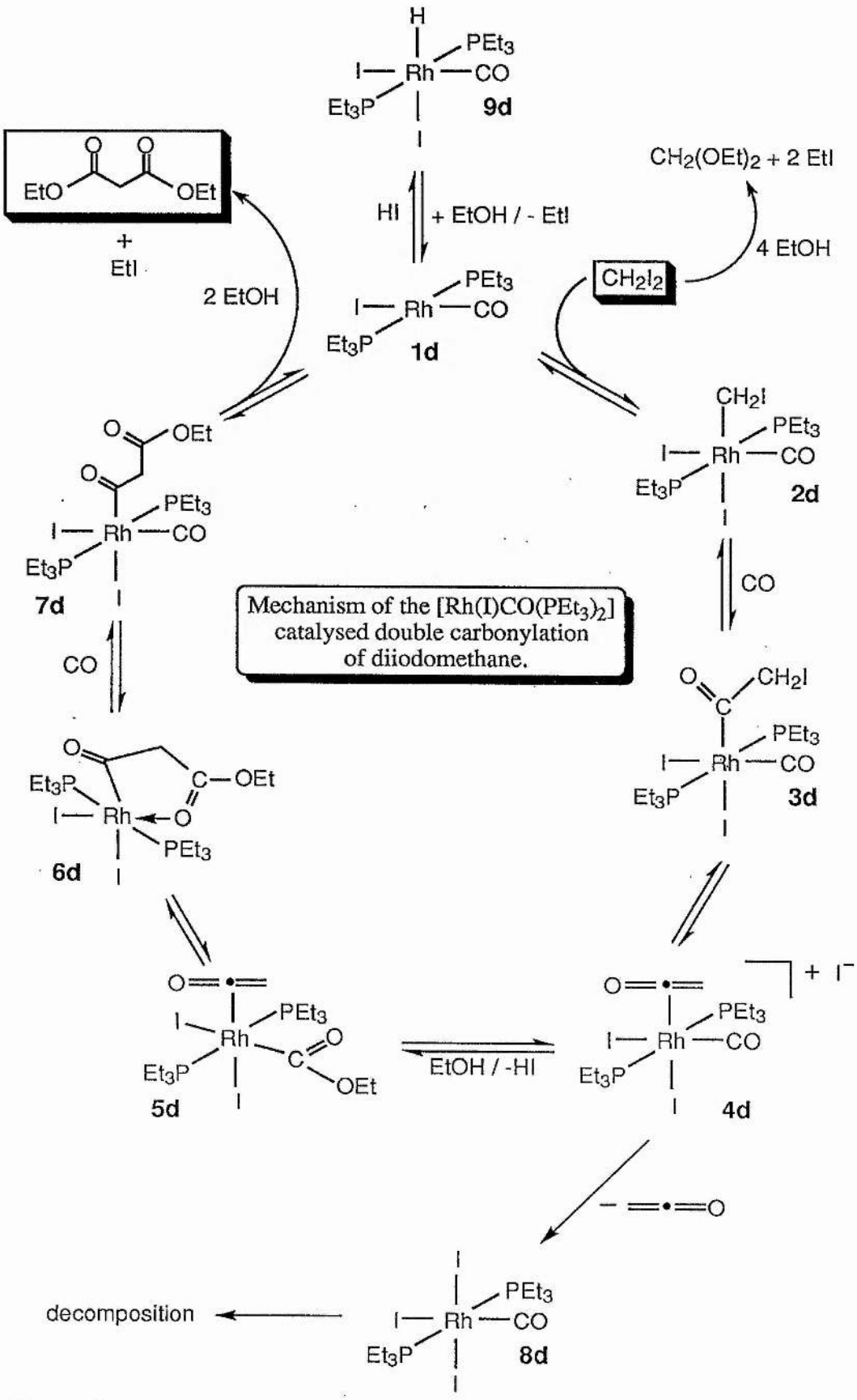
Mechanism of the [Rh(I)CO(PEt3)2] catalysed double carbonylation of diiodomethane.
9d
1d
2d
3d
4d
5d
6d
7d
8d
HI
+ EtOH / - EtI
2 EtOH
+ EtI
CH2I2
CH2(OEt)2 + 2 EtI
4 EtOH
CO
EtOH / -HI
decomposition

Figure A

CHAPTER ONE

Introduction and literature review

1.0 Preface

The first report of a transition metal catalysed double carbonylation reaction of an organohalide appeared in 1975.[1] This reaction used $[Co(CO)_4]^-$ to catalyse the synthesis of phenyl pyruvic acid* from benzyl chloride in the presence of $Ca(OH)_2$.

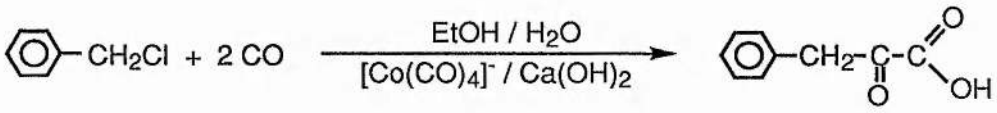

Pyruvic acids and their derivatives can be used in the synthesis of biologically important α-hydroxy acids and also α-amino acids. Both natural and unnatural amino acids can be made from via the appropriate α-keto-acid. Later work in the field of double carbonylation has focused on the catalytic synthesis of α-keto-esters and α-keto-amides as more useful organic synthons.

The double carbonylation of both geminal and non-geminal dihalides is also reported (see sections 2 and 3). Geminal dihalides such as diiodomethane can be used as substrates for the synthesis of malonic acid derivatives. Malonate esters are the starting point for the synthesis of barbituric acid and other important pharmaceutical compounds. The most common class of non-geminal dihalide substrates are 1,3 and 1,4 halo-substituted benzenes. When such substrates are doubly carbonylated in the presence of diols or diamine nucleophiles they form the basis for efficient polyester or polyamide syntheses (see section 3.3).

The work discussed in this thesis involves the mechanistic elucidation of the rhodium / phosphine catalysed double carbonylation of diiodomethane. To place this work in context the following review concentrates on the mechanistic understanding of all the catalytic double carbonylation reactions of halocarbons yet reported. For clarity the reports are arranged according to product, substrate, and the metal centre of the catalyst which is used.

---

* For clarity, acids of the type $RCOCO_2H$ and their derivatives will be referred by their trivial name 'pyruvic acids' rather than by IUPAC nomenclature as 2-oxo-carboxylic acids.

SECTION 1 Preparation of Derivatives of Pyruvic Acid

PART A Preparation of α-Keto-Acids

1.1 Introduction

The first reported example of a double carbonylation reaction was the cobalt catalysed synthesis of phenyl pyruvic acid.[2] Of all the transition metal catalysed double carbonylation reactions, the synthesis of substituted pyruvic acids has received the most attention.

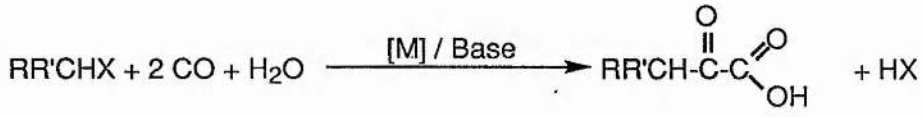

Cobalt catalysis, particularly the use of $[Co(CO)_4]^-$, has dominated the field of α-keto-acid synthesis. Tanaka[3,4] has reported species of the type $[PdX_2(PR_3)_2]$ (R = alkyl, aryl) to be very efficient catalysts for the synthesis of keto-acids also. Given the wide use of palladium complexes in the catalytic synthesis of α-keto-esters (Part B) and α-keto-amides (Part C) it is perhaps surprising to find so little work reported on the use of palladium catalysts in α-keto-acid synthesis. All the catalytic systems reported to date require the use of (at least) a stoichiometric quantity of base, normally an alkali or alkaline earth metal hydroxide. The catalytic synthesis of lactones and other products formed via substituted pyruvic acids and their derivatives will be covered in Part D.

1.2 Cobalt carbonyl based catalytic systems

The catalytic species used in these reactions is $[Co(CO)_4]^-$ which is either introduced pre-synthesised, e.g. $Na[Co(CO)_4]$, or is formed in-situ from the reduction of $[Co_2(CO)_8]$ by CO in the presence of a base.

Figure 1.2.1

Given the breadth of this area it will be divided into sections according to the class of substrate; benzyl halides (section 1.3), aryl halides (1.4), primary phenylethyl halides (1.5), secondary phenylethyl halides (1.6) and finally simple alkyl halides (1.7).

1.3 Preparation of phenyl pyruvic acids from benzyl halides

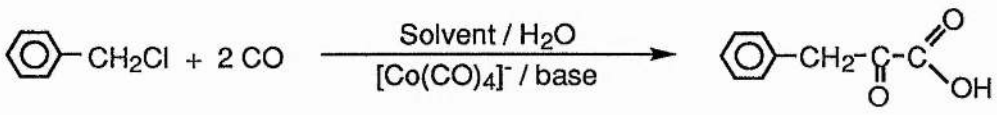

The first catalytic synthesis of phenyl pyruvic acid (PPA) from a benzyl halide was reported in 1975 by Perron at Rhone Poulenc.[2] This patent reports the synthesis of PPA from benzyl chloride in up to 73% yield using $Na[Co(CO)_4]$ in aqueous ethanol with $Ca(OH)_2$ (1.5 equiv. wrt benzyl chloride) as the base. The major side product of this reaction was the single carbonylation product, phenyl acetic acid (PAA). The double / single carbonylation ratio was shown to increase with increasing CO pressure. Other minor side products were the ethanolysis products $PhCH_2CO_2Et$ and $PhCH_2OEt$. When $M(OH)_n$ is replaced by a tertiary amine as the base no double carbonylation products are observed. Since 1976 a number of other reports of the synthesis of phenyl pyruvic acid from benzyl halides have appeared in the literature.[5-10] The syntheses of a range of substituted PPA's from ring-substituted benzyl halides have also been reported.[2,5,11-16]

A review on cobalt catalysed carbonylation has summarised the effect of the solvent and the CO pressure upon the double carbonylation of benzyl chloride.[17] The selectivity for PPA over PAA is observed to increase, with respect to the alcoholic solvent used, in the order; MeOH < EtOH < i-PrOH < t-BuOH < t-amyl-OH. An increased PPA / PAA ratio is also observed when the CO pressure is increased. The proposed mechanism[12] for the cobalt carbonyl catalysed double carbonylation of benzyl halides is shown in figure 1.3.1 below; the evidence for this mechanism will be discussed at the end of this section.

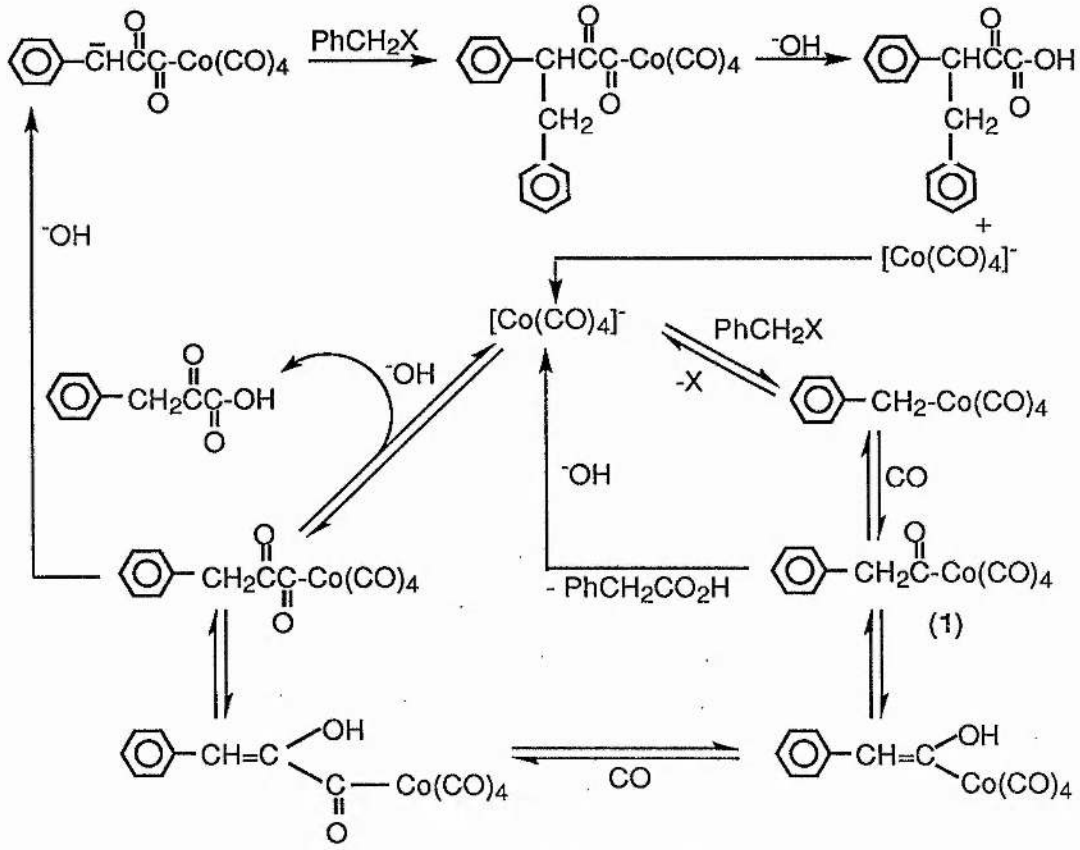

Figure 1.3.1: The proposed mechanism for the cobalt carbonyl catalysed double carbonylation of benzyl halides.

Figure 1.3.1 shows that it is the fate of the benzylacyl intermediate (**1**) which determines the ratio of the single / double carbonylation products. If this species isomerises to its enol form then inserts another CO then PPA will be the product, whereas nucleophilic attack of (**1**) will yield the single carbonylation product PAA. Thus an increase in CO pressure favours the double carbonylation product as does a decrease in the efficacy of the nucleophile. As this proposed mechanism would predict the PPA / PAA ratio increases with the basicity of the solvent alcohol.

A later patent by Perron[6] investigates the use of a range of alcoholic solvents on the double carbonylation of benzyl chloride. In this report the catalyst $Na[Co(CO)_4]$ is prepared in-situ from $CoCl_2 \cdot 6\ H_2O$ and CO using $Na_2S_2O_3$ and/or Na_2S as reducing agents. Using these catalyst precursors in propan-2-ol an 80% yield of PPA is achieved after 2 hours rising to 94% after 20 hours. Using methanol as the solvent a 94% yield of PPA after 20 hours is also observed.

Alkali or alkaline earth metal hydroxides are the best bases for this reaction.[2,5,6,18] $Ca(OH)_2$ or LiOH are reported[2,5,6,13,18] as the favoured bases. One report[18] suggests that CaO can be used in place of $Ca(OH)_2$. In a paper on the double carbonylation of phenylethyl bromide[19] the direct interaction between a Ca^{2+} ion and a cobalt-enolate intermediate is proposed to promote the second carbonyl insertion; This work will be covered in depth in section 1.5.

The effect of the reaction temperature on the carbonylation of benzyl chloride and 3-phenyl propylbromide has been studied by Fell.[18] With both organohalide substrates (RX) the major products are the keto acid (RCOCOOH), the carboxylic acid (RCOOH) and the alcohol (ROH). With either substrate the yield of the alcohol is very low below 70 °C but then increases with temperature; Conversely the yield of the carbonylation products reaches a maximum then drops off with increasing temperature. For either substrate the maximum selectivity for the keto-acid is achieved at a lower temperature than for the acid. The nature of the temperature profiles is reported to show that the keto-acid is not formed via the free single carbonylation product. The selectivity maximum for the keto-acid is presumably due to the entropically driven decarbonylation of the keto-acid at elevated temperatures. At higher temperatures still the competition between the hydroxide anion and the $[Co(CO)_4]^-$ may explain the predominance of the alcohol over the two carbonylation products.

The effect of the substituents on the carbonylation of substituted benzyl halides has investigated by Foà[13], des Abbayes[11,12] and Perron et al.[1] The substituents play a key role when double carbonylation is attempted via phase transfer catalysis (PTC). Under PTC at 1 atm CO neither unsubstituted nor m-CF_3 substituted benzyl chloride give any double carbonylation products.

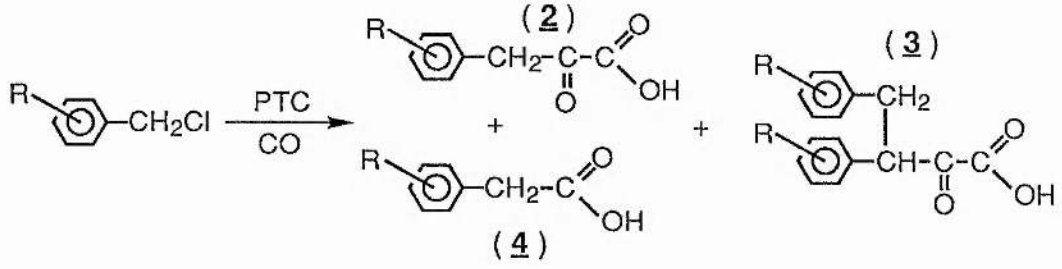

Figure 1.3.2

When a single methyl substituent, in any position, is present then significant amounts of the alkylated double carbonylation product (3) are observed, but none of the non-

alkylated product[11] (2). Keto-acid (3) is presumably formed by the attack of the starting material upon a pyruvyl cobalt intermediate. The use of 1-chloromethyl-2,4,6-trimethylbenzene gives a 1:1 mixture of (2) and (4) but in low yield - the alkylated product (3) not being formed because of the steric protection afforded by the ortho-methyl groups. A review on phase-transfer catalysis by Cassar[20] indicated that under PTC electron donating substituents favour double carbonylation and vice versa.

In the studies mentioned above $NaOH_{(aq)}$ formed one phase of a two phase PTC system. Perron[1] reports high conversions of a wide range of mono-substituted benzyl chlorides with good double / single carbonylation selectivity and with no mention of the formation of alkylated products (3). This is achieved by the use of aqueous ethanol in a homogeneous system with $Ca(OH)_2$ as the base. Good yields starting from chloro-substituted benzyl chlorides are also quoted in a patent by Foà.[13]

Alper[12] has proposed a mechanism for the cobalt catalysed double carbonylation of benzyl halides which is shown in figure 1.3.1 above. The effect of substituents on the phenyl ring of the substrate, discussed above, is consistent with Alper's mechanism but the first concrete evidence to support his proposal was provided by Foà[21] some six years later. Foà et al investigated the double / single carbonylation of α-phenylethyl bromide and the α-deuterium labelled analogue. They observed that the replacement of the α-hydrogen by a deuterium atom strongly inhibited double carbonylation. This primary kinetic isotope effect provides evidence for an enolic intermediate in the mechanism as the necessary keto-enol isomerisation requires the cleavage of the α-hydrogen / deuterium bond - exemplified in figure 1.3.3 below.

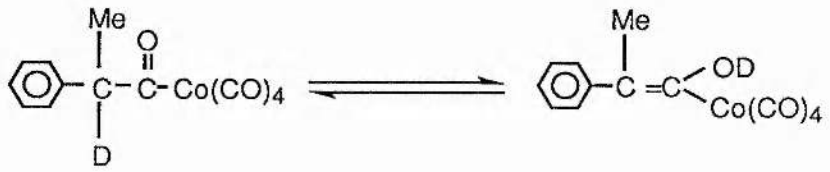

Figure 1.3.3

In one account of the double carbonylation of ortho-methyl benzylbromide the nature of the minor reaction products is also reported.[12] The presence of ortho-xylene (5%) and $(o\text{-}CH_3\text{-}C_6H_4\text{-}CH_2)_2$ (7%) suggests that a radical mechanism may be operating. In a careful mechanistic study of the single carbonylation of benzyl bromide, des Abbayes[22] invokes a metallocarboxylic acid species (5) to explain such products - see figure 1.3.4. The evidence used to support this intermediate comes from measuring the CO_2 formed in the reaction, which is in fair agreement with a mechanism involving

(5) but not a radical mechanism which would involve the coupling of $[Co(CO)_4]^{\cdot}$ radicals to generate $Co_2(CO)_8$ followed by its reduction back to $[Co(CO)_4]^-$ (which yields carbonate ions - the source of CO_2) shown in figure 1.2.1.

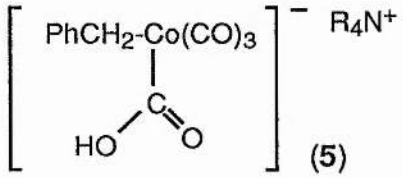

Figure 1.3.4

1.4 Preparation of phenyl glyoxylic acids from aryl halides

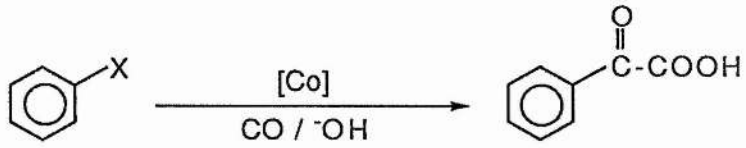

The double carbonylation of aryl halides requires, in addition to a stoichiometric amount of base, a stoichiometric amount of a methylating agent[23,24] or photo-stimulation[25] to achieve catalysis. The methylating agent is employed to form $[MeCo(CO)_4]$ which is known[26] to be the active catalyst for the carbonylation of aryl iodides. Photostimulation probably photodissociates a CO ligand to form a species capable of insertion into the phenyl-carbon to halogen bond. Alkaline hydrolysis is often required at the end of the reaction to liberate the keto-acid product from the aldol condensation adduct with pyruvic acid.[23]

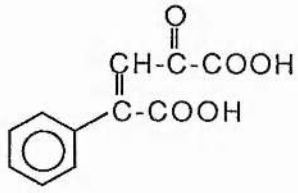

Figure 1.4.1: Aldol condensation product of 2-oxo benzoic acid with pyruvic acid.

This must mean that these systems are also able to doubly carbonylate the methylating agent, ie MeI, to yield pyruvic acid. Miura,[24] like Perron[6] reports the use of $CoCl_2$ and a reducing agent (either Na_2S or $NaBH_4$) under CO as catalyst precursors forming $[Co(CO)_4]^-$ in-situ. The use of in-situ reducing agents reduces some of the keto-acid product to yield α-hydroxy acid derivatives - ArCH(OH)COOH (normally 2-9% wrt ArX).

Miura reports propan-2-ol to be a better solvent than dioxane for their $CoCl_2$ precursor based system.[24] In a more extensive study[26] the effect of a number of polar solvent systems upon the carbonylation of 1-bromonaphthalene and para-substituted benzenes was studied. For these organohalides (RX) the following products were observed; RCOMe, RCO_2H, $RCOCO_2H$, $RCHOHCO_2H$. With a water / co-solvent system the ratio of water / co-solvent and the nature of the co-solvent was investigated but no clear trends were observed. When the effect of a range of alcoholic solvents upon the homogeneous carbonylation of bromobenzene was investigated[23] the same trend in selectivity seen for the carbonylation of benzyl halides[17] was observed; t-BuOH > i-PrOH > EtOH > MeOH. Presumably it is the attack of an alkoxide ion upon a cobalt-acyl intermediate which forms the single carbonylation product; thus the more acidic alcohols give rise to a lower selectivity.

As with other double carbonylation systems yielding pyruvic acid derivatives the double / single carbonylation selectivity is found to be inversely proportional to the temperature.[23,24] By changing the temperature[24] of the carbonylation of 1-bromonaphthalene from 60 °C to 20 °C, for example, the selectivity to the keto acid rose by a factor of 5. A 60 fold increase in selectivity is observed for the carbonylation of bromobenzene by changing from 40 °C to 20 °C with no keto-acid formed at all at 55 °C.[23]

The effect of substituents on the phenyl ring of the substrate has been investigated by Foà et al[23] but no clear trends were observed. Other work[25] has shown that, by using substrates with a carboxyl group ortho to the halogen, photo-stimulation can facilitate double carbonylation in the absence of a methylating agent. This is shown in figure 1.4.2 below.

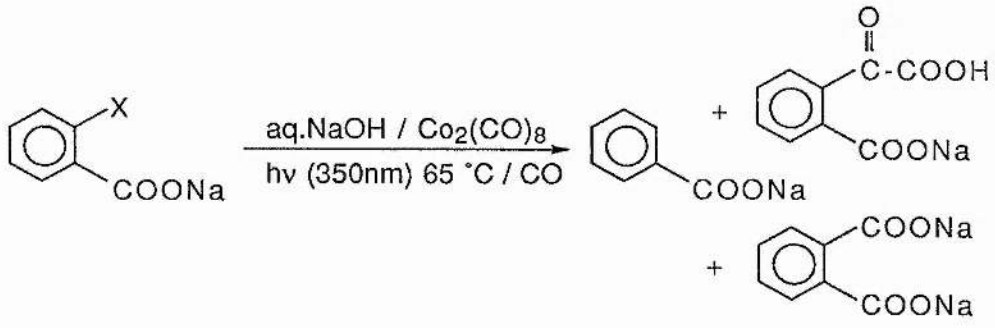

Figure 1.4.2: Photostimulated carbonylation of ortho-carboxyl halobenzenes.

The double carbonylation of o-dihalobenzenes[25] is also reported, with o-halobenzoic acid being formed in addition to the products shown above. The fact that o-dihalobenzenes do not yield any o-halophenyl glyoxylic-acids or bis-keto-acids suggests that the o-carboxyl group plays a role in the second CO insertion. The mechanism proposed by Kashimura is based on this premise and is shown in figure 1.4.3.[25]

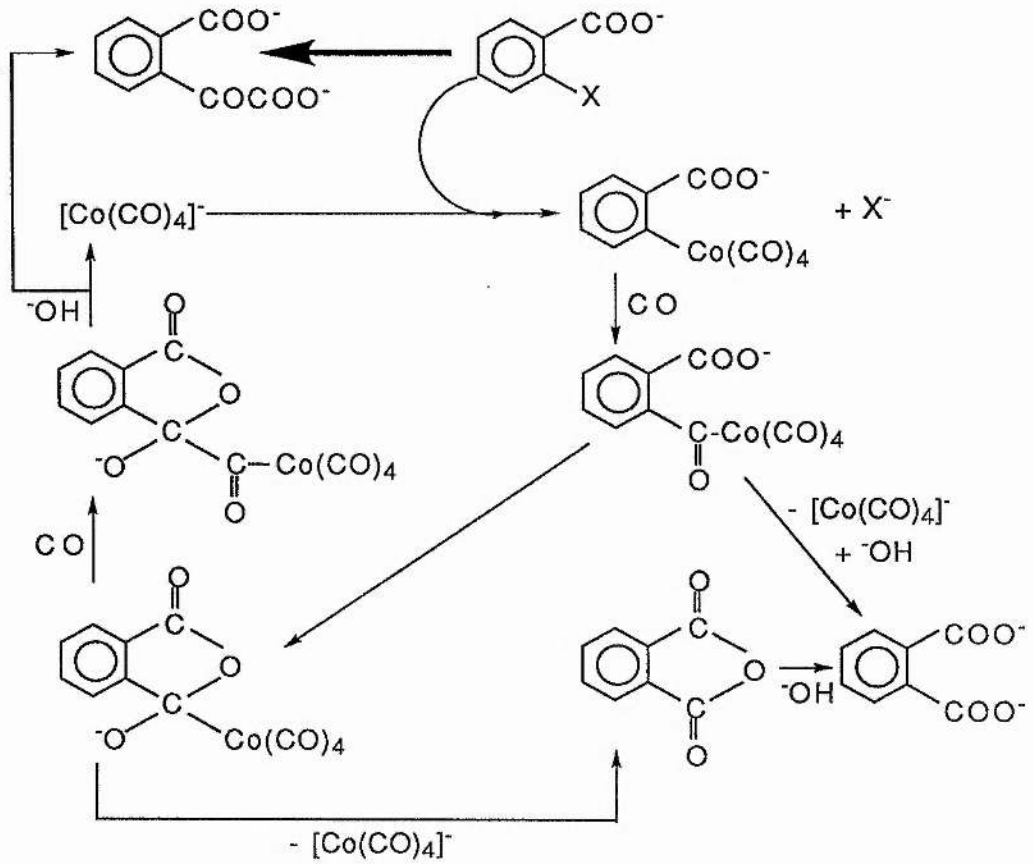

Figure 1.4.3: Proposed mechanism for the photostimulated carbonylation of ortho-carboxyl halobenzenes.

1.5 Preparation of α-keto acids from primary phenylethyl halides

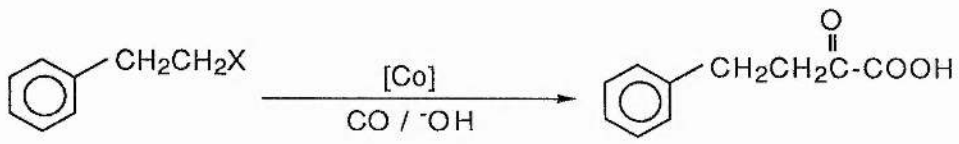

Most of the work on the double carbonylation of primary phenylethyl halides has centred on $PhCH_2CH_2Br$[18,19,27,28] with only one report[18] of the double

carbonylation of $PhCH_2CH_2Cl$. The favoured solvents for this transformation are 2-methyl propan-1-ol[19] and t-butanol.[18,27,28]

A patent by Lee and Wolfram[28] elegantly demonstrated the effect of temperature and reaction time upon the double / single carbonylation selectivity of phenylethyl bromide. As has been alluded to with all the other keto-acid forming reactions the selectivity was shown to decrease when the temperature was raised. Lee and Wolfram showed that at 20 atm CO the yield of the keto-acid reached a maximum and then dropped off with time. This suggests that the keto-acid is being formed and subsequently decomposes under the reaction conditions. When the same series of experiments was run at 60 atm CO it was observed that, once formed, the keto acid was stable. This indicates that the loss of CO from the keto-acid (forming phenyl propionic acid) is the route of the decomposition. The work of Fell[18], discussed in section 1.3, adds support to this hypothesis by demonstrating that as the concentration of the double carbonylation product falls the concentration of the single carbonylation product rises.

A comparison of alkali metal hydroxides as bases showed[18] that the yield of and selectivity to the keto acid increased in the order; KOH < NaOH < LiOH. A study of the effects of both group I and II $M(OH)_n$ showed $Ca(OH)_2$ to be the base of choice. If a base of too low a solubility[19] (ie $Mg(OH)_2$ in t-BuOH / H_2O) is used then this enhances side reactions. These side reactions give neutral hydrocarbon products and probably result from both HBr elimination and radical pathways. In a similar study[19] Mortreux et al propose that the superiority of $Ca(OH)_2$ as the base in most if not all keto acid yielding reactions is due to a favourable interaction between the calcium ion and one or more of the catalytic intermediates - these ideas are summarised in figure 1.5.1 and below.

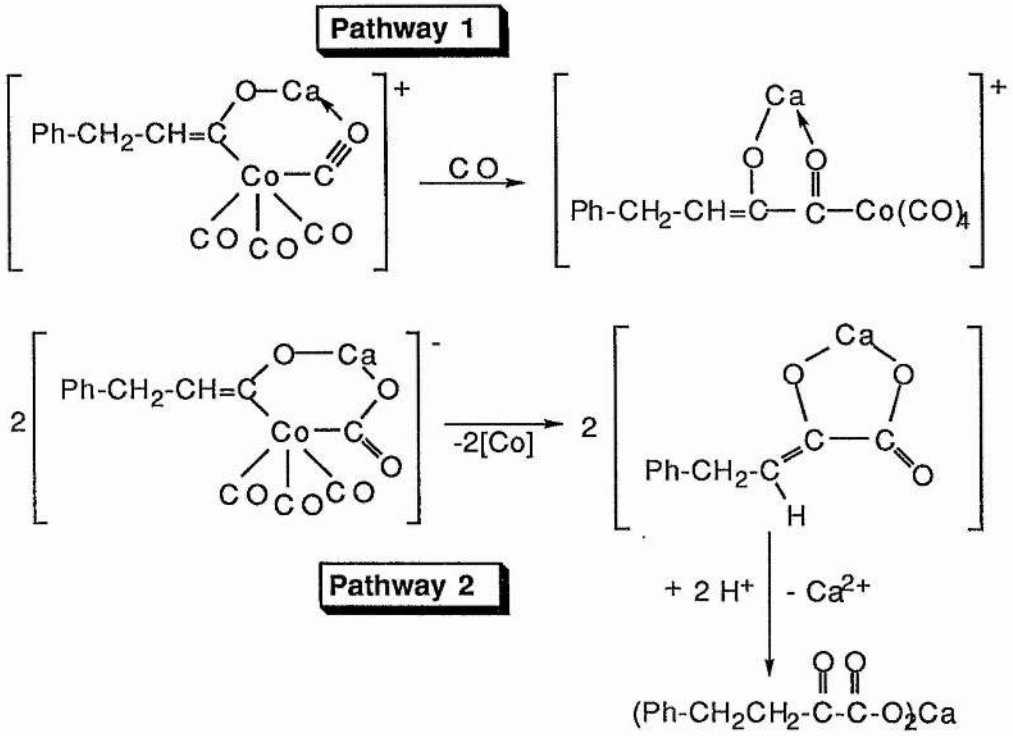

Figure 1.5.1: The potential roles of Ca^{2+} in the double carbonylation of phenyl ethyl halides.

The work of Shriver et al[29-31] uses Lewis acids to stabilise transition metal acyls which increasing the carbonyl insertion rate into M-C bonds - this precedent would favour Pathway 1 (Figure 1.5.1). Mortreux quotes the work of Miura[26,32] and des Abbayes[22] as precedents for Pathway 2: des Abbayes proposes a metallocarboxylic acid species ([**5**] - figure 1.3.4) to explain the product distribution in the $[Co(CO)_4]^-$ / PTC catalysed carbonylation of benzyl bromide. Miura has observed a remarkable change in selectivity in the carbonylation of 1-bromonaphthalene; In the presence of $Ca(OH)_2$ the reaction gave a 52% yield of 1-naphthyl glyoxylic acid but when NaOH was used no double carbonylation occurred at all.

The mechanism proposed for the double carbonylation of primary phenylethyl halides[19] is analogous to that proposed by Alper[12] for benzyl halides - see section 1.3.

1.6 Preparation of α-keto acids from secondary phenylethyl halides

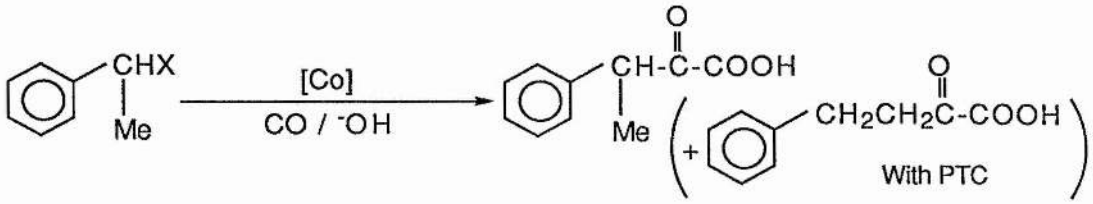

The double carbonylation of PhCHMeX (X = Cl, Br) has been achieved in aqueous alcohols[17,23] and 2 phase systems using PTC.[33,34] For homogeneous systems branched alcohols are the favoured solvents and $Ca(OH)_2$ is the preferred base - as seen for most other substrates. Again an inverse relationship between reaction temperature and the double / single carbonylation ratio is observed. Yields of up to 84% are reported with selectivity of up to 96%.

Foà et al[33] have also carried out an extensive study of the oxidative addition of PhCHMeX (X = Cl, Br) to $Na[Co(CO)_4]$. The rate of oxidative addition of PhCHMeCl is observed to be over 10 times slower than for benzyl chloride. The rate is faster in low polarity, non-coordinating solvents ie t-amyl alcohol rather than THF or DMF which would stabilise the $[Co(CO)_4]^-$ anion and increase the activation energy for the addition reaction. All these observations point to an S_N2 pathway for the oxidative addition step. In actual catalytic reactions low polarity solvents would disfavour the attack of hydroxide ions or other nucleophiles which explains the increased yield of keto acids in these solvents. When a water / toluene solvent system is used the importance of phase transfer catalysts is highlighted as this increases the concentration of the active catalytic species in the organic phase where the carbonylation reactions takes place. An increased yield of neutral coupling products {ie $(PhCHMe)_2$} is observed at higher CO pressures and this is attributed to a faster regeneration of $[Co(CO)_4]^-$ from dicobaltoctacarbonyl.

With 2 phase PTC systems both primary and secondary carbonylation products are observed.[21,33] The results of a labelling study[21] involving the single-carbonylation of PhCDMeBr gave a range of products indicative of an isomerisation of the substrate via an alkenyl cobalt intermediate as exemplified in figure 1.6.1 below

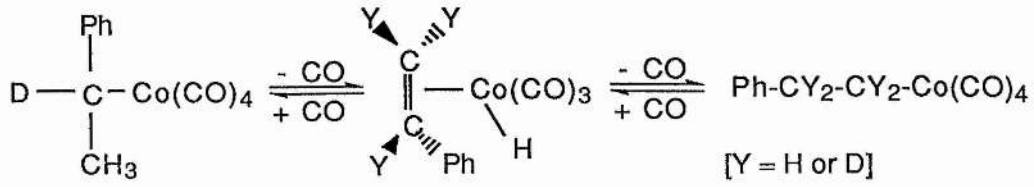

Figure 1.6.1

Such isomerisation is specifically reported[23] as not being observed in homogeneous systems.

1.7 Preparation of alkyl α-keto acids from alkyl halides

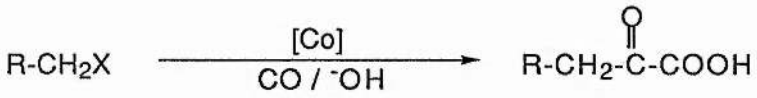

The conditions required for the double carbonylation of alkyl halides are more forcing that those used for aryl or benzyl halides, usually between 3 and 12 hours at 80-110 °C and 50-60 atm CO in the presence of a base. Examples of the double carbonylation of primary[35]and secondary[36] alkyl halides have been reported as well as the double carbonylation of bis-halo alkanes.[37-39] t-BuOH is the preferred solvent, with M(OH) or $M(OH)_2$ as the base. As observed with other substrates there is an inverse effect of the temperature upon the selectivity to the keto-acid. The main products from the carbonylation reactions of RX are usually $RCOCO_2H$, RCO_2H and the hydrolysis product ROH. Only reactions involving substrates containing four or more carbons have been reported which seems strange given the precedent for the carbonylation of MeI to give pyruvic acids in the MeI mediated carbonylation of phenyl halides.[23, 24]

The reactivity of 1-bromo-2-methyl pentane towards double carbonylation is observed[36] to be lower than for linear primary alkanes - presumably due to a lower rate of oxidative addition cf. phenylethyl halides.[33]. The reactions of 1-bromo-2-methyl-heptane or secondary halo-octanes are far from clean as the substrate not only carbonylates but also undergoes chain isomerisation to give a range of simple acids and keto acids.[33] When the substrate is 2-bromo-n-octane the main products are the 1 and 2 substituted acid and keto acids but with 3 and 4-bromo-n-octane the products are a distribution of all the possible primary and secondary isomers.

It is reported in patents covering the carbonylation of haloalkanes of the type X-CHR-$(CH_2)_n$-CHR-X that 3 different classes of product can be formed by subtle changes in reaction conditions.[37-39] These conversions are all shown in figure 1.7.1 below. For example, 1,12-dibromododecane can be doubly carbonylated to 14-bromo-2-oxo-tetradecanoic acid (**6**)[38] Another patent[39] reports the formation of cyclic keto-acids (**8**). Presumably this occurs by linking a double carbonylation with an HBr elimination, C-C coupling reaction. Yet another patent[37] reports the carbonylation of 1,7-dibromoheptane to give 1,9-bis-2,8-dioxo-nonandioic acid (**7**) by what could formally be called a double-double or a quadruple carbonylation!

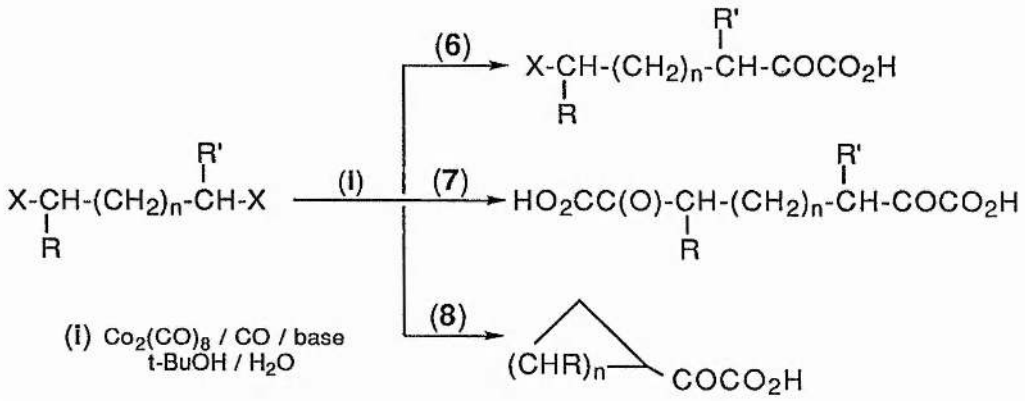

Figure 1.7.1

1.8 Substituted cobalt carbonyl based catalytic systems

There are only 2 references in the literature on the double carbonylation of organic halides by cobalt-phosphine complexes. The first[40] is a patent which reports the double carbonylation of n-butyl bromide into 2-oxohexanoic acid (in 20% yield) using dicobaltoctacarbonyl in the presence of the bidentate phosphine dppe. The second is a study by Mortreux et al[41] into the effects of hydrophobic versus water soluble phosphines on the double carbonylation of primary phenylethyl bromide.

The catalyst precursors used by Mortreux et al were of the type $[Co_2(CO)_6L_2]$,where L is a tertiary phosphine or tertiary sulphonated phosphine. When the di-cobalt complexes containing either PPh_3 or $P(p\text{-}C_6H_4Cl)_3$ ligands were added to the system only single carbonylation and no double carbonylation products were observed. This was rationalised on the basis of i) the insolubility of these complexes in the solvent system used (t-BuOH / water); and ii) the reduction of $[Co_2(CO)_6L_2]$ to $[Co(CO)_3L]^-$ being less facile than the reduction of $[Co_2(CO)_8]$. Thus pre-formed $Na[Co(CO)_3PPh_3]$ was tried as the catalyst. This species did mediate the formation of

the desired keto-acid, but only in 2% yield (cf. 66% when $[Co_2(CO)_8]$ was used under identical conditions).

Sulphonated phosphine complexes such as $[Co_2(CO)_6(P(m\text{-}C_6H_4SO_3Na)_3)_2]$ (**1**) are less basic that their PPh_3 analogues and are also soluble in polar solvents thus the potential of these sulphonated phosphine complexes were also investigated. Using (**1**) as the catalyst precursor gave a 40-50% yield of the desired keto-acid, but interestingly the double / single carbonylation selectivity was much lower than observed for $[Co_2(CO)_8]$. Even more puzzling was that, unlike all the cobalt carbonyl systems discussed above, increasing the CO pressure had no effect on the selectivity to or yield of the keto-acid. It would appear that the replacement of any of the CO's on the metal centre by a phosphine makes the metal too basic to favour the second carbonyl insertion.

One isolated report exists of the use of $[Co(CO)_3NO]$ to catalyse the double carbonylation of benzyl chloride[42] but although the yields of PAA are comparable with those of $[Co_2(CO)_8]$ the yield of the double carbonylation product (PPA) is extremely low. The reaction was carried out in a benzene-water system using PTC. Aqueous two-phase systems have a high base availability and thus the low PPA yield is probably due to an increased liberation of PAA from the metal by hydroxide ions. This in-turn will be favoured by the lower electron density at the metal caused by the highly electron withdrawing nitrosyl ligand.

1.9 Palladium phosphine complex based catalytic systems

Tanaka and co-workers[3,4] have been the first and only group to report the palladium catalysed double carbonylation of organic halides into α-ketoacids. As with the cobalt based systems a base is required and the most effective bases are again LiOH and $Ca(OH)_2$. Complexes of the type $PdCl_2L_2$ - where L is a tertiary phosphine - were the species used and the substrates which have been reported to yield double carbonylation products were; PhI, PhBr, p-Me-PhI and 2-iodothiophene. Unlike the cobalt systems polar aprotic solvents such as dioxane, THF or acetonitrile are the preferred solvents for the reaction. The major difference between the cobalt and $PdCl_2L_2$ based catalysts is the CO pressure required for a high conversion of the organic halide. At a CO pressure of 30 atm the conversion of PhBr using $PdCl_2(PPh_3)_2$ is only 42%. To attain conversions of PhI over 90% a CO pressure of 150 atm is required. With a halobenzene as the substrate, in addition to phenyl glyoxylic acid, the other major products were benzoic acid and benzaldehyde. Tanaka

assumed that the mechanism for this reaction will be analogous to that found for the Pd catalysed α-keto amide synthesis.[43-45] On this basis the following mechanism (Figure 1.9.1) was proposed.

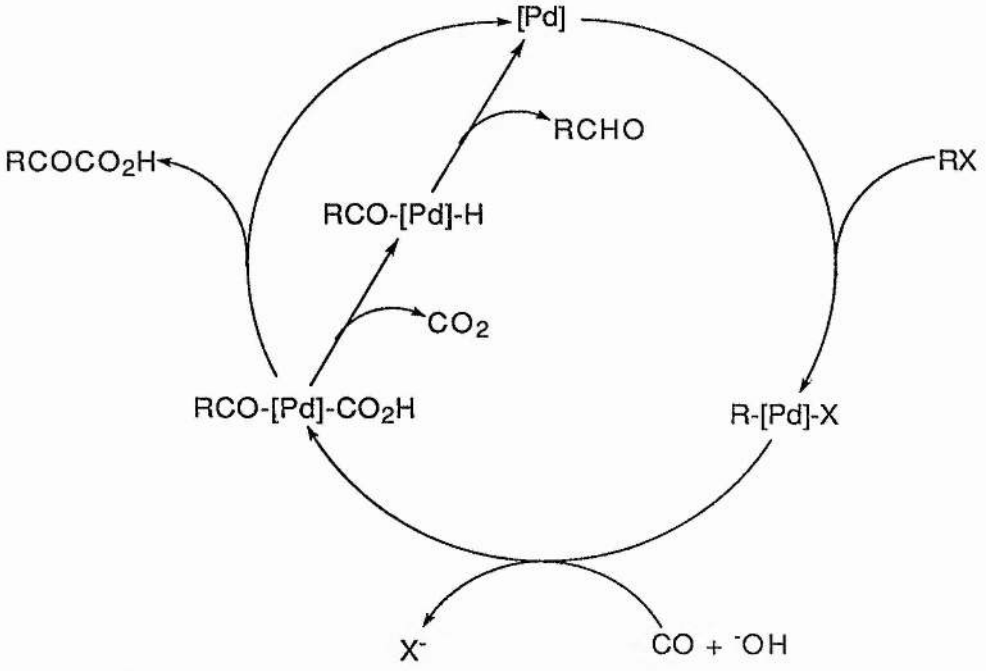

Figure 1.9.1

More basic phosphines gave a higher selectivity to the desired keto-acid.[4] Very bulky, yet still basic, phosphines such as PCy_3 gave a poor selectivity. The optimal yield of phenylglyoxylic acid was achieved using $PdCl_2(PMe_3)_2$ in dioxane with $Ca(OH)_2$ as the base under a CO pressure of 300 atm - this gave 100% conversion of PhI with a keto-acid yield of 84%.

1.10 One step preparation of α-Hydroxy Acids from halo aromatics

$$ArX + 2CO + H_2O + 2[H] \xrightarrow{[Pd^0L_n(PR_3)_2]} ArCH(OH)COOH + HX$$

One of the uses of α-keto-acids is in the synthesis of biologically important α-hydroxy acids. The one step catalytic preparation of α-hydroxy acids can be achieved by the palladium bis-phosphine catalysed double carbonylation of aryl halides with i-PrOH as the solvent and $Ca(OH)_2$ as the base.[46] The selective reduction of the α-keto carbonyl is achieved in-situ by i-PrOH / $Ca(OH)_2$ which perform a Meerwein-Ponndorf type transfer hydrogenation as well as acting as a good solvent / base for the

reaction. The reduction is believed to operate via the mechanism shown in figure 1.10.1

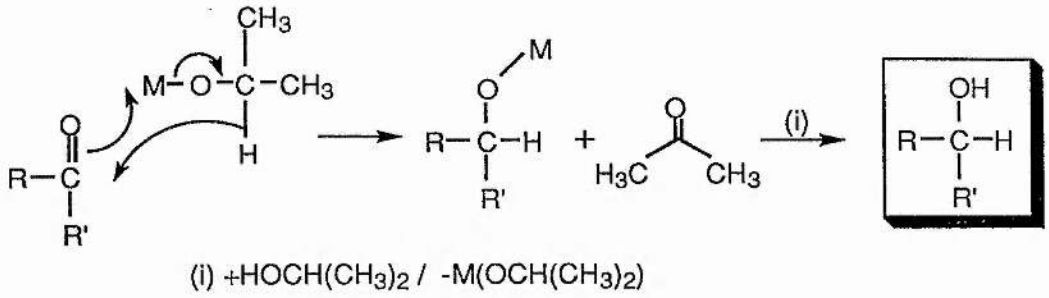

(i) +$HOCH(CH_3)_2$ / -$M(OCH(CH_3)_2)$

Figure 1.10.1

Phenyl iodide, substituted derivatives thereof, 2-iodothiophene and 1-bromonaphthalene have been converted to the respective α-hydroxy acids using this catalytic system. The products of the reaction of RX are $RCH(OH)CO_2H$, $RCOCO_2H$ and RCO_2H. The selectivity of the reaction toward the α-hydroxy acid is observed to be higher in bulky alcohols. Basic phosphines such as PMe_3 also lead to higher selectivities.

1.11 Summary

The mechanism of the synthesis of α-keto acids using cobalt based catalysts, where reported, appears to be accepted by most researchers. This mechanism first proposed by Alper[12] was later validated by a labelling study[21] reported by Foà and co-workers. A feature that all the $[Co(CO)_4]^-$ catalysed reactions have in common is the increase in double / single carbonylation selectivity achieved by either increasing the CO pressure or decreasing the temperature. The supremacy of $Ca(OH)_2$ as a base for all the reactions discussed has been tentatively accounted for by the proposal of the direct involvement of the Ca^{2+} ion in assisting the second carbonyl insertion reaction. Rather than $Ca(OH)_2$ having an ideal pK_b it appears that it is the ionic radius and divalent nature of the Ca^{2+} ion that could be important.

Both phosphine and nitrosyl substituted cobalt systems have been observed to be less effective than cobalt carbonyl based catalysts. The one other active metal so far reported, palladium, requires a far higher CO pressure to achieve a comparable conversion of phenyl halides to that of cobalt based catalysts. The mechanism by which it operates seems to be significantly different from that for the cobalt systems.

PART B Preparation of α-Keto-Esters

1.12 Introduction

Keto-esters are seen as attractive organic synthons, being activated with respect to keto-acids and keto-amides. The catalytic double carbonylation of organohalides to give keto-esters was first reported in 1985 by Tanaka[47] using the catalyst precursor $[PdCl_2(PPh_3)_2]$. The catalyst precursor $[PdX_2(PR_3)_2]$ (X = halogen; R = alkyl, aryl) is common to all the reported double carbonylation reactions yielding keto-esters. The active catalytic species is believed to be a bis-phosphine Pd^0 species[48,49] but is as yet uncharacterised. The most commonly studied substrate[47-53] is PhI, but organobromides[52] can also yield keto-esters though their rate of reaction is much slower. No reports of the double carbonylation of organochlorides into keto-esters have been reported. Substituted phenyl iodides,[38,47,50,52,53] vinyl halides[47] and some heterocycles[38,50,52] have yielded keto-esters also.

All accounts of this reaction report that a base is required and careful studies[48,49] have shown NEt_3 to be the base enabling the highest yields and selectivities. With NEt_3 as the base only two products are observed in the alkoxy-carbonylation of PhI; The ester ($PhCO_2R$) and the desired α-keto-ester ($PhCOCO_2R$). The preferred alcohol for this reaction should be basic and of moderate bulk - ie 2-BuOH or t-$BuCH_2OH$. The size of the phosphine is reported[48,49] to have a far more important effect on the reaction than its electronic character, the ideal cone angle[54] being between 140-170 °.

The best reported example of the double carbonylation of PhI into a keto-ester uses the catalyst precursor $[PdCl_2(PPh_3)_2]$ in 2-PrOH / NEt_3 for 24 hours at 60 °C and under 300 atm CO. This reaction gave (2-propyl)glyoxylate in a 92% yield with 92% selectivity.[49] It should be noted that the conditions (temperature and pressure) under which the palladium catalysed double carbonylation of organohalides (into keto-acid derivatives) are carried out become harsher in the order; keto-amides < keto-esters < keto-acids. Presumably this reflects the relative nucleophilicity of the nucleophile which increases; H_2O < ROH < R_2NH. This is also reflected in the observation that the double carbonylation of PhI into keto-esters is a relatively slow reaction[48] compared to the analogous keto-amide synthesis.

Yamamoto,[48] Tanaka and co-workers[49] have carried out exhaustive studies into the optimisation of the double carbonylation of PhI into keto-esters and their work dominates the field.

1.13 The effect of the reaction time and temperature

This kind of double carbonylation is a slow reaction, so elevated temperatures are required for a reasonable rate of reaction; 60-80 °C is quoted by most workers. As the temperature is increased the rate of carbonylation increases but the selectivity to the keto-ester drops dramatically. Yamamoto et al[48] have shown that the selectivity of the reaction towards the keto-ester is 50% for the first 10 hours but then drops to 40% from 20 hours until the end of the study at a 100 hour reaction time. This loss in selectivity has been linked to a build up of $O=PPh_3$ observed by in-situ ^{31}P NMR, suggesting that the loss of PPh_3 from the metal centre forms a palladium species with a decreased double / single carbonylation selectivity.

1.14 The effect of the carbon monoxide pressure

The effect of the CO pressure upon the yield and selectivity of the carbonylation of PhI depends upon the solvent and the phosphine ligands used. With $[PdCl_2(PPh_3)_2]$ and NEt_3 in either EtOH or 2-PrOH the yield of and selectivity to the keto-ester increases with CO pressure[49] - See figure 1.14.1 The selectivity to the keto-ester is less sensitive to CO pressure in EtOH than in 2-PrOH. A very similar change in selectivity with CO pressure is observed in 2-BuOH, although in this case the overall yield is unaffected. This difference could be due to the relative solubility of CO in these alcohols. With $[PdCl_2(PCy_3)_2]$ and NEt_3 in 2-BuOH the conversion (ie rate) increases with CO pressure but both the yield and selectivity to the keto-ester drop at elevated pressures. These data are shown in figure 1.14.1 below.

The difference between PPh_3 and PCy_3 complexes relates to the greater cone angle of the latter ligand. Being larger it can be more easily displaced from the metal and then quaternised by HI or PhI, especially at higher CO pressure. The increased basicity of PCy_3 over PPh_3 also favours the quaternisation of free PCy_3. Mono-phosphine complexes show lower selectivity than bis-phosphine species - see section 1.17.

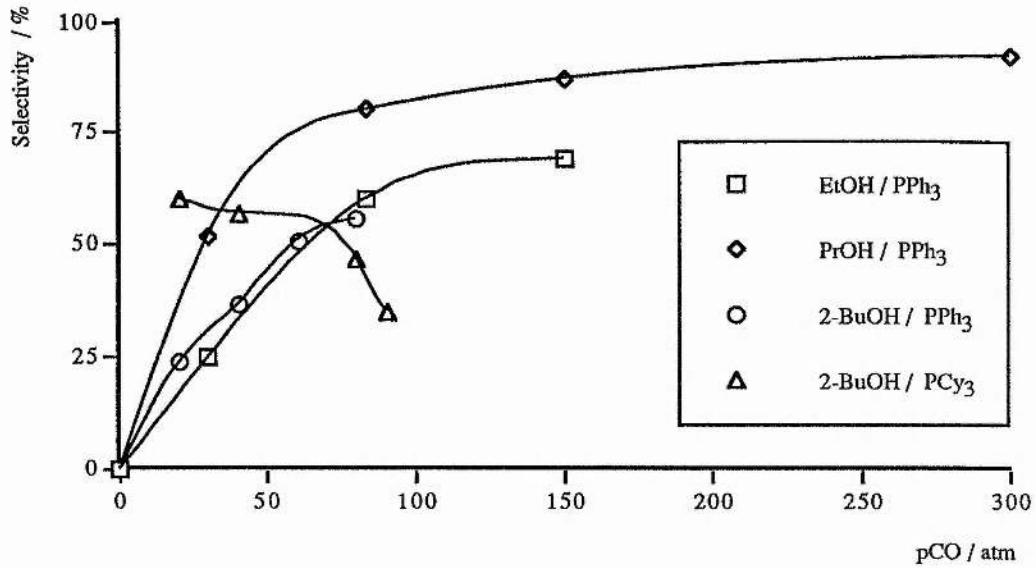

Figure 1.14.1 - Showing the selectivity to keto ester in the carbonylation of PhI catalysed by $[PdCl_2(PR_3)_2]$ (R = Ph, Cy) plus NEt_3 in EtOH, 2-PrOH and 2-BuOH.

1.15 The effect of the alcohol and co-solvents

The choice of the alcohol used in these reactions is a major determinant in the double / single carbonylation ratio. The single carbonylation reaction is normally much faster than the double carbonylation reaction and thus the conversion is increased by favouring the single carbonylation reaction. The ideal alcohols to achieve a high double / single carbonylation ratio are basic with a moderate bulk. For primary alcohols the double / single carbonylation ratio is observed[49] to decrease in the order; t-$BuCH_2OH$ > i-$BuCH_2OH$ > n-BuOH > EtOH > MeOH. t-BuOH is reported exclusively to yield single carbonylation products. Yamashita et al[48] report secondary alcohols of moderate bulk to give the highest selectivities, choosing 2-BuOH for their studies.

The use, in addition to the alcoholic solvent / reagent, of a co-solvent can have a marked effect on the reaction selectivity. Low polarity co-solvents are observed to give higher selectivities to keto-esters. These effects are rationalised in section 1.18.

Normally the double / single selectivity of carbonylation reactions carried out in the presence of MeOH is very low, but higher selectivities to methoxy keto-esters can be achieved by using methyl formate (MeOCHO) as the methoxide source.[51] Either the methyl formate slowly decarbonylates (yielding CO and MeOH) or MeOH present as

an impurity in the methyl formate is responsible for the reaction.[55] Although an improved selectivity is observed, the yield is extremely poor, unfortunately this is a 'catch-22' situation as alkanolysis is the rate determining step in the formation of keto-ester by double carbonylation, but only by having low methoxide concentration can high selectivity be achieved.

1.16 The effect of tertiary amines and inorganic bases

Poor selectivities are reported when inorganic bases are used, tertiary amines being preferred as bases for the synthesis of keto-esters by double carbonylation. When NEt_3 is the base employed only the desired keto-ester and the single carbonylation product are observed. With ^{i}PrOH and KOAc, the products were; $PhCO_2H$ (32.0 %), 2-PrOAc (38.4 %), $PhCO_2{}^{i}Pr$ (11.8 %), $PhCOCO_2{}^{i}Pr$ (5.5 %) and a trace amount of $PhCOCO_2H$.[53]

Tertiary amines with a pK_a of 10-11 give the highest selectivities.[49] By examining a variety of tertiary amines in this pK_a range the ideal steric properties of the amine can be isolated - it is found that the selectivity decreases with steric congestion. NEt_3 is thus observed to be the ideal base for this reaction.

1.17 The steric and electronic effects of the phosphine and the Pd/PR_3 ratio

The conversion of PhI falls with an increasing PR_3:Pd ratio, where as the selectivity to the keto-ester peaks at PR_3:Pd = 2:1.[48] It should be noted that double carbonylation is observed in the absence of any phosphine but for the highest selectivity a 2:1 PR_3:Pd ratio has been observed to be ideal, suggesting that a bis-phosphine complex is the active species of choice. Tertiary phosphines having a cone angle of between 140-170 ° give the highest conversion (ie rate) and selectivities towards keto-esters. The use of a range of para-substituted triphenylphosphines has been used to study the effect of the electronic nature of the phosphine upon the reaction[49] whilst keeping the cone-angle constant. Both the conversion and the selectivity increase with more electron withdrawing phosphines, but the significance of the electronic effects are minor in comparison with that of the steric influence of the phosphine upon the reaction.

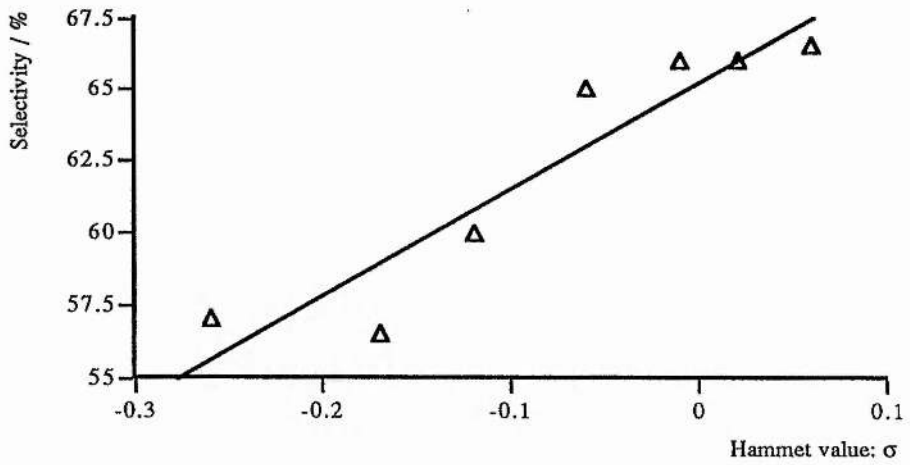

Figure 1.17.1 - Showing the electronic effect of a variety of para-substituted triaryl phosphine ligands upon the selectivity of the [$PdCl_2(PAr)_3$] catalysed carbonylation of PhI.[49]

Mechanistic studies suggest that larger phosphines differentially protect the site of attack of alcohol / alkoxide ion leading to the ester - [Pd(COPh)I$(PR_3)_2$] - over the site of attack which yields the desired keto-ester - [Pd(COPh)I(CO)$(PR_3)_2$]. (See figure 1.18.1 below)

1.18 Mechanistic studies

An in-situ NMR study[48] of a catalytic reaction employing [$PdCl_2(PPh_3)_2$], NEt_3, PhI and 2-BuOH revealed [Pd(COPh)I$(PPh_3)_2$] to be the predominant species under standard catalytic conditions. During the course of the reaction the build up of $OPPh_3$ and unidentified palladium-phosphine species were observed. The selectivity towards the keto-ester decreases with time and it is proposed that the formation of a palladium mono-phosphine complex at the expense of the more selective bis-phosphine complex is responsible for this.

The oxidative addition of PhI to palladium and the subsequent carbonyl insertion to give [Pd(COPh)I$(PR_3)_2$] are known to be fast[56] which is consistent with [Pd(COPh)I$(PPh_3)_2$] being involved in the rate determining step as suggested by the in-situ NMR study. The reactivity of [Pd(Ph)I$(PPh_3)_2$] (**9**) and [Pd(COPh)I$(PPh_3)_2$] (**10**) with CO / ROH / NR_3 was observed[57] to be identical. The keto-ester / ester ratio and yields being the same for a range of alcohols and amines. Tanaka concluded

therefore that **10** is a common intermediate in the formation of both esters and keto-esters. The mechanism shown in figure 1.18.1 has been proposed.[48, 49]

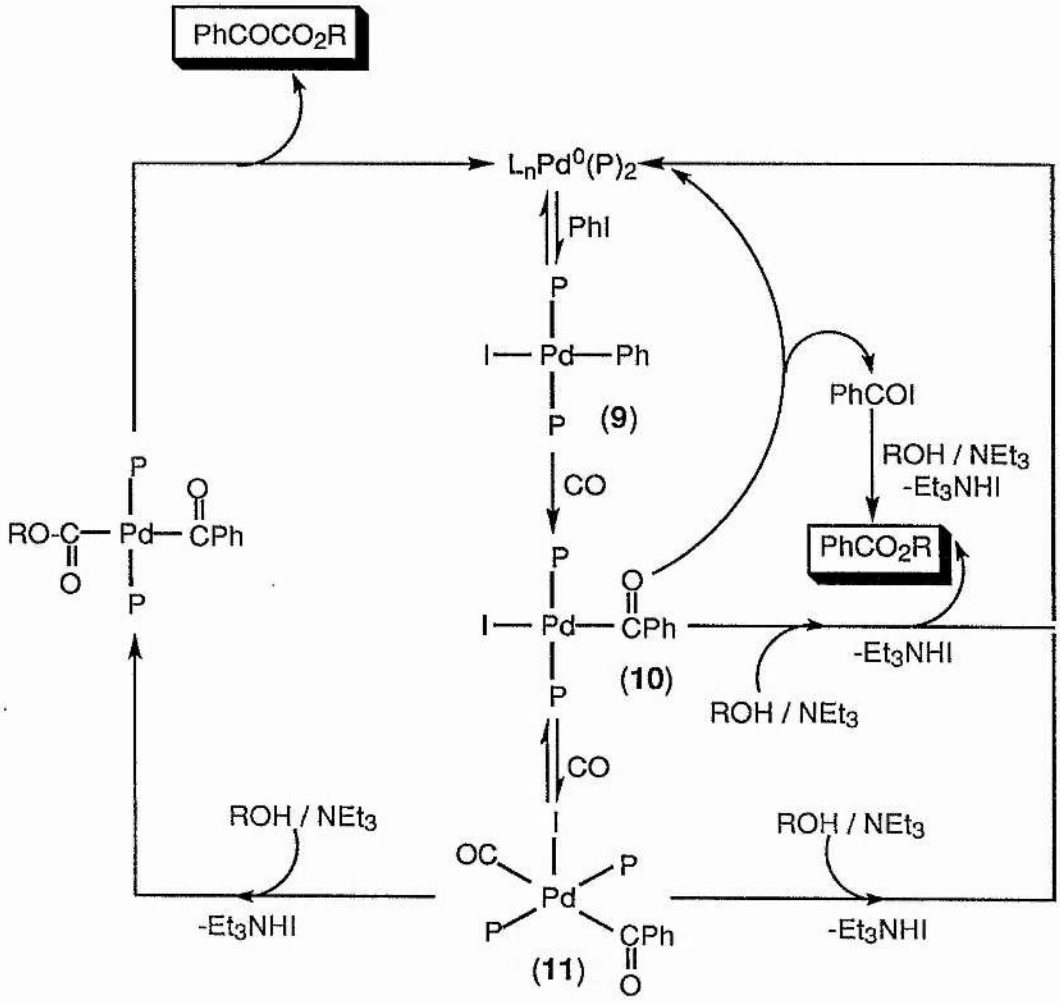

Figure 1.18.1: Proposed mechanism for the palladium / phosphine catalysed alkoxy-double carbonylation of PhI.

The reaction of **10** to give **11** (see figure 1.18.1 above) has been observed by HPIR and has been shown to be reversible. Examining analogous complexes containing a range of different phosphines showed that this equilibrium position was biased towards **11** in species with the larger phosphines.[48]

The reductive elimination and alkanolysis of PhCOI has been shown[57] to be a minor route to the single carbonylation product, but there are two potential major routes to this product. These two routes are illustrated in figure 1.18.2.

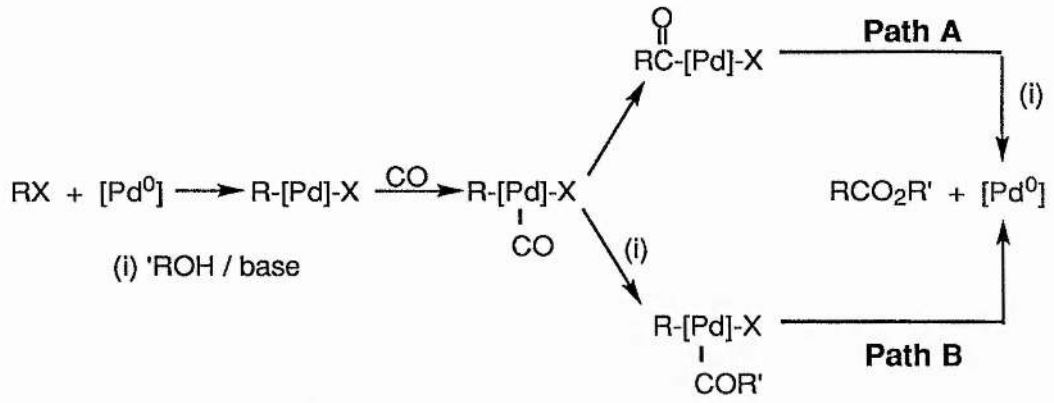

Figure 1.18.2: The possible major routes to RCO_2R by the carbonylation of RX.

When $[Pd(PhCH_2)Cl(PPh_3)_2]$ is reacted with MeOH / NEt_3 / CO no organometallic intermediates could be observed.[56] Since both CO insertion and alkoxide attack are disfavoured by electron donating phosphines, Milstein[56] has used palladium bis-PMe_3 complexes to stabilise the potential intermediates shown in figure 1.18.2. By this approach Milstein observed the intermediates in this process and has shown that Path A (figure 1.18.2) is the major route to the single carbonylation product. The nucleophilic attack of RO^- on the CO of $[PdX(CO)(PR_3)_2]$ (Path B) does not form a route to the ester. A ^{13}CO labelling study of the CO insertion into the Pd-C bond has shown this reaction to be irreversible in both phenyl and benzyl complexes. A kinetic study[48] of the reaction of **10** with EtOH / Et_3N shows the reaction to be first order in [EtOH], $[NEt_3]$ and [Pd] and inversely proportional to $[PPh_3]$. This indicates that the loss of phosphine from the metal is required for the formation of the ester. The high negative entropy of activation of this reaction suggests a very ordered transition state, and solvent effects on the rate point to an ionic intermediate. This, and other evidence already discussed, leads Yamamoto to propose that the amine plays an intimate role in the formation of the ester.[48] The two proposed potential roles of the amine are shown in figure 1.18.3

The observed increase in yield of the single carbonylation product in polar solvents implies that cationic species are involved in the pathway responsible for ester production. Examination of the reaction of $[Pd(COPh)(PPh_3)_2](ClO_4)$·acetone with ^iPrOH / NEt_3 under CO shows the organic reaction product ratios (9% selectivity to keto-ester) to be very different from those observed in standard catalytic reactions (94% selectivity to keto-ester). On this basis it is excluded as a potential intermediate in the catalytic cycle.[57]

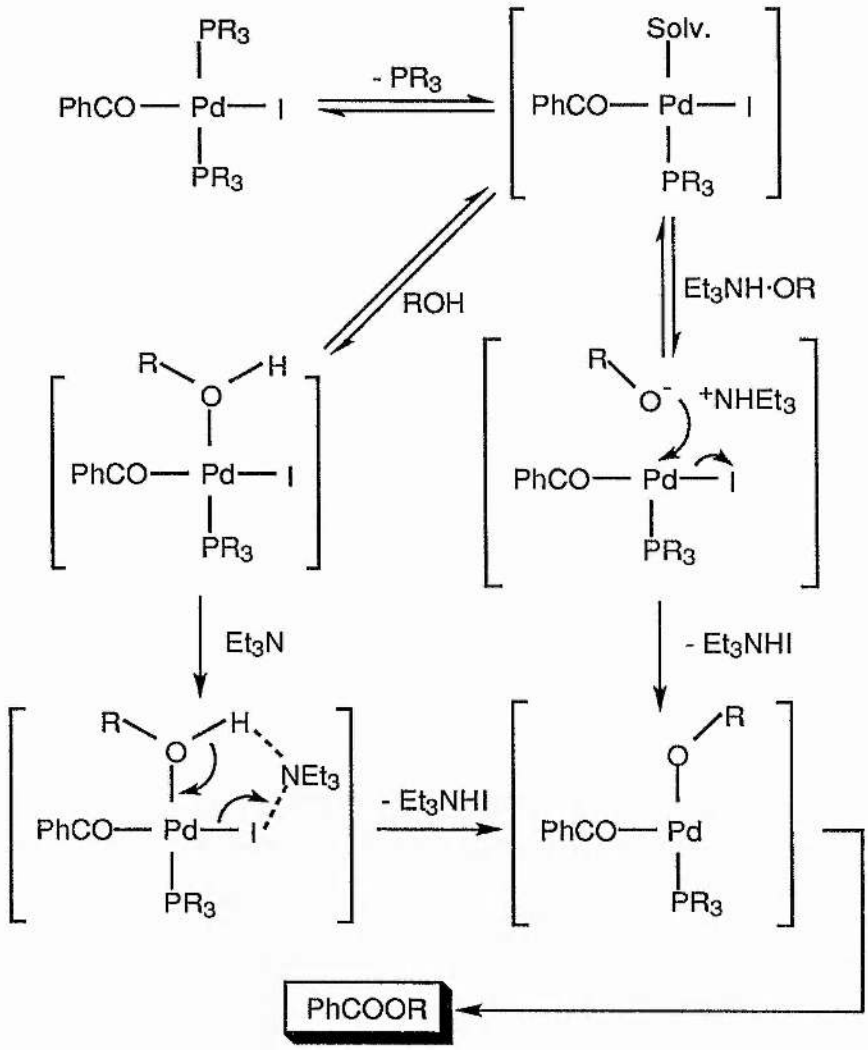

Figure 1.18.3: Potential roles for NEt_3 in the alkoxy-carbonylation of PhI.

The origin of the effect of different alcohols upon the catalytic reaction was probed[48] by comparing the reaction of a series of pairs of alcohols (ROH & R'OH) with $[Pd(COPh)I(PPh_3)_2]$. This was carried out under CO in the presence of NEt_3. Analysis of the product ratios - PhCOCOR / PhCOCOR' / PhCOOR / PhCOOR' - gave a relative reactivity of a range of alcohols towards the intermediates which yield the ester and the keto-ester. This showed that small acidic alcohols were preferentially found in the ester products whereas more basic alcohols of a moderate size were found in the keto-ester products.

The key to understanding the mechanistic reasons behind the trends in the reactivities of alcohols and the effect of the choice of tertiary amine for the reaction can be understood on the basis of the reactions shown in figure 1.18.4.

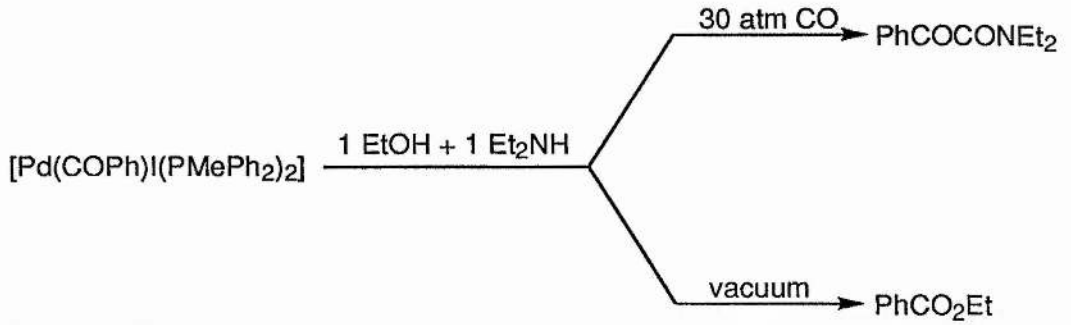

Figure 1.18.4

It is the attack of an anionic nucleophile which yields the single carbonylation product, and thus the ester is formed from alkoxide attack. Conversely, the keto amide is formed under CO pressure as a neutral nucleophile is required to react with the CO ligand (leading in turn to reductive elimination of the ester or amide) and amines are better nucleophiles than alcohols. The effect of a variety of alcohols on the double / single carbonylation selectivity of the catalytic reaction was discussed in section 1.15. More acidic the alcohols give rise to lower selectivities because of more of the alcohol is instead found in the alkoxide form.

Another potential mechanism for double carbonylation yielding keto-esters which has been investigated is centred on the steps shown in figure 1.18.5.

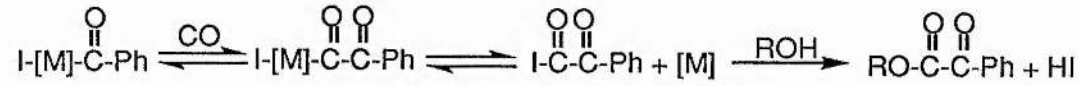

Figure 1.18.5: Potential route to keto esters via a pyruvyl complex.

Pyruvyl complexes of Pd,[45,58,59] Pt[58,60] and Fe[61,62] have been synthesised, all by reaction with Cl-C(O)CO_2R. The palladium complexes undergo rapid decarbonylation at 25 °C to yield aroyl complexes,[45,58,60] where the more stable platinum analogues only decarbonylate when heated to > 60 °C. Both platinum and palladium species can be stabilised with respect to decarbonylation by adding excess phosphine to the solution. These observations led Angelici, Sen and co-workers[58,60] to propose that a phosphine ligand is temporarily lost to allow for acyl migration to the metal before the CO is lost. This idea is illustrated in figure 1.18.6

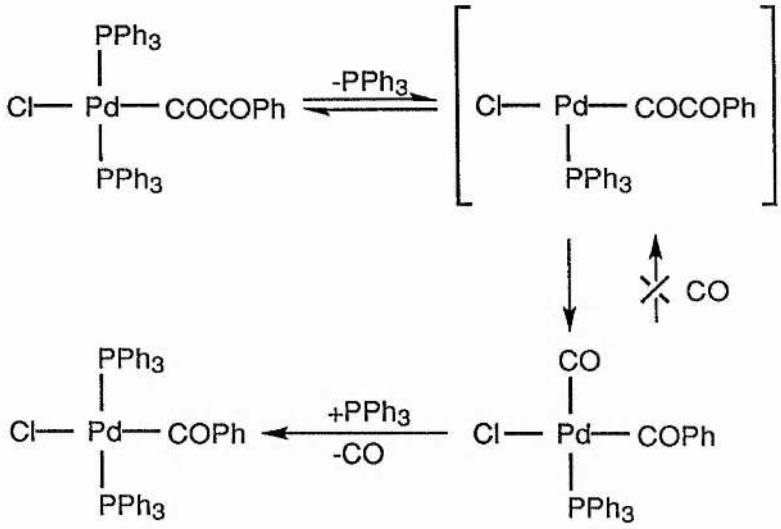

Figure 1.18.6: Proposed decarbonylation pathway of $[Pd(COCOPh)Cl(PPh_3)_2]$.

The pyruvyl trimethylphosphine palladium complex $[Pd(PhCOCO)(solvent)(PMe_3)_2]^+$ was observed[59] to be less susceptible to decarbonylation than the other analogues. This allowed the study of its reactivity with nucleophiles. When exposed to a source of RO^- at -40 °C the organic moieties $PhCOCO_2R$ and $PhCO_2R$ were observed as products. These observations could have suggested that [Pd-COCOR] complexes were involved as intermediates in the catalytic cycle except that a ^{13}CO labelling experiment demonstrated that although keto-amides could be formed from the reaction of $[Pd(COCOPh)Cl(PPh_3)_2]$ with $HNEt_2$ the reaction did not involve the direct cleavage of the pyruvyl moiety from the metal but instead proceeded via the reductive coupling of PhCO and $^{13}CONEt_2$ moieties.[43]

Attempts to insert CO into the Pd-C(O)Ph bond to re-form the initial pyruvyl complex -even at 67 atm CO - were unsuccessful.[58,60] Sen and co-workers[60] have also observed that the rate of the decarbonylation reaction is unaffected by up to 47 atm CO which shows that inserting CO into such Pd-C(O)R bonds is at least difficult, if not impossible. This indicates that $[PdCl(COPh)(CO)(PPh_3)_2]$ is thermodynamically favoured with respect to the pyruvyl complex $[PdCl(COCOPh)(PPh_3)_2]$. Given that catalytic reactions have been reported at these temperatures and pressures, the route shown in 1.18.5 can probably be dismissed. Only two examples[63,64] of the insertion of CO into a metal-acyl bond have been reported, these were achieved by a one electron oxidation followed by NO addition - shown in figure 1.18.7.

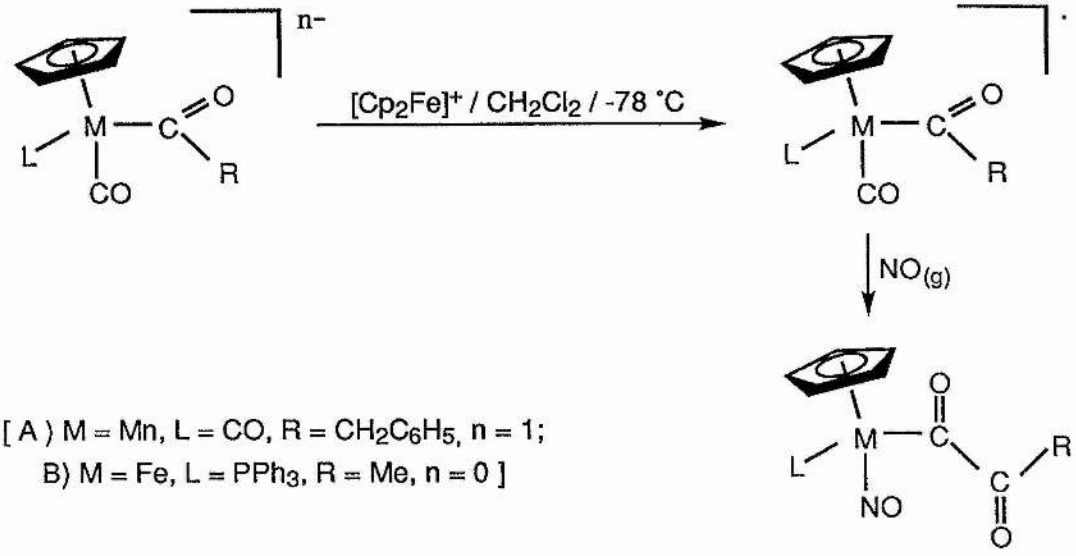

[A) M = Mn, L = CO, R = $CH_2C_6H_5$, n = 1;
B) M = Fe, L = PPh_3, R = Me, n = 0]

Figure 1.18.7: Examples of CO insertion into metal acyl bonds.

1.19 Summary

The synthesis of keto esters by the double carbonylation of organic iodides and bromides can be achieved using palladium phosphine complexes. Although the active catalytic species has yet to be fully characterised, all the evidence suggests that it is a Pd(0) bis-phosphine complex (ie $[Pd(CO)_n(PR_3)_2]$ n = 1, 2). Although the exact nature of the catalytic species is not definitively known a mechanism has been proposed which is consistent with all the experimental data. Large phosphines such as PPh_3 or PCy_3 lead to a better selectivity with the electronic nature of the phosphine only playing a minor role. The preferred base for the reaction is NEt_3 and a number of observations point to the base playing an intimate part in the mechanism, not just acting as a arbitrary sink for HI. The ideal alcohols for the highest double / single carbonylation selectivity are weakly acidic alcohols of moderate bulk. The importance of these parameters is probably due to the role of alkoxide ions in ester formation, but unionised alcohols in keto-ester formation.[48]

PART C Preparation of α-Keto-Amides

1.20 Introduction

Of all the derivatives of α-keto-acids, amides require the mildest conditions in their preparation via double carbonylation. The first reports of the catalytic double carbonylation of organohalides to give keto-amides appeared in 1982. The groups of both Tanaka[65] and Yamamoto[66] reported the catalytic double carbonylation of a range of organohalides by Pd(II) bis-phosphine precursors. A range of organobromide and iodide substrates can be converted to keto-amides; aryl and substituted aryl halides,[65-69] vinyl halides,[65,66,70] alkyl halides[71] and heterocycles.[65,66] Most of the work in this field has, though, been carried out using aryl halides

Only 2 accounts of the activation of an organo-chloride yielding a keto-amide have appeared. Basset et al [72] have reported the activation of chlorobenzene using [(η^6-chloroarene)$Cr(CO)_3$] as the substrate the C-Cl bond is activated by the electron withdrawing $Cr(CO)_3$ moiety. The C-Cl bond in allyl chlorides is activated by the adjacent allyl moiety. Yamamoto[73] has utilised this feature and has published a brief account of the double carbonylation of 2-methyl allyl chloride into the corresponding keto-amide.

A range of metal phosphine complexes has been observed[67] to form active catalysts for the double carbonylation of PhBr: $CuBr(PPh_3)_3$; $NiCl_2(PEt_3)_2$; Co(I) tris-PPh_3 complexes and Pd(II) bis-phosphine complexes. Palladium(II) complexes without phosphine ligands are not observed to form active double carbonylation catalysts for the formation of keto-amides. Of all the species screened, the Pd(II) bis-phosphine precursors were the most effective and all the other work on double carbonylation yielding keto-amides has been based on such species. The species proposed as the active catalyst in these reactions is a Pd(0) complex formed from the Pd(II) precursor in situ. Typical yields for the double carbonylation of phenyl iodide often exceed 90%.[65] Starting from PhI with $HNEt_2$ as solvent / base / reagent and using [$PdCl_2$dppb] at 60 °C and 40 atm CO for 4 hours, the keto-amide is formed in 98% yield.[65] Iodostyrene also yields the corresponding keto-amide in 93% yield using [$PdMe_2(PMePh_2)_2$] in $HNEt_2$ at 25 °C and 70 atm CO for 70 hours.[70]

1.21 α-Keto-amides from aryl (and substituted aryl) halides

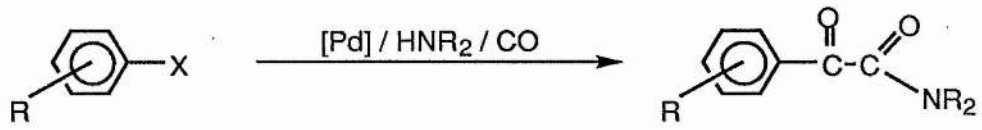

1.22 The effect of temperature and carbon monoxide pressure

A common feature of double carbonylation reactions yielding α-keto-acid derivatives is the increase in selectivity at lower reaction temperatures or at elevated CO pressures (See Parts A and B). This is observed for the amino-double carbonylation of both phenyl bromides and iodides.[65,67,68] An unusual feature of amino-double carbonylation is the observed[67] increase in reaction rate with increasing CO pressure for PhI, but decrease of reaction rate with CO pressure for PhBr. Yamamoto suggests that this points to the rate determining step for the PhBr reaction being the initial oxidative addition, a different rate determining step rather than the expected attack of amine upon CO. The decrease in reaction rate is propounded as being due to a greater number of CO ligands on the initial Pd(0) catalyst at higher CO pressures leading to a reduced nucleophilicity of the metal centre.

1.23 The effect of amine bases

Diethyl amine ($HNEt_2$) is reported to be the ideal base for these reactions.[65,67] It should be noted that $HNEt_2$ acts not only as a base but as one of the reagents also - in addition to this many of the reported studies use it as the solvent as well. A systematic study[67] of the effect of various secondary amines has revealed the following: Conversion is directly related to the basicity of the amine but inversely proportional to the size of the amine (with $pK_b \approx 3.0$). The selectivity to the keto-amide increased with amine size up to a certain size. Smaller amines are thus more reactive, yet less selective - an observation which is also backed by work on the reactivity of amines with the proposed reaction intermediate $[Pd(COPh)X(PMePh_2)_2]$. (See section 1.27)

When primary amines are used in these reactions only Shiff base products (ie PhC(=NHCy)C(O)NHCy from the condensation of the keto-amide with the amine) are normally observed[65] unless t-$BuNH_2$ is employed when a high selectivity to the desired keto-amide is regained.[67]

1.24 The effect of the solvent and the substrate

In the majority of the reports of these reactions $HNEt_2$ is used as the solvent (as well as base / reagent). Yamamoto[44] has investigated solvent effects upon the reactions of proposed intermediates in the catalytic cycle. Although conventional organo chloride reagents are observed to be inactive the reactivity of proposed intermediates where PhCl was presumed as the substrate were also investigated. The two series of reactions are shown in figure 1.24.1.

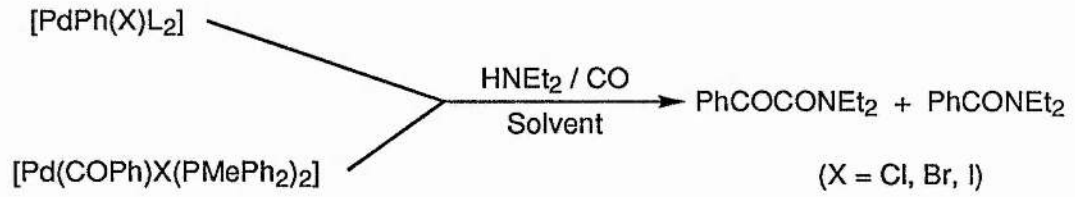

Figure 1.24.1

When X is bromide or iodide the selectivity of the reaction to the keto-amide rises with the polarity of the solvent with both the phenyl and the acyl complexes. When, on the other hand, the chloro complexes are investigated their selectivity to the keto-amide is observed to be highest in non-polar solvents. Since, with one exception,[72] only organo bromides and iodides are suitable reagents this could suggest that the catalytic mechanism goes via an ionic intermediate. The proposed catalytic cycle, discussed later, is believed to involve cationic palladium intermediates (section 1.27).[44]

A variety of para-substituted phenyl bromides undergo double carbonylation[67] to give keto-amides. Electron withdrawing substituents give a high conversion but a low selectivity, correspondingly, electron donating groups give higher selectivities but lower overall conversions. These different conversions are observed for reactions of the same time duration and thus reflect the rate of reaction. The introduction of an ortho-methyl group onto the substrate greatly retards the reaction, the two methyl groups in 2-6 dimethyl bromobenzene almost stop the carbonylation reaction entirely; amide (0 %), keto-amide (2 %).

1.25 The effect of the phosphine ligands

Both mono and bidentate phosphine ligands can give active catalytic complexes. The two best ligands are observed to be $PMePh_2$ and $Ph_2P\text{-}(CH_2)_4\text{-}PPh_2$ (dppb).[65,67,68] A range of bidentate phosphines was investigated by Tanaka[65] the ability of dppb to be change between being a bidentate and unidentate ligand is conceivably the reason behind its suitability for this reaction (see section 3.2).

1.26 Polymer bound palladium catalysts

Palladium complexes with three classes of polymer supported ligands have been investigated for the double carbonylation of phenyl halides in the presence of secondary amines.[69] The polymer supported ligands investigated were: diphenylphosphinomethyl polystyrene (PSP), poly-2-vinyl pyridine (PVP) and poly-2-N-vinyl pyrolidone (PNVP). PSP and PNVP were stable to the leaching of palladium under the reaction conditions, but only the PSP based catalyst gave good yields of the keto-amide. The PSP system with a P:Pd ratio of 5.9:1, PhI as the substrate with $HNEt_2$ under 2.8 atm CO at 100 °C gave a quantitative conversion with a 90% selectivity to the keto-amide. This reaction is unusual as both the yield and the double / single carbonylation selectivity is proportional to the reaction temperature. The selectivity is virtually independent of the CO pressure, but the rate of reaction does increase with increasing CO pressure. The unusual effects of temperature and pressure upon these reactions suggests that the mechanism operating with the supported catalysts is significantly different from that in standard homogeneous systems.

1.27 Mechanistic Studies

The mechanism shown in figure 1.27.1 describes the $[Pd^0L_n(PR_3)_2]$ catalysed double carbonylation of aryl bromides and iodides.[67]

The reactivity of complexes of the type $[Ph\text{-}PdX(PR_3)_2]$ (**1**) has been examined by Yamamoto.[44,67] In addition to the single carbonylation pathway shown in figure 1.27.1 [Path A] there was another potential route to the amide product which had to be considered. This route, Path B, is shown in figure 1.27.2.

The reaction of **12** with ^{13}CO to give **13** has been shown to be irreversible.[56,67] It has also been observed that the reaction of **12** with piperidine[67] or diethylamine[43] exclusively gives the amide product whereas under the same conditions **13** gives the keto-amide exclusively. These observations show that **13** is not an intermediate in the conversion of **12** to the free amide and thus gives good evidence for Pathway A in figure 1.27.1 as the mechanism of amide production.

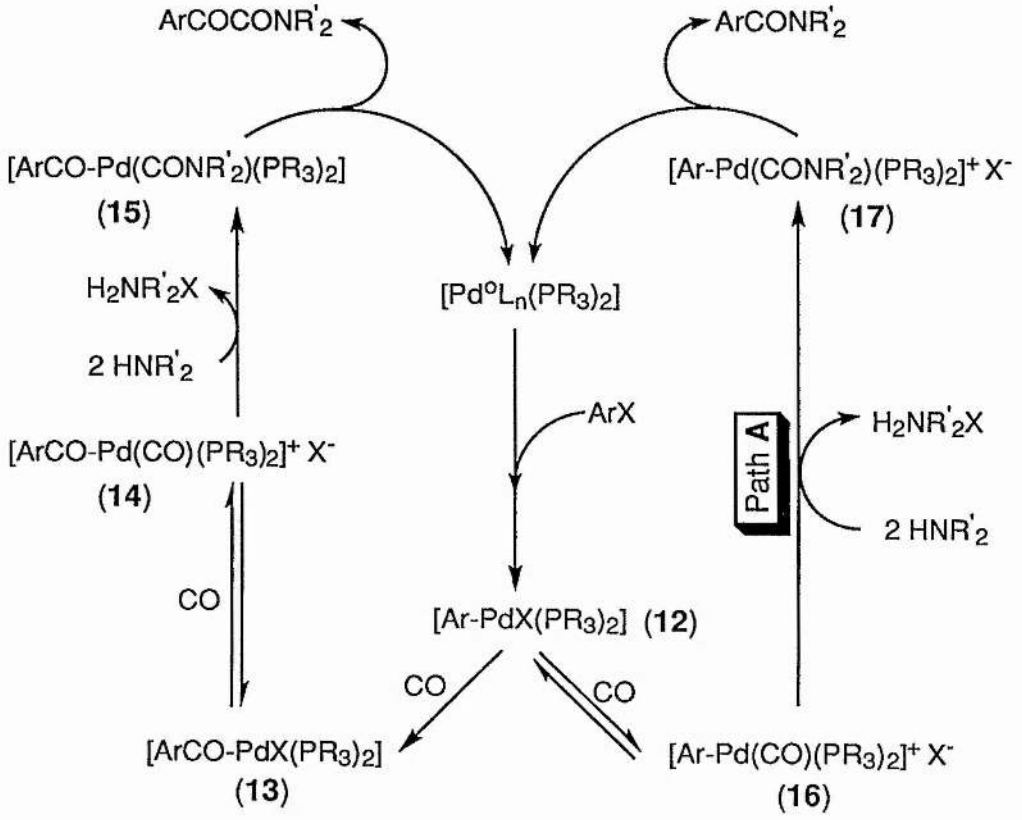

Figure 1.27.1: Proposed mechanism for the palladium / phosphine catalysed amino-double carbonylation of aryl halides.

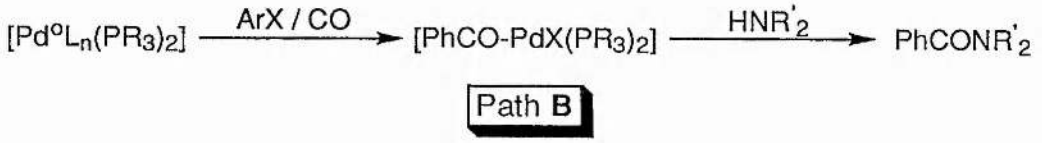

Figure 1.27.2: Alternative amino-single carbonylation pathway.

The observation that the yield of keto-amide from phenyl halides is higher in polar solvents[44] suggests that an ionic intermediate is involved in the mechanism. When **13** is examined by HPIR and is subjected to CO (20 atm) in CH_2Cl_2 no new carbonyl bands are observed. Addition of methanol to the solution gives rise to the observation of a new terminal CO band. When the model ionic complex trans-

$[Pd(COPh)(PMePh_2)_2][ClO_4]$ is examined by HPIR under a CO atmosphere the carbonyl bands observed are nearly identical to the solution of **13** in CH_2Cl_2 / MeOH under CO. The reaction of **13** with CO is shown to be reversible. This reaction[44] models the proposed mechanistic step converting **13** to **14**. The reaction of trans-$[Pd(COPh)CO(PMePh_2)_2][ClO_4]$ with CO and a secondary amine gives mainly keto-amide with a little amide. The reaction of the cationic species is observed to occur more rapidly than the reaction of the analogous neutral complex and thus its involvement in the catalytic cycle is proposed.

As with the first carbonyl insertion into the Pd-Ph bond two pathways for the reaction of **13** with a second mole of CO have been suggested,[43,45,74] these are shown in figure 1.27.3.

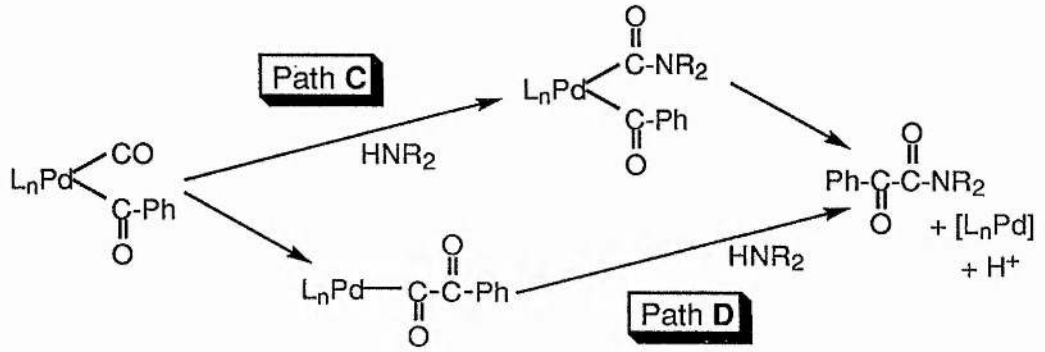

Figure 1.27.3 : The two plausible pathways for the second CO insertion step of the palladium / phosphine catalysed amino-double carbonylation reaction.

Transition metal pyruvyl complexes can be prepared[43,45,75,76] but readily decarbonylate even at room temperature. Sen has studied the chemistry of the Pt and Pd analogues.[43] The decarbonylation of $[Pd(COCOPh)Cl(PPh_3)_2]$ (**18**) is inhibited by the addition of excess phosphine, but the rate of decarbonylation is unaffected by even 47 atm CO. When a solution of the acyl complex $[Pd(COPh)Cl(PPh_3)_2]$ (**13**) is placed under 67 atm CO no reaction is observed. Thus even if the step **13**⇔**18** is reversible the equilibrium is strongly towards the acyl species (**13**).

$[M(COCOPh)Cl(PPh_3)_2]$ (M = Pt, Pd(**18**))[43] react with $HNEt_2$ (with or without CO) to form the keto-amide $PhCOCONEt_2$. Sen presents irrefutable evidence that the second CO insertion occurs exclusively via Path C with the following elegant experiment. When **18** is allowed to react with $HNEt_2$ under ^{13}CO the reaction yields $Ph^{12}CO^{13}CONEt_2$ with ≥ 96% label integrity. This labelling study can only be explained in terms of the initial decarbonylation of **18** yielding the acyl species **13**

which can then undergo a reversible exchange of the terminal CO ligand with ^{13}CO. The acyl species must then form the keto-amide via Path C.

The coupling of the two carbonyl groups to form the keto-amide is proposed to occur by the reductive elimination of cis-acyl and carbamoyl ligands from the palladium centre. Carbamoyl complexes are widely reported in the literature.[73,74,77-85] The requirement for the two organic moieties to be in a cis-configuration has been observed by Yamamoto.[81,83] trans-$[Pt(COPh)(CONEt_2)(PPh_3)_2][BF_4]$ is known[74] to decompose in $CDCl_3$ to yield $HNEt_2$ and $PhCOCONEt_2$ as the main organic products. This reaction of trans-$[Pt(COPh)(CO)(PPh_3)_2][BF_4]$ with HNR_2 has also been studied in-situ by NMR,[83] the series of reaction steps observed is shown in figure 1.27.4.

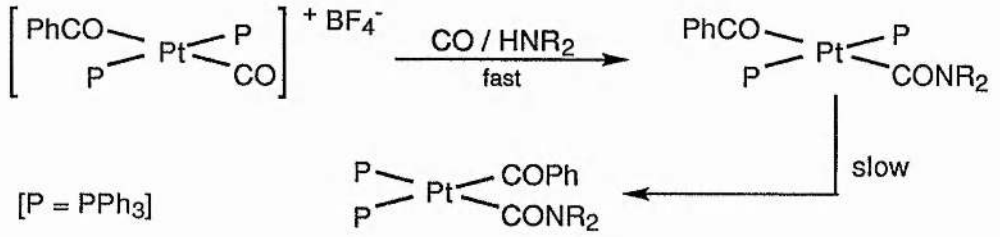

Figure 1.27.4

The rate of formation of the cis carbamoyl complexes from both neutral and cationic model acyl complexes is observed[83] to be dependent upon the presence of both $HNEt_2$ and CO. Another pair of model reactions elucidate the mechanistic reasons behind this, these are shown in figures 1.27.5 and 1.27.6.

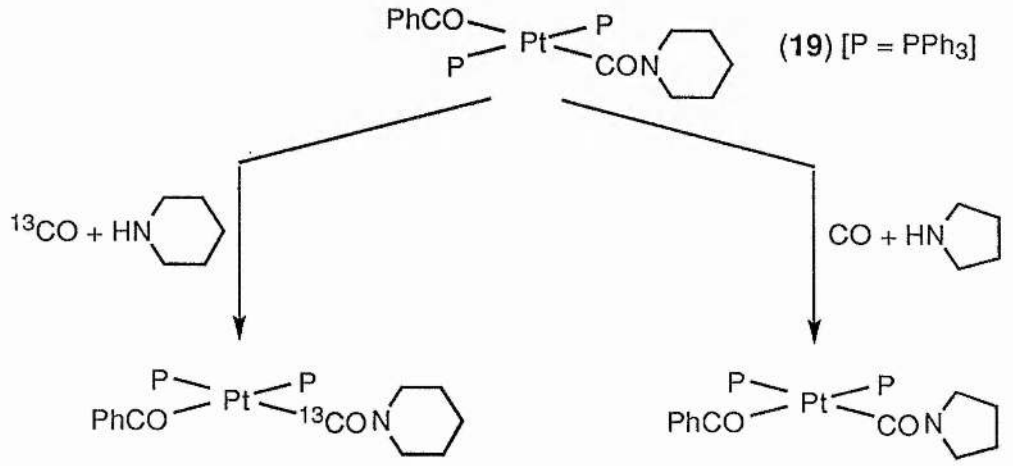

Figure 1.27.5

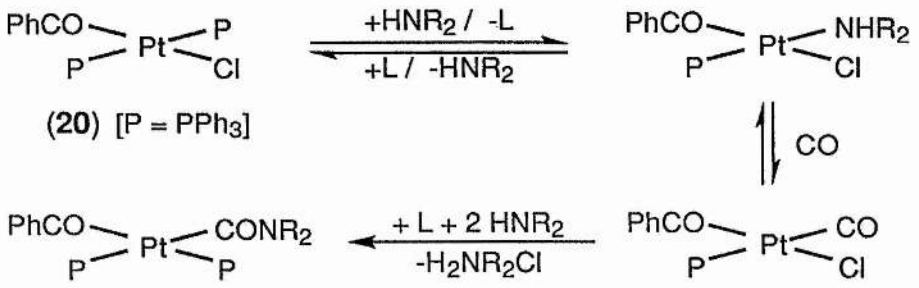

Figure 1.27.6

The reaction of a model carbamoyl complex **19** clearly shows that both amine and CO dissociation are required for the cis-trans isomerisation. The reaction of the neutral model complex trans-[Pt(COPh)Cl(PPh_3)$_2$] (**20**) with $HNEt_2$ and CO was followed by NMR. Free amine is required to displace the phosphine and is then itself displaced by CO before the phosphine rebinds to give the cis-complex. The importance of phosphine dissociation observed in these platinum model systems is mirrored by the improved catalytic performance of catalyst precursors with bulky, less basic, phosphines such as PPh_3 - see section 1.25. Initially one would consider that the displacement of a phosphine from the metal in the presence of PhI could lead to its quaternisation. It appears that either the size of PhI or the low basicity of PPh_3 prevents this from occurring to a significant extent in this system.

Platinum complexes are often used to model catalytically active palladium species as they generally display a lower reactivity. Yamamoto has also studied palladium trans-bis-PMe_3 complexes[80-82] as the small basic phosphine is less easily dissociated from the metal and they are observed to stabilise a number of the proposed reaction intermediates. Although the complexes based on the more basic PMe_3 do not undergo dissociative trans to cis isomerisation their reactivity is very similar to the platinum models discussed above - This helps validate the significance of the information gained from the platinum based model reactions. The work of Yamashita in this area is summarised by the scheme shown in figure 1.27.7.

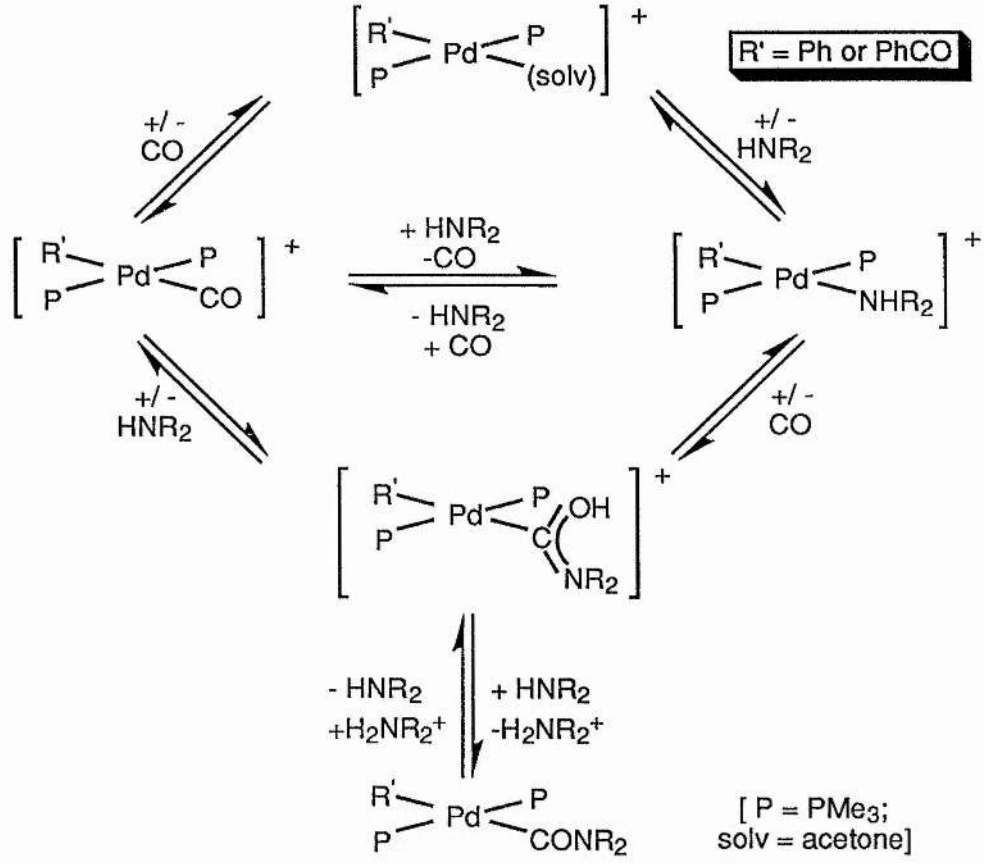

Figure 1.27.7

1.28 α-Keto-amides from other substrates

The double carbonylation of vinyl halides yielding keto-amides has been reported.[65,70] The reactivity of a range of substituted vinyl bromides and iodides has been studied by Yamamoto.[70]

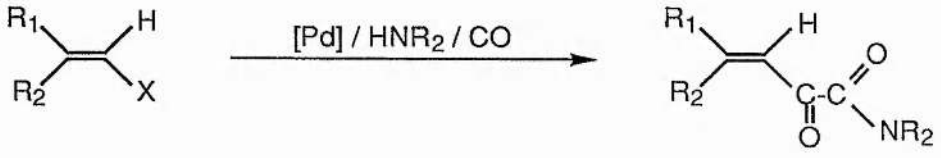

It is observed that only phenyl substituted vinyl halides give the double carbonylation product, when no phenyl substituent is present in the substrate the only product is the amide formed by single carbonylation. The configuration of the substrate (ie Z or E) is not found to be important The extended conjugation in phenyl substituted vinyl halides could be the important factor. Selectivity is seen to be higher for the iodides than for the bromides, the best catalyst precursor was found[70] to be [$PdCl_2$(dppb)].

The double carbonylation of styryl bromide using [$PdCl_2$(dppb)] at 50 °C under 57 atm CO with $HNEt_2$ as solvent / reagent gave 70% of the E-isomer of the keto-amide and 30% of a mixture of E and Z isomers of the amide.

The reaction is best run at 50 °C with the selectivity falling above and below this temperature. The double / single carbonylation selectivity is proportional to CO pressure. The mechanism of this reaction has been probed by the synthetic reactions shown in figure 1.28.1 below.[70]

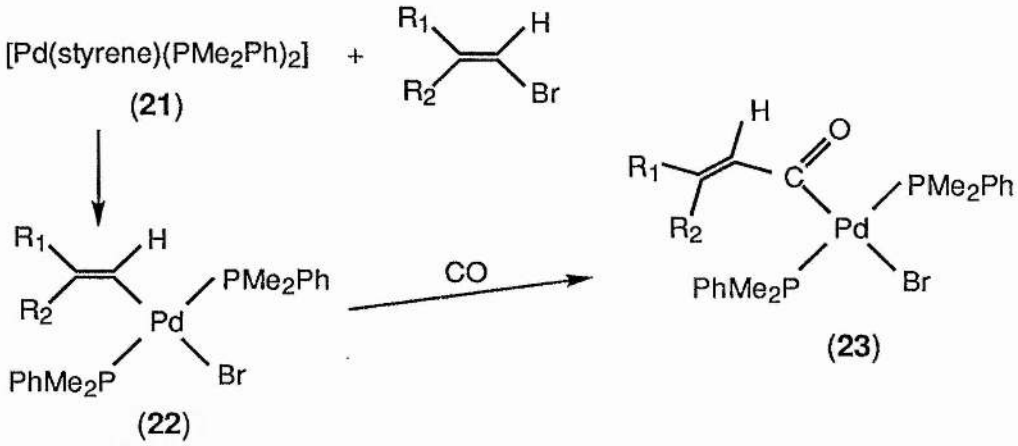

Figure 1.28.1

The reactions shown in figure 1.28.1 occur with retention of the trans-configuration when carried out at room temperature. Both complexes **22** and **23** react with a secondary amine and 50 atm CO at room temperature to yield a mixture of keto-amide and amide products. Investigation of the reactivity of a range of secondary amines with **22** showed that conversion was higher with smaller and thus most reactive amines (ie pyrrolidine). The selectivity to the formation of the keto-amide from **22** was highest with $HNEt_2$. The same trend in reactivity was seen with the reaction of the acyl species **23**. Here though the selectivity to the keto-amide followed a similar trend to the reactivity; $Pr_2NH < Et_2NH <$ pyrrolidine $\approx$ piperidine. It is interesting to note that both **22** (R_1 = Me; R_2 = H) and **23** (R_1 = Me; R_2 = H) react with R'_2NH and CO to give the appropriate keto-amide selectively. This reaction should model the use of 1-bromoprop-2-ene as a substrate which under catalytic conditions gives no keto-amide product. Another interesting yet unexplained observation is that the addition of 1-bromoprop-2-ene to the catalytic reaction of phenyl substituted substrate inhibits the double carbonylation reaction. In the synthetic reaction of **21** with 1-bromoprop-2-ene in the absence of excess phosphine the products are butadiene and [$Pd^{II}Br_2(PMePh_2)_2$], formed by an unexplained mechanism. This suggests that

perhaps 1-bromoprop-2-ene may inhibit the catalytic reactions by irreversibly oxidising the active palladium(0) species.

Using the information discussed above, together with that from a kinetic study, the mechanism shown in figure 1.28.2 was proposed.[70]

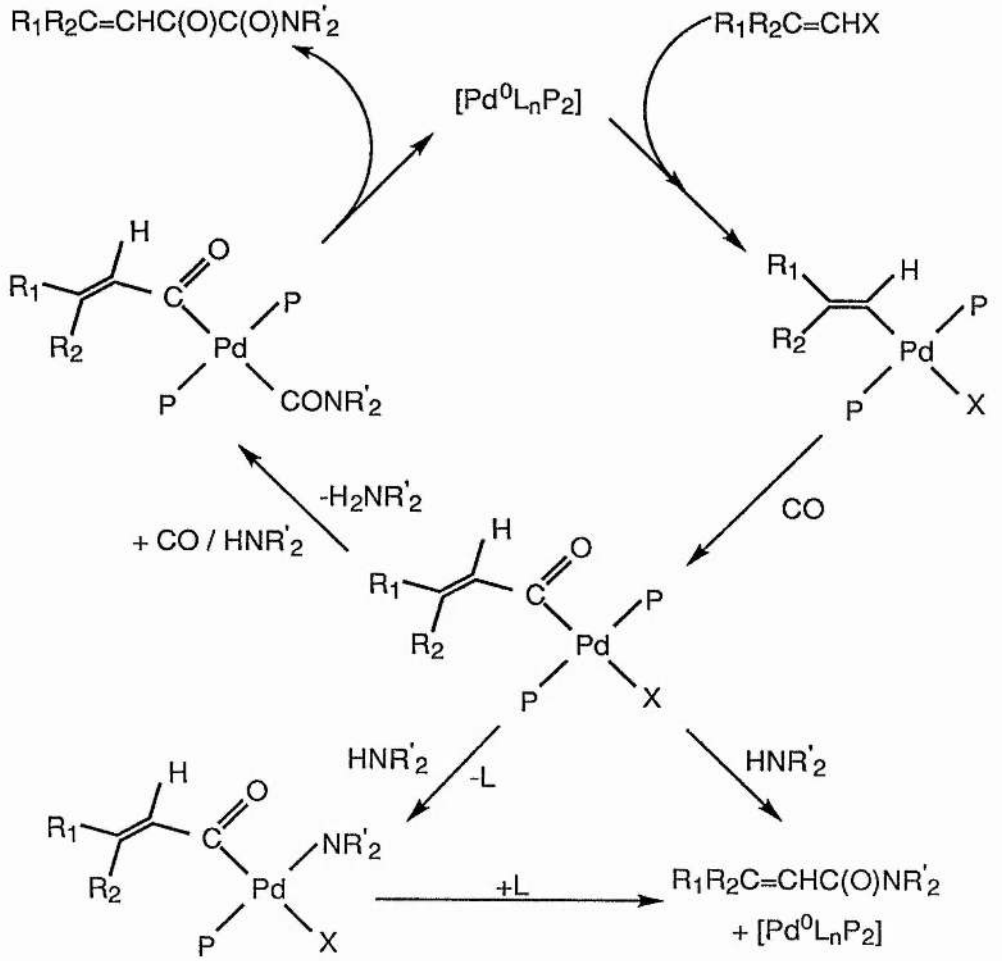

Figure 1.28.2: Proposed mechanism for the palladium / phosphine catalysed amino-double carbonylation of alkenyl halides.

A brief account[73] of the double carbonylation of 2-substituted allyl chlorides (ie crotyl chloride) has appeared. $[PdCl_2(PPh_3)_2]$ proves to be a good catalyst precursor for this reaction. The reaction required $HNEt_2$ as a base, with benzene as the solvent. When 1 atm CO is used, no carbonylation is observed, only the metathesis of the chloride to an amine. The CO pressure has to be increased to above 100 atm to achieve good double / single carbonylation selectivity, but under optimised reaction conditions (not reported) a yield of over 95% of the desired keto-amide was achieved.

Preliminary evidence suggests that the mechanism for the double carbonylation of 2-methyl allyl chloride is analogous to that proposed for aryl halides - see figure 1.27.1.

One isolated example of the double carbonylation of alkyl iodides has been reported.[71] Perfluoroalkyl iodides are used as the substrates with the catalyst precursor $[PdCl_2(PR_3)_2]$. Bulky phosphines such as PPh_3 or PCy_3 are found to be best for this reaction as are aliphatic hydrocarbon solvents. When a 5:1 excess of $HNEt_2$ / substrate is used at 100 °C with 50 atm CO the yield of keto-amides from a range of perfluoroalkyl iodides varies between 33-66% with a double / single carbonylation selectivity of up to 83%.

Part D Preparation of other α,β -Dicarbonyls

1.29 Introduction

The syntheses of α,β-dicarbonyls other than α-keto-acid derivatives can be split into two classes: i) The synthesis of an α-keto-acid derivative followed by an second inter or intra-molecular reaction carried out in situ; lactones, α-keto-lactones and α-keto-lactams have been made by this methodology. ii) The synthesis of α-diketones.

1.30 Preparation of lactones, α-keto lactones and α-keto lactams

Two accounts of the direct synthesis of α-keto lactones and α-keto lactams from the double carbonylation of aryl halides have emerged. The first is a palladium bis-phosphine catalysed double carbonylation of aryl iodides with ortho alcohol or amine groups.[86] In this system an intra-molecular ring closure gives the product. A wide range of bi-functional substrates was examined and it was observed that the size of the lactone / lactam ring formed directed the double / single carbonylation product ratio. The smallest α-keto-lactam ring synthesised via double carbonylation formed a 5 membered ring, given the nature of the reagents no smaller ring would be possible. Both a six membered α-keto-lactam and an eight membered α-keto-lactone could made by this method. No attempt was made to synthesis seven membered rings. Larger α-keto-rings would have to be formed via palladocycles of an unprecedented ring size. Thus only the three substrates shown in figure 1.30.1 gave the desired double carbonylation products.

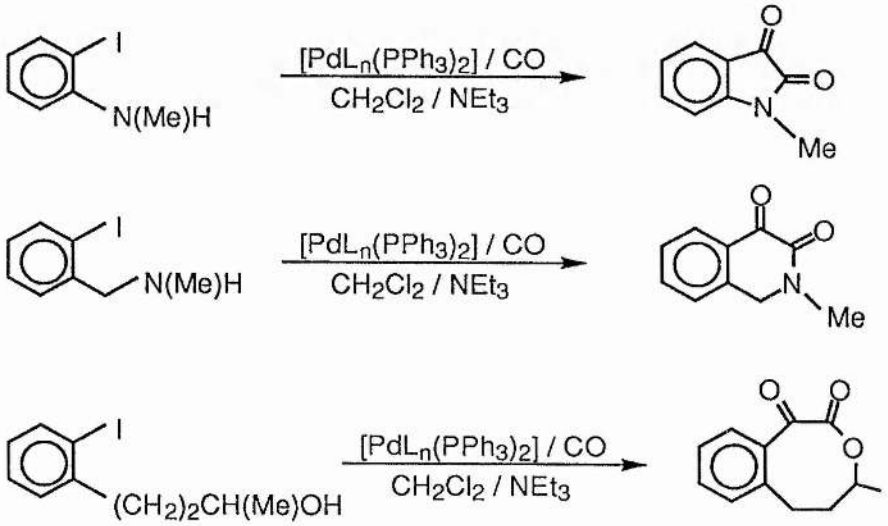

Figure 1.30.1

The mechanistic proposal for this reaction, as it would apply to 2-iodo-N-methyl aniline, is shown in figure 1.30.2.

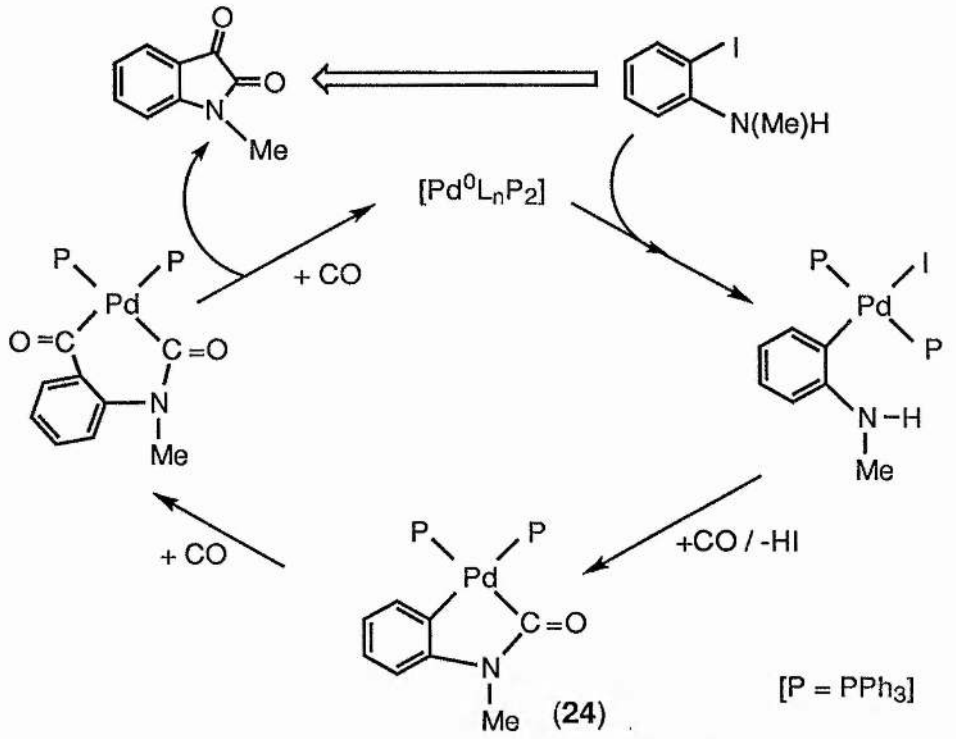

Figure 1.30.2: Proposed mechanism of the palladium / phosphine catalysed amino-double carbonylation of 2-iodo-N-methylaniline.

It is clear from the mechanism shown in figure 1.30.2 that it is the size of intermediate palladocycles, acyl or a di-carbonyl, that will govern the nature of the product. Thus double carbonylation / intramolecular cyclisation is only observed with a limited range of substrates. A competition between intramolecular cyclisation and intermolecular ester / amine formation was observed due to the substrate being the only nucleophile present in the reaction mixture. The mechanistic proposal in figure 1.30.2 is unusual in that it suggests that the attack of the amine upon the carbon monoxide occurs before carbonyl insertion into the Pd-C bond formed by the substrate. This sequence is proposed on the basis of the reported isolation of complex **24**.[87]

The other account of the preparation of α-keto lactones is the $[Ni(CO)_3CN]^-$ catalysed double carbonylation of halo dienes which has been reported by both Alper[88] and Amer.[89,90] An example of this conversion is shown in figure 1.30.3.

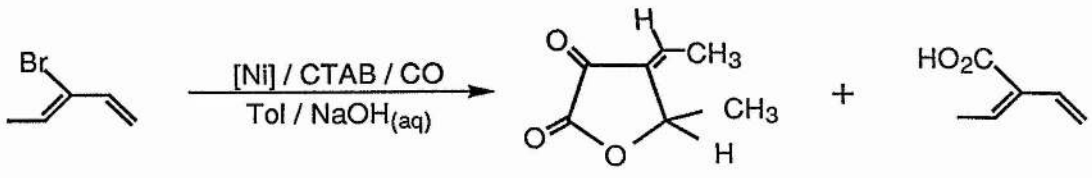

Figure 1.30.3

One unusual feature of this catalytic system is that the double / single carbonylation selectivity increases with increasing reaction temperature. Although less reactive than their bromo-analogues, chloro-dienes can also be doubly carbonylated. The carbonylation of a wide range of monoenes and dienes showed that particular structural features enabled double carbonylation whilst others inhibited the formation of the α-keto lactone with the unsaturated acid as the only observed product. Monoenes, dienes which have a fixed s-cis configuration or halo-dienes without the 2-bromo-1,3-diene unit gave only the single carbonylation product. Unlike the palladium catalysed amino-double carbonylation of alkenyl halides[70] no electronic substituent effect at the 1-position was observed, but bulky groups at the 4-position were observed to disfavour double carbonylation. Both Alper[88] and Amer[90] proposed broadly similar mechanisms for this reaction. In the light of the observations of the effect of the structure of the substrate on the reaction, Amer proposes that only by involving the co-ordination of the C(3)=C(4) can these results and the effect of temperature on the reaction be satisfactorily explained. Amer's preferred mechanism is shown in figure 1.30.4 overleaf.

The one example of a catalytic double carbonylation reaction leading to a simple lactone involves the double carbonylation of phenylethyl bromide followed by an aldol (self) condensation reaction[91] (see figure 1.30.5 overleaf). The catalyst precursor used for this reaction was the bi-metallic [$Sn(Co(CO)_4)_4$] species. The reaction was carried out in aqueous alcoholic media. This is another example of a catalytic system which is dependant on this use of $Ca(OH)_2$ as a base. As suggested previously by Mortreux[19] for similar α-keto-acid yielding reactions, it is proposed that the calcium ion plays an intimate role in the reaction. (See also Part A, section 1.5). It is shown that the $[Co(CO)_4]^-$ moiety catalysed the double carbonylation reaction and that it is a tin species formed in-situ (a Lewis acid) which catalyses the aldol condensation.

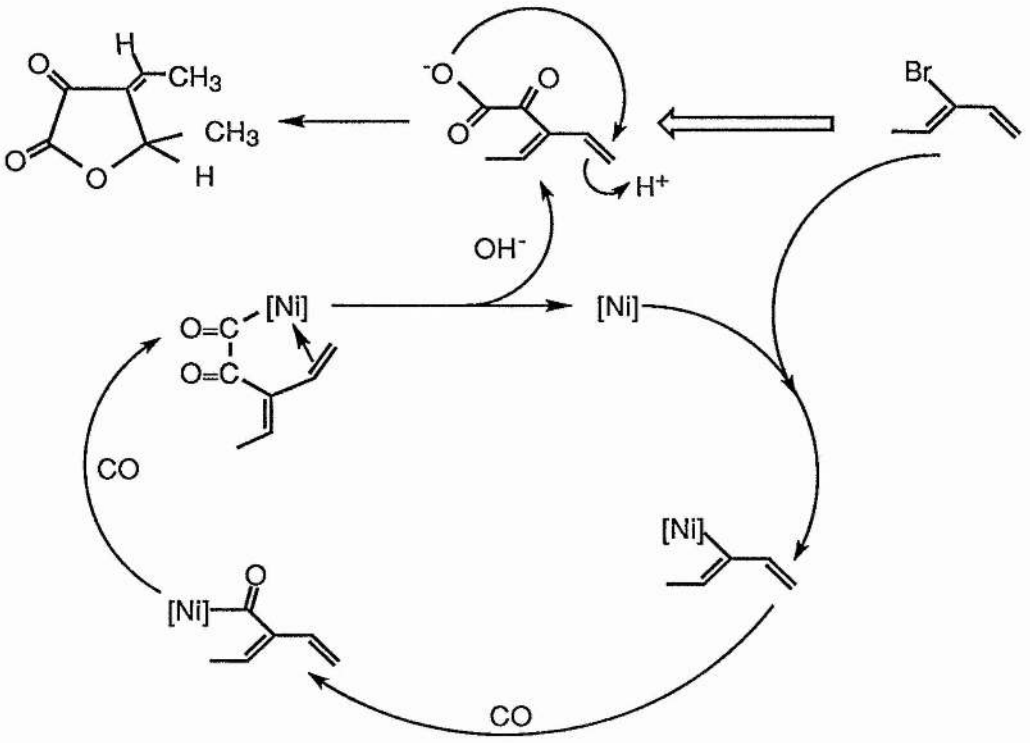

Figure 1.30.4: Proposed mechanism of the nickel catalysed synthesis of α-keto lactones from halo-dienes.

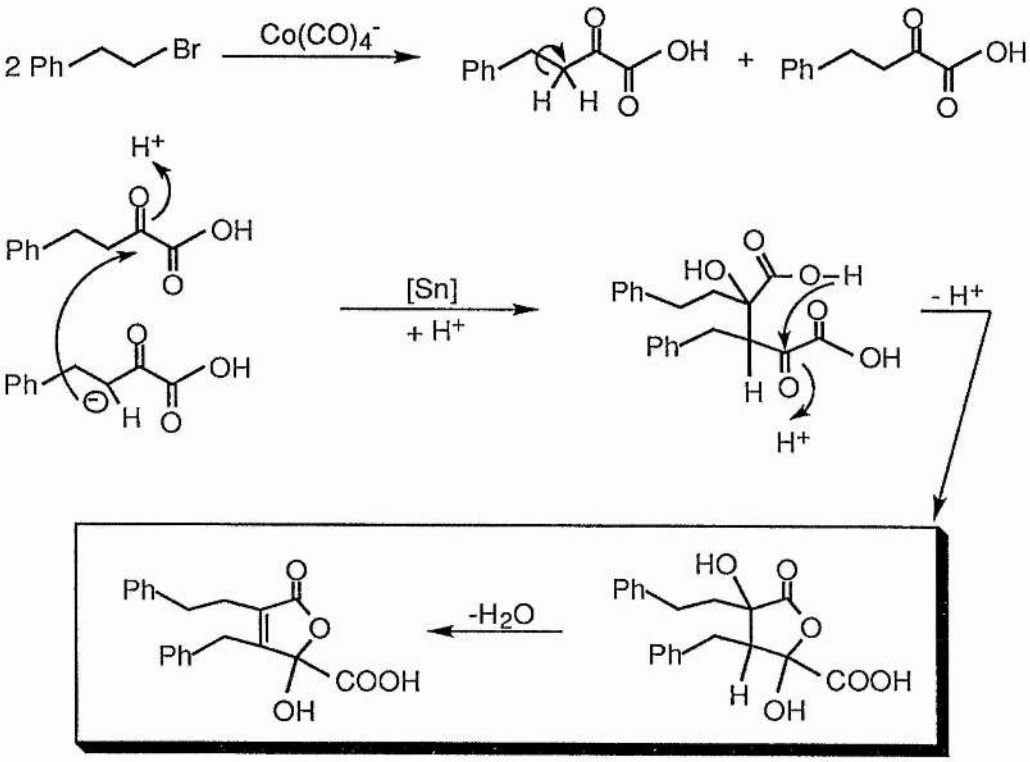

Figure 1.30.5: Route to substituted lactone by the combined cobalt catalysed double carbonylation linked to tin catalysed aldol condensation and cyclisation.

1.31 Preparation of diketones

Only two accounts of the catalytic synthesis of diketones, by the double carbonylation of organohalides, have appeared. The first example uses the iodonium salt $[Ph_2I][Cl]$ as the substrate[92] but the double / single carbonylation selectivity is extremely low (≈4:10). The second example yields diaryl α-diketones from either phenyl or substituted phenyl iodides.[93] Although the yield of this reaction is only between 50-61% (depending on the substrate) the selectivity is excellent (<99%) with the desired diketone sometimes being the sole product. A range of palladium complexes are observed to catalyse this reaction, but the best catalyst precursor was found to be $[PdCl_2(PPh_3)_2]$. A range of substituted aryl iodides proved successful substrates. The substituents on the substrate were observed to have virtually no effect upon the yield or selectivity of the reaction. The one exception to this was 4-iodophenol which only gave a 40% yield of the α-diketone. The reaction was observed to give higher yields of α-diketones in more polar solvents. A plausible mechanism has been suggested, this is shown in figure 1.31.1.

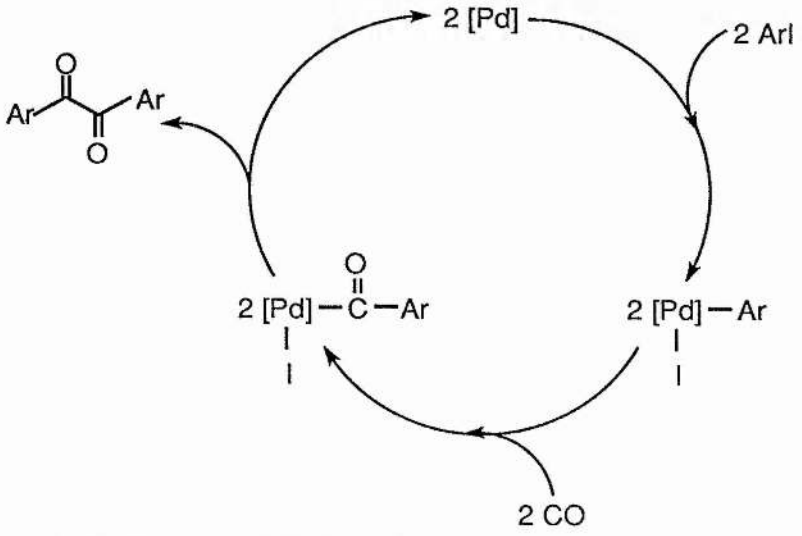

Figure 1.31.1: Plausible mechanism for the palladium catalysed synthesis of α-di-ketones from aryl iodides.

Synthetic studies by Eisenberg,[94,95] Chen,[96] Yamamoto and co-workers[44,97] may be relevant to the mechanism of this palladium bis-phosphine catalysed α-diketone synthesis. Yamamoto[44,97] has observed that the reaction of cis-$[PdMe_2(PR_3)_2]$ with CO yields MeCOCOMe. Chen[96] has studied the related complexes cis-$[Pt(COR)(COR')(PPh_3)_2]$ which thermally decompose to give RCOCOR' and RCOR'. Under an inert atmosphere the mono ketone is the major products, but the diketone predominates under a CO atmosphere. Eisenberg[94,95] has studied the di-

rhodium complexes (**25,26**) shown in figure 1.31.2. Both these complexes yield diketones upon reaction with CO and it has been shown that this reaction occurs via a radical pathway.

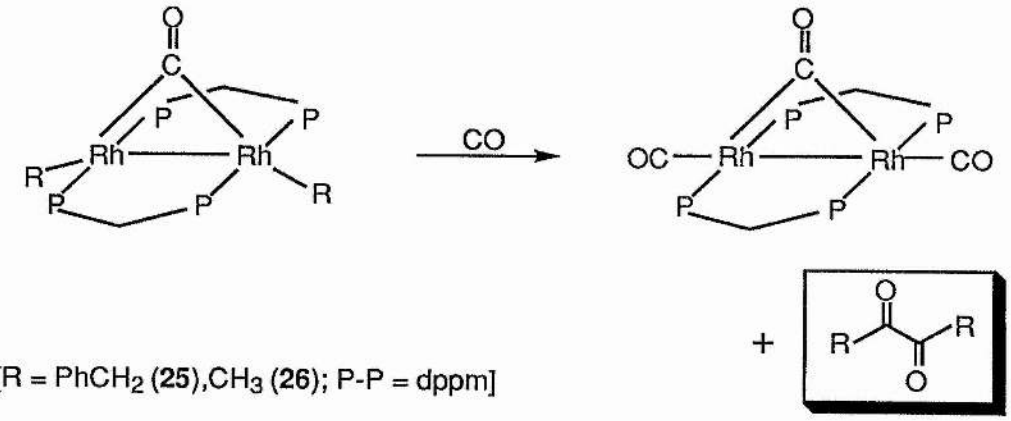

[R = $PhCH_2$ (**25**),CH_3 (**26**); P-P = dppm]

Figure 1.31.2: Stoichiometric formation of diketones from bis-rhodium alkyl complexes.

SECTION 2

Preparation of derivatives of Malonic Acid

2.0 Introduction

Derivatives of malonic acid can be prepared by the double carbonylation of geminal di-halides e.g. CH_2I_2.

$$CH_2X_2 + 2CO + 2ROH \longrightarrow CH_2(COOR)_2 + 2HX$$

Often the nature of the solvent is chosen to determine whether the product is an ester or an amide. When the solvent is an alcohol or amine it not only acts as solvent / reagent but also as a sink for the hydrogen halide produced.

Catalytic systems based on cobalt, rhodium and palladium have been reported, but the majority of the mechanistic elucidation has centred on $[Co_2(CO)_8]$ and $[RhX(CO)(PEt_3)_2]$ systems. CH_2Br_2 is the most commonly reported substrate but malonyl derivatives have been synthesised from CH_2Cl_2, CH_2I_2 and $RR'CBr_2$ (R, R' = H, CH_3). In all but the rhodium catalysed system, which is the subject of this thesis, the addition of a base has been required to act as a sink for the hydrogen halide produced.

2.1 Cobalt carbonyl based catalytic systems

The majority of the work in this area has been carried out by Miyashita et al[98-100] who in 1989 were the first to report the cobalt catalysed double carbonylation of a geminal di-halide.[100] This work has centred on the carbonylation of $R^1R^2CBr_2$ (R^1, R^2 = H, CH_3) using $[Co_2(CO)_8]$ in the presence of either Zn or NEt_3. Earlier work from this group had shown the potential of a range of metal complexes to catalyse the single alkoxy- / aminocarbonylation of $R^1R^2CBr_2$ forming acetyl derivatives. $[Co_2(CO)_8]$ was shown to be the most effective potential catalyst for this reaction.

$$R^1R^2CX_2 + CO + HY + Zn \xrightarrow{[M]} R^1R^2CHCOY + ZnX_2$$

[M] = $[MX_2(PPh_3)_2]$ (M = Ni, Pd, Pt; X = Cl, Br) or $[Co_2(CO)_8]$

(R^1, R^2 = H, CH_3; Y = OCH_3, NEt_2)

Figure 2.1.1

Miyashita had previously shown that η^2-ketene complexes could be isolated from the reaction of a range of transition metal complexes of the type MX_2L_2 with CH_2Br_2 under CO in the presence of Zn[101, 102]. These species were shown to be intermediates in the single-carbonylation and when the cobalt complex $[Co_2(CH_2{=}C{=}O)(CO)_7]$ (**27**) was carbonylated at 50 atm CO in methanol, DMM (7%) was observed[100] in addition to the main product, methyl acetate (77%).

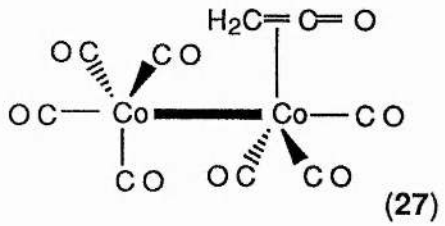

(27)

To provide further information on the nature of the cobalt ketene complex (**27**) its reaction with a range of nucleophiles and hydrogen was investigated.

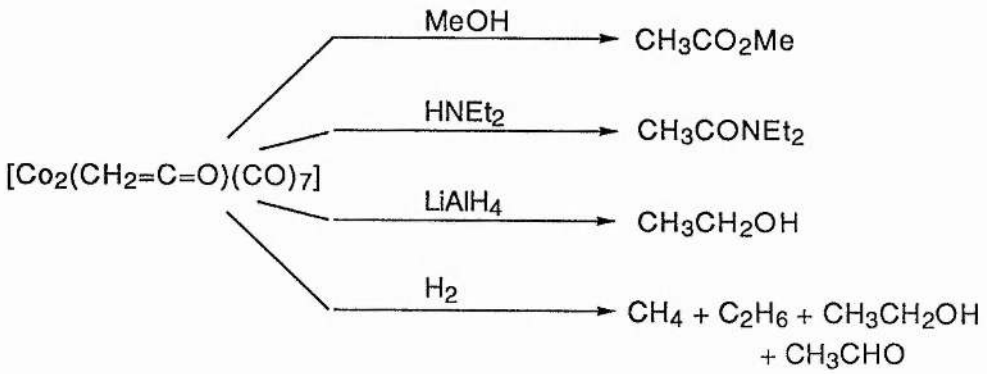

Figure 2.1.2

It was concluded that the high reactivity of (**27**), along with its spectral data, pointed to the ketene being bound to only one cobalt atom as bridging ketene complexes are known to be less reactive particularly towards hydrogen.

An extension of the above work was the $[Co_2(CO)_8]$ amino single / double carbonylation[99] shown in figure 2.1.3;

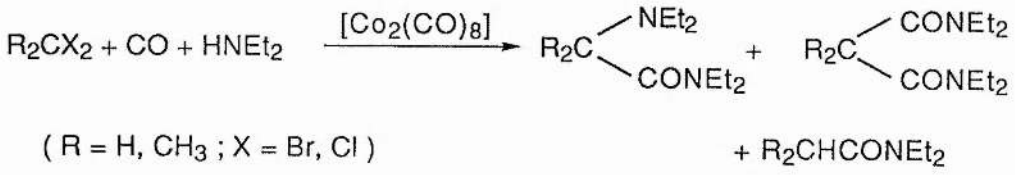

Figure 2.1.3

In this reaction the yield of and selectivity towards the malonamide derivative is reported to be higher with THF or benzene as the solvent than with hexane or 1,1-dichloroethane and using potassium carbonate as the base rather than NEt_3. The reactivity of $HNEt_2$ causes the aminocarbonylation reaction to be less clean than the methoxycarbonylation[100] - $HCONEt_2$, $(CONEt_2)_2$ and $CO(NEt_2)_2$ were observed as side products. The optimum yield reported is for the double carbonylation of CH_3CHBr_2 in THF / K_2CO_3 which at 50 atm CO and 100 °C / 48hrs gives a 28% yield of and 71% selectivity to the malonamide. It is worth noting that although the yield is low (2%) CH_2Cl_2 can also be carbonylated to the corresponding malonamide under similar reaction conditions. A range of Ir, Ru, Cr, Mo and W carbonyls were shown to have no activity towards the double carbonylation of CH_3CHBr_2 under identical conditions.[99]

In the light of the mechanistic studies carried out on the $[Co_2(CO)_8]$ / $[Co(CO)_4]^-$ double carbonylation reactions yielding pyruvates (see part 1, section C) the cobalt carbamoyl complex $[Co(CONEt_2)(CO)_4]$ was synthesised and was shown[99] to promote the amino single / double carbonylation of 1,1-dibromoethane but no mechanistic cycle was proposed.

Pályi[103] has carried out some interesting work on chloromethyl and chloroacyl complexes of cobalt which is summarised in figure 2.1.4 below.

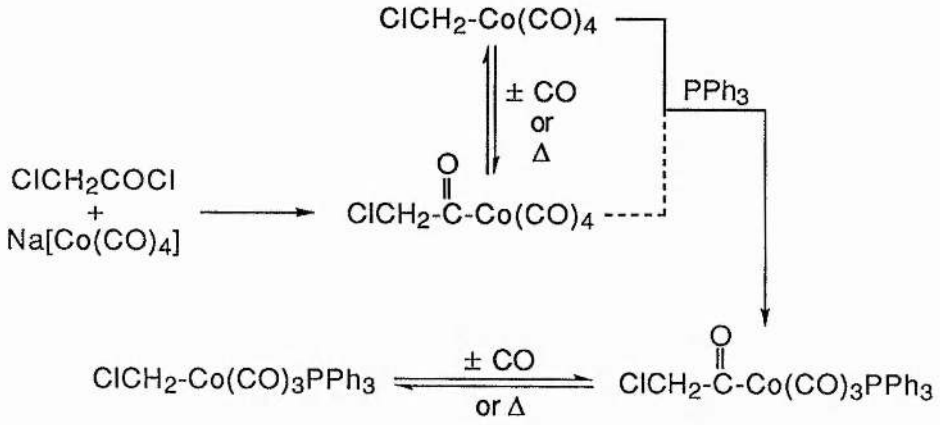

Figure 2.1.4

The position of the carbonylation / decarbonylation equilibria could either be altered either by changing the temperature of the reaction solution or by applying a pressure of CO. The application of CO pressure (5 atm) to the $[RCo(CO)_4]$ system favoured the chloroacyl species, lowering the temperature to -10 °C was observed to have the same effect on the equilibrium position. The decarbonylation of the phosphine substituted

complex required a higher temperature and this was attributed to the acyl ligand being a better π-acceptor than the alkyl group conferring an increased thermal stability on the chloroacyl complex. Pertinent to the mechanism of alkoxy-double carbonylation of geminal dihalides is the reaction of $[ClCH_2Co(CO)_4]$ with the methoxide ion at low temperature (-40 °C).

$$ClCH_2\text{-}Co(CO)_4 \xrightarrow[-40\ ^\circ C]{MeO^-} [ClCH_2\text{-}Co(CO_2Me)(CO)_3]^- \xrightarrow{\Delta} CoL_n + CH_2(CO_2Me)_2$$

The yield of the DMM is reported as 10-55% (wrt Co) and this may be because the only source of CO is the cobalt carbonyl. Thus the malonate is presumably formed from the methylene and methoxyacetyl moieties from one cobalt centre and the CO unit from another. This suggests a di-metallic mechanism.

Two other reports of the cobalt carbonyl catalysed double carbonylation of geminal dihalides have appeared.[104,105] One is a patent[104] which claims the formation of malonate esters from diiodo- or dibromomethane, however even the most promising example it cites has a very low substrate / catalyst ratio. The other report[105] describes the catalytic activity of a range of metals (including cobalt) supported on activated carbon towards the single / double methoxycarbonylation of dibromo- and dichloromethane. The activity of $[Co_2(CO)_8]$ / CH_2Br_2 was compared to the heterogeneous cobalt system under identical conditions (140 °C, 31 atm CO, 1 hr) and approximately double the yield of DMM is observed along with a higher selectivity towards the malonate ester vs. single carbonylation and methanolysis products. When CH_2Cl_2 was used as the substrate a higher double / single carbonylation ratio was observed which was attributed to the rapid carbonylation reported for chloromethyl acetate.[106]

2.2 Cobalt phosphine complex based catalytic systems

Phosphine substituted cobalt carbonyl systems have been reported to catalyse the double carbonylation of geminal dihalides.[107,108] The highest yielding catalytic synthesis of malonate esters yet reported was recently published by Mortreux et al.[107] They describe the use of the electrogenerated species $[Co(CO)_3PBu_3]^-$ (**28**), in a methanol-methyl formate solvent system with NaOMe as a base, as being capable of carbonylating dichloromethane in up to a 75% yield. The conditions of 80 °C / 15 atm CO / 15 hr are not harsh but a large excess of base (54:1) appears to be required. The products of a $[Co(CO)_3PBu_3]^-$ catalysed reaction of CH_2Cl_2 with CO and NaOMe are:

DMM; methyl methoxyacetate; and dimethoxy methane with traces of methyl acetate. The 80:20 methanol-methyl formate solvent system (equilibrium ratio under 15 atm CO at 80 °C) was chosen so that the methoxide catalysed MeOH to methyl formate reaction did not starve the desired carbonylation reaction of carbon monoxide. The active catalytic species from $[Co_2(CO)_8]$ or $[Co_2(CO)_6L_2]$ are believed to be $[Co(CO)_4]^-$ or $[Co(CO)_3L]^-$ respectively[107] which is why the work of Mortreux uses electrochemistry within the autoclave to generate the highly air and moisture sensitive mononuclear anion from $[Co_2(CO)_6(PBu_3)_2]$ in situ. A DMM yield enhancement is observed when a greater number of electrons are delivered to the system than would be required for the formation of (**28**) and this could be explained by the electroregeneration of the catalyst or electroreduction of inactive cobalt complexes formed from decomposition pathways reintroducing them into the catalytic cycle. When dichloromethane is replaced by methyl chloroacetate as the substrate, it is quickly consumed to give methyl methoxy acetate and DMM. This evidence together with literature precedents[17,103] leads Mortreux to suggest the two potential catalytic mechanisms shown in figure 2.2.1 below.

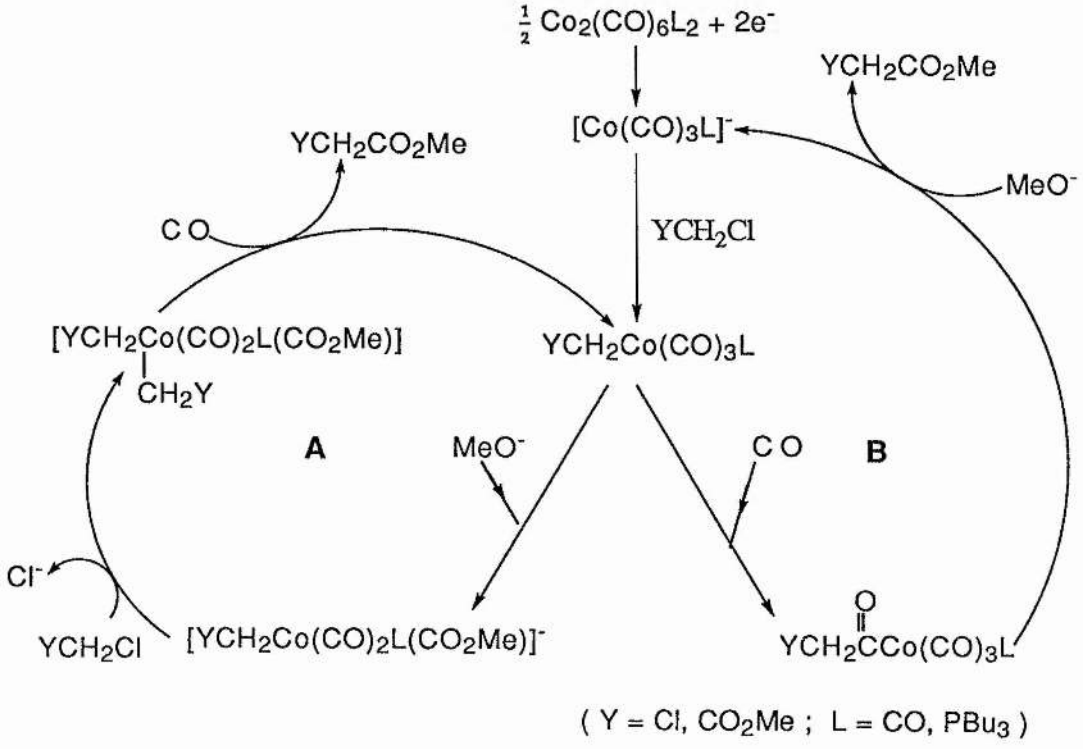

Figure 2.2.1: The proposed mechanism for the electroassisted $[Co(CO)_3L]^-$ catalysed double carbonylation of dichloromethane.

Given the work of Miyashita[100], ourselves and others[109-113] the observation of methyl acetate as a minor product probably points to a somewhat different mechanism in operation. The most likely source of the methyl acetate is from the reaction of ketene (from the decomposition of a metallo-ketene intermediate) with the methanol present in the catalytic system.[114]

Cutler and Tso[115] have investigated CO insertion reactions in Co-C bonds using $[PMePh_2(CO)_3Co\text{-}R]$ (R = Me, CH_2OMe or $CH_2C(O)OEt$). It was observed that the methyl and methoxy methyl compounds rapidly insert CO at ambient pressure to yield stable acyl derivatives. A simple CO insertion into the $Co\text{-}CH_2C(O)OEt$ bond was not observed up to 4.7 atm. Given that all the reported catalytic dihalomethane double carbonylation reactions reported require a CO pressure of at least 20 atm this is perhaps not such a surprising result. The product of a CO insertion into the $Co\text{-}CH_2C(O)OEt$ bond would be a malonyl complex. Cutler and Tso also report two direct syntheses of $[PMePh_2(CO)_3Co\text{-}C(O)CH_2CO_2Et]$ by either the reaction of $[PMePh_2(CO)_3Co]Na$ with ethyl malonyl chloride or by the reaction of $[(CO)_4Co\text{-}C(O)CH_2CO_2Et]$ with $PMePh_2$. The malonyl complex is observed to be unstable with respect to a decarbonylation yielding $[PMePh_2(CO)_3Co\text{-}CH_2C(O)OEt]$.

2.3 Rhodium and Palladium based catalytic systems

Two non-cobalt based catalytic systems have been reported in the literature. The most recent[116] is the $[RhX(CO)(PEt_3)_2]$ based system which will be discussed in detail in the following chapters. The other[112,117] uses a palladium (II) bis-phosphine catalyst $[PdX_2(PPh_3)_2]$ (X = halide, acetate, $\text{-}C(O)OCH_3$).

Using $[PdX_2(PPh_3)_2]$, CO (50 atm) and a strong aromatic or tertiary amine base at 100 °C DMM is produced from CH_2Cl_2 in 11% yield after 8 hours, and 2-phenyl-DMM can be synthesised from $PhCHCl_2$ in 55% yield. The use of product yields when trying to compare catalytic systems can be misleading, perhaps a more helpful statistic to consider is the TON of the catalyst. With the carbonylation of CH_2Cl_2 catalysed by $[PdCl_2(PPh_3)_2]$ a catalyst TON of 11 is achieved and with the carbonylation of $PhCHCl_2$ by $[Pd(OCOCH_3)(COOCH_3)(PPh_3)_2]$ the TON is 19. The work of Rudler[112] on a similar Pd(II) system is discussed in section 2.4.

2.4 Mechanistic models based on metals other than cobalt

A number of μ-alkylidene complexes have been shown to react stoichiometrically with CO to yield malonates, acetates or ketenes.[109,112,113] Rudler[112] has studied the two μ-methylene complexes, **29** and **30**.

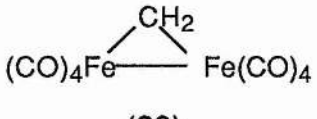

(29)

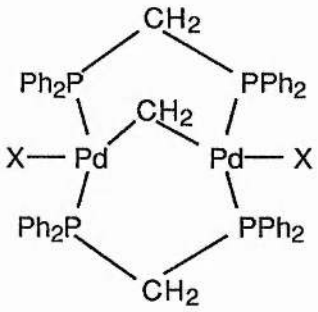

(30)

(**29**) was reacted with dodecan-1-ol under CO (40 atm) in hexane and gave dodecyl acetate (46%) and di-dodecyl malonate (5%). When the CO pressure was altered at a constant reaction temperature the yield of the carbonylated products increased but the selectivity was unaffected. If a tertiary phosphine or tertiary amine was added instead of altering the CO pressure the same products of carbonylation were observed. Presumably these π-donor ligands stabilise the metal by binding to the site on the metal vacated by the CO. When NEt_3 was used in addition to CO (40 atm) an enhancement in both yield and selectivity was observed. Interestingly when the primary alcohol was exchanged for a secondary alcohol the selectivity was reversed in favour of the malonate but the overall yield was lower. Two products of the reaction of (**29**) with CO were isolated and one was characterised by X-ray crystallography. The X-ray structure revealed a mono-nuclear complex of $Fe(CO)_4$ with a trimer of ketene (**31**). The reaction of (**29**) with CO and norbornene is reported to give a lactone moiety (**32**) consistent with the trapping of an acyl intermediate.

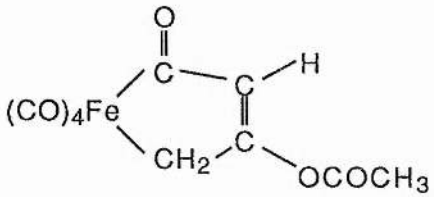

(31)

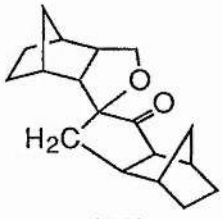

(32)

Complex (**30**) gives the same carbonylation products as (**29**), it reacts far more slowly but shows a better selectivity towards the malonate ester.- {CO (40 atm), 70 °C, 20 hr - malonate (25%), acetate (9%)} Unlike the iron species the palladium

complex (**30**) does not show any dependence upon CO pressure above 10 atm. As PdI_2(dppm) was isolated at the end of all the reactions with (**30**) the reactivity of a range of mononuclear palladium(II) phosphine complexes towards the carbonylation of CH_2I_2 (or CH_2Cl_2) was investigated. These species showed a very low TON - lower than $[PdX_2(PPh_3)_2]$[117] (see section 2.3).

Keim[113] has carried out an informative deuterium labelling study with the iron complex **29** (figure 2.4.1). The D label is exclusively found on the acetate methyl group and thus the position of the deuterium label can only be explained by attack of D^+ on ketene.

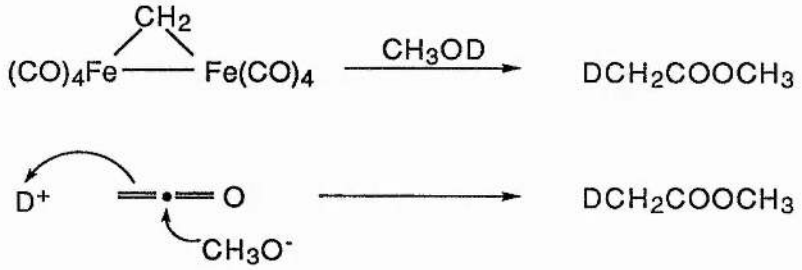

Figure 2.4.1

The reaction of (**29**) with $ClCH_2COCl$ gives a species (not isolated) that reacts with MeOH to give methyl acetate. This presumably occurs by the formation of a transient iron chloroacyl species which undergoes β-chloride abstraction[110,111,118] to give a ketene complex, which itself reacts with methanol to give methyl acetate. Transition metal mediated reactions of acid chlorides to give ketenes have also been reported for platinum,[111] ruthenium[110] and rhodium.[118]

The reaction of an iridium bis-phosphine complex $[IrCl(N_2)(PPh_3)_2]$ with various acyl chlorides to yield coordinatively unsaturated acyl Ir(III) compounds[119] may help in understanding the mechanistic pathway for the catalytic double carbonylation of dihaloalkanes - see figure 2.4.2 overleaf. Upon oxidative addition of the acyl chloride the N_2 was lost from the metal and 5 co-ordinate Ir(III) acyl species were isolated. When heated in solution these 5 co-ordinate species decarbonylated and gave stable 6 co-ordinate $[IrCl_2(Alkyl)CO(PPh_3)_2]$ species. Of particular interest was the reaction with ethyl malonyl chloride (shown below) and the subsequent reactions of the complex formed.

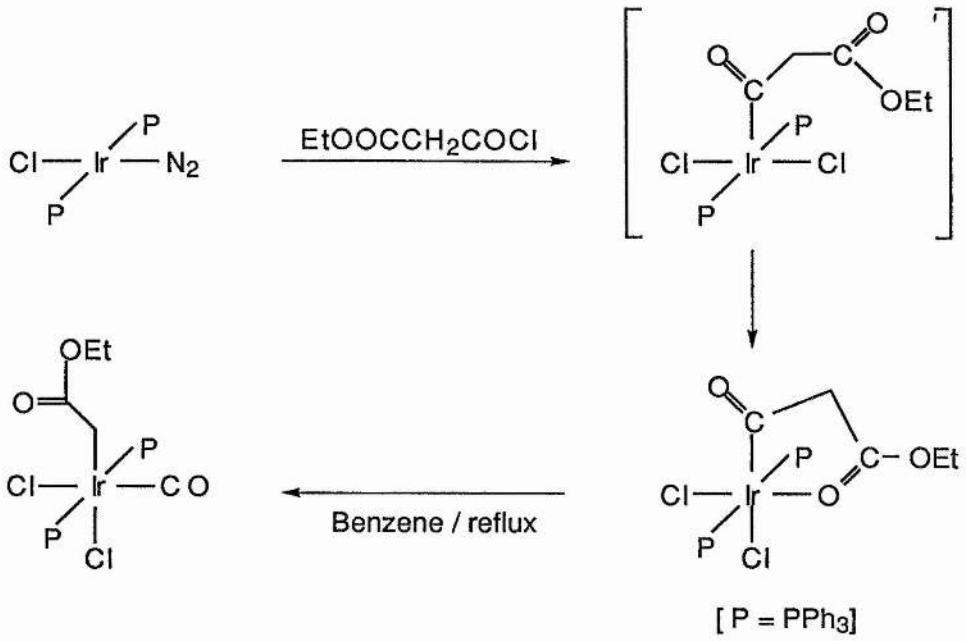

Figure 2.4.2

The initial oxidative addition gave a 5 co-ordinate 16 e Ir(III) complex. This rearranged in solution so that the lone pairs on the carbonyl oxygen co-ordinated to the metal centre giving a 6 co-ordinate Ir(III) η^2-malonyl complex. This species was stable enough to be isolated and characterised, but when it is refluxed in benzene it decarbonylates yielding a 6 co-ordinate, 18 e Ir(III) carboethoxymethyl complex, with the CO from the malonyl moiety remaining on the metal to fill the hitherto vacant co-ordination site.

In summary it may be said that most of the studies of the mechanism of the transition metal catalysed double carbonylation of geminal di-halides implicate ketene as an important intermediate.

SECTION 3 Double Carbonylation at Two Separated Sites within One Molecule

3.0 Introduction

The products of the reactions covered in this section come from the inclusion of two CO moieties at two distinct sites in one molecule. Although the mechanisms of such reactions have not been investigated they are likely to bear more similarity to that of standard single carbonylation reactions than those reactions reported in sections 1 and 2. The substrates fall into two basic classes, the first are non-geminal dihalocarbons such as para-dichlorobenzene which can undergo two concomitant single carbonylations. Di-acids and their derivatives are the cornerstone of the condensation polymer industry and the applications of double carbonylation reactions to polymer synthesis will be covered in a separate section to the preparation of discrete di-acid, ester or amide, molecules.

The second class of substrates are monohalo alkenes in which both of the functionalities undergo carbonylation. These reactions yield cyclic γ-keto esters which result from an intra-molecular cyclisation - this cyclisation is similar to that described in section 1.30.

3.1 Cobalt catalysed double carbonylation of non-geminal dihalides

Foà[120] has reported the use of cobalt alkyl carbonyl catalysts for the double carbonylation of para-dihalo benzenes and dihalogenated thiophene derivatives. The best results are observed when the catalytic species - $[ECH_2Co(CO)_4]$ where E = electron withdrawing group - is made in situ from dicobaltoctacarbonyl and ECH_2I. Bromo compounds give higher conversions than their chloro derivatives under the same conditions, but this may just reflect their relative rate of reaction. As an illustration, the double carbonylation of para-dibromobenzene in CH_3OH / CH_3ONa under 1 atm CO at 25 °C gives a 98% yield of the di-ester. A patent[37] reports that $[Co(CO)_4]^-$ catalyses the carbonylation of 1,7-dibromoheptane to give 1,9-bis-2,8-dioxo-nonandioic acid by what could formally be called a double-double or a quadruple carbonylation! The synthesis of other α-keto-acid derivatives from halo-alkanes is covered in depth in section 1.7.

Photolytically driven cobalt carbonyl catalysed double and triple carbonylation of polyhalogenated benzenes and polyhalogenated benzoic acids has been investigated by Kashimura and co-workers.[25,121] Such catalytic systems are observed to yield both polyacid benzene moieties and / or α-keto-acid moieties. Only the synthesis of aromatic poly acids such as 1,2,4,5-tetrabenzoic acid (pyromellitic acid), 1,2,4-tribenzoic acid (trimellitic acid) 1,3,5-tribenzoic acid (trimesic acid) will be discussed in detail as the work of Kashimura on the synthesis of related α-keto-acid species was covered in section 1.3.

The synthesis of aromatic poly acids was achieved in an irradiated $NaOH_{(aq)}$ solution at 65 °C under CO (2 atm) using $[Co_2(CO)_8]$ as the catalyst precursor. These reactions clearly occur by a radical pathway as some of the products observed have often lost one or more halogen functionality via hydrogen abstraction. A sample of these reactions is illustrated in figures 3.1.1-3.1.2 with the double carbonylation products (and yields) highlighted.

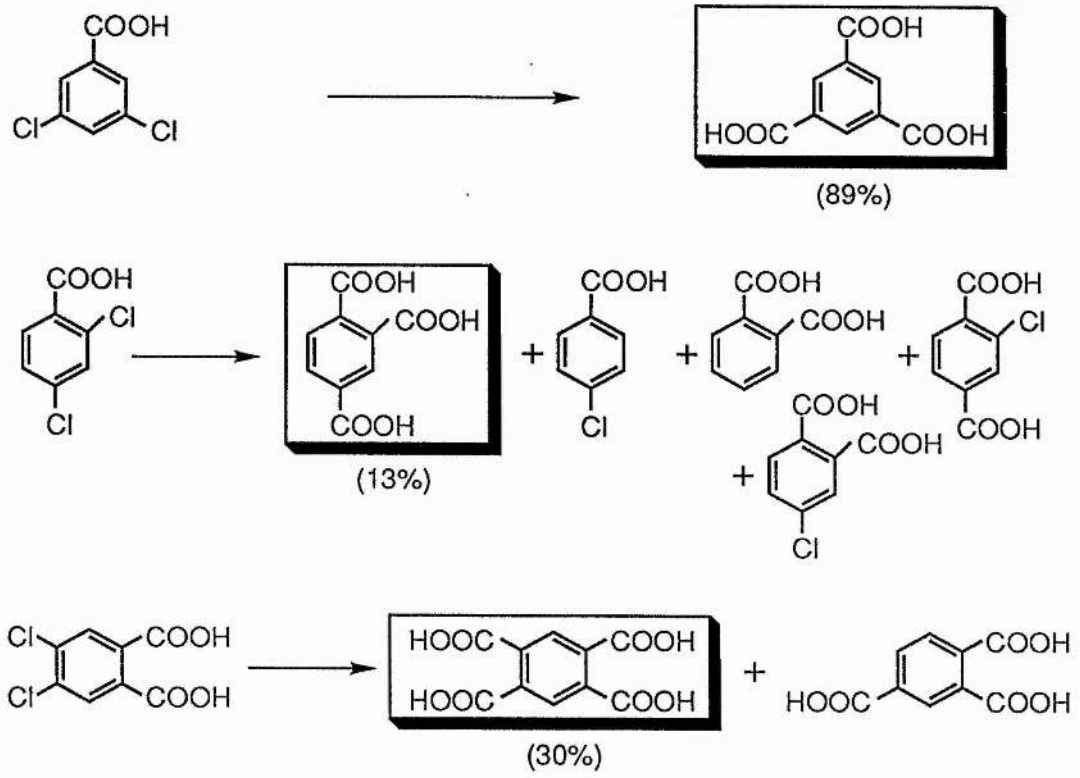

Figure 3.1.1

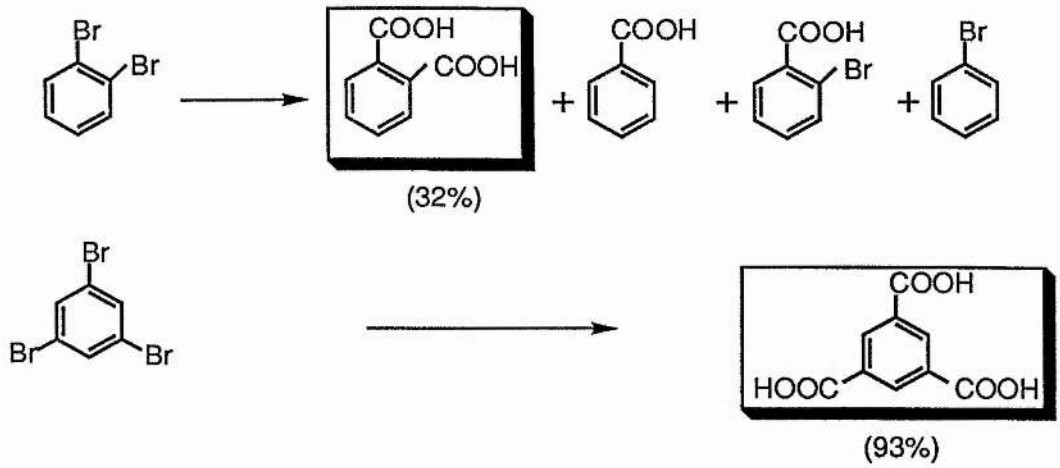

Figure 3.1.2

It can been seen from figures 3.1.1-3.1.2 that substrates with adjacent functionality (either with respect to halogen or acid groups) react in a very non-selective manner. Where the substrates do not exhibit such adjacent functionality, ie with 3,5-dichlorobenzoic acid, selective high yielding double carbonylation can be achieved.

3.2 Palladium catalysed double carbonylation of non-geminal dihalides

The first example of a palladium catalysed double carbonylation of this type was reported by Milstein[122]and co-workers using the catalyst [Pd(dippp)$_2$] (dippp = di-isopropylphosphinopropane). This electron rich species is peculiar in being able to catalyse the carbonylation of a range of aryl chlorides. Amongst these is 1,4-dichlorobenzene which can be doubly carbonylated into 1,4-dimethyl dibenzoate (82% in 20 hr) in DMF with NaOAc as the base at 150 °C under just 4.7 atm CO. A range of mono and di-phosphines were investigated for use with this reaction, dippp proved to be the most effect di-phosphine. Mono-dentate phosphine complexes showed no activity at all towards the carbonylation of chlorobenzenes. In solution ^{31}P NMR studies show that one ligand of [Pd(dippp)$_2$] is bi-dentate and the other mono-dentate. Mechanistic work shows that dippp is lost from the metal and re-bound during the course of the catalytic cycle and this can be achieved reversibly despite the presence of HCl in the reaction system. No catalyst decomposition is observed at the end of a reaction and it was shown that the [Pd(dippp)$_2$] could be recycled. Milstein highlights what he believes are the advantageous features of dippp; it is i) highly basic, ii) can form a stable 6 membered chelate complex, and iii) very bulky.

The double carbonylation of 4,4'-dibromobiphenyl gives aryl esters using the catalyst precursors $PdCl_2$ / dppp.[123-125] An extremely strong N-centred base is required to achieve high yields from this reaction, MTBD (7-methyl-1,5,7-triazobicyclo[4.4.0]dec-5-ene - $pK_a = 13.0$) being a good example. Less exotic bases such as DBU and t-BuOK can also furnish respectable yields. A range of substituted phenols can be used as nucleophiles, but it was observed that the reaction was hindered by the use of sterically hindered phenols (ie 2,6-di-t-butyl-3-methylphenol). The reaction was also hindered by bases where the N-centre was sterically crowded.

Ethoxy-double carbonylation of 4,4'-dibromobiphenyl can be achieved using phosphinated polystyrene (PSP) palladium complexes.[125] The highest yield and selectivity were achieved with a P:Pd ratio of 4:1. The P-Pd bond energy for polymeric phosphines is often lower than for conventional (ie PPh_3) complexes and thus a higher P:Pd ratio is required for stable polymer ligand complexes than for 'free' phosphine complexes.[124] Two unusual features of the polymer based catalytic system were noted. A small, but significant decrease in both the yield and selectivity of the double carbonylation reaction occurred as the CO pressure was increased. The use of any of a wide range of aprotic co-solvents (the primary solvent / reagent being ethanol) significantly inhibited the reaction. This was tentatively attributed to a change in the polymer conformation in aprotic media. An alternative explanation might involve the requirement of ethoxide ions to drive unfavourable equilibria in the reaction such as the reductive elimination of the acyl halide carbonylation product or of HBr from the palladium centre.

3.3 Polymer synthesis achieved by double carbonylation

Most condensation polymers are formed by the reaction of di-carboxylic acid derivatives with either diamines (polyamides) or diols (polyesters). Palladium[126-129] and nickel[127,130] catalysts have been used for the double carbonylation of non-geminal organic dihalides in the presence of di-functional nucleophiles (ie diols) to yield the desired polymers in a one pot reaction.

The rate of carbonylation of aryl bromides has been shown to be inversely proportional to CO pressure whereas the rate of carbonylation of aryl iodides is proportional to CO pressure[67] - see section 1.22. This feature led to improvements in the molecular weight of polyamides over those derived from 1,3-dibromobenzene.[129] By using 1,3-diiodobenzene instead, with aromatic diamines at elevated CO pressures

in the presence of $[PdCl_2(PPh_3)_2]$ and DBU in DMA, linear high molecular weight polyamides were obtained.[129] This reaction has been shown to be tolerant of a range of fuctionalised aromatic monomer units.

Double carbonylation / polycondensation reactions catalysed by a Pd-phosphine complex[128] can also yield wholly aromatic polyesters of molecular weight 10,000-100,000. A range of amine bases was investigated for the reaction and DBU again proved the most effective. Only aprotic solvents could be used for this reaction and this was accounted for on the basis of the solubility of the growing polymer in these media. Interesting observations of the effect of the amount and nature of the phosphine upon this reaction were made. The ideal P:Pd ratio was found to be 1:4 even though the probable catalyst would be a bis-phosphine species. Possibly the excess phosphine stabilises the catalyst towards cluster formation and therefore de-activation. The use of dppe is observed to give a faster initial rate of carbonylation than PPh_3, but PPh_3 gives higher molecular weight products. This could be due to the dppe activating the palladium centre not only towards the di-bromo substrate but also towards the phenyl chloride which was normally used as the solvent. Clearly the incorporation of a mono-functional unit such as benzoic acid (from the carbonylation of PhCl) would terminate the polymer chain growth. When the CO pressure was increased above 10 atm the molecular weight of the product decreased and this was accounted for on the basis of the suppression of reactivity of organobromides with palladium bis-phosphines at elevated CO pressures.[67] Aromatic diols were found to yield higher molecular weight polymers than aliphatic diols, this is probably due to their higher acidity and thus reactivity towards the intermediate aroyl complexes (see Part B section 1.15).

$[NiCl_2(bpy)]$, $[NiCl_2]$ / bpy, $[NiBr_2]$ / bpy and $NiCl_2$ are all equally effective catalyst precursors for the synthesis of polyamides from a range of non-geminal dibromides with $H_2N\text{-}C_6H_4\text{-}O\text{-}C_6H_4\text{-}NH_2$ and CO.[130] Conversions of over 95% are observed when DBU is used as a base for this reaction, but when inorganic bases are employed no polymerisation is observed. Polar aprotic solvents are found to be ideal for this reaction. It should be noted that the ideal temperature is 150 °C, somewhat higher that the 115-120 °C required for palladium based systems.[127, 128]

3.4 The double carbonylation of monohalo alkenes

The title reaction can be catalysed by starting from a range of palladium precursors; $[PdCl_2(PPh_3)_2]$, $Pd(OAc)_2$ or Pd(dibenzylidene-acetone)$_2$. It is achieved by the carbonylation first of the carbon-halogen bond[131] then the carbonylation of the alkene unit. A concerted intramolecular attack of the initial (C-Halogen derived) acyl unit upon the alkene as it undergoes carbonylation leads to cyclic γ-keto esters. Examples of such reactions[131,132] are shown in figure 3.4.1. Since the double carbonylation of alkenes falls outside of the scope of this review, just pertinent examples of this class of double carbonylation are shown below and the coverage should not be considered comprehensive.

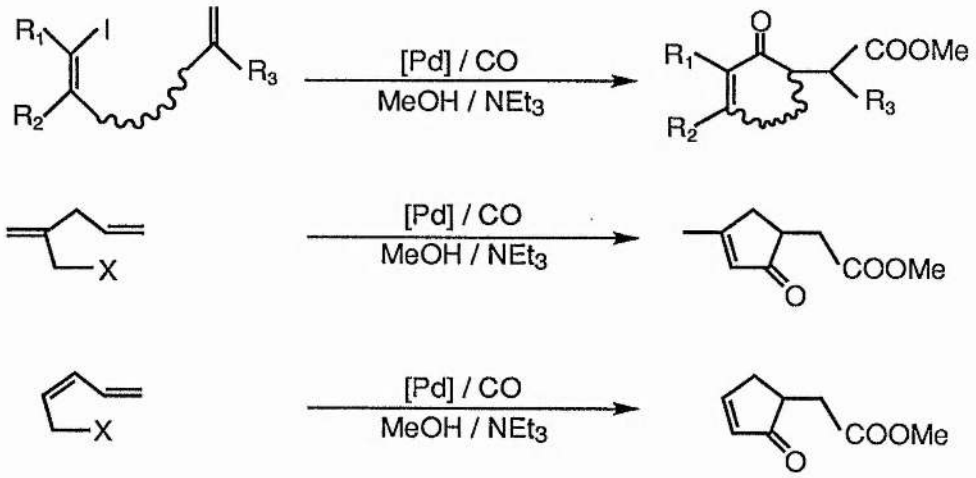

Figure 3.4.1

These reactions are carried out in a 1:1 benzene / acetonitrile solvent system, with NEt_3 as the base and also in the presence of MeOH. It is observed that unless an alcohol is present (to trap the carbonylation product as an ester) polymerisation occurs. The proposed mechanism of these reactions is shown overleaf in figure 3.4.2.

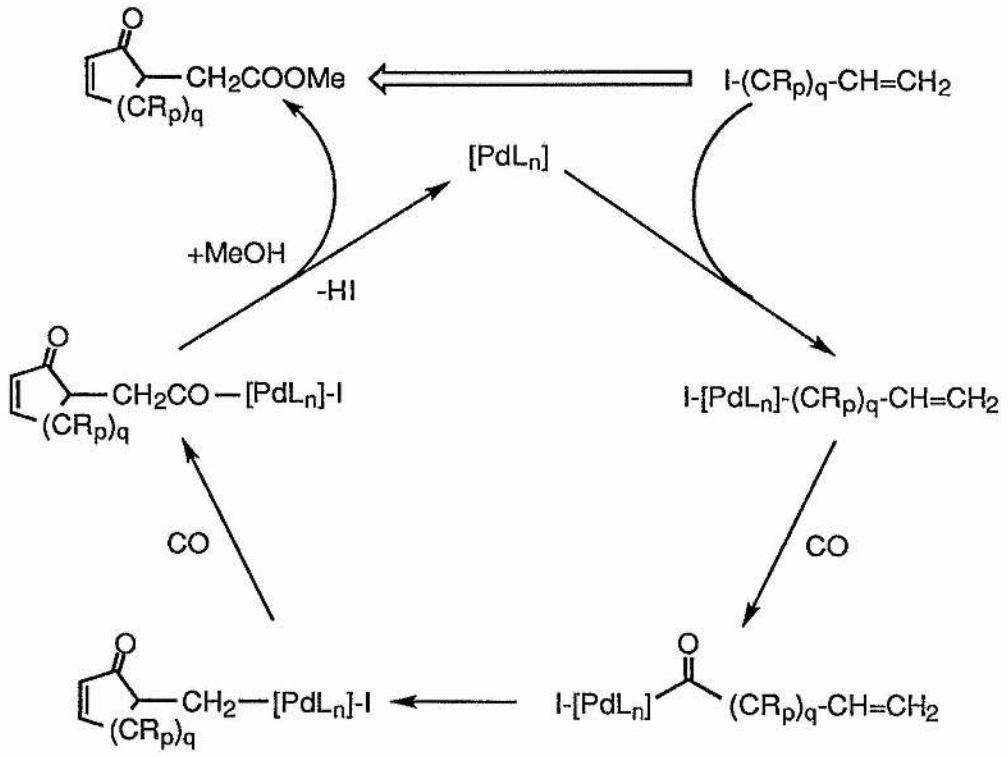

Figure 3.4.2: Proposed mechanism for the palladium catalysed double carbonylation of halo-enes at two distinct sites.

CHAPTER TWO

Catalytic Carbonylation of Diiodomethane

2.0 Introduction

The subject of this thesis is the catalytic double carbonylation of diiodomethane (CH_2I_2). The initial work which prompted this study showed that using the catalyst precursors $[Rh_2(OAc)_4]$ / PEt_3 / CO (with both PEt_3 and CO in a large excess with respect to rhodium) the reaction of a solution of CH_2I_2 in ethanol yielded diethylmalonate (DEM) and ethyl iodide as the major products.[133]

$$CH_2I_2 + 2CO + 2EtOH \xrightarrow{[Rh_2(OAc)_4] / PEt_3 / CO} CH_2(COOEt)_2 + 2HI$$

The ethyl iodide is formed by the reaction of EtOH and HI, presumably forming equal amounts of water. The other minor products from the reaction (detected by GC) were diethoxymethane ($CH_2(OEt)_2$) formed from the ethanolysis of the substrate, ethyl propanoate ($EtCO_2Et$) and a trace of ethyl acetate (CH_3CO_2Et). The nature of the reaction products was confirmed by GC-MS and ^{13}C / ^1H NMR. It was shown that the diethoxymethane is formed by a route independent of the catalyst and ethyl propanoate is assumed to be formed by the carbonylation of EtI formed in-situ. The significance of the trace quantities of ethyl acetate in the product mixture will be discussed in chapter four. A typical product yield (wrt initial $[CH_2I_2]$) from this reaction carried out under optimised conditions was; DEM (20%), $CH_2(OEt)_2$ (0.6%), $EtCO_2Et$ (0.6%). Although the conversion of diiodomethane is low, the selectivity to the malonate ester is very high - ie 97%. It is also important to note here that this is the only reported catalytic double carbonylation system reported that does not require the use of a base - see Chapter One. The effect of bases on this system is discussed in section 2.4.

As will be highlighted in section 2.9 the active catalyst for this reaction only has a short lifetime under the reaction conditions. It has been shown that the standard 4 hour reaction time used for catalytic runs is in excess of the lifetime of the catalytic species and this (along with the other factors discussed in section 2.9) demonstrates a direct relationship between the yield of DEM and the catalyst lifetime. To quantify the lifetime of the catalyst the term catalyst Turn Over Number (TON) is defined as the average number of catalytic cycles the active rhodium species performed before irreversible decomposition. The unstable nature of the catalytic system prevented its examination by kinetic methods. Conclusions that can be drawn from the catalytic

reactions which give evidence pertaining to the mechanism of the title reaction will be summarised in chapter five rather than here.

The catalytic reactions reported here were carried out in a glass liner inside a (250 cm^3) stainless steel autoclave, heated to between 50 and 170 °C. The standard conditions were a reaction time of 4 hours at 120 °C under 40 atm CO. The majority of the reactions reported here were carried out using CH_2I_2 (1 cm^3, as substrate) in EtOH (4 cm^3) with $[Rh_2(OAc)_4]\cdot 2MeOH$ (*ca.* 0.01 g) with various amounts of phosphine, the P:Rh ratio of 3:1 being typical. In the result tables it should be assumed that these conditions apply unless otherwise stated.

It should be stated at the outset that the results gained from these catalytic runs were never found to be consistently reproducible. When a series of identical runs were carried out there were obvious modal yield values, but the variation observed under seemingly identical reaction conditions could be very large. Another problem with these data presented is the accuracy of the determination of the final concentrations of CH_2I_2 and EtI. The quantitative analysis was carried out using a GC using a narrow bore capillary column (BP-1) linked to a FID detector. FID detectors are noted for their insensitivity towards halogenated compounds. Thus the data for the final $[CH_2I_2]$ and [EtI] for these reactions has a very large margin of error and therefore it will not be presented here.

2.1 Effects of the P:Rh ratio

Table 2.1.1 shows the product yields from a series of reactions carried out with fixed amounts of the rhodium precursor $[Rh_2(OAc)_4]$ but with varying amounts of added PEt_3. It can be seen that the best yields of DEM are achieved with either a P:Rh ratio of 3:1 or with no phosphine present at all. These results are best viewed graphically and are presented thus in figure 2.1.1.

Table 2.1.1: Showing the effect of the P:Rh ratio upon the reaction.

		Yield / %[a]				
Run	**P:Rh**	**DEM**	**$CH_2(OEt)_2$**	**$EtCO_2Et$**	**TON**	**Selectivity[b]**
31	1:1	4.1	0.6	<0.1	12.9	87%
32	2:1	3.1	0.5	<0.1	9.7	86%
33	3:1	5.9	1.3	<0.1	18.5	82%
34	4:1	3.7	1.5	<0.1	11.6	71%
45	None[c]	9.5	2.7	0.9	29.8	78%
51	None[d]	-	2.4	-	-	-

a) Calculated from GC peak area, wrt initial [CH_2I_2]; b) Calculated as ratio of yield of DEM to yield of (DEM + $CH_2(OEt)_2$); c) [$Rh_2(OAc)_4$] only, no PEt_3; d) PEt_3 only, no [$Rh_2(OAc)_4$].

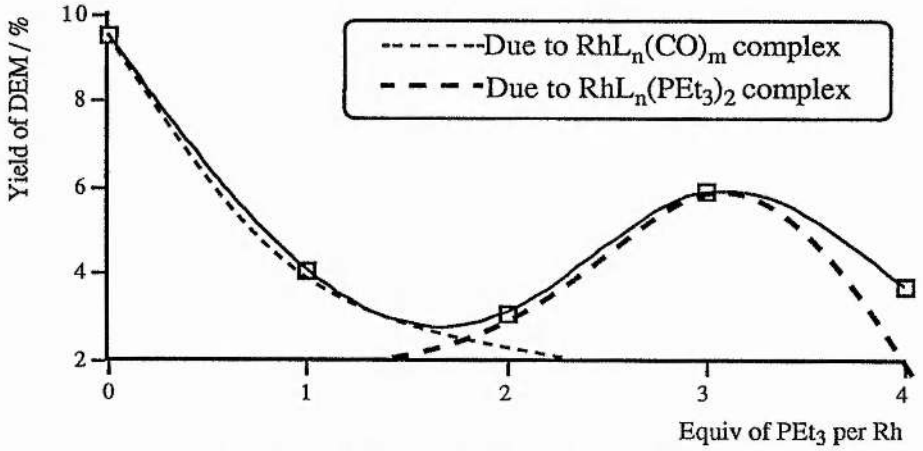

Figure 2.1.1: Graph showing yield of DEM vs. amount of PEt_3 added.
L = non-phosphorus based ligand.

These data show that there are two potential catalytic systems which can operate in this P:Rh ratio region, a rhodium carbonyl species (Run 45) and a rhodium phosphine complex. The synthesis of DEM (—) at low P:Rh is catalysed by a rhodium carbonyl complex(--) whose action is inhibited by PEt_3. At higher P:Rh a rhodium phosphine complex(--) is the active catalyst thus the second maxima of DEM yield in figure 2.1.1. The dashed lines show how the observed effect of the P:Rh ratio on the DEM yield could potentially be due to the superposition of the action of two different but catalytically active rhodium species.

The reaction conditions for run 45 (No PEt_3) are very similar to those used in a report of the synthesis of [$Rh_6(CO)_{16}$].[134] To assist in understanding this result a separate autoclave run was carried out in the absence of the substrate and the major

organometallic product from this reaction was observed, by IR, MS, and microanalysis, to be $[Rh_6(CO)_{16}]$. The role of $[Rh_6(CO)_{16}]$ in this process will be discussed in section 2.2.

The work presented in chapter three (section 3.1) showed that the species formed from the precursors $[Rh_2(OAc)_4]$ / 6-8 PEt_3 under standard reaction conditions was $[Rh(OAc)CO(PEt_3)_2]$. So why is the ideal P:Rh ratio observed as 3:1 and not 2:1? This potential anomaly is explained by the slow reaction that takes place between PEt_3 and CH_2I_2 forming the quaternary salt $[Et_3PCH_2I][I]$ (described in chapter four). Thus, in order to 'assemble' the bis-phosphine species $[Rh(OAc)CO(PEt_3)_2]$ in the presence of CH_2I_2 a slight excess of phosphine is required to allow for the removal of some by slow quaternisation by CH_2I_2. $[Et_3PCH_2I][I]$ is shown in chapter 4 to be detrimental to the catalyst stability / lifetime.

Since phosphines make excellent spectroscopic handles for NMR studies it was decided to concentrate our study on the potential of rhodium phosphine complexes as catalysts for the title reaction.

2.2 Study of other potential catalysts / catalyst precursors

Having shown that $[Rh(OAc)CO(PEt_3)_2]$ is the species formed from the catalyst precursors under standard reaction conditions (chapter three, section 3.1), a range of Rh(I) bis-phosphine species and rhodium carbonyls were investigated for their catalytic activity.

Table 2.2.1: Showing the product yields for a variety of catalytic species.

		Yield / %			
Run No.	*Catalyst*[a]	**DEM**	**$CH_2(OEt)_2$**	**$EtCO_2Et$**	**TON**
62	A	3.2	1.0	-	10.1
87	A+1 PEt_3	2.0	0.3	<0.1	8.0
63	B	3.2	1.0	-	10.1
123	C+1 PEt_3	1.0	0.2	0.2	3.1
84	D	5.0	0.8	<0.1	15.7
138	E	trace	trace	trace	-
51	None[b]	-	2.4	-	-

a) A = $[Rh(OAc)CO(PEt_3)_2]$; B = $[Rh(I)CO(PEt_3)_2]$; C = $[Rh(Cl)CO(PEt_3)_2]$; D = $[Rh(CO)_2I_2]^-$ formed in-situ from $[Rh_2(OAc)_4]$ + 5 I_2; E = $[Rh_6(CO)_{16}]$. b) No catalyst precursors used.

This now shows that $[Rh(X)CO(PEt_3)_2]$ (X = I, Cl, OAc) are all active catalysts for the double carbonylation of diiodomethane. Note that in runs 87 and 123 the addition of one equivalent of free phosphine inhibits the reaction; A 3:1 P:Rh ratio is only required when the catalyst is made in-situ when the excess phosphine allows the catalyst to 'assemble' in the presence of diiodomethane as discussed above. The above data confirms that rhodium carbonyl species are able to catalyse the reaction. It also suggests that $[Rh_2(OAc)_4]$ and CH_2I_2 in the absence of PEt_3 do not form $[Rh_6(CO)_{16}]$, but instead forms the Monsanto catalyst $[Rh(CO)_2I_2]^-$ (compare runs 84 and 138).

2.3 Effects of reaction temperature

A series of reactions using a 6:1 PEt_3:$[Rh_2(OAc)_4]$ ratio (P:Rh = 3:1) with 1 cm^3 CH_2I_2 and 4 cm^3 EtOH under 40 atm CO were carried out at a range of temperatures. Figure 2.3.1 below shows the change in the yield of DEM with temperature.

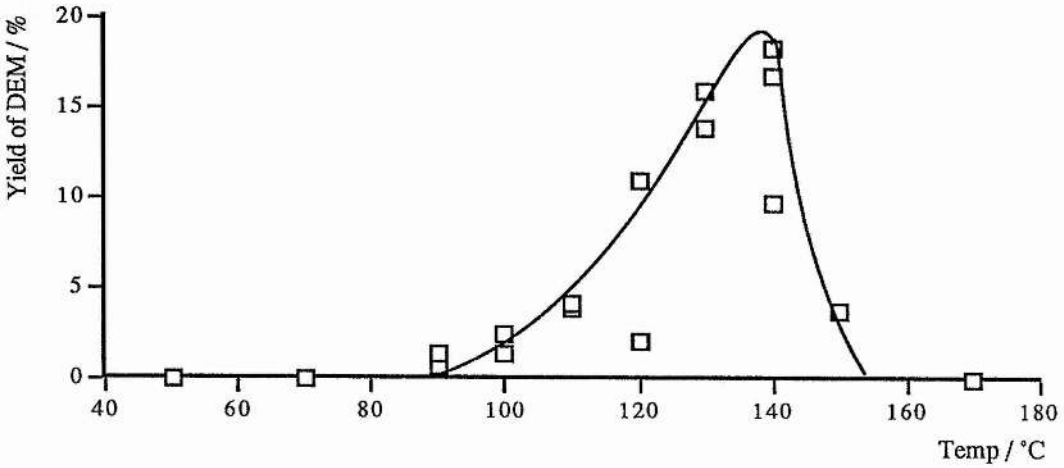

Figure 2.3.1: Graph showing DEM yield vs. reaction temperature

No reaction is observed below 90 °C. Above 90 °C the yield of DEM increases with temperature, the optimum reaction temperature range being 120-140 °C. Elevating the temperature above 140 °C presumably decomposes the active $[Rh(X)CO(PEt_3)_2]$ species.

2.4 Effects of an added base

The effect of a very wide range of both inorganic bases and N-centred organic bases on the reaction was examined. Without exception all bases were observed to inhibit the double carbonylation reaction. A possible reason for this, linked to the proposed mechanism for this reaction, is discussed in chapter four (section 4.2).

2.5 Effects of the solvent system

It should be noted that the alcohol used in this reaction acts not only as a solvent, but also as a reagent / HI sink. A wide range of alcoholic solvents was employed in this reaction; MeOH, EtOH, i-PrOH and n-BuOH. All these alcohols (ROH) were suitable, with the malonate ester and acetal $CH_2(OR)_2$ being observed in all cases. Malonate esters were not observed when either t-BuOH or $MeOCH_2CH_2OH$ were used as solvents. In the case of MeOH, methyl acetate was produced and with EtOH, ethyl propanoate. The activity of $[Rh(X)CO(PEt_3)_2]$ towards the carbonylation of MeOH will be discussed in section 2.11. Ethyl propanoate is presumed to arise from the carbonylation of EtI. Quantitative data was only obtained for the EtOH based system.

It was reasoned that the addition of a non-protic co-solvent 1:1 v/v with EtOH would reduce the ethoxide concentration and thus inhibit the side reaction which gives rise to the acetal - see figure 2.5.1.

$$CH_2I_2 + 2\ EtO^- \longrightarrow CH_2(OEt)_2 + 2\ I^-$$

Figure 2.5.1

A range of co-solvents were investigated. THF and DMSO were observed to decompose under the reaction conditions. 1,2-dimethoxyethane (DME) proved too reactive giving rise a number of unidentifiable oxygenated products, but no malonate ester. The co-solvents which did prove stable and allowed carbonylation to occur were; toluene DMF, DMA, CH_3CN, acetone and CH_2Cl_2. All of these co-solvents did decrease the yield of $CH_2(OEt)_2$ as predicted thus improving the selectivity. The results of these catalytic runs are shown in Table 2.5.1.

Table 2.5.1: Showing the effect of co-solvents upon the reaction.

		Yield / %				
Run	**Co-solvent**	**DEM**	**$CH_2(OEt)_2$**	**$EtCO_2Et$**	**TON**	**Selectivity**
33	None	5.9	1.3	<0.1	18.5	82%
38	Toluene	4.7	1.0	-	14.7	82%
41	DMF	6.6	<0.1	<0.1	20.7	>99%
182	DMA[a]	9.1	0.5	-	28.5	95%
181	CH_3CN[a]	8.7	0.4	0.2	27.3	96%
200	CH_2Cl_2[a]	2.1	0.4	0.3	6.6	84%
202	Acetone[a]	2.2	0.2	-	6.9	92%

a) pCO = 84 atm

A 4:1 v/v mixture of EtOH / CH_2I_2 forms two layers, the top layer rich in EtOH and the bottom layer rich in the more dense CH_2I_2. An additional benefit of the use of co-solvents is that a one phase solution is obtained which could be quantitatively analysed after the reaction with greater accuracy. Although the yield of DEM observed using any of these co-solvents at 40 atm CO was similar to that observed using EtOH alone the increase in catalyst TON with CO pressure(described in section 2.8) was not observed in these dual solvent system reactions.

This, and mechanistic work to be presented in chapters three and four, shows the great importance of an alcoholic solvent for this reaction. The alcohol appears to play at least two crucial roles in addition to being a reagent and a suitably polar solvent; i) as a non-basic sink for HI and ii) to shift the equilibrium position in reductive elimination reactions yielding RX (R = H, alkyl, acyl; X = Halogen).

2.6 Effect of changing the initial diiodomethane concentration

Figure 2.6.1 shows the effect of changing the initial diiodomethane (substrate) concentration upon the catalyst TON. It is observed that higher concentrations of diiodomethane are advantageous to catalyst stability. A potential explanation of this effect is discussed in detail in chapter three. An increase in diiodomethane concentration would increase the rate of the first step in the catalytic cycle causing an advantageous shift in the equilibrium position (according to Le Chatelier's principle) in the final step of the proposed mechanistic cycle (section 3.13).

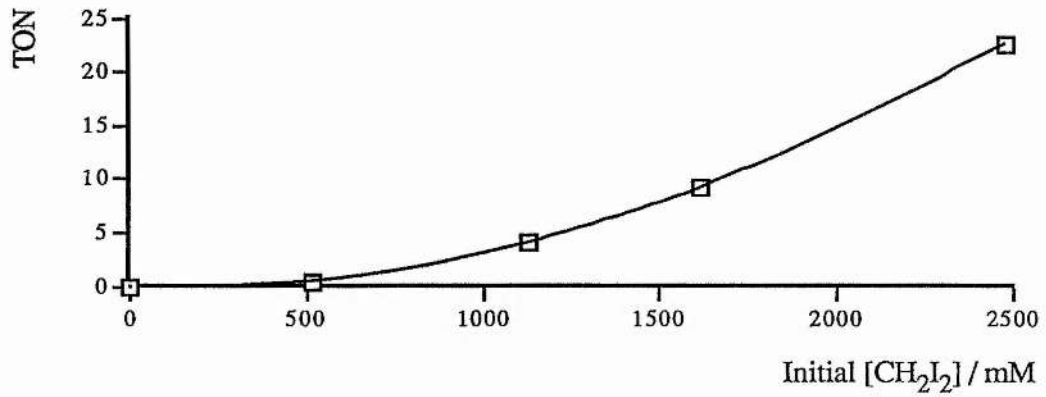

Figure 2.6.1: Graph showing TON vs. initial diiodomethane concentration.

2.7 Effects of changing the phosphine ligand

A range of phosphines and a phosphite were investigated as possible catalyst precursor units in systems were the catalyst was allowed to form in-situ from $[Rh_2(OAc)_2]$ / 6 PR_3. These results are presented in table 2.7.1.

Table 2.7.1: Showing the effect of a variety of phosphine ligands upon the reaction.

		Yield / %[a]				
Run	**Phosphine**	**DEM**	**$CH_2(OEt)_2$**	**$EtCO_2Et$**	**TON**	**Selectivity**
81	PMe_3	4.6	1.6	-	14.4	74%
33	PEt_3	5.9	1.3	<0.1	18.5	82%
75	P^iPr_3	2.2	0.6	-	6.9	79%
36	$P(OEt)_2$	6.2	1.9	<0.1	19.4	77%
80	PPh_3	7.1	1.0	<0.1	22.3	88%
59	dmpe	2.6	0.6	-	8.2	81%

a) P:Rh = 3:1 for all reactions except for dmpe P:Rh 2:1

As table 2.7.1 shows, a range of phosphine ligands can form active catalytic species. The majority of the ligands result in very similar yields of DEM, with no obvious trend related to the electronic character of the ligand being observed. The use of either dmpe or P^iPr_3 leads to significantly lower yields than the other ligands. The steric bulk of P^iPr_3 could inhibit the oxidative addition of the bulky diiodomethane thus

lowering the DEM yield. Recent work from within our group on the reaction of $RhCl_3$ with dmpe and CO has shown that the 5 co-ordinate species $[RhCl(CO)_2(dmpe)]$ forms in preference to $[RhCl(CO)(dmpe)]$.[135] This 5 co-ordinate 18 e species would have to lose a CO molecule before any oxidative addition reaction could occur. This different behaviour (compared to $[Rh(X)CO(PR_3)_2]$) probably explains the poor catalytic performance of the dmpe derived species.

2.8 Effects of varying the carbon monoxide partial pressure

The mechanism proposed for this reaction in chapter three includes a competition step between CO insertion and catalyst decomposition. This step is illustrated in figure 2.8.1.

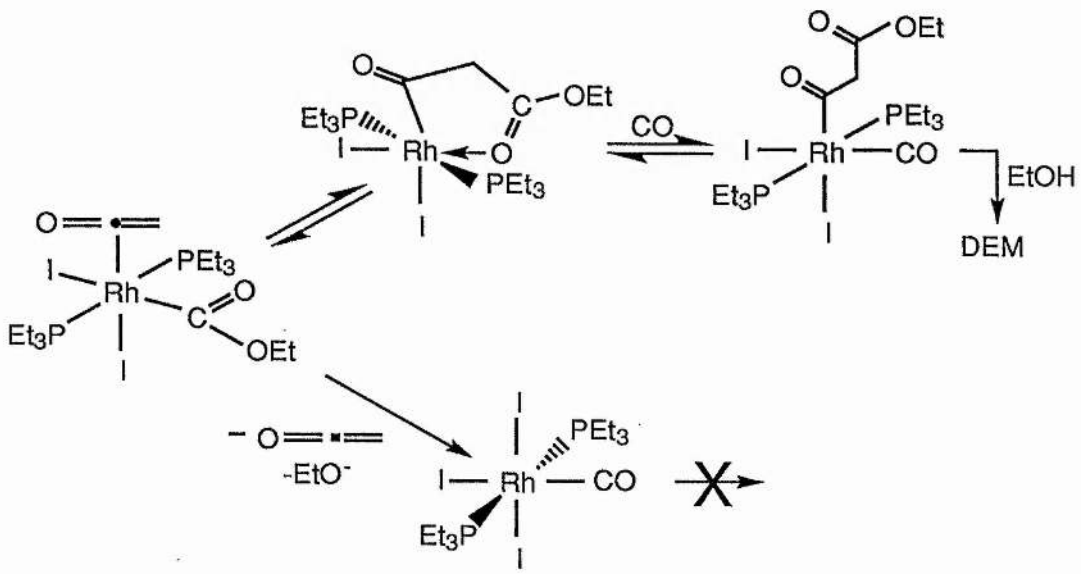

Figure 2.8.1

With the proposed existence of a competition step, such as shown above, a direct relationship between CO pressure and catalyst TON would be expected. The observed effect of CO pressure on TON is shown in figure 2.8.2 and the predicted trend is indeed observed.

If the trend observed in figure 2.8.2 could be extrapolated to much higher pressures, complete conversion of the diiodomethane substrate by this catalyst may be expected at approximately 700 atm CO. In order to test this hypothesis a series of reactions were carried out at 300-350 atm CO using ultra-high pressure equipment in the labs of Prof.

W Keim in Aachen, Germany. Sadly the yields of DEM achieved at 300-350 atm CO are similar to those achieved at 40 atm CO under the same conditions.

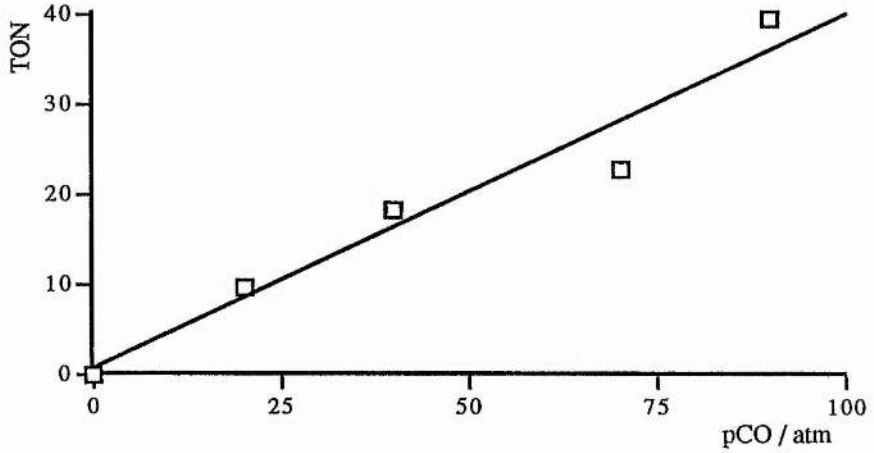

Figure 2.8.2: Graph showing effect of pCO on Catalyst TON.

Two potential explanations for this are; i) the displacement of the phosphine ligands from the metal centre by CO given the high CO concentrations achieved at these pressures and ii) competition between CH_2I_2 and CO for co-ordination sites on the initial Rh(I) species. The second explanation has also been proposed by Yamamoto[67] for the decrease in rate for the double carbonylation of PhBr at elevated CO pressures. Although evidence for the displacement of PEt_3 by CO at high CO pressures could potentially be obtained by HPIR, independent work[136] on the reactions of $[Rh(I)CO(PEt_3)_2]$ under CO from within our group has not implied the occurrence of such a phenomenon at up to 100 atm. This does not rule out the possibility of this displacement occurring during reactions carried out at 300-350 atm. A reversible reaction between $[Rh(Cl)CO(PEt_3)_2]$ and CO has been observed[137] and this is shown in figure 2.8.3.

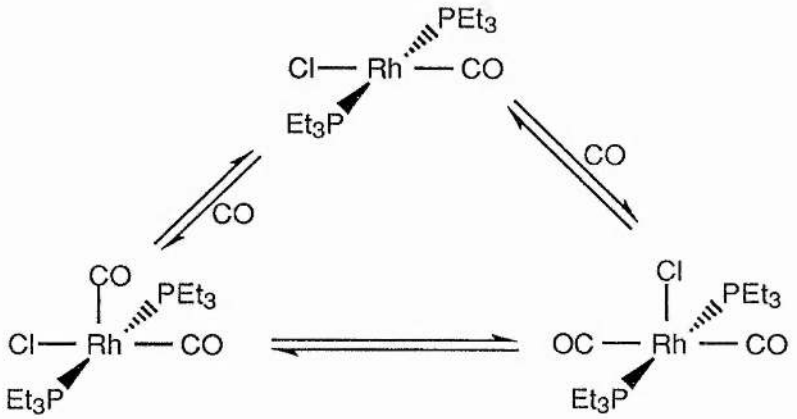

Figure 2.8.3: The reactions of $[Rh(Cl)CO(PEt_3)_2]$ with CO.

In light of the work of Yamamoto and other work within our group the blocking of the reaction of $[Rh(X)CO(PEt_3)_2]$ with CH_2I_2 by CO co-ordination appears, at present, to be the best explanation for low DEM yields at 350 atm CO.

2.9 Study of catalyst stability and effects of catalyst reducing agents

The low yields of DEM observed could conceivably be due to one of two reasons: i) Catalyst decomposition; ii) the reaction reaching an unfavourable equilibrium limiting the yield of DEM. If catalyst decomposition is occurring within 4 hours then increasing the reaction time beyond 4 hours should not increase the yield of DEM. An increase in the catalyst concentration should increase the yield of DEM if the catalyst's lifetime is lower than 4 hours. If it is an unfavourable equilibrium which is limiting the DEM yield, altering the concentration of the catalyst should not alter the position of the equilibrium and the DEM yield should not change. It was observed that the yield of DEM did not increase from its value at 4 hours after a 21 hour reaction time and that increasing the catalyst concentration increases the yields of all the products. These results of changing the reaction time and catalyst concentration demonstrate that it is catalyst stability that is the limiting factor in this reaction. Further evidence confirming catalyst decomposition comes from 'snapshots' of the rhodium phosphine species present in solution at different reaction times. These data are discussed in chapter four (section 4.6).

The major catalyst decomposition step has been shown to be the competition reaction illustrated in figure 2.8.1 above (see also chapter four). It was thought that this inactive Rh(III) species might be reduced in-situ and thus the metal centre re-introduced into the catalytic cycle. An analogous reduction is achieved in the Monsanto process using hydrogen.[138]

$$[RhI_4(CO)_2]^- + H_2 \longrightarrow [RhI_2(CO)_2]^- + 2\,HI$$

Figure 2.9.1

A comparison of two nearly identical catalytic runs, one with pCO = 40 atm and pH_2 = 40 atm (run 149) and one with pCO = 40 atm and no hydrogen shows that the hydrogen has no effect on the catalyst stability - see table 2.9.1

Table 2.9.1: Showing the effect of hydrogen as a potential reductant upon the TON.

		Yield / %			
Run No.	**Gas used**	**DEM**	**$CH_2(OEt)_2$**	**$EtCO_2Et$**	**TON**
33	CO only	5.9	1.3	<0.1	19
149	CO/H_2	4.6	1.0	0.2	14
146	CO only[a]	9.3	1.0	trace	29

a) Mg amalgam added as the reducing agent.

Although the route which allows hydrogen to reduce $[RhI_4(CO)_2]^-$ does not operate with $[RhI_3(CO)(PEt_3)_2]$, the effect of the Mg amalgam suggests that catalyst oxidation is responsible for its loss of activity.

2.10 Effect of promoters and other additives

The addition of molecular sieves (run 93) to remove any water present in the CO or generated in-situ was not observed to have any significant effect on the reaction. When a large volume of water was added to the reaction (by replacing 1 cm^3 of EtOH by water) no carbonylation was observed. Thus it appears that the reaction is unaffected by a low water concentration but inhibited by a larger one. The effect of water on the system is probably complex and merits further study. It has been shown that when the same catalyst is used for the carbonylation of MeI the addition of small volumes of water helps to stabilise the active Rh(I) species.[136]

The addition of metal iodide salts is often observed to promote the transition metal catalysed carbonylation of organic iodides.[139] The addition of KI (10:1 vs. Rh) is not observed to promote the reaction. The addition of Na(OAc) had no significant effect on the yield of DEM, but appeared to enhance the yield of ethyl propanoate. $Li(OAc)\cdot 2H_2O$ was observed to strongly inhibit the double carbonylation reaction. $Sn^{II}I_2$ was used as a potential sink for I_2 ($SnI_2 + I_2$ ' SnI_4) but rather than improve the TON it totally inhibited the carbonylation reaction.

Table 2.10.1: Showing the effect of additive and promotors upon the reaction.

		Yield / %				
Run	**Additive**	**DEM**	**$CH_2(OEt)_2$**	**$EtCO_2Et$**	**TON**	**Selectivity**
33	None	5.9	1.3	<0.1	18.5	82%
97	KI[a]	3.4	2.3	0.3	10.7	70%
155	NaOAc	5.3	trace	5.3	16.6	>95%
153	LiOAc	trace	-	trace	-	-
129	SnI_2	-	-	-	-	-

a) pCO = 35 atm.

2.11 Studies of other halogenated substrates

The versatility of $[RhX(CO)(PEt_3)_2]$ as a carbonylation catalyst was examined by the investigation of a number of other halocarbon substrates: MeI, CH_2Cl_2, CH_2ICl, PhCl, $PhCH_2Cl$ and ICH_2CH_2I. Carbonylation / double carbonylation was not observed with CH_2Cl_2, CH_2ICl, PhCl or ICH_2CH_2I. Both MeI and $PhCH_2Cl$ could be successfully carbonylated in ethanol to give ethyl acetate and 2-phenylethyl acetate respectively. Both of these reactions can be carried out under mild conditions, 100 °C and 40 atm CO without the need for an added base. These preliminary studies have been extended into two individual Ph.D projects; the methyl iodide promoted carbonylation of methanol[136] and the carbonylation of allyl and benzyl halides.[137]

2.12 Attempts towards use of para-formaldehyde as a substrate

The original aim of this project was to find a catalytic system capable of carbonylating formaldehyde promoted by iodide. (cf. iodide promoted methanol carbonylation - Monsanto Process) It was assumed that diiodomethane would be a good model for a system containing CH_2O / 2 HI as illustrated in figure 2.12.1.

$$CH_2O + 2\,HI \longrightarrow ? \longrightarrow CH_2I_2 + H_2O$$

Figure 2.12.1

A previous study[133] reported preliminary studies into the activation of formaldehyde. When para-CH_2O was used as the substrate and acetyl iodide as the source of HI (formed in-situ from MeI and CO) under the reaction conditions found optimal for the

diiodomethane work, the products of the reaction were observed to be CH_2O, EtI, EtOAc (from AcOI + EtOH),$CH_2(OEt)_2$ and $(EtOCH_2)_2O$. These were the same products observed in the earlier work by Gash.[133] The species which is characterised as $(EtOCH_2)_2O$ was previously observed but never identified, being previously known just as 'Product A'. An investigation of early literature revealed that the reaction shown in figure 2.12.1 does not in fact occur, instead that shown in figure 2.12.2 has been observed[140,141] for the reaction of para-CH_2O with LiBr in c.H_2SO_4 (a source of H^+ and Br^- cf. HBr)

$$2\ CH_2O + 2\ HBr \longrightarrow BrCH_2\text{-}O\text{-}CH_2Br + H_2O$$

Figure 2.12.2

In the trial catalytic system ICH_2-O-CH_2I will react with the solvent / reagent EtOH to give the observed tris-ether. Synthetic reactions of para-CH_2O with a source of H^+ and I^-, in ethanol or diethyl ether as the solvent, did not yield either I-CH_2OH or CH_2I_2.

Since para-CH_2O reacts in ethanol to form $CH_2(OEt)_2$ it was reasoned that this might be used as a substrate (in the presence of an iodide promoter) that more closely modelled para-CH_2O than CH_2I_2. Attempted transformations of $CH_2(OEt)_2$ into CH_2I_2 using H^+ / I^- in a range of solvents and using neat anhydrous $CH_2(OEt)_2$ did not yield any iodinated product.

The results of all the work on para-CH_2O / $CH_2(OEt)_2$ lead us to conclude that the initial assumption that formaldehyde could be transformed into diiodomethane with HI is incorrect. Although [$RhX(CO)(PEt_3)_2$] can selectively catalyse the double carbonylation of CH_2I_2 there is no potential for the activation of formaldehyde via diiodomethane.

2.13 Summary

The catalytic reaction carbonylation of diiodomethane may presently give only low yields of malonate esters but selectivities of up to 99% can be achieved in EtOH / DMF. It has been shown that the optimal P:Rh ratio for the catalyst precursors is 3:1 and that the pre-formed catalytic species [$RhX(CO)(PEt_3)_2$] can also be used in the absence of excess phosphine. The role of an alcohol as a non-basic HI sink for this reaction has been shown to be crucial. Due to a competition step in the reaction

mechanism, the catalyst TON is proportional to the CO pressure up to a limit of between 100-300 atm. The ideal reaction temperature range is 120-140 °C. Unusually no base is required for this reaction and in fact all the bases which were investigated were observed to inhibit the double carbonylation reaction. A wide range of phosphine ligands is suitable to form an active Rh(I) catalyst. The major limitation of this catalytic system is the instability of the catalyst under moderate CO pressures. The same catalyst is also active for the mono carbonylation of allyl halides[137] and methyl iodide.[136]

2.14 Experimental

Several, heating, stirring and analytical procedures have been investigated during the course of this work in the hope of achieving consistently reproducible data. When compared under the standard reaction conditions all the methods gave the same yields for the oxygenated products within experimental error. The general experimental procedures such as the drying of solvents, the nature of the equipment used in this work and the sources of the chemicals are summarised in Appendix One.

Runs 30-106 – The catalytic runs were carried out in a stainless steel autoclave (250 cm^3) fitted with a glass liner. Approximately 0.01 g ($1.98x10^{-5}$ mol) of $[Rh_2(OAc)_4]\cdot 2MeOH$ was used each time with the various phosphine ligands and solvent systems in varying amounts. The conditions used are summarised in Sections 2.1-12. All the reagents were weighed or injected into a Schlenk tube under an inert atmosphere and then transferred into the autoclave, previously flushed 3 times with the reagent gas, whilst under a positive pressure of this gas. The only exception to this was for insoluble, but air stable, species which were pre-weighed directly into the autoclave. All solvents were distilled and degassed with nitrogen before use (See Appendix 1) The CH_2I_2 was degassed and stored over 4 Å molecular sieves. The autoclaves were heated to the prescribed temperature for 4 hr using an electric fan assisted oven and at the end of the 4 hr period cooled rapidly by placing into a bath of cold water. The product analysis was carried out using a GC (within 48 hr) and GCMS if unrecognised products were observed.

Runs 106-221 – Two changes were made to the above method for the following runs; i) The amount of $[Rh_2(OAc)_4]$ was measured by using an ethanolic solution of known concentration such that each 4 cm^3 contained $1.98x10^{-5}$ mol. ii) The autoclave was heated by clamping a cylindrical electrical heating band around the autoclave (with a thermocouple inserting between the band and the autoclave) and heating the

autoclave to the prescribed temperature controlled electronically and adjusted by the feedback from the thermocouple. The reaction mixture was also stirred at between 900-1000 rpm using a magnetic follower (flea) inside the glass liner. At the end of the 4 hr period the autoclave was removed from the heating band and cooled rapidly by placing into a bath of cold water.

GC Analysis of Product Mixtures from Catalytic Reactions 30-221 – After releasing the pressure from the autoclave, the resultant solution from the catalytic run was removed from within, and around, the glass liner in the autoclave and a measurement of volume recovered made. When the product solution formed two liquid phases they were diluted 1:1 with Et_2O to give a homogeneous solution before analysis. A 2 cm^3 aliquot of the homogeneous solution was removed and 3 μl p-xylene added as an internal standard. The GC syringe was washed with this solution 3 times and a sample (0.1 μl) injected into the GC.

The temperature program for the GC was; 5 min at 50 °C followed by raising the temperature to 150 °C at 16 °C·min^{-1} (6.25 min), then maintaining this temperature for a further 2.75 min. The concentrations of the product components were calculated from calibration curves, plotted from data obtained from solutions of known concentration, also using p-xylene as the internal standard.

The potential error in the concentrations of the halogenated products calculated by GC analysis was as follows; CH_2I_2 (± 40%), EtI (± 20%). The error associated to the concentrations calculated for the oxygenated products (diethoxymethane, ethyl propanoate and DEM) was acceptable at only ± 5%.

CHAPTER THREE

Synthetic and Mechanistic Studies - Steps and Species within the Catalytic Cycle

3.0 Introduction

In order to improve a catalytic process, an understanding of the underlying mechanism is first required. If a species acts as a catalyst its mechanism of action must be cyclic. The subject of this chapter is the evidence for the mechanistic cycle, or Tolman Loop, which is proposed for the rhodium / phosphine catalysed double carbonylation of diiodomethane. Any irreversible exit from this cycle amounts to catalyst decomposition and details of such steps are the subject of chapter four.

The proposed mechanistic cycle for the rhodium / phosphine catalysed double carbonylation of diiodomethane is shown in figure 3.0.1. This mechanism stems from the study of the synthesis and reactivity of proposed intermediates within the cycle. The most salient feature of this proposed mechanistic cycle is the involvement of a metallo-ketene intermediate. Ketene intermediates have also been proposed for the $[Co_2(CO)_8]$ catalysed double carbonylation of geminal di-bromides[98-100] and the stoichiometric reaction of a di-iron methylene species[112] with CO and an alcohol which yields a malonate ester.

Evidence for each reaction intermediate and step, where available, will be presented in turn throughout this chapter as we take a journey around the proposed catalytic cycle. The spectroscopic data (NMR and IR) for all the organo-rhodium species discussed are collected together in Tables 3.1 - 3.4 at the end of this chapter.

3.1 Discovering the nature of the catalytic species

This project was initiated by the discovery that a solution of $[Rh_2(OAc)_4]$ and PEt_3 (P:Rh = 50:1) in ethanol under a CO pressure of 40 atm could catalyse the double carbonylation of diiodomethane (CH_2I_2) into diethylmalonate (DEM). The first step in understanding this catalytic process was to identify the nature of the species responsible for this catalysis. Autoclave studies (chapter two; section 2.1) had identified that the ideal P:Rh ratio for the double carbonylation reaction was 3:1 so the reaction of $[Rh_2(OAc)_4]$ with 6 PEt_3 in ethanol under a CO atmosphere was investigated.

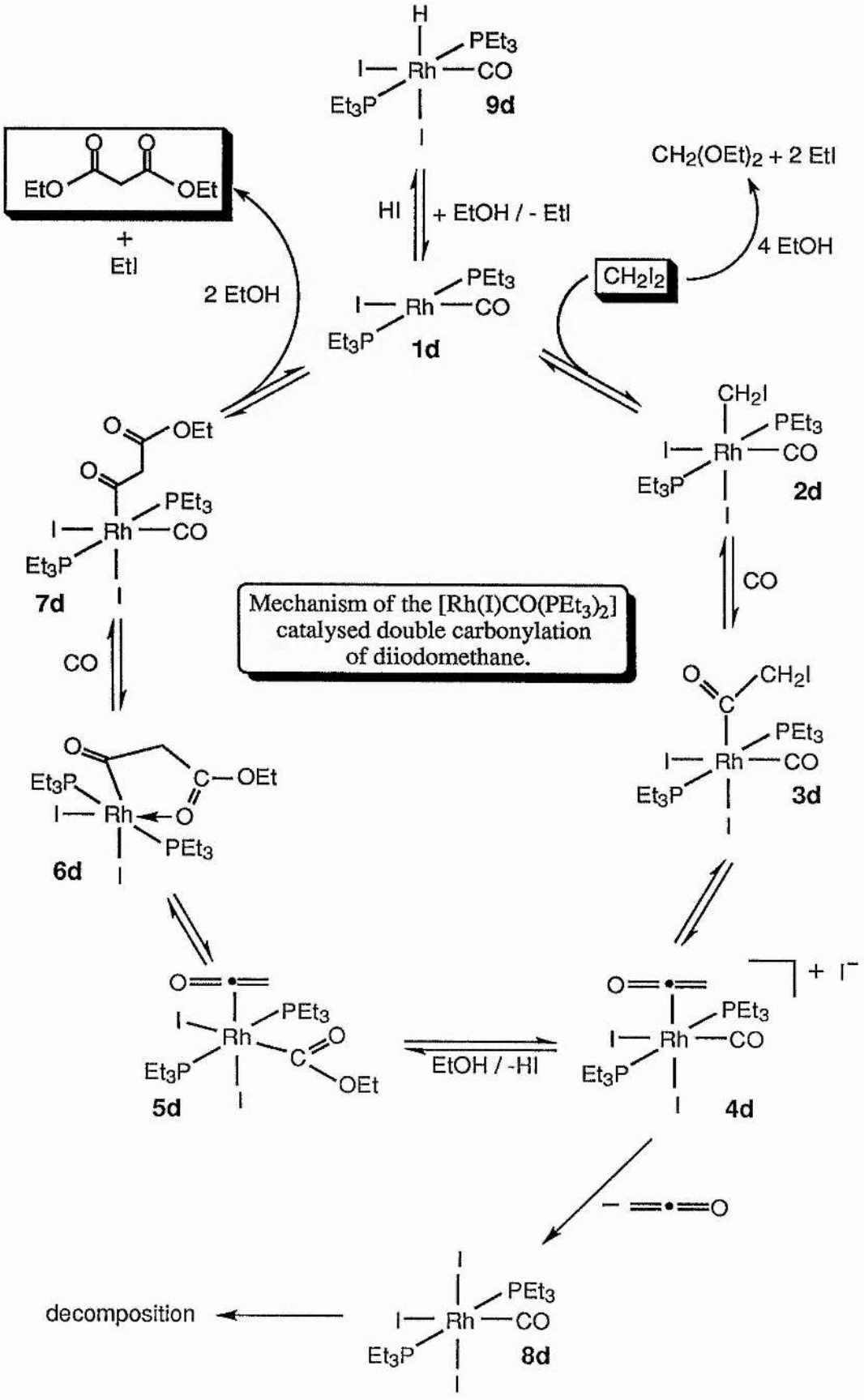
Mechanism of the [Rh(I)CO(PEt3)2] catalysed double carbonylation of diiodomethane.
9d
1d
2d
3d
4d
5d
6d
7d
8d
HI
+ EtOH / - EtI
2 EtOH
+ EtI
CH2(OEt)2 + 2 EtI
4 EtOH
CH2I2
CO
EtOH / -HI
decomposition

Figure 3.0.1

The reaction of $[Rh_2(OAc)_4]\cdot 2MeOH$ with 6 PEt_3 in CH_3CH_2OD under 40 atm CO was followed by ^{31}P NMR spectroscopy in-situ using a sapphire HP-NMR cell. The deuterium label in the ethanol was used to provide a lock for the NMR instrument. After the reaction solution was transferred under an inert atmosphere to the HP-NMR cell it was pressurised to 40 atm with CO. The ^{31}P NMR spectrum of this solution at room temperature is shown in figure 3.1.1 and the tentative assignments of the data summarised in table 3.1.1.

Chemical Shift δ / ppm	Assignment	Coupling J / Hz	Assignment
54.4 (s)	O**P**Et_3	-	-
22.7 (dd)	OC·$[Rh_2(OAc)_4]$·**P**Et_3	12.3 109.9	$J^2_{Rh\text{-}P}$ $J^1_{Rh'\text{-}P}$
21.3 (dd)	Et_3**P**·$[Rh_2(OAc)_4]$·**P**Et_3	30.5 128.2	$J^2_{Rh\text{-}P}$ $J^1_{Rh\text{-}P}$

Table 3.1.1: ^{31}P NMR Data from the reaction of $[Rh_2(OAc)_4]\cdot 2MeOH$ with 6 PEt_3 in CH_3CH_2OD under 40 atm CO after a few minutes at room temperature.

The initial reaction at room temperature appears to be the substitution of the axial solvent molecules on the rhodium dimer by either CO or PEt_3 which are better ligands than MeOH or EtOH.

The reaction was then heated (in-situ) to 373K for 2 hours and a second ^{31}P NMR spectrum recorded. The spectrum was now much simplified and is shown in figure 3.1.2. It consisted of two signals; δ = 53.4(s) ppm (from $OPEt_3$) and δ = 22.5(d) ppm ($J_{P\text{-}Rh}$ = 124.6 Hz). Upon cooling the sample back to 300K the same ^{31}P NMR signals were observed with the doublet slightly shifted to δ = 22.2(d) ppm ($J_{P\text{-}Rh}$ = 123.7 Hz). A single doublet with a splitting of 70-130 Hz is characteristic of either a mono-phosphine rhodium(I) complex or a trans-bis-phosphine rhodium(I) complex (^{103}Rh, I = 1/2). In order to discover the exact nature of the sole rhodium phosphine species formed under these conditions a complementary synthetic reaction was carried out.

When dissolved in ethanol $[Rh_2(OAc)_4]$ gives a green / blue coloured solution, upon addition of PEt_3 (4 equivalents wrt Rh) the solution turns red. Bubbling CO through this solution for 30 min at room temperature yields a bright yellow solution characteristic of Rh(I). The oil isolated from this solution was purified at low

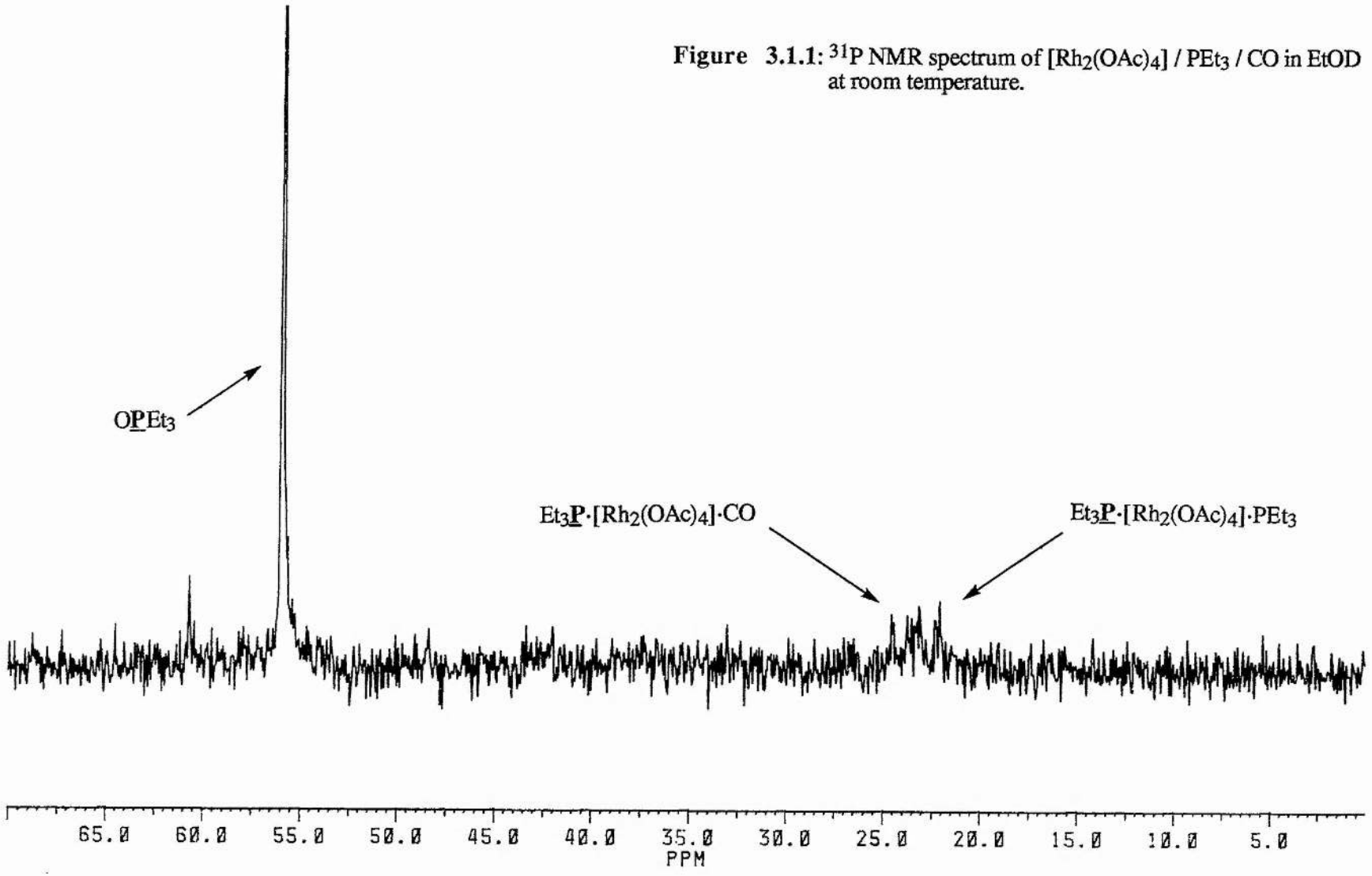

Figure 3.1.1: ^{31}P NMR spectrum of $[Rh_2(OAc)_4]$ / PEt_3 / CO in EtOD at room temperature.

Figure 3.1.2: ^{31}P NMR spectrum of $[Rh_2(OAc)_4]$ / PEt_3 / CO in EtOD after 2 hr at 373K.

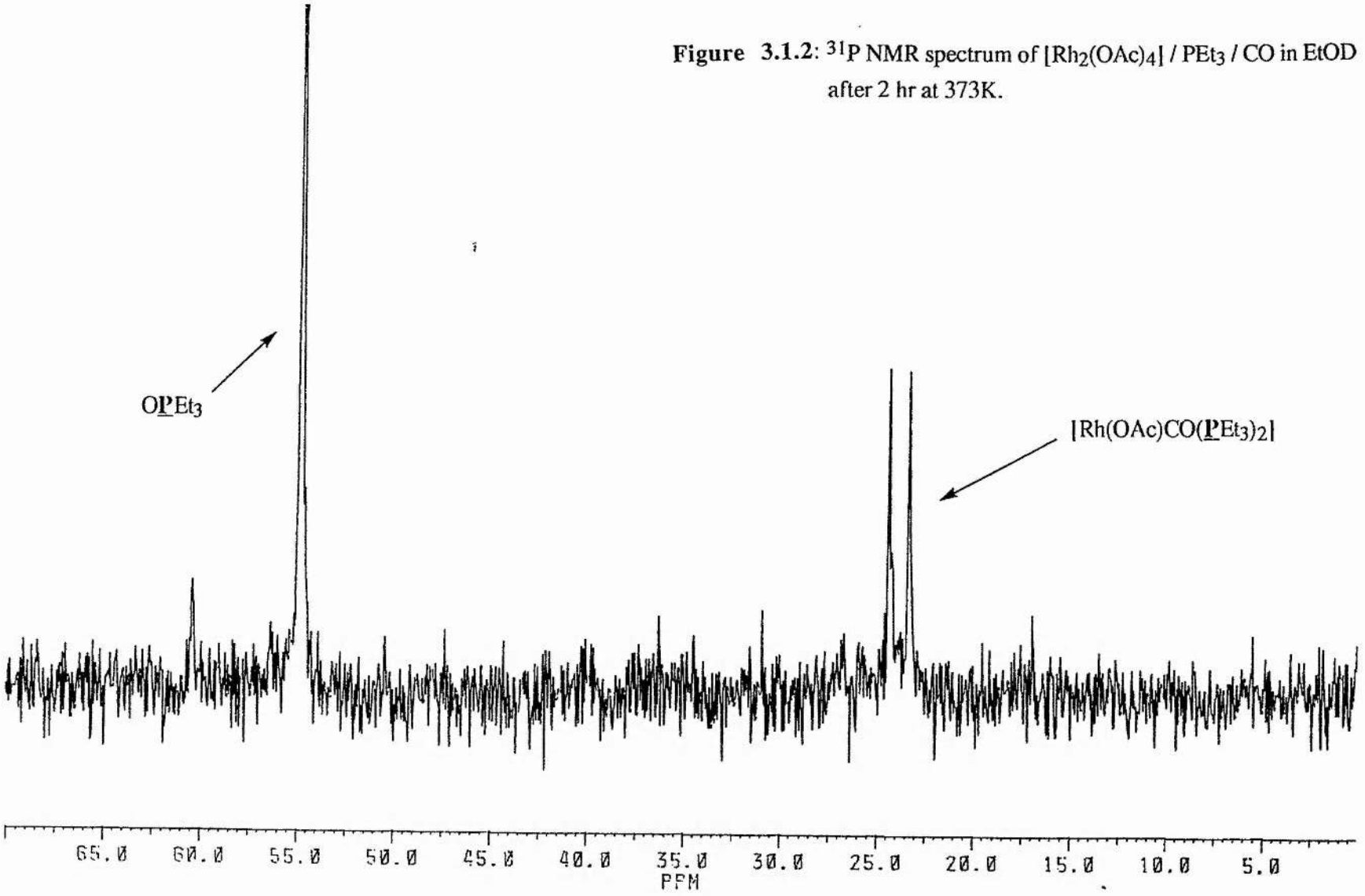

temperature yielding [Rh(OAc)CO(PEt$_3$)$_2$] (**1a** - 75% yield). The species was characterised by ^{31}P, ^{13}C, ^{1}H NMR spectroscopy and microanalysis. The ^{31}P NMR spectrum of this species matched the doublet observed in the in-situ HP-NMR experiment establishing that [Rh(OAc)CO(PEt$_3$)$_2$] (**1a**) is the species formed from the catalyst precursors under the conditions of the catalytic reaction.

Throughout this project the lability of the anions on Rh(I) and Rh(III) trans-bis-phosphine complexes has become obvious; evidence of this is presented in this chapter and chapter four and has also been widely reported in the literature.[118,142,143] Thus, in the presence of the high iodide concentration found in the catalytic reaction the active catalytic species is expected to be [Rh(I)CO(PEt$_3$)$_2$] (**1d**) rather than its acetate analogue. Evidence from ^{31}P NMR 'snapshots' of the actual catalytic system at different times during the reaction supports this and is presented in chapter four (section 4.6). Both **1a** and **1d** were shown in chapter two (section 2.2) to catalyse the double carbonylation of CH_2I_2 and to give identical product distributions when used in separate catalytic runs.

3.2 The Synthesis of [Rh(X)CO(PEt$_3$)$_2$] (X = Cl, Br, I)

The synthesis of the halide analogues of **1a**, [Rh(X)CO(PEt$_3$)$_2$] (X = Br (**1b**), Cl (**1c**) and I (**1d**)) has been achieved by methods subtly adapted from those reported for the synthesis of **1c** and **1d** by Chatt and Shaw.[143] Crude **1c** can be synthesised by the method described, but is best recrystallised from diethyl ether rather than the aqueous methanol suggested. This preparation has been found to be the highest yielding, the most time efficient and cost effective of those investigated. What makes this preparation particularly cost effective is that the yield of pure **1c** obtained is unaffected by the use of cheaper low grade $RhCl_3 \cdot 3H_2O$. **1d** is obtained in quantitative yield by the metathesis of **1c** using NaI in dry acetone and **1b** using LiBr in place of NaI.[143]

3.3 The oxidative addition of diiodomethane to [Rh(X)CO(PEt$_3$)$_2$]

Having established the active catalytic species as [Rh(X)CO(PEt$_3$)$_2$] the oxidative addition of CH_2I_2 to **1a**, **1c**, and **1d** was investigated. This constitutes the first step in the proposed reaction mechanism.

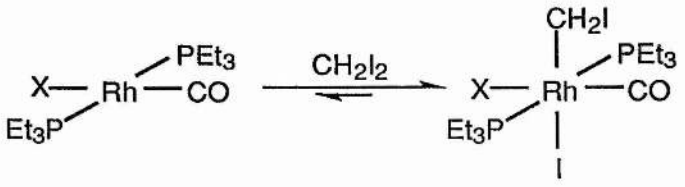

1 2

3.3.1 The reaction of [Rh(Cl)CO(PEt$_3$)$_2$] (**1c**) with diiodomethane

The results of an investigation into the synthesis and reactivity of **1c** has been published by Gash et al.[118] After several failed attempts to repeat the synthesis of [RhCl(I)(CH_2I)CO(PEt$_3$)$_2$] (**2c**) from **1c** and CH_2I_2 this reaction was studied in-situ by ^{31}P / ^{1}H VT-NMR spectroscopy. The spectra from this in-situ reaction are shown in figure 3.3.1.

To a solution of **1c** (in a NMR tube) in CD_2Cl_2 at 213 K (-60 °C) was added 0.96 equivalents of CH_2I_2 and this was examined by ^{31}P NMR spectroscopy at 213 K. At 213 K only the starting material (**1c**) was observed. Upon warming a second doublet due to [RhCl(I)(CH_2I)CO(PEt$_3$)$_2$] (**2c**), the expected product, was observed. Upon further warming to 283 K, then 313 K, **2c** continued to form as the sole product of the reaction, but its rate of formation was observed to be slow. When the sample was heated to 343 K for 70 min the product distribution changed dramatically. No longer was **2c** the only observed product as can been seen from figure 3.3.1. The predominant Rh(III) species now contained the chloromethyl rather than iodomethyl unit, the products being formed by isomerisation of **2c**; [RhI$_2$(CH_2Cl)CO(PEt$_3$)$_2$] (**2g**) and isomerisation followed by halogen scrambling; [RhCl(I)(CH_2Cl)CO(PEt$_3$)$_2$] (**2h**), [RhCl$_2$(CH_2Cl)CO(PEt$_3$)$_2$] (**2i**) and [RhI$_2$(CH_2I)CO(PEt$_3$)$_2$] (**2d**). Also observed was [RhCl(I$_2$)CO(PEt$_3$)$_2$] (**8c**), which was presumably formed from **2c** via the loss of 'CH_2'. Although the initial species **2c** was still predominant a large amount of [Rh(I)CO(PEt$_3$)$_2$] (**1d**) was also observed, possibly formed as part of the halogen scrambling process or via reductive elimination of ICH_2Cl from **2c**, **2g** or **2h** or ICl from **8c**. Similar halogen exchange reactions have previously been reported.[118]

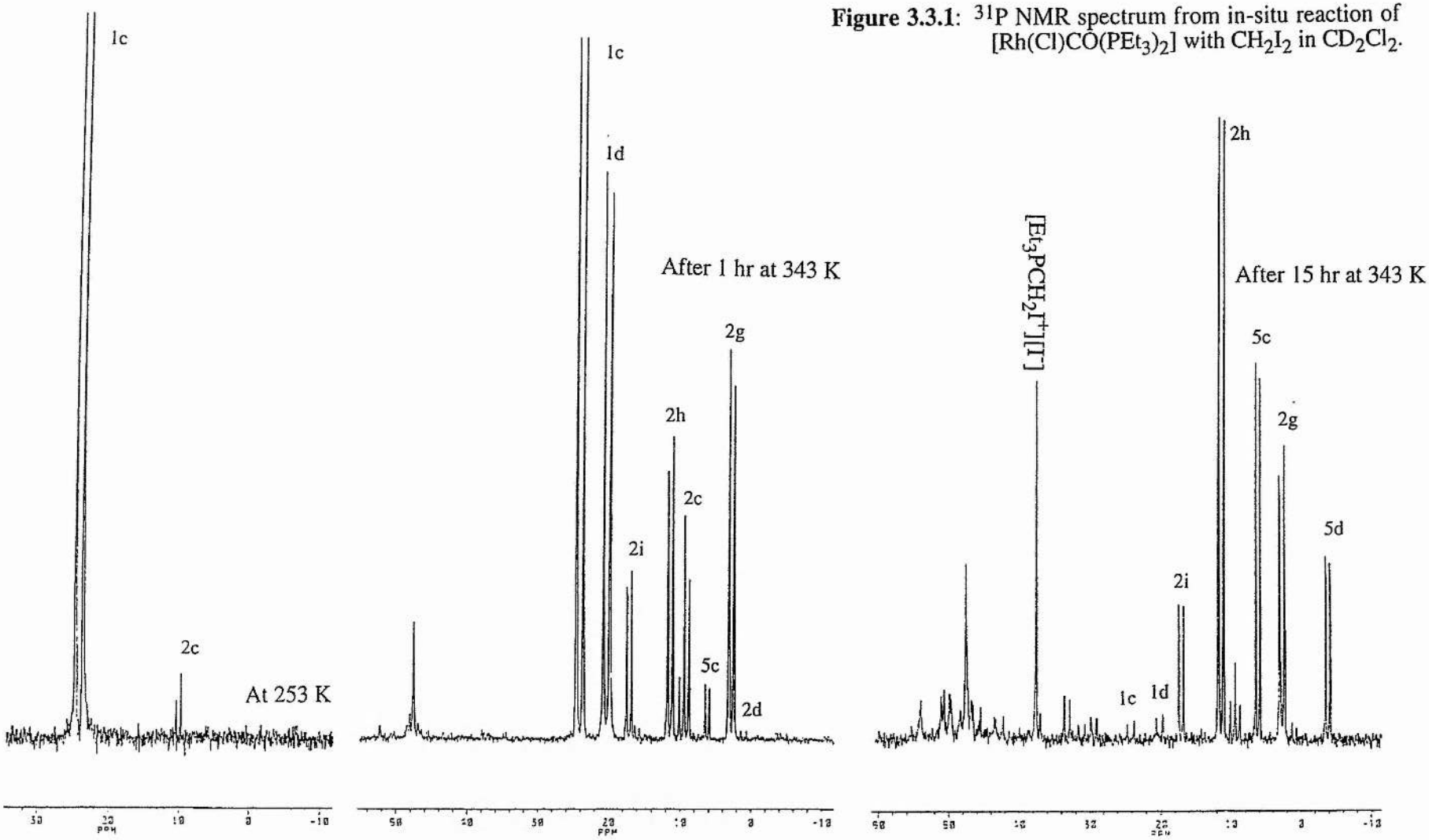

Figure 3.3.1: ^{31}P NMR spectrum from in-situ reaction of $[Rh(Cl)CO(PEt_3)_2]$ with CH_2I_2 in CD_2Cl_2.

When the sample was heated to 343 K for a further 14 hours complete conversion of the CH_2I_2 was observed and only very minor amounts of Rh(I) species were still present in the sample. The major product class present at this stage was still the Rh(III) chloromethyl species; **2h > 2g > 2i**. No Rh(III) iodomethyl species could be identified from the ^{31}P / ^{1}H spectra. Apart from small amounts of residual Rh(I) (**1c** & **1d**) the other two identified products were of the type $[RhI_2(X)CO(PEt_3)_2]$; **8c > 8d**.

These in-situ study results point to $[RhCl(I)(CH_2I)CO(PEt_3)_2]$ (**2c**) being the kinetic product from the reaction of **1c** and CH_2I_2. Chloromethyl complexes **2g-i** are clearly the thermodynamically favoured products. The loss of 'CH_2' from the initially formed halomethyl complexes is observed to yield tri-halo species of the type $[RhI_2(X)CO(PEt_3)_2]$; **8c > 8d**. It should be noted that only tri-halo products **8c-d** and not $[RhCl_2(X)CO(PEt_3)_2]$ (X = Cl (**8a**), I (**8b**)) are observed. This product distribution may imply that 'CH_2' is lost solely from Rh-CH_2I species **2c,d,f** and not from the more thermodynamically stable Rh-CH_2Cl species **2g-i**. Unfortunately the complex halogen scrambling reactions which occur in the overall reaction makes it impossible to be certain of this hypothesis.

The halogen scrambling reactions of complexes of the type **2a-i** are known to be favoured in polar solvents[118] and at elevated temperatures (see above) thus the clean synthesis of **2c** from **1c** + CH_2I_2 should be best achieved at room temperature and in a non-polar solvent. This is precisely the procedure of Gash et al,[118] the previous failures to repeat this procedure were found to be due to attempting to carry out the reaction at too small a scale. When the reaction is carried out using at least a 0.5 g (1.3 mmoles) (**1c**) scale the reaction is clean (at or below 40 °C) and goes to completion at room temperature in 24 hours; it is the difficulty in isolating **2c** from solution which leads to low yields (26-29%).

3.3.2 The reaction of $[Rh(OAc)CO(PEt_3)_2]$ (1a) with diiodomethane

A 50 fold excess of CH_2I_2 was added to a solution of **1a** in THF and the reaction stirred in the dark under a nitrogen atmosphere for 18 hours. Removal of the solvent gave an orange oil which was analysed by NMR. Three products were identified by ^{31}P NMR spectroscopy . The two major species were characterised by ^{31}P / ^{13}C / ^{1}H NMR spectroscopy as the isomers **2a** and **2b**, shown in figure 3.3.2, the third species could not be characterised.

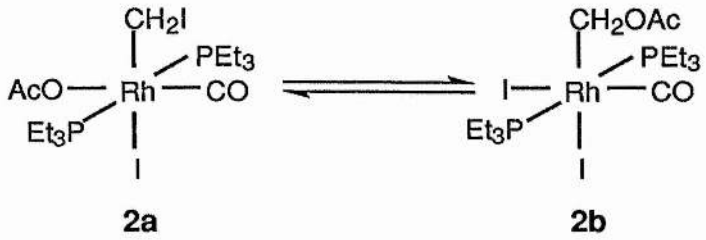

2a **2b**

Figure 3.3.2: Major products from the reaction of **1a** with CH_2I_2.

Given that **2a** and **2b** are isomeric they are presumably in equilibrium in solution. In an attempt to synthesise a pure Rh(III) iodomethyl complex the reaction of [Rh(I)CO(PEt_3)$_2$] with CH_2I_2 was investigated as the isomerisation seen between **2a** and **2b** would not be observed as both 'anions' are iodide.

3.3.3 The reaction of [Rh(I)CO(PEt_3)$_2$] (**1d**) with diiodomethane

A 50 fold excess of CH_2I_2 was added to a solution of **1d** in THF and the reaction stirred in the dark under a nitrogen atmosphere for 18 hours. Removal of the solvent gave an orange oil which was analysed by NMR. In addition to residual starting material, three products were identified by ^{31}P NMR spectroscopy. These species were characterised by ^{31}P / ^{13}C / ^{1}H NMR spectroscopy as **8d** and the isomers **2d** and **2e** shown in figure 3.3.3.

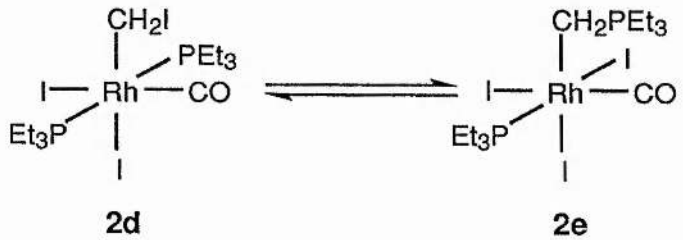

2d **2e**

Figure 3.3.3: The isomeric products from the reaction of **1d** with CH_2I_2.

Again the selective synthesis of the desired species (ie **2d**) was not achieved, with the isomerisation of **2d** to the ylide **2e** being observed. The ^{31}P NMR spectrum of **2e** consists of a doublet (δ = -1.9 ppm; $J_{Rh\text{-}P}$ = 78 Hz) due to the phosphine on the metal and a singlet (δ = 49.3 ppm) due to the phosphorus ylide. The carbon and hydrogen nuclei of the 'CH_2' unit of the ylide are observed as a doublet of doublets of doublets (ddd) in both the ^{13}C and ^{1}H NMR spectra respectively. These splitting patterns are generated by coupling to both rhodium and to two inequivalent phosphorus atoms.

An analogous equilibrium between an iodoacyl iodide and the isomeric ylide complex has been observed by Werner[144] for the complex [CpRhI(CH_2I)PMe_3]. He suggests that on such Rh(III) species it is the most nucleophilic species on the metal (or from solution) that will exchange with the methylene substituent. This would suggest that the nucleophilicity of the ligands used here increases in the order I < PEt_3 < OAc. The product mixture from the reaction of **1a** with CH_2I_2 consisted of **2a** and **2b** in approximately equal amounts (assessed by the peak areas in the ^{31}P NMR spectrum). When a solution of **2d** and **2e** is studied by ^{31}P NMR spectroscopy and heated in-situ the intensity of the signal for **2d** is seen to decrease in favour of **2e** and by loss of 'CH_2' to form [$RhI_3(CO)(PEt_3)_2$]. A similar loss of 'CH_2' was also observed by Werner. This loss of 'CH_2' could occur with the subsequent formation of ethylene but neither Werner nor ourselves have ever detected ethylene as a result of such a transformation.

3.4 The reaction of [RhCl(I)(CH_2I)$CO(PEt_3)_2$] with Me_4NCl

Since halogen scrambling reactions of [RhXY(CH_2Z)$CO(PEt_3)_2$] (X, Y, Z = halide) are known to be facilitated in polar solvents[118] the synthesis of [$RhCl_2(CH_2Cl)CO(PEt_3)_2$] (**2i**) from [RhCl(I)(CH_2I)$CO(PEt_3)_2$] (**2c**) and Me_4NCl in MeOH was attempted. The reagents were stirred, in the dark, under nitrogen for 25 hours and then the non-ionic rhodium species extracted into Et_2O. After attempts to crystallise the product failed, the solvent was removed to yield an orange oil which was re-dissolved in CD_2Cl_2 and analysed by ^{31}P / ^{1}H NMR spectroscopy. The ^{31}P NMR spectrum revealed, in addition to residual starting material, one major product δ = 17.1 ppm (J_{Rh-P} = 82 Hz) and two minor products δ = 24.2 ppm (J_{Rh-P} = 116 Hz), δ = 11.5 ppm (J_{Rh-P} = 82 Hz). This ^{31}P NMR spectrum is shown in figure 3.4.1. The ^{1}H NMR spectrum revealed two doublets of triplets at around 4 ppm, characteristic in position and couplings to the chloromethyl group of [RhXY(CH_2Cl)$CO(PEt_3)_2$] (X, Y = Cl, I) and another at 3.4 ppm. These species could all be identified with reference the ^{31}P NMR library resulting from this project and the work of Gash et al.[118] The major product was identified from its ^{31}P / ^{1}H signals as [$RhCl_2(CH_2Cl)CO(PEt_3)_2$] (**2i**) and the two other species as: [Rh(Cl)$CO(PEt_3)_2$] (**1c** - 24.2(d) ppm) and [RhCl(I)(CH_2Cl)$CO(PEt_3)_2$] (**2h** - 11.4(d) ppm). The assignment of the doublet δ_P = 17.1 ppm to **2i** is contrary to the assignment of Gash et al who claimed this species to be [RhI(Cl)(CH_2Cl)$CO(PEt_3)_2$] where I is trans to CH_2Cl. They report that the reaction between **1c** and ICH_2Cl gives two products and their suggestion was that ^{31}P NMR shift should move significantly down field for the species where I was trans to CH_2Cl with respect to the structural

Figure 3.4.1: ^{31}P NMR spectrum of product mixture from reaction of $[RhCl(I)(CH_2I)CO(PEt_3)_2]$ with Me_4NCl in MeOH (recorded in CD_2Cl_2).

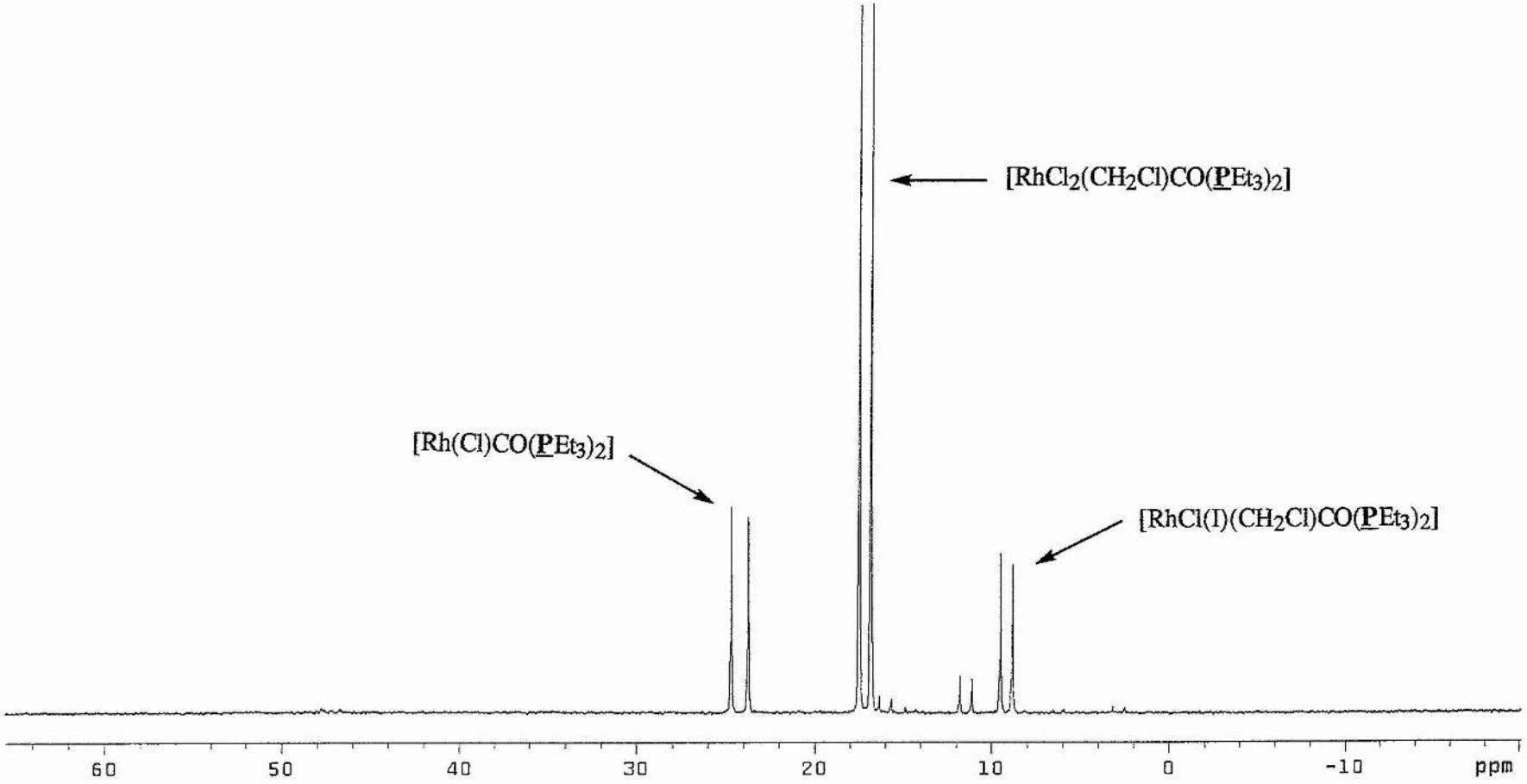

isomer where Cl was trans to CH_2Cl. This suggestion seems without precedent, and since this synthetic reaction was carried out in the presence of excess chloride in a polar solvent δ_P = 17.1 ppm was reassigned as the all chloride species **2i**. A sample of **2i** was required to study its reaction with CO and since **2i** was the major product (63%) and all the contaminants were well known species this crude oil was used without further purification - see section 3.5 below.

3.5 The reaction of $[RhX_2(CH_2Cl)CO(PEt_3)_2]$ (2)with CO

Unlike Rh(III) iodoacyl species (**3d-e**), the chloroacyl species **3c** is stable towards β-chloride elimination at room temperature (see section 3.6.2). Thus, it should be possible to observe directly the insertion of CO into a Rh-CH_2Cl bond because the product is known (at room temperature) to be stable towards further reaction. Since purification of Rh-CH_2X species has proved problematic, a sample of crude $[RhCl_2(CH_2Cl)CO(PEt_3)_2]$ (**2i** - see section 3.4) was studied by ^{31}P / ^{1}H HPVT-NMR spectroscopy under 50 atm CO.

No changes in the ^{31}P / ^{1}H spectra were observed upon heating the sample, in 20-30 K stages, up to 340 K (67 °C). After cell re-pressurisation followed by sustained heating of the sample at 370 K the major new species observed by ^{31}P NMR spectroscopy gave rise to a doublet at 19.3 ppm (J_{Rh-P} = 70 Hz). These ^{31}P NMR parameters match those for $[RhCl_3CO(PEt_3)_2]$ (**8a**). The final ^{31}P NMR spectrum is shown in figure 3.5.1. Examination of this solution by ^{1}H NMR spectroscopy reveals a decrease in signals due to Rh-CH_2X species (observed also in the ^{31}P spectrum) and new singlet at 4.60 ppm. This singlet comes in the characteristic region for the protons of the type $XC\underline{H}_2COY$ but it is not due to $ClC\underline{H}_2COCl$ (δ_H = 4.55 ppm) or $[RhCl_2(COC\underline{H}_2Cl)CO(PEt_3)_2]$ (δ_H = 4.67 ppm). Examination of the solution by IR spectroscopy shows 4 broad signals in the carbonyl region, 3 due to carbon monoxide ligands on Rh(I) and Rh(III) (2100-1900 cm^{-1}) and also a broad signal in the acyl region (1700 cm^{-1}). This suggested that there could be a [Rh]-$COCH_2X$ species present in solution, so the ^{13}C NMR spectrum was examined. The acyl carbonyl of species of the type [Rh]-$COCH_2X$ has been found to give a characteristic doublet of triplets at around 217 ppm. No multiplet in this region of the ^{13}C NMR spectrum was observed so it is unclear what interpretation of the other evidence should be. Given that the major organometallic species present at the end of the reaction was **8a**, the presence of diketene might be expected in the solution if **8a** had formed via a chloroacyl species. Signals due to diketene where not observed in the ^{13}C / ^{1}H spectra.

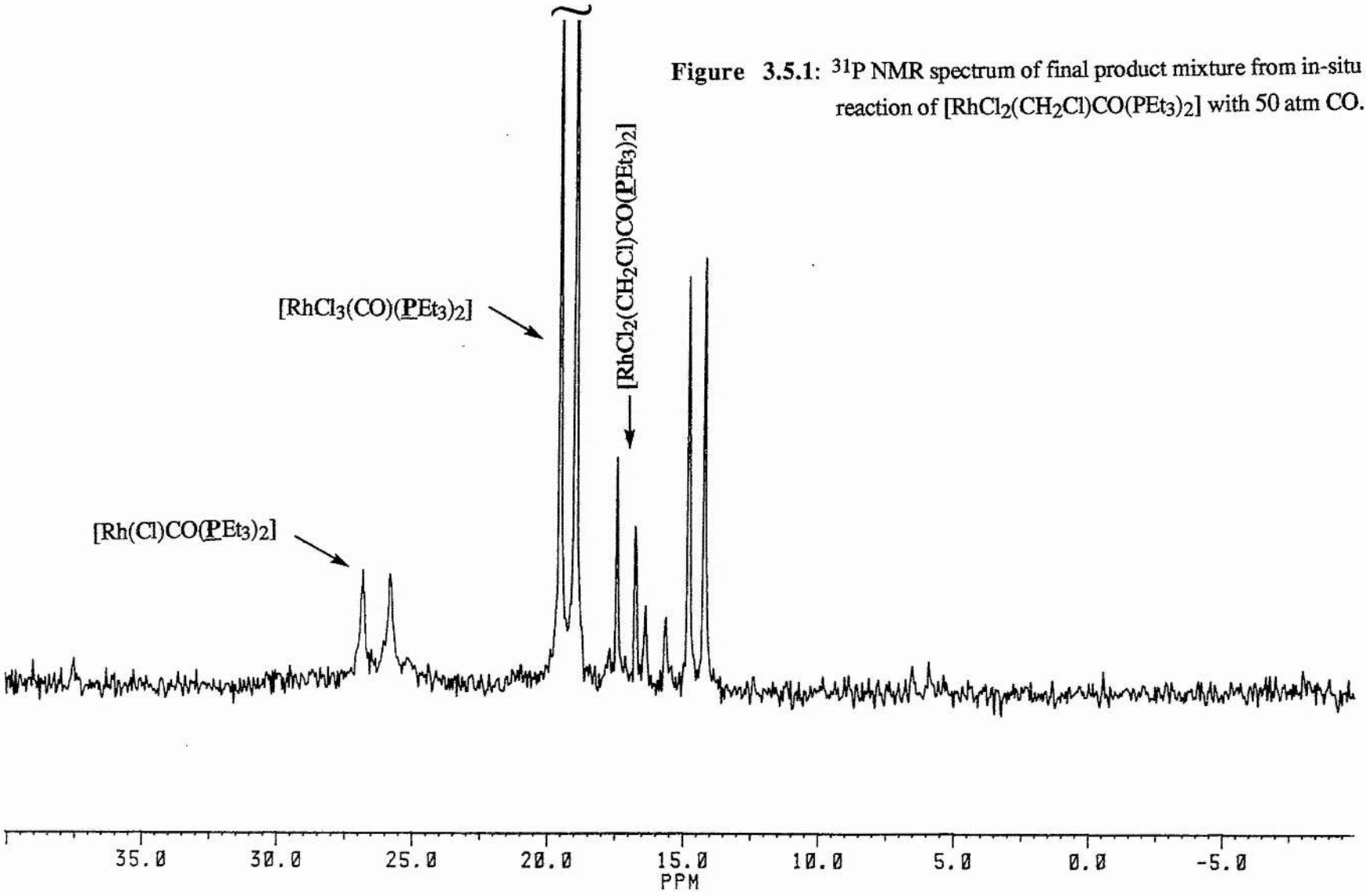

Figure 3.5.1: ^{31}P NMR spectrum of final product mixture from in-situ reaction of $[RhCl_2(CH_2Cl)CO(PEt_3)_2]$ with 50 atm CO.

Since the results of this in-situ experiment cannot be reasonably explained, future work could try a different approach towards the attempt to observe the conversion of **2i** to **3c**. One potential approach[103] would be to heat **3c** in an attempt to observe the entropy driven decarbonylation reaction yielding **2i**. An alternative approach would be remove the CO ligand from **2c** photochemically thus driving the chloroacyl ligand to de-carbonylate forming complex **2i** - these strategies are shown in figure 3.5.1.

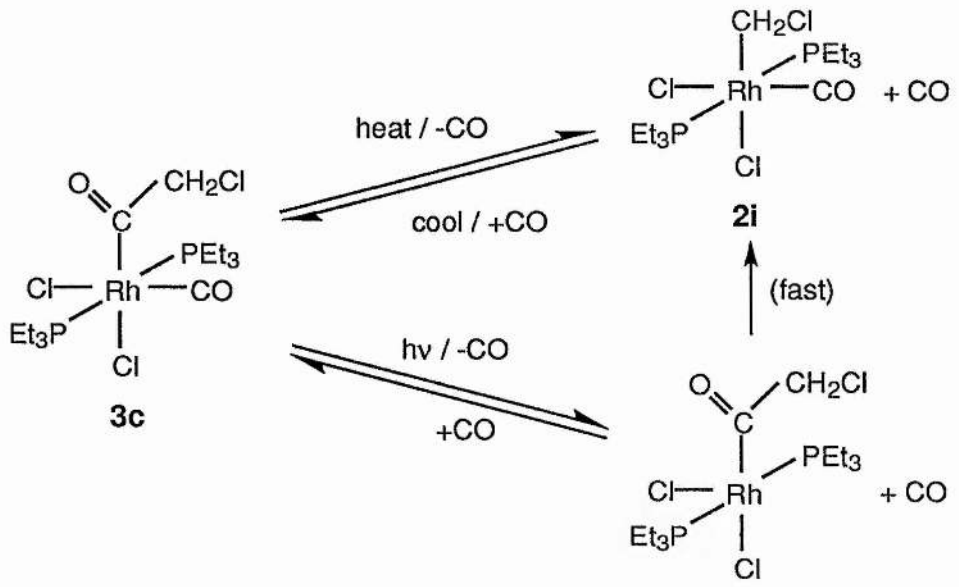

Figure 3.5.1: Potential routes to study the decarbonylation of complex **3c** followed as a method to allow observation of the reverse, carbonyl insertion reaction.

If this reaction were studied in-situ by HPVT-NMR under 1 atm CO then subsequent cooling of the reaction could allow for observation of the reformation of **3c** by the desired CO insertion reaction.

3.6 The direct synthesis of haloacyl species $[RhX_2(COCH_2X)CO(PEt_3)_2]$

According to the proposed catalytic cycle, the reaction of the iodomethyl intermediate **2d** with CO should yield an iodoacyl species $[RhI_2(COCH_2I)CO(PEt_3)_2]$ (**3d**).

3.6.1 The attempted synthesis of $[RhCl(I)(COCH_2I)CO(PEt_3)_2]$ (3e)

In an effort to model intermediate **2d** the synthesis of $[RhCl(I)(COCH_2I)CO(PEt_3)_2]$ (3e) was attempted[145] by the stoichiometric reaction of $[Rh(I)CO(PEt_3)_2]$ **1d** with ICH_2COCl (iodoacetyl chloride). The product of this reaction was not **3e** as expected but was instead a mixture of rhodium tri-halo species (**8**). Close examination of the

^{13}C / ^{1}H NMR spectra of the crude reaction products revealed the presence of diketene. The most probable mechanism[146] to explain the formation of these products is shown in figure 3.6.1.

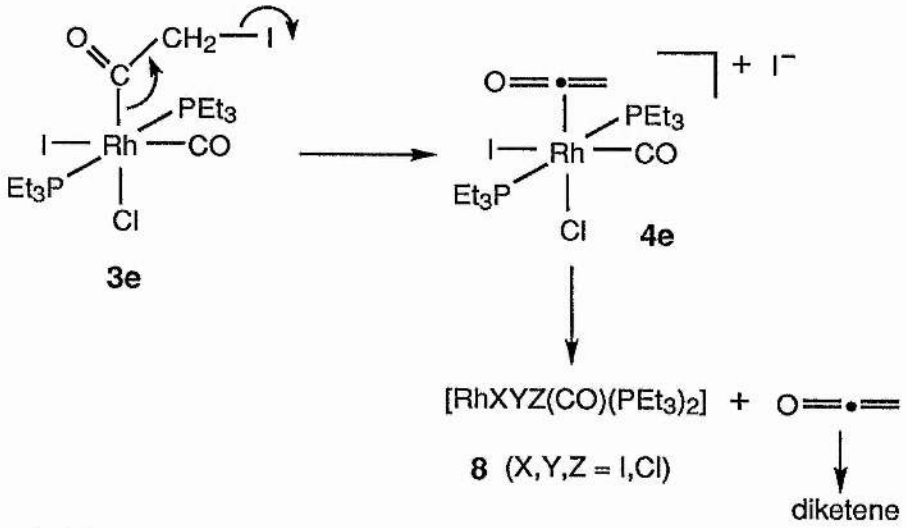

Figure 3.6.1

The oxidative addition of iodoacetyl chloride forms the desired iodoacyl species **3e** but this undergoes a β-iodide elimination to yield the ketene complex **4e** which decomposes releasing ketene. This work was carried out in CD_2Cl_2 which does not react with ketene, it thus dimerised because free ketene is not a stable species at room temperature. The interpretation of the reaction shown in figure 3.6.1 forms the cornerstone of the mechanism which is proposed for the catalytic reaction under investigation. Strong evidence from a range of sources, in addition to this, establishes the role of a metallo-ketene intermediate in this catalytic mechanism and this will be presented in sections 3.6.6, 3.9 below and in chapter four (sections 4.1 and 4.2).

3.6.2 The synthesis of $[RhCl_2(COCH_2Cl)CO(PEt_3)_2]$ (3c)

Since the decomposition of **3e** appears to be due to the weakness of the carbon-iodine bond it was reasoned that were this replaced with the stronger C-Cl bond then the resulting species may be stable towards β-halide elimination.

The reaction of **1c** with chloroacetyl chloride in CD_2Cl_2 was studied in-situ by ^{31}P / ^{1}H VT-NMR spectroscopy but this did not reveal anything unusual about the reaction. The trans oxidative addition occurs without any intermediates which are observable on the NMR time scale.

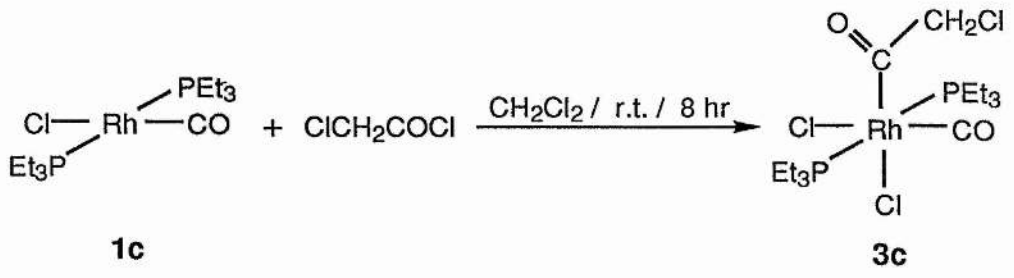

1c **3c**

Figure 3.6.2

The reaction of **1c** with a stoichiometric quantity of chloroacetyl chloride in CH_2Cl_2 gave, on work up, a pale yellow oil. Two recrystallisations from hot Et_2O gave $[RhCl_2(COCH_2Cl)CO(PEt_3)_2]$ as pale yellow crystals which were characterised as **3c** by ^{31}P / ^{13}C / ^{1}H NMR, IR and microanalysis. The crystals also proved of suitable quality for X-ray diffraction analysis, the crystal structure of **3c** is discussed in section 3.6.3.

3.6.3 The crystal structure of $[RhCl_2(COCH_2Cl)CO(PEt_3)_2]$ (3c)

The X-ray diffraction data was acquired at 220 K, yet unresolvable disorder in the ethyl groups of the phosphine ligands reduced the quality of fit of the solution to the diffraction data, giving a high R-factor (R = 0.164). The source of this disorder cannot yet be understood. Thus it is not possible to comment in detail upon the bond lengths and angles observed in the structure shown in figure 3.6.3. The structure shows the phosphine ligands to be trans and the chloroacyl moiety to be trans to a chloride rather than the CO ligand. This structure is consistent with the structure determined by the NMR and IR spectra.

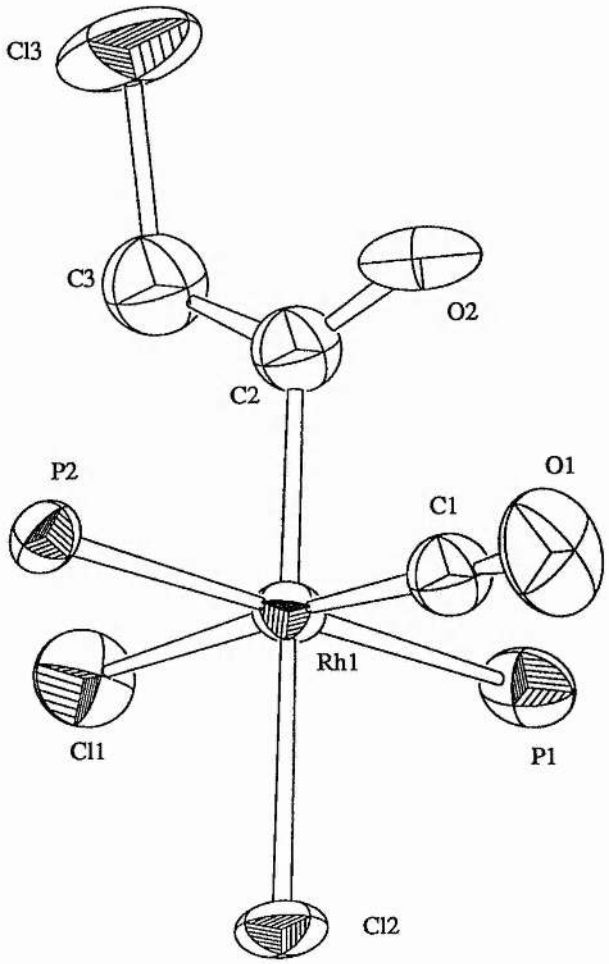

Figure 3.6.3: A simplified ORTEP plot of the structure of **3c**.

3.6.4 The synthesis of $[RhCl_2(COCH_2Cl)CO(PMe_3)_2]$

The quality of the data from X-ray structure of **3c** was greatly limited by the disorder of the ethyl groups of the two phosphine moieties. In an attempt to gain more accurate structural data about this important intermediate the trimethylphosphine analogue of **3c**

was synthesised. [Rh(Cl)CO(PMe$_3$)$_2$] was synthesised according to the method of Field and Partridge[147] and then reacted with chloroacetyl chloride in an analogous fashion to **3c**. The desired product [RhCl$_2$(COCH$_2$Cl)CO(PMe$_3$)$_2$] was characterised by ^{31}P / ^{13}C / ^{1}H NMR and IR. Unfortunately the initial crystals did not prove suitable for X-ray diffraction studies and a lack of time prevented attempts to grow suitable crystals.

3.6.5 The synthesis of [RhBr$_2$(COCH$_2$Br)CO(PEt$_3$)$_2$] (3b)

The synthesis of [RhBr$_2$(COCH$_2$Br)CO(PEt$_3$)$_2$] (**3b**) can be achieved in an analogous fashion to that of **3c** using a stoichiometric ratio of **1b** and bromoacetyl bromide. [RhBr$_2$(COCH$_2$Br)CO(PEt$_3$)$_2$] was isolated as orange powder and characterised by ^{31}P / ^{13}C / ^{1}H NMR, IR and microanalysis. **3b** can also be synthesised by the metathesis of **3c** with LiBr in acetone. The product of the metathesis reaction was identified as **3b** by ^{31}P / ^{13}C / ^{1}H NMR and IR.

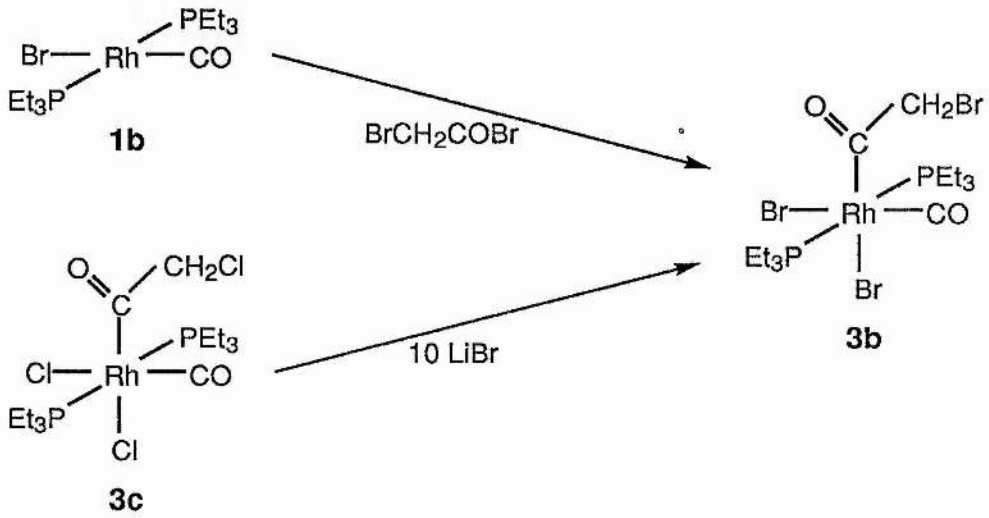

Figure 3.6.4: The two synthetic routes to complex **3b**.

3.6.6 The reaction/s of [RhCl$_2$(COCH$_2$Cl)CO(PEt$_3$)$_2$] (3c)with NaI

Since the synthesis of **1b**, **1d** and the bromoacyl species **3b** can be achieved by halide exchange from their chloro substituted analogues (**1c**, **3c**) an indirect synthesis of the mechanistic intermediate **3d** might perhaps be achieved the metathesis of **3c**.

Figure 3.6.5: ^{31}P NMR spectra from reaction of $[RhCl_2(COCH_2Cl)CO(PEt_3)_2]$ with NaI in acetone after various reaction times.

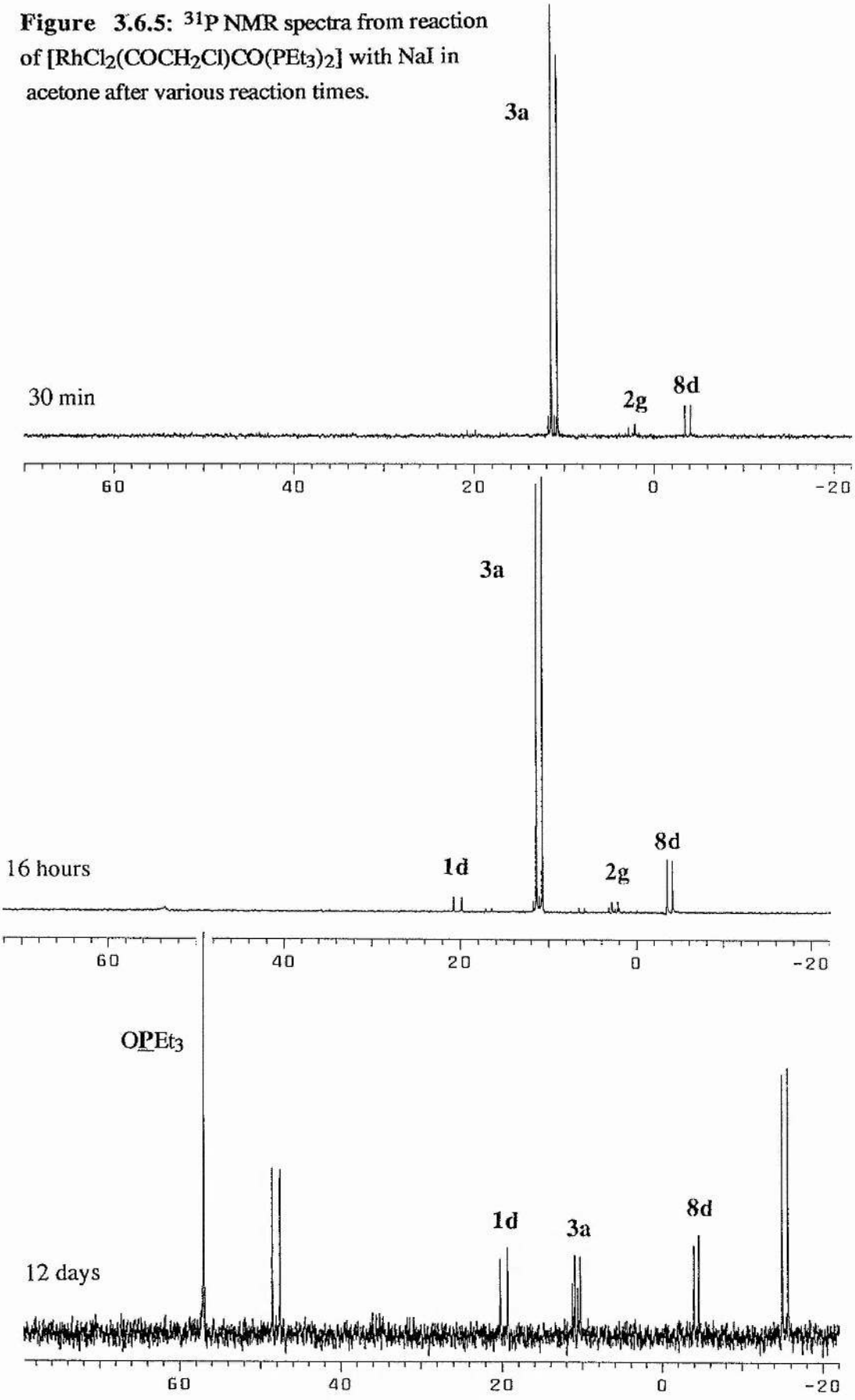

The reaction of $[RhCl_2(COCH_2Cl)CO(PEt_3)_2]$ (**3c**) with NaI (10 equiv.) in acetone was examined (following work-up and re-dissolution in CD_2Cl_2) by ^{31}P / ^{13}C / ^{1}H NMR spectroscopy after a 30 min, 16 hour and then a 12 day reaction time. These spectra are shown in figure 3.6.5.

After 30 min none of the starting material is observed by ^{31}P NMR spectroscopy (CD_2Cl_2), instead a major new species was observed giving a doublet at δ = 11.1 ppm (J_{Rh-P} = 84.5 Hz). A minor amount of $[RhI_3(CO)(PEt_3)_2]$ (**8d**), traces of $[Rh(I)CO(PEt_3)_2]$ (**1d**) and two other unknown species δ = 11.4 ppm (J_{Rh-P} = 83.0 Hz), δ = 2.5 ppm (J_{Rh-P} = 83.0 Hz) were also observed. The ^{1}H NMR spectrum reveals a strong singlet at 4.75 ppm characteristic of [Rh]-$COC\underline{H}_2Cl$ and thus the major product was characterised as $[RhI_2(COCH_2Cl)CO(PEt_3)_2]$ (**3a**) where the two chlorides on the metal have been exchanged for iodide but the chloroacyl unit remains intact. The minor products remain uncharacterised, but from their ^{31}P NMR data they could plausibly be $[RhCl(I)(COCH_2Cl)CO(PEt_3)_2]$ ((**3f**) - unknown at 11.4 ppm), a potential intermediate species in the synthesis of **3a** from **3c**, and $[RhI_2(CH_2Cl)CO(PEt_3)_2]$ (**2g** - 2.5 ppm). The ^{13}C NMR spectrum of this mixture contains small peaks in the alkyl region which are consistent with the chloromethyl group of **2g** (2 singlets at approx. 30 ppm)

After 16 hours the same solution was examined by ^{31}P NMR spectroscopy as described above. The major species was still **3a** (11.1 ppm) but the growth of the peaks due to **8d** and **1d** was observed. The relative intensities of the other species was not observed to change significantly. The reaction was then allowed to proceed for 12 days after which a significant change in the product distribution was observed by ^{31}P NMR spectroscopy. The major signals in the ^{31}P spectrum were now at 56.9(s) ppm ($OPEt_3$), 48.0(d) ppm, J_{Rh-P} = 117 Hz and -15.4(d) ppm, J_{Rh-P} = 83 Hz. The minor products were common to those observed after 16 hours, **1d**, **8d**, **3f** and residual $[RhI_2(COCH_2Cl)CO(PEt_3)_2]$ (**3a**). The two unknown species fall outside the ^{31}P NMR field range for any of the wide range rhodium bis-phosphine species identified during this or other work from within the group. The species at 48.0(d) ppm is tentatively characterised as a mono-phosphine species $Rh(PEt_3)L_n$ from: i) Its position and P-Rh coupling constant; ii) the observation of $OPEt_3$ (56.9 ppm) showing the break down of the bis-phosphine skeleton of one or more of the products. The nature of the species observed at -15.4 ppm remains a mystery. It is likely that is a Rh(III) trans-bis-phosphine species given: i) The reaction conditions and ii) a characteristic P-Rh(III) coupling constant of 83 Hz.

To identify the source of the species whose rhodium bis-phosphine skeleton was observed to break down in the above study the thermal stability of $[RhI_3(CO)(PEt_3)_2]$ (**8d**) in acetone was assessed. The ^{31}P NMR spectrum of **8d** in d^6-acetone at room temperature consists of one doublet at -2.6 ppm ($J_{P\text{-}Rh}$ = 77 Hz) as expected. After heating the sample to 100 °C for 1 hour the sample was re-examined by ^{31}P NMR spectroscopy. **8d** was still the major species in solution, but it had also decomposed / reacted to give 5 new species: Signals at 81.3(s) ppm, 48.7(d) ppm ($J_{Rh\text{-}P}$ = 117 Hz), 26.2 ppm ($J_{Rh\text{-}P}$ = 104 Hz), 22.0 ppm ($J_{Rh\text{-}P}$ = 115 Hz) and 14.2 ppm ($J_{Rh\text{-}P}$ = 80 Hz) were observed. The singlet at 81.3 ppm is assigned to $OPEt_3$ and the doublet at 22.0 ppm to **1d**. Both these species are observed in the metathesis reaction described above. The species responsible for the doublet at 48.7 ppm ($J_{Rh\text{-}P}$ = 117 Hz), allowing for a slight solvent shift from CD_2Cl_2 to d^6-acetone, was also observed in the initial metathesis reaction. The doublet at 26.2 ppm is probably due to another rhodium mono-phosphine species, given its coupling constant, but the doublet at 14.2 ppm remains as yet unassigned. These data show that **8d** is thermally unstable in acetone with respect to to loss of I_2 and PEt_3 which gives rise to **1d** and the uncharacterised mono-phosphine complexes observed in the reaction of **3c** with NaI after 12 days. A reaction scheme which summarises these results is shown in figure 3.6.6.

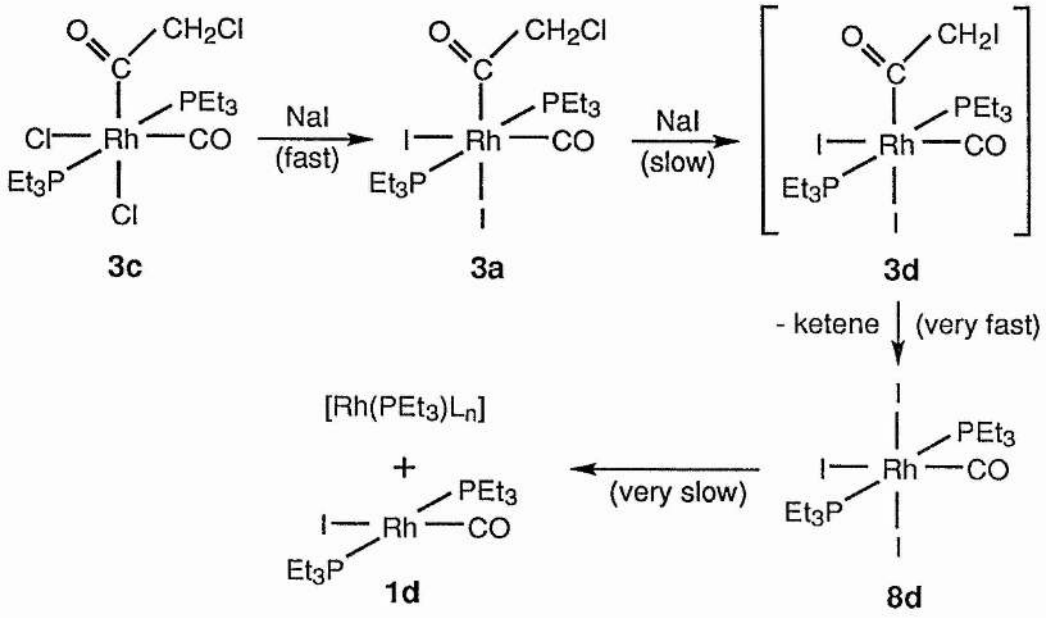

Figure 3.6.6: The reactions of complex **3c** with excess NaI over a 12 day period.

3.7 Attempted reaction of $[RhCl_2(COCH_2Cl)CO(PEt_3)_2]$ (**3c**) with $[Rh(Cl)CO(PEt_3)_2]$ (**1c**)

Since diiodomethane is a difunctional molecule, the possibility of a dimetallic catalytic mechanism had to be considered. The low concentration of organometallic species in homogeneous catalysis reactions might be thought to preclude the reaction between two metal centres, but one example is known. Evidence for the formation of di-rhodium complexes in the catalytic photochemical dehydrogenation of cyclohexane by $[RhCl(L)(PR_3)_2]$ (L = CO, H_2; R = Me, Cy) has attracted a number of studies of the role of di-metallic species in such catalysis.[148-150]

The reaction of either a rhodium iodomethyl complex or an iodoacyl complex with a Rh(I) centre are plausible and would potentially lead to the species shown in figure 3.7.1.

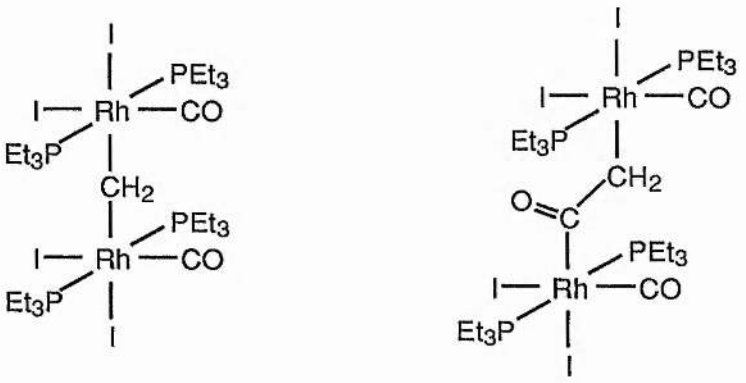

Figure 3.7.1

The reaction of iodomethyl species **3c** with $[Rh(Cl)CO(PEt_3)_2]$ (**1c**) has been studied previously and does not yield a di-rhodium methylene bridged species as might be expected.[133] Thus the reaction between the chloroacyl species **3c** and **1c** was investigated. A 1:1 mixture of **3c** and **1c** was stirred in CH_2Cl_2 for 19 hours. Work up of this reaction showed only the return of the starting materials. Since no reaction has ever been reported between dichloromethane and **1c** it is perhaps not surprising that the C-Cl bond of the chloroacyl complex did not undergo oxidative addition to the Rh(I) centre of **1c** either. Ideally the reaction between an iodoacyl species (ie **3d**) and a Rh(I) centre would be attempted, but the instability of iodoacyl species toward β-iodide elimination prevents this. A kinetic study of a catalytic reaction should prove to be the best method by which to determine whether a mono or dimetallic mechanism is operating. Unfortunately the rapid decrease in concentration of the active organo-rhodium species during this catalytic reaction due to their short lifetime makes kinetic data complex and difficult to obtain.

3.8 Attempts to model the metallo-ketene intermediate

It is the rapid β-iodide elimination from the iodoacyl complex **3d** which confers the high selectivity for this catalytic reaction. In all other examples of catalytic double carbonylation the product of the attack of a nucleophile upon the singly carbonylation organometallic intermediate is observed (see chapter one). It is this nucleophilic attack which yields the singly carbonated organic product, often in significant amounts, thus lowering the selectivity of the reaction. The product of a β-iodide elimination from $[RhI_2(COCH_2I)CO(PEt_3)_2]$ (**3d**) should be a Rh(III) ketene complex. The first attempted synthetic strategy to such a species is shown in figure 3.8.1.

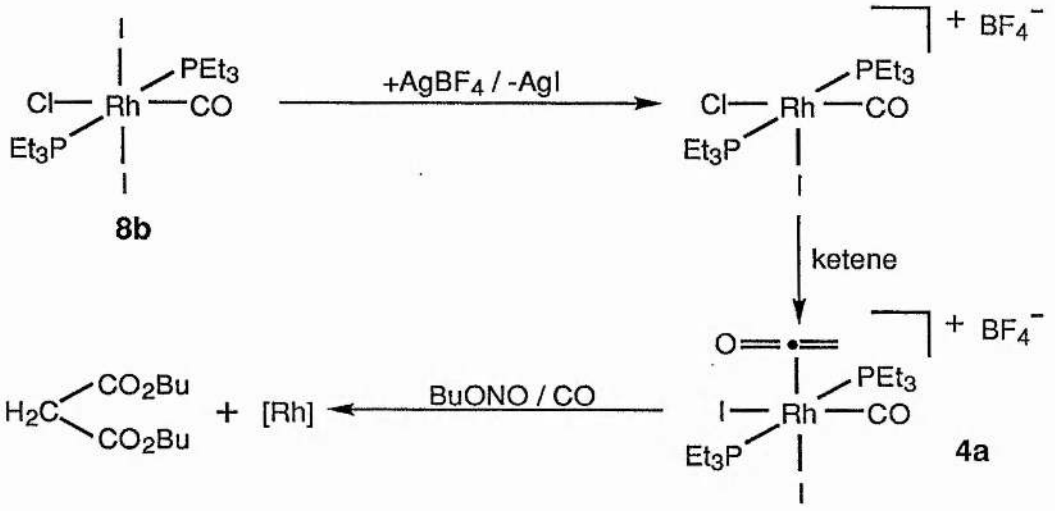

Figure 3.8.1: Potential route to the in-situ generation of complex **4a**.

The strategy was to introduce the reagents, **8b** / $AgBF_4$ / BuONO into an a cooled (-100 °C) autoclave and then to condense freshly prepared ketene into the vessel followed by the addition of 20 atm CO. Allowing the vessel to warm to room temperature would have boiled the ketene (T_b = -41 °C) allowing the reaction to occur. The hope was to observed dibutyl malonate in the product solution thus showing the intermediary of ketene in the $[Rh(X)CO(PEt_3)_2]$ catalysed synthesis of malonate esters from CH_2I_2. BuONO was chosen as a source of RO^- which would not react directly with ketene (unlike ROH). The use of n-butanol in a standard catalytic reaction was previously checked and found to be viable for the production of $CH_2(CO_2Bu)_2$ (chapter two, section 2.5). Ketene was freshly prepared by the pyrolysis of acetone. A number of attempts on this reaction failed to yield any $CH_2(CO_2Bu)_2$ (or related products) at the end of the reaction. This was probably due to the technical problems encountered with the o-rings required to seal the metal pressure vessel at below the boiling point of ketene (-41 °C). The autoclave leaked significant quantities of gas

past the o-ring seal at up to room temperature despite many attempts to cure the leaking with a variety of different o-rings. A potential solution to this was the use of a ketene with a higher boiling point, thus dimethylketene (T_b = 34 °C) was subsequently investigated.

Dimethylketene was synthesised by the thermal decomposition of dimethylmalonic anhydride[151]. Initially the reaction of dimethyl ketene with **8b** / $AgBF_4$ in CD_2Cl_2 was studied in-situ by ^{31}P / ^{13}C / ^{1}H VT-NMR spectroscopy starting the reaction at -78 °C and gradually warming the sample to room temperature. No reaction of **8b** was observed to occur. Since there was no reaction observed in the small scale low temperature experiment, the reaction was scaled up to a synthetic scale and a mixture of **8b**, $AgBF_4$ and dimethylketene (1:1:10) was stirred under N_2 in the dark for 16 hours. Work up yielded an oil which was examined by ^{31}P NMR spectroscopy. The ^{31}P spectrum showed a forest of signals in the region of δ = 35-55 ppm indicative of a breakdown of the rhodium bis-phosphine skeleton and no signals in the region where trans-bis-PEt_3 rhodium complexes are usually observed.

Since the direct reaction of Rh(III) species with a free ketene moiety did not prove a viable route to models of the metallo-ketene intermediate **4d** a new synthetic strategy was required. In the actual catalytic cycle the metallo-ketene intermediate **4d** is not formed by a direct reaction with free ketene, but by the intramolecular synthesis of the ketene ligand. The metallo-ketene intermediate **4d** is then either attacked by iodide to form the decomposition product **8d** or reacts with CO and continues within the catalytic cycle. If a model for **4d** is to have more than just a transient lifetime then the counter ion must not be able to displace the ketene ligand. A non-coordinating counter ion would fulfil this role. The reason why [Rh]-$COCH_2I$ (ie **4d**) species are unstable yet their chloro or bromo analogues are stable isolable species is due to the nature of the halide leaving group. If a species [Rh]-$COCH_2X$ could be synthesised where X was a good leaving group, yet a poor nucleophile then perhaps this could undergo a β-anion elimination yielding a stable metallo-ketene moiety. A possible example is illustrated in figure 3.8.2.

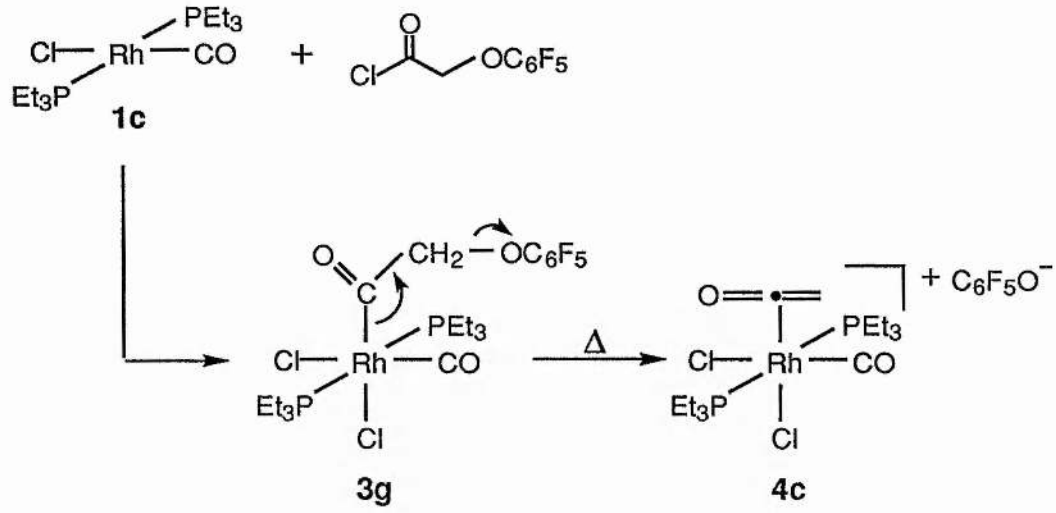

Figure 3.8.2: Potential synthetic route to a stable metallo-ketene complex **4c**.

A stoichiometric quantity of Cl-C(O)$CH_2OC_6F_5$ was added to a solution of **1c** in CD_2Cl_2 at 213 K and the reaction examined in-situ using ^{31}P / ^{1}H VT-NMR spectroscopy. As the temperature of the sample was increased the reaction of **1c** was observed to form a new doublet in the ^{31}P spectrum; δ = 16.5 ppm (J_{Rh-P} = 84 Hz). This doublet continued to grow with rising temperature at the expense of the doublet due to **1c**. The ^{1}H NMR spectra showed the growth of two multiplets in the alkyl region due to the formation of a new rhodium(III) bis-PEt_3 species. The intensity for the signal due to the methylene protons (5.1(s) ppm) in Cl-C(O)$CH_2OC_6F_5$ was observed to decrease at the expense of a new singlet at 4.8 ppm. The changes in the ^{31}P and ^{1}H NMR spectra were analogous to those observed in an earlier study of the oxidative addition of chloroacetyl chloride to **1c**. These changes indicate the formation of the oxidative addition complex **3g**. Prolonged heating (50 °C, 18 hr) of the sample only lead to an increased yield of **3g** and not to the formation of any new species observed by ^{31}P NMR spectroscopy. It is possible that the elimination of the perflurophenoxide leaving group was hindered by the low polarity of the solvent (CD_2Cl_2). d^8-THF was added to the sample and it was allowed to stand for 2 days after which ^{31}P NMR spectroscopy revealed the formation 5 new Rh(III) species but they were in too low a concentration to be identified. This study is very promising should be repeated in a more polar (aprotic) NMR solvent such as neat d^8-THF.

3.9 Indirect evidence for role of ketene as an intermediate

It was shown in section 3.6 that the complex [RhCl(I)($COCH_2I$)CO(PEt_3)$_2$] (**3e**) undergoes a rapid β-iodide elimination in CD_2Cl_2 which (in the absence of CO) yields

ketene, observed as its dimer. Ketene is known to react readily with alcohols, the product from its reaction with EtOH being EtOAc (ethyl acetate).[114,152] Thus if free ketene were ever present in a catalytic reaction traces of EtOAc should be observed amongst the products. Before it was possible to be sure that ketene was the source of the trace amount of EtOAc observed, all other potential sources of EtOAc had to be eliminated. It is known (chapter 2, section 2.11) that $[Rh(X)CO(PEt_3)_2]$ catalyses the synthesis of acetate esters from the carbonylation of MeI which is often found as a minor impurity in commercial CH_2I_2. Also standard catalytic runs use $[Rh_2(OAc)_4]\cdot 2MeOH$ as a catalyst precursor, this is another potential source of EtOAc. Thus a catalytic reaction was carried out using pre-synthesised $[Rh(I)CO(PEt_3)_2]$ as the catalyst, ethanol as the solvent and doubly distilled MeI free CH_2I_2 as the substrate. Traces of EtOAc were still observed in the product mixture.

The importance of the concentration of the EtOAc observed in this experiment and its bearing on the significance of ketene loss to catalyst decomposition is discussed in chapter four (section 4.1). To confirm ketene as the source of the EtOAc a labelling study was carried out, the rationale for this is shown in figure 3.9.1.

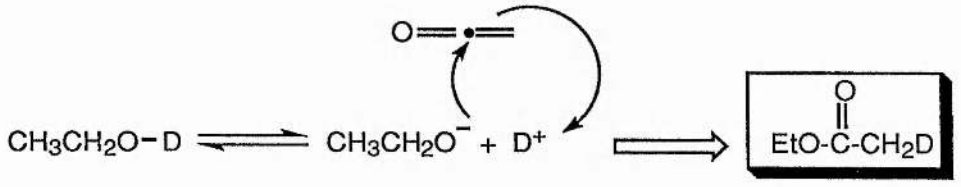

Figure 3.9.1: The reaction of ketene with CH_3CH_2OD.

Once again a catalytic system free of all sources of ethyl acetate (except ketene) was employed but with 1:1 toluene / d^1-EtOD as the solvent. After the reaction, the organic products were distilled from the spent catalyst and excess solvent and were examined by a series of NMR techniques. All the spectra are shown in figures 3.9.2 and 3.9.3. A ^{13}C NMR DEPT spectrum clearly showed a negative signal (associated with CH_2 groups) in the CH_3 region where all the other signals were positive. The signal for the $\underline{C}H_2D$ carbon should be a 1:1:1 triplet, only two of the three peaks were observed (at 75.5 MHz) with one of the peaks masked under a positive peak from the $\underline{C}H_3CH_2$- signal of another product species (ie EtI, EtOD or $CH_2(OEt)_2$). The $^2D\{^1H\}$ spectrum showed a singlet at 1.6 ppm indicative of a deuterium on the acetate methyl group of $CH_2DCO_2CH_2CH_3$. Final confirmation came from the comparison of 125.7 MHz $^{13}C\{^1H\}$ and $^{13}C\{^1H, ^2D\}$ spectra where the (now well resolved) 1:1:1 triplet in the $^{13}C\{^1H\}$ spectrum collapsed to a singlet in the $^{13}C\{^1H, ^2D\}$ spectrum as the ^2D coupling was lost.

The proposed mechanism for this reaction shows that, once formed, the ketene complex **4d** can either lose ketene to form **8d** and thus irreversibly leave the cycle or react with a second molecule of CO. The dependence of the catalyst TON on CO was shown in chapter two. There is plenty of precedence for invoking ketene as an intermediate in the double carbonylation of a geminal dihalide. Miyashita and co-workers have shown the involvement of a ketene complex in the double carbonylation of geminal dibromides by $[Co_2(CO)_8]$.[98-100] An account of the stoichiometric formation of malonate esters from both a di-palladium and a di-iron complex[112] when first reacted with CH_2I_2 then CO has been reported. Both of these reactions have been shown to go via ketene; This work is covered in depth in section 2.4 of chapter one.

Other reports have shown that ketene (pre-synthesised) can act as a precursor to malonate esters. Ube Industries of Japan[153-156] have published patents on the synthesis of malonate esters by the cobalt catalysed carbonylation of ketene in the presence of an alkyl nitrite (RONO). An alkyl nitrite is employed as a source of RO^- which does not react directly with the ketene substrate.

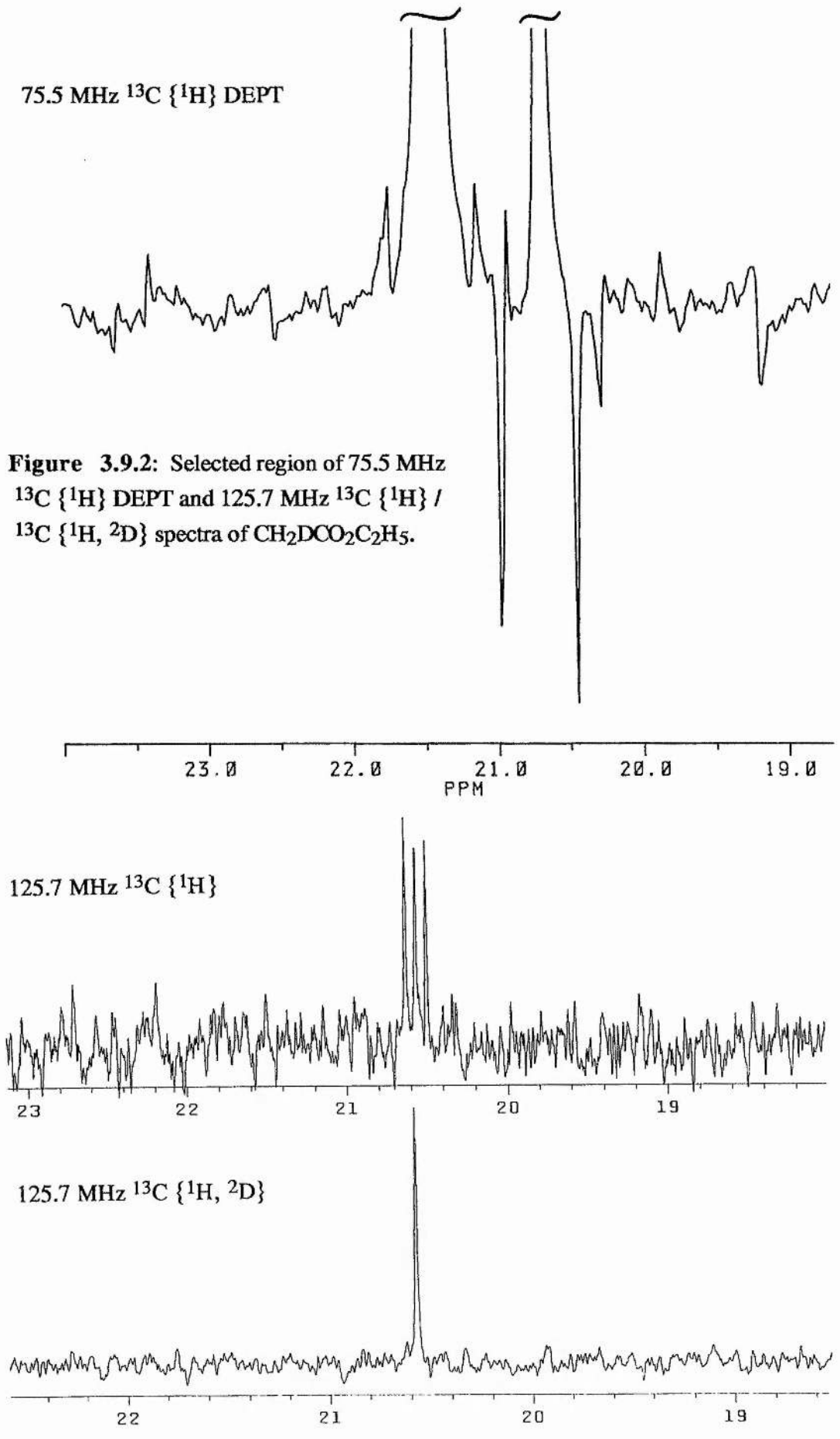

Figure 3.9.2: Selected region of 75.5 MHz ^{13}C {^{1}H} DEPT and 125.7 MHz ^{13}C {^{1}H} / ^{13}C {^{1}H, ^{2}D} spectra of $CH_2DCO_2C_2H_5$.

Figure 3.9.3: ^{2}D NMR spectrum of $CH_2DCO_2C_2H_5$ in $CDCl_3$ / d^1-EtOD.

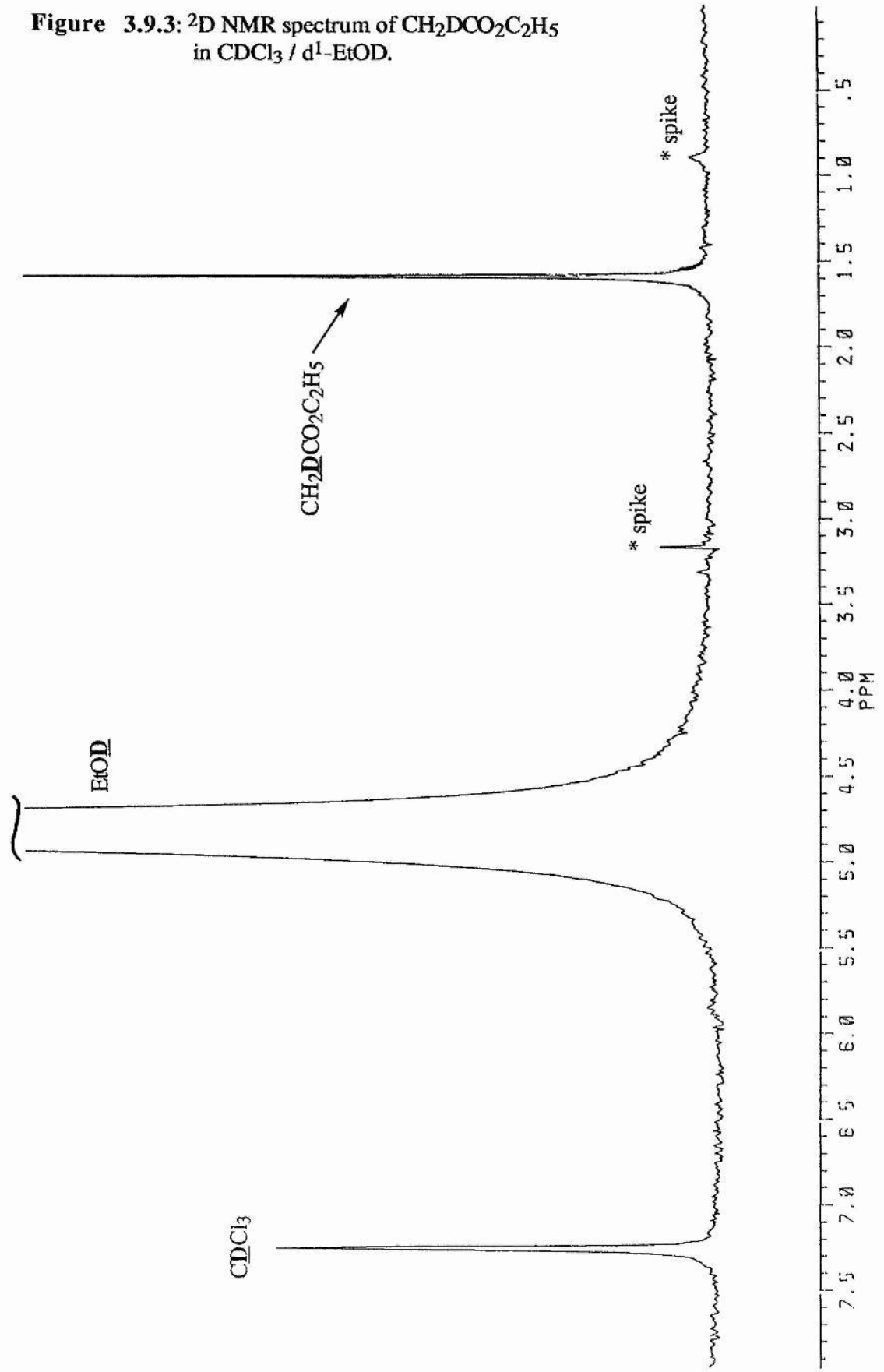

3.10 The use of ICH_2COR (R = Cl, OEt) as substrates

An alternative to a mechanism involving a metallo-ketene intermediate (ie **4d**) could be that shown in figure 3.10.1 overleaf. In this mechanism the singly carbonylated intermediate ICH_2COI would be observed, however briefly, free from the metal centre. The cycle in figure 3.10.1 would continue by the insertion of a Rh(I) species into the I–CH_2COR (R = I, OEt) bond and the subsequent (second) carbonyl insertion giving DEM as the organic product of the overall catalytic reaction. If such a mechanism were operating then $[Rh(X)CO(PEt_3)_2]$ should be an active catalyst for the single carbonylation of ICH_2COR as well as the double carbonylation of CH_2I_2. When either ICH_2COCl or ICH_2CO_2Et was examined as substrate in a standard catalytic reaction, no carbonylation reaction was observed and $EtOCH_2CO_2Et$ was returned in both cases. Since the formation of ICH_2CO_2Et from ICH_2COI and EtOH yields also a stoichiometric quantity of water it is possible that this could play a vital role in the reaction and perhaps this was why the carbonylation of ICH_2COR was not observed. To test this hypothesis ICH_2CO_2Et was used as the substrate when an equal amount of water had also been added to the reaction solution. Again no carbonylation was observed and only the ethanolysis product $EtOCH_2CO_2Et$ was returned.

Secondly, if the alternative mechanism shown in figure 3.10.1 were operating the product/s of the reaction of free ICH_2COI with the solvent (EtOH) should be observed in the product solution, even if only in low concentration. Such species would be ICH_2CO_2Et and / or $EtOCH_2CO_2Et$. Such products have never been observed, even in trace amounts, in any of the catalytic runs carried out under a wide range of reaction conditions. The combined evidence presented above leads to the conclusion that the mechanism shown in figure 3.10.1 is not operating in this catalytic reaction.

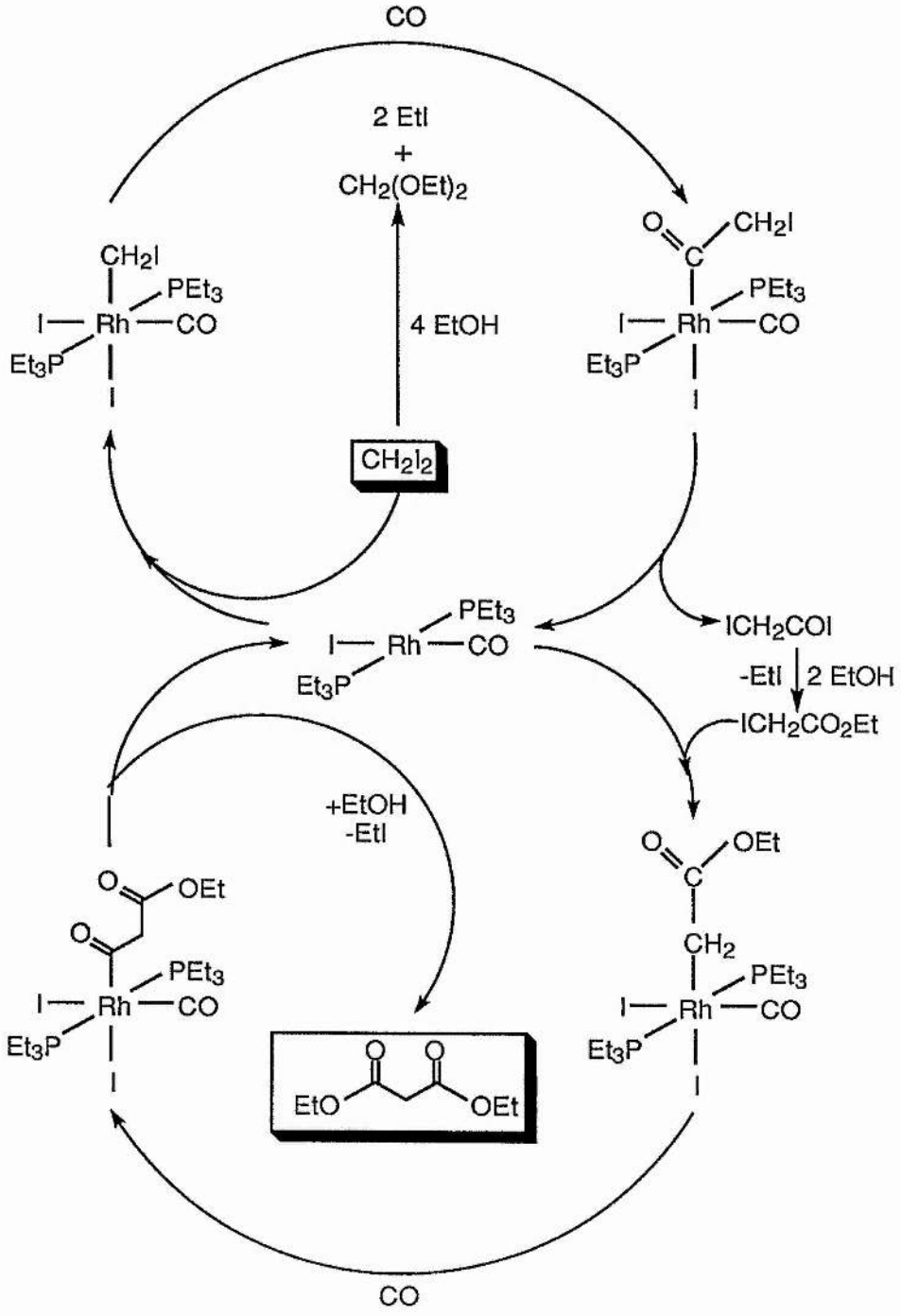

Figure 3.10.1: An alternative catalytic cycle to explain the [Rh(I)CO(PEt_3)$_2$] catalysed double carbonylation of diiodomethane.

3.11 The synthesis of $[RhCl_2(COCH_2CO_2Et)CO(PEt_3)_2]$ (7c)

The final intermediate in the proposed catalytic cycle is the malonate complex $[RhI_2(COCH_2CO_2Et)CO(PEt_3)_2]$ (**7d**) - see figure 3.0.1. The final step of the proposed mechanism is the reductive elimination of ethyl malonyl iodide, followed by the reaction of free ethyl malonyl iodide with ethanol yielding DEM. $[RhCl_2(COCH_2CO_2Et)CO(PEt_3)_2]$ (**7c**) was synthesised as a model of this final intermediate.

The synthesis of **7c** is achieved by the reaction of **1c** with a stoichiometric quantity of ethyl malonyl chloride (EtO_2C-CH_2-COCl) in CH_2Cl_2 at room temperature for 16-20 hours. After work-up the product is obtained as a pale yellow oil which when recrystallised twice from hot Et_2O yields pale yellow / white crystals.

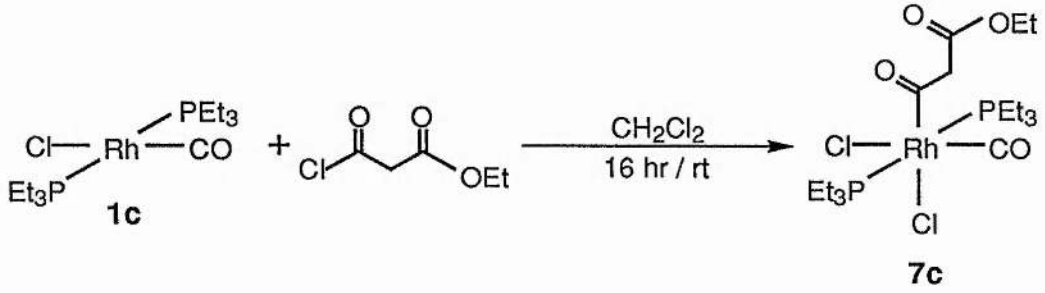

Figure 3.11.1

Characterisation of these crystals by ^{31}P / ^{13}C / ^{1}H NMR, IR and microanalysis showed the product to be **7c**. The crystals also proved of suitable quality for X-ray diffraction analysis (see section 3.12). The product is found to be stable for at least six months if stored under nitrogen at -30 °C, but to decompose within 1-2 weeks if kept at room temperature.

In a separate study the in-situ reaction of **1c** with ethyl malonyl chloride in CD_2Cl_2 was monitored by ^{31}P / ^{1}H VT-NMR spectroscopy. As the temperature of the sample was raised in 20-30 K steps from 223K to 293K the expected oxidative addition was observed with the malonyl complex giving rise to a doublet (δ = 16.1 ppm; J_{Rh-P} = 85 Hz). No intermediates with lifetimes on the NMR time scale were observed.

3.12 The crystal structure of $[RhCl_2(COCH_2CO_2Et)CO(PEt_3)_2]$ (7c)

The X-ray diffraction data was acquired at 293 K, but unresolvable disorder in the ethyl groups of the phosphine ligands reduced the quality of fit of the solution to the diffraction data, giving a high R-factor (R = 0.191). The source of this disorder cannot yet be understood. It was shown for complex **3c** that acquisition of the X-ray diffraction data at 220 K did not significantly decrease the disorder. Therefore it is not possible to comment in detail upon the bond lengths and angles observed in the structure shown in figure 3.12.1. The X-ray structure shows the phosphine ligands to be trans and the malonyl moiety to be trans to a chloride rather than the CO ligand. This structure is consistent with the structure determined by the NMR and IR spectra.

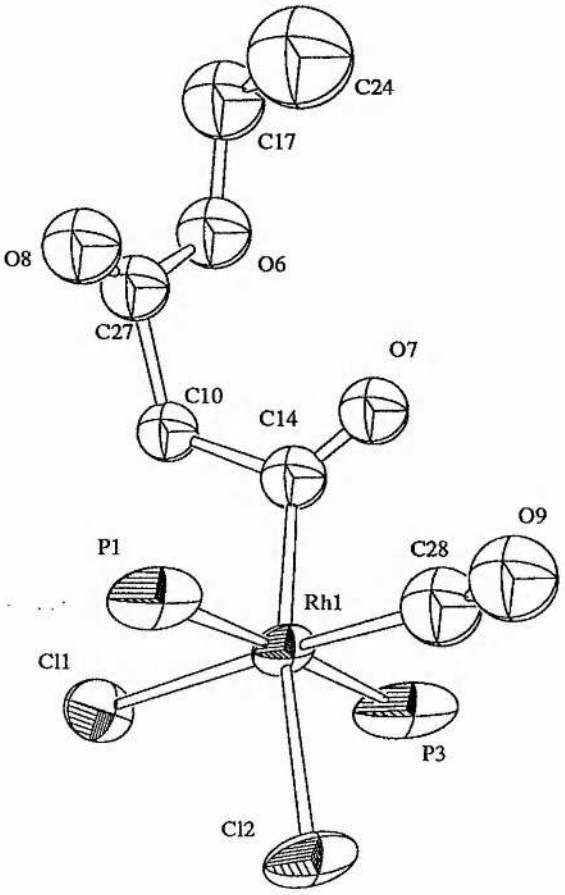

Figure 3.12.1: A simplified ORTEP plot of the structure of **7c**.

3.13 The reaction of $[RhCl_2(COCH_2CO_2Et)CO(PEt_3)_2]$ with EtOH

The final step in the proposed mechanism is the release of the malonyl moiety and the consequent regeneration of the Rh(I) active catalytic species. When the in-situ reaction described in section 3.11 had gone to completion, ethanol (approx. 1:1 with initial **1c**) was added and ^{31}P VT-NMR spectroscopic observation continued. At room temperature the ^{31}P spectrum was somewhat more complicated (see figure 3.13.2) Stepwise raising of the temperature simplified the spectrum until at 100 °C the sole product (in addition to residual **7c**) was another Rh(III) species, δ = 19.1 ppm; J_{Rh-P} = 73 Hz. Technical problems prevented further examination of the sample, but the most likely reaction occurring here is shown in figure 3.13.1

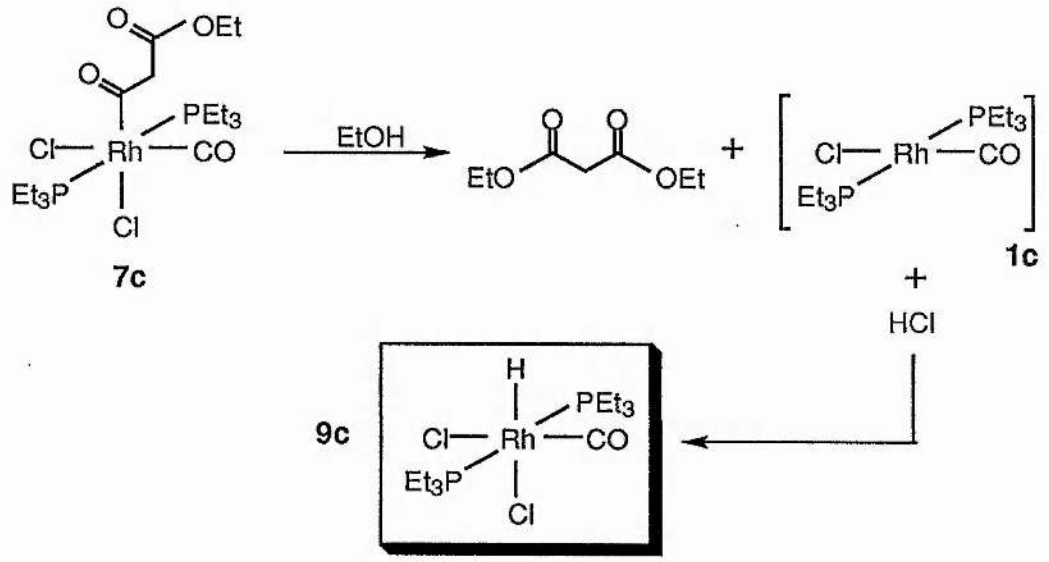

Figure 3.13.1: The reaction of **7c** with 1 equivalent of ethanol.

This proposal should be confirmed by the synthesis of the hydride complex **9c** which time has not allowed. In the real catalytic system, EtOH is present not just in a stoichiometric quantity but in vast excess and so it acts as a sink for HX. Work to be presented in chapter four also shows that the formation of $[Rh(H)I_2CO(PEt_3)_2]$ (**9d**), the analogue of **9c** which would form under catalytic conditions, does not constitute catalyst decomposition. **9d** is observed to react readily with EtOH to yield EtI (and therefore H_2O) and thus regenerate the catalytically active species $[Rh(I)CO(PEt_3)_2]$ (**1d**).

Figure 3.13.2: ^{31}P NMR spectra of in situ reaction of $[RhCl_2(COCH_2CO_2Et)CO(PEt_3)_2]$ with EtOH.

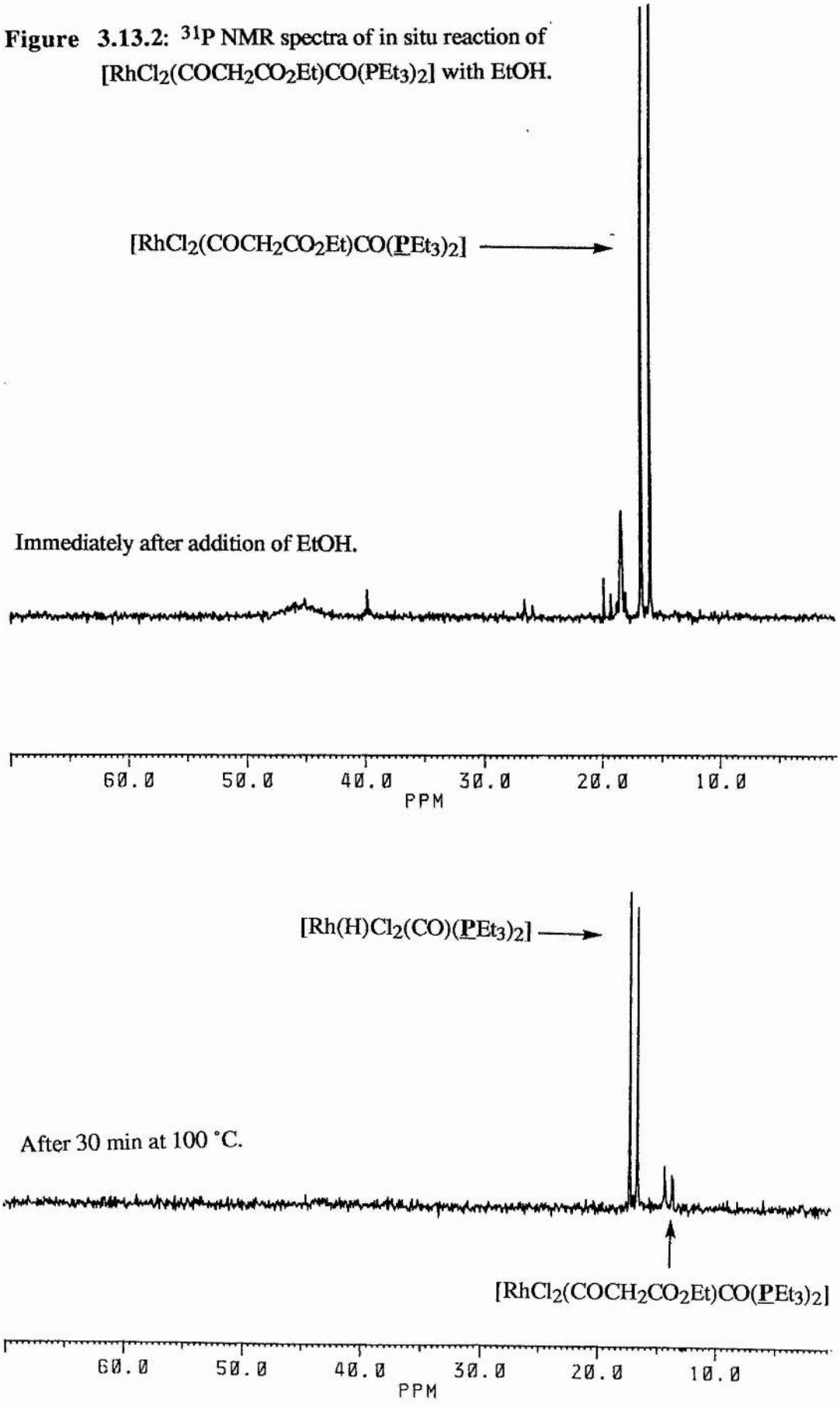

To study the reductive elimination of the malonyl moiety further a synthetic scale reaction of the model complex **7c** was refluxed in the presence of 1 equivalent of EtOH in CH_2Cl_2 for 2 hours. It was hoped that this would yield a significant quantity of the unknown product observed during the in-situ experiment discussed above. The major organometallic product from this synthetic reaction was re-crystallised giving pale yellow crystals. These crystals were shown by ^{31}P NMR spectroscopy to be the pure starting material (**7c**).

Although this model reaction was carried out with the same stoichiometry of EtOH / **7c** as the in-situ experiment the concentration of the species was much lower than those used in-situ. Thus, the reaction was repeated with an increased concentration of EtOH. With a 30:1 ratio of EtOH / **7c** the main isolated species was again unreacted **7c**. After the volatile products were removed from the filtrate obtained from the re-crystallisation of this product mixture the resultant oil was examined by ^{31}P NMR spectroscopy and was found to be mainly $[Rh(Cl)CO(PEt_3)_2]$ (**1c**). The volatile products from the filtrate were also examined by GCMS and ^{13}C NMR spectroscopy. Apart from the solvent, DEM was observed as the only species present. This reaction is summarised in figure 3.13.1.

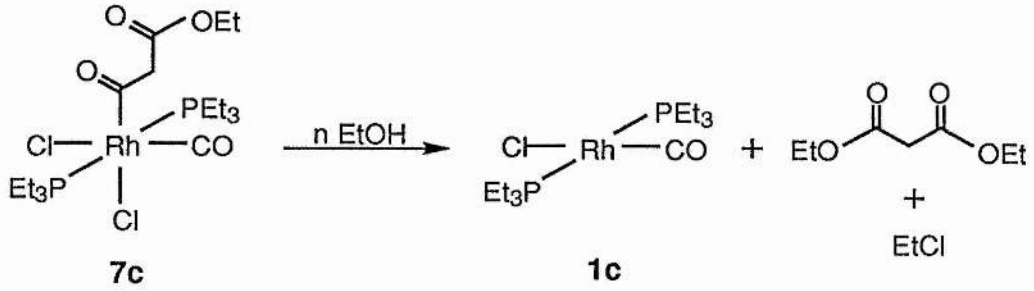

7c **1c**

Figure 3.13.1: The reaction of complex **7c** with excess ethanol.

Although we did not observe the species seen in the in-situ reaction of **7c** with EtOH (thought to be **9c**), what was observed at this higher EtOH / **7c** ratio was **1c** and DEM, a model of the final step in the proposed mechanism. It should be noted that in the real catalytic system, where ethanol is the solvent, the ethanol concentration is much higher than in these model reactions were it is only present in a stoichiometic amount. The position of the equilibrium of the reaction **7c** to **1c** (plus free ethyl malonyl chloride) is observed to be strongly thermodynamically biased towards **7c**. The equilibrium can only be driven to yield **1c** in significant quantities when the subsequent reaction of either ethyl malonyl chloride (ie irreversibly reacting with ethanol yielding DEM) or **1c** (ie reaction with diiodomethane) occurs and the position of the equilibrium is forced to alter according to Le Chatelier's principle.

If the reaction of **7c** to **1c** is a good model of the catalytic step **7d** to **1d** then the catalytic reaction should show a dependence on both the concentration of alcohol and substrate (diiodomethane). It has been shown throughout this thesis (chapters 2,4,5) that an alcohol plays a vital role in this catalytic system. The use of co-solvents was studied in chapter 2 and the consequent decrease in alcohol concentration was observed to have a detrimental effect upon catalyst stability (section 2.5). Also in chapter two a positive relationship between catalyst TON and the initial diiodomethane concentration was established (section 2.6). If all the steps in catalytic mechanism from **7d** back to the ketene complex **4d** are reversible then the slow reductive elimination of **7d** giving **1d** would allow time for organo-rhodium species to shuffle back through the cycle to the unstable ketene complex thus increasing their chance of being irreversibly lost from the cycle.

Table 3.1 - NMR and IR Spectral Data on complexes of the type $[RhX(CO)(PR_3)_2]$

COMPLEX		δ_P (ppm)	J_{Rh-P} (Hz)		δ_C (ppm)	J_{Rh-C} (Hz)		δ_H (ppm)	ν_{CO} (cm^{-1})	Lit. Ref.
$[Rh(OAc)CO(PEt_3)_2]$	**1a**	25.4 (d)[a]	124	$\underline{C}O$	192.3 (dt)	70.6	$OCOC\underline{H}_3$	1.9 (m)	-	This work
				$O\underline{C}OCH_3$	137.4 (s)		$PC\underline{H}_2CH_3$	1.6 (m)		
				$OCO\underline{C}H_3$	23.1 (s)		$PCH_2C\underline{H}_3$	1.0 (m)		
	1a	21.2 (d)[b]	124							
$[RhBr(CO)(PEt_3)_2]$	**1b**	22.5 (d)	116				$PC\underline{H}_2CH_3$	1.9 (m)	1957	137
							$PCH_2C\underline{H}_3$	1.2 (m)		
$[RhCl(CO)(PEt_3)_2]$	**1c**	24.2 (d)	116							157
$[RhI(CO)(PEt_3)_2]$	**1d**	20.5 (d)[c]	115	$P\underline{C}H_2CH_3$	19.2		$PC\underline{H}_2CH_3$	2.0 (m)	1961	This work
				$PCH_2\underline{C}H_3$	9.1		$PCH_2C\underline{H}_3$	1.1 (m)		
$[RhCl(CO)(PMe_3)_2]$	**1e**	-9.9 (d)	114	$P\underline{C}H_3$	16.3 (t)[d]		$PC\underline{H}_3$	1.5 (s)	-	147

Unless otherwise indicated all species are fully characterised trans-phosphine complexes and their spectra are recorded in CD_2Cl_2 at 298 K.

a) Spectra recorded in C_7D_8. b) Spectra recorded in CH_3CH_2OD at 300 K. c) Spectra recorded in C_6D_6. d) $^J_{P-\underline{C}H_3}$ = 15 Hz.

Table 3.2 - NMR and IR Spectral Data for complexes of the type $[RhXY(CH_2Z)(CO)(PEt_3)_2]$

COMPLEX		δ_P (ppm)	J_{Rh-P} (Hz)	$\delta_{C\underline{H_2}X}$ (ppm)	J_{Rh-H} (Hz)	J_{P-H} (Hz)		δ_H (ppm)	ν_{CO} (cm^{-1})
$[Rh(OAc)I(CH_2I)CO(PEt_3)_2]$	**2a**	3.1 (d)	85	3.5 (dt)	2.1	6.8			
$[RhI_2(CH_2OAc)CO(PEt_3)_2]$	**2b**	0.9 (d)	82	5.8 (dt)	2.9	5.9			
$[RhCl(I)(CH_2I)CO(PEt_3)_2]$[a]	**2c**	9.8 (d)	80	3.3 (dt)	2.2	4.3	$PC\underline{H_2}CH_3$	2.3 (m)	2053
							$PCH_2C\underline{H_3}$	1.1 (t)	
$[RhI_2(CH_2I)CO(PEt_3)_2]$	**2d**	1.0 (d)	82	3.6 (dt)	2.1	5.7	$PCH_2C\underline{H_3}$	1.2 (t)	
$[RhI_3(CH_2PEt_3)CO(PEt_3)]$	**2e**	-1.9 (d)	78	3.0 (ddd)					
		49.3 (s)			J^2_{Rh-H} = 2.4 Hz, J^2_{P-H} = 11.0 Hz, J^3_{P-H} = 10.0 Hz				
$[RhI_2(CH_2Cl)CO(PEt_3)_2]$[a]	**2g**	2.7	80	4.4	2.7	6.4	$PC\underline{H_2}CH_3$	2.5 (m)	2055
							$PCH_2C\underline{H_3}$	1.3 (t)	
$[RhCl(I)(CH_2Cl)CO(PEt_3)_2]$[b]	**2h**	11.3	82	4.4	2.8	5.0	$PC\underline{H_2}CH_3$	2.2 (m)	
							$PCH_2C\underline{H_3}$	1.3 (t)	
$[RhCl_2(CH_2Cl)CO(PEt_3)_2]$[c]	**2i**	17.2	80	4.5	2.9	4.6	$PC\underline{H_2}CH_3$	2.3 (m)	
							$PCH_2C\underline{H_3}$	1.3 (t)	

Unless otherwise indicated all species are trans-PEt_3 complexes, characterised by solution NMR and their spectra are recorded in C_6D_6 at 298 K.
a) Fully Characterised. b) Spectra recorded in d^8-THF. c) Spectra recorded in CD_2Cl_2. d) Data for complexes **2c**, **2g**, **2h** supplied by Gash.[133]

Table 3.3 - Selected NMR and IR Spectral Data for complexes of the type $[RhXY(COCH_2R)(CO)(PR_3)_2]$

COMPLEX		δ_P (ppm)	J_{Rh-P} (Hz)		δ_C (ppm)		δ_H (ppm)	ν_{CO} (cm^{-1})	$\nu_{C(O)CH_2R}$ (cm^{-1})
$[RhI_2(COCH_2Cl)CO(PEt_3)_2]$[a]	**3a**	11.1 (d)	85			Rh-COC**H**$_2$Cl	4.7 (s)	-	-
						PC**H**$_2$CH$_3$	2.2 (m)		
						PCH$_2$C**H**$_3$	1.2 (m)		
$[RhBr_2(COCH_2Br)CO(PEt_3)_2]$	**3b**	14.4 (d)	85	Rh-**C**OCH$_2$Br	212.9	Rh-COC**H**$_2$Br	4.7 (s)	2063	1671
				Rh-CO**C**H$_2$Br	29.7 (s)	PC**H**$_2$CH$_3$	2.2		
						PCH$_2$C**H**$_3$	1.2		
$[RhCl_2(COCH_2Cl)CO(PEt_3)_2]$	**3c**	16.8 (d)	80	Rh-**C**OCH$_2$Cl	217.6 (dt)	Rh-COC**H**$_2$Cl	4.7 (s)	2050	1660
				Rh-CO**C**H$_2$Cl	55.0	PC**H**$_2$CH$_3$	2.2 (m)		
						PCH$_2$C**H**$_3$	1.2 (m)		
$[RhCl_2(COCH_2OC_6F_5)CO(PEt_3)_2]$[a] ($R = OC_6F_5$)	**3g**	16.3	85			Rh-COC**H**$_2$R	4.8 (s)	-	-

Unless otherwise indicated all species are fully characterised trans-phosphine complexes and their spectra are recorded in CD_2Cl_2 at 298 K.

a) Characterised in solution by NMR.

Table 3.3 (continued) - Selected NMR and IR Spectral Data for complexes of the type $[RhXY(COCH_2R)(CO)(PR_3)_2]$

COMPLEX		δ_P (ppm)	J_{Rh-P} (Hz)		δ_C (ppm)		δ_H (ppm)	ν_{CO} (cm^{-1})	$\nu_{C(O)CH_2R}$ (cm^{-1})
$[RhCl_2(COCH_2Cl)CO(PMe_3)_2]$	-	-5.5 (d)	86			Rh-COC**H**$_2$Cl	4.6 (s)	2065	1668
$[RhCl_2(COCH_2CO_2Et)CO(PEt_3)_2]$	**7c**	16.1 (d)	85	Rh-**C**OCH$_2$R'	220.5	Rh-COC**H**$_2$R'	4.0 (s)	2050	1700
(R' = CO_2Et)				Rh-CO**C**H$_2$R'	61.5	PC**H**$_2$CH$_3$	2.2 (m)		(1645[a])
				Rh-COCH$_2$**C**O$_2$Et	168.1	PCH$_2$C**H**$_3$	1.2 (m)		

Unless otherwise indicated all species are fully characterised trans-phosphine complexes and their spectra are recorded in CD_2Cl_2 at 298 K.
a) ν_{CO} for [Rh]-COCH$_2$**CO**OEt

Table 3.4 - NMR and IR Spectral Data for complexes of the type $[RhX_2Y(CO)(PR_3)_2]$

COMPLEX		δ_P (ppm)	J_{Rh-P} (Hz)		δ_H (ppm)	J_{Rh-H} (Hz)	J_{P-H} (Hz)	ν_{CO} (cm^{-1})
$[RhCl_3CO(PEt_3)_2]$[a]	**8a**	19.4	71					-
$[RhCl(I)_2CO(PEt_3)_2]$	**8c**	6.2	73					-
$[RhI_3CO(PEt_3)_2]$	**8d**	-3.8	73					2057
$[RhH(I)_2CO(PEt_3)_2]$[b]	**9d**	13.6	84	$PC\underline{H}_2CH_3$	2.3 (m)			2037
				$PCH_2C\underline{H}_3$	1.2 (m)			
				[Rh]-<u>H</u>	-11.1	16	10	

Unless otherwise indicated all species are fully characterised trans-phosphine complexes and their spectra are recorded in CD_2Cl_2 at 298 K.
a) Spectroscopically characterised only. b) Full ^1H spectral data for complex **9d** confirmed by Rankin.[160]

3.14 Experimental

All the following reactions (unless specified) were carried out in dry deoxygenated solvents under a dry nitrogen atmosphere. The general experimental procedures such as the drying of solvents, the nature of the equipment used in this work and the sources of the chemicals are summarised in Appendix One. All NMR and IR data from the organorhodium species are collected in tables 3.1-3.4 presented on the immediately preceding pages.

3.14.1 — *In-situ ^{31}P HPVT-NMR study of the reaction of $[Rh_2(OAc)_4]\cdot 2MeOH$ with PEt_3 / CO.*

$[Rh_2(OAc)_4]\cdot 2MeOH$ (0.01 g 0.02 mmol) and PEt_3 (20 µl 0.14 mmol) were dissolved in CH_3CH_2OD (2 cm^3) and an aliquot of this solution (0.5 cm^3) transferred into a HP-NMR Cell (Sheffield Univ.). The head and gas supply tube were purged 3 times with CO (10 atm) and then the cell pressurised to 40 atm with CO. The ^{31}P NMR spectrum of the reaction mixture in the HP-NMR cell was recorded at room temperature. The HP-NMR cell was left in the spectrometer, heated to 373K in-situ and the ^{31}P NMR spectrum recorded after 2 hr. The HP-NMR cell was then cooled to 300K in situ and the ^{31}P NMR spectrum recorded again.

3.14.2 — *Synthesis of $[Rh(OAc)CO(PEt_3)_2]$ (1a).*

$[Rh_2(OAc)_4]\cdot 2MeOH$ (0.2666 g 0.53 mmol) was dissolved in ethanol (30-40 cm^3) and 8 equivalents of PEt_3 (0.6 cm^3 4.1 mmol) injected into the reaction mixture. A steady flow of CO was bubbled through the solution for approximately 30 min. The solution went from red to yellow during the reaction. The solvent was removed from the yellow solution *in vacuo* and the resultant yellow oil dissolved in a little light petroleum (1 cm^3). This solution was cooled to -100 °C, yielding a yellow microcrystalline solid from which the petroleum was removed by filtration. The solid was washed with light petroleum, filtered again and then pumped vigorously as it was allowed to warm to room temperature. The product was obtained as a yellow oil (Yield 75%) which was identified as $[Rh(OAc)CO(PEt_3)_2]$ by ^{31}P / ^{1}H NMR spectroscopy, IR and microanalysis: Found; C 41.64 %, H 7.79 %. $C_{15}H_{33}O_3P_2Rh$ requires; C 42.35 %, H 7.76%.

3.14.3 — *Synthesis of [Rh(Cl)CO(PEt$_3$)$_2$] (1c).*

This was carried out using a method adapting from the method published by Chatt and Shaw.[143] $RhCl_3 \cdot 3H_2O$ (1.0317 g 3.92 mmol) was dissolved in ethanol (20 cm^3). The red solution was refluxed for 3 hr whilst a steady flow of CO was bubbled through the solution. After 3 hr the resultant pale yellow solution was allowed to cool to room temperature and 3 equivalents of PEt_3 (1.7 cm^3 11.5 mmol) were added slowly. As the PEt_3 was added, evolution of CO from the solution was observed. The reaction was then refluxed under nitrogen for a further 30 min yielding a yellow / green solution. The solvent was removed *in vacuo* to give a green oil. The desired product was extracted from the green oil into diethyl ether (40 cm^3) and the supernatant removed by filtration. The yellow etheral solution was evaporated to 5-10 cm^3 and then cooled to -30 °C for 2-3 days to allow crystallisation to occur. The resultant bright yellow crystals were filtered at -50 °C and dried *in vacuo*, yield 79%. The product was identified as [Rh(Cl)CO(PEt_3)$_2$] by ^{31}P / ^1H NMR spectroscopy and IR by comparison to literature values.[157]

3.14.4 — *Synthesis of [Rh(Br)CO(PEt$_3$)$_2$] (1b).*

[Rh(Cl)CO(PEt_3)$_2$] (0.2220 g 0.55 mmol) was dissolved in acetone (20 cm^3) and approx. 20 equivalents of LiBr (0.95 g 10.94 mmol) were added with stirring. The yellow solution was stirred for 2 hr then the volume reduced *in vacuo* to approx. 5 cm^3. Light petroleum (50 cm^3) was added to precipitate the Li salts and the supernatant removed by filtration. The Li salts were washed with a second volume of light petroleum (20 cm^3) and the filtrates combined. The petroleum was removed *in vacuo* to give a yellow oil which was re-dissolved in a minimum volume of hot diethyl ether (5-7 cm^3). The etherial solution was cooled to -78 °C for 6 hr to allow crystallisation to occur. The resultant bright yellow micro-crystals were filtered at -78 °C and dried *in vacuo*, quantitative yield. The product was identified as [Rh(Br)CO(PEt_3)$_2$] by ^{31}P / ^1H NMR spectroscopy and IR by comparison to literature values.[137]

3.14.5 — *Synthesis of [Rh(I)CO(PEt$_3$)$_2$] (1d).*

[Rh(Cl)CO(PEt_3)$_2$] (0.2204 g 0.55 mmol) was dissolved in acetone (20 cm^3) and approx. 5 equivalents of NaI (0.41 g 2.73 mmol) added with stirring. The solution was stirred in the dark for 5 min during which time NaCl was observed to precipitate.

The volume of the yellow / orange solution was reduced to approx. 5 cm^3 then light petroleum (30 cm^3) added to precipitate the excess NaI and the supernatant removed by filtration. The Na salts were washed with a second volume of light petroleum (30 cm^3) and the filtrates combined. The volume of the combined filtrates was reduced to approx. 5-10 cm^3 *in vacuo* and the yellow solution cooled to -100 °C for 4 hr to allow crystallisation to occur. The resultant bright yellow micro-crystals were filtered at -100 °C and dried *in vacuo,* 98 % yield. The product was identified as $[Rh(I)CO(PEt_3)_2]$ by ^{31}P / ^{1}H NMR spectroscopy, IR and microanalysis: Found; C 32.23 %, H 5.16%. $C_{13}H_{30}OP_2IRh$ requires; C 31.6 %, H 6.12 %.

3.14.6 — *The reaction of $[Rh(OAc)CO(PEt_3)_2]$ (1a) with CH_2I_2.*

$[Rh(OAc)CO(PEt_3)_2]$ (0.1255 g 0.29 mmol) and 50 equivalents of CH_2I_2 (1.2 cm^3 14.9 mmol) were dissolved in THF (50 cm^3) and stirred in the dark at room temperature for 18 hr. Two attempts to crystallise the product failed {The resultant orange solution was reduced to 1/3 of original volume *in vacuo* and i) Et_2O (30-40 cm^3) added then the solution the cooled to -100 °C} and thus the solvent(s) were removed *in vacuo* yielding an orange/brown oil. A sample of this oil was analysed by ^{31}P / ^{13}C / ^{1}H NMR spectroscopy and the major products were characterised as $[Rh(OAc)(CO)I(CH_2I)(PEt_3)_2]$ and $[Rh(CH_2OAc)CO(I)_2(PEt_3)_2]$.

3.14.7 — *The reaction of $[Rh(I)CO(PEt_3)_2]$ (1d) with CH_2I_2.*

$[Rh(I)CO(PEt_3)_2]$ (0.1029 g 0.21 mmol) and 40 equivalents of CH_2I_2 (0.8 cm^3 9.92 mmol) were dissolved in THF (40 cm^3) and stirred in the dark at room temperature for 18 hr. The solvent was removed from the resultant orange/brown solution *in vacuo*. A sample of the resultant crude oil was examined by ^{31}P / ^{1}H NMR spectroscopy and identified as a mixture of trans-$[RhI_2(CH_2I)CO(PEt_3)_2]$ and $[RhI_3(CH_2PEt_3)CO(PEt_3)_2]$. No attempt was made to purify the reaction mixture.

3.14.8 — *In-situ ^{31}P / ^{1}H VT-NMR study of the reaction of $[Rh(Cl)CO(PEt_3)_2]$ (1c) with CH_2I_2.*

$[Rh(Cl)CO(PEt_3)_2]$ (0.0936 g 0.23 mmol) was dissolved in CD_2Cl_2 (0.7 cm^3) then cooled to 213 K (-60 °C). 0.97 equivalents of CH_2I_2 (18 µl 0.22 mmol) were added to the solution and the mixture was transferred to an NMR tube (pre-cooled to 213 K)

and sealed under nitrogen. The sample was initially examined by ^{31}P / ^{1}H NMR spectroscopy in-situ at 213K. The sample was warmed in-situ to 233K and allowed to equilibrate at this temperature for 10 min before examination by ^{31}P / ^{1}H NMR spectroscopy again. This procedure was repeated at a range of temperatures; 253 K, 283 K, 313 K and 343 K. Finally the sample was heated to 343 K ex-situ for 14 hr and then examined by ^{31}P NMR spectroscopy.

3.14.9 — *Synthesis of [RhCl(I)(CH_2I)CO(PEt_3)$_2$] (2c).*

The synthesis of [RhCl(I)(CH_2I)CO(PEt_3)$_2$] was achieved using the method of Gash and Cole-Hamilton.[118]

3.14.10 — *The reaction of [RhCl(I)(CH_2I)CO(PEt_3)$_2$] (2c) with Me_4NCl in methanol.*

[RhCl(I)(CH_2I)CO(PEt_3)$_2$] (0.2452g 0.37 mmol) was dissolved in MeOH (20 cm^3) and approx. 40 equivalents of Me_4NCl (1.60 g 14.6 mmol) added to the solution with stirring. The reaction solution was stirred in the dark for 25 hr at room temperature yielding a pale yellow solution. The volume of the solution was reduced to approx. 5 cm^3 *in vacuo* then diethyl ether (40 cm^3) added to precipitate the ammonium salts and the supernatant removed by filtration. The ammonium salts were washed with a second volume of diethyl ether (10 cm^3) and the filtrates combined. Attempts to crystallise the product from this solution were unsuccessful so the solvent was removed *in vacuo* to yield a yellow oil. A sample of the oil was examined by ^{31}P / ^{1}H NMR spectroscopy and identified as a mixture of [$RhCl_2$(CH_2Cl)CO(PEt_3)$_2$] (**2i** - major) with [Rh(Cl)CO(PEt_3)$_2$] (**1c**) and [RhCl(I)(CH_2Cl)CO(PEt_3)$_2$] (**2h**) as minor products. No further attempts were made to purify the reaction mixture.

3.14.11 — *Reaction of [Rh(I)CO(PEt_3)$_2$] (1d) with ICH_2COCl*

[Rh(I)CO(PEt_3)$_2$] (0.1000g 2.02 mmol) was dissolved in CD_2Cl_2 (0.7 cm^3) and ICH_2COCl (0.1 cm^3) added. The solution was mixed and transferred to the NMR instrument and examined by ^{31}P / ^{1}H NMR spectroscopy at room temperature. The major products where observed to be [RhCl(I)$_2$CO(PEt_3)$_2$] (**8c**) and [RhI_3CO(PEt_3)$_2$] (**8d**). ^{1}H NMR spectrum showed the presence of diketene in solution. Very similar results were achieved when the procedure was repeated at 213 K.[145]

3.14.12 — *Synthesis of [$RhCl_2(COCH_2Cl)CO(PEt_3)_2$] (3c).*

[Rh(Cl)CO(PEt_3)$_2$] (0.3088 g 0.77 mmol) was dissolved in CH_2Cl_2 (30 cm^3) and 1 equivalent of $CH_2ClCOCl$ (62 µl 0.77 mmol) added with stirring. The reaction solution was stirred at room temperature for 8 hr then the solvent removed *in vacuo* giving a pale yellow oil. The oil was re-dissolved in hot diethyl ether (15 cm^3) then cooled to -30 °C for 3 days to allow crystallisation to occur. The resultant white / pale yellow crystals were filtered at -50 °C and dried *in vacuo*, yield 56%. The product was identified as [$RhCl_2(COCH_2Cl)CO(PEt_3)_2$] by ^{31}P / ^{13}C / ^{1}H NMR spectroscopy, IR, X-ray diffraction and microanalysis: Found; C 34.94 %, H 5.93 %. $C_{15}H_{32}Cl_3O_2P_2Rh$ requires; C 34.94 %, H 6.25 %.

3.14.13 — *Synthesis of [$RhCl_2(COCH_2Cl)CO(PMe_3)_2$].*

[Rh(Cl)CO(PMe_3)$_2$] (0.3672 g 1.15 mmol)[147] was dissolved in CH_2Cl_2 (15 cm^3) and 1 equivalent of $CH_2ClCOCl$ (95 µl 1.11 mmol) added with stirring. The reaction solution was stirred at room temperature for 18 hr then the solvent removed *in vacuo* giving a sticky pale yellow solid. This solid was twice recrystallised from hot Et_2O / CH_2Cl_2 (with cooling to -30 °C for 9 days to allow crystallisation to occur). The resultant colourless crystals were filtered at -78 °C and dried *in vacuo*, yield 68%. The product was identified as [$RhCl_2(COCH_2Cl)CO(PMe_3)_2$] by ^{31}P / ^{13}C / ^{1}H NMR spectroscopy and IR.

3.14.14 — *Synthesis of [$RhBr_2(COCH_2Br)CO(PEt_3)_2$] (3b).*

This can be achieved by direct reaction of [Rh(Br)CO(PEt_3)$_2$] (**1b** - see section 3.14.4) with bromoacetyl bromide [Route A] or by the metathesis of [$RhCl_2(COCH_2Cl)CO(PEt_3)_2$] (**3c** - see section 3.14.12) with LiBr [Route B].

[Route A] - [Rh(Br)CO(PEt_3)$_2$] (0.2464 g 0.55 mmol) was dissolved in CH_2Cl_2 (15 cm^3) and 1 equivalent of $BrCH_2COBr$ (49 µl 0.56 mmol) added with stirring. The reaction solution was stirred at room temperature for 18 hr then the solvent removed *in vacuo* giving a sticky yellow solid. The sticky solid was re-dissolved in a minimum volume of hot diethyl ether then cooled to -30 °C for 4 days to allow crystallisation to occur. The resultant yellow / cream powder was filtered at -50 °C and dried *in vacuo*, yield 87%.

The product was identified as $[RhBr_2(COCH_2Br)CO(PEt_3)_2]$ by ^{31}P / ^{13}C /^{1}H NMR spectroscopy, IR and microanalysis: Found; C 28.84 %, H 5.14 %. $C_{15}H_{32}Br_3O_2P_2Rh$ requires; C 27.77 %, H 4.97 %.

[Route B] - $[RhCl_2(COCH_2Cl)CO(PEt_3)_2]$ (0.1056 g 0.21 mmol) was dissolved in acetone (15 cm^3) and approx. 10 equivalents of LiBr (0.197 g 2.2 mmol) added with stirring. The reaction solution was stirred at room temperature for 1 hr then the volume reduced to 5 cm^3 *in vacuo*. The product was extracted into hot diethyl ether (2 x 30 cm^3) and the supernatant filtered from the lithium salts. The resultant yellow solution was evaporated *in vacuo* to approx. 7-10 cm^3 then cooled to -30 °C for 3 days to allow crystallisation to occur. The resultant yellow micro-crystals were filtered at -50 °C and dried *in vacuo*. The product was identified as $[RhBr_2(COCH_2Br)CO(PEt_3)_2]$ by ^{31}P / ^{13}C NMR spectroscopy and IR by comparison with the sample made by route A.

3.14.15 — *The reaction of $[RhCl_2(COCH_2Cl)CO(PEt_3)_2]$ (3c) with NaI.*

$[RhCl_2(COCH_2Cl)CO(PEt_3)_2]$ (0.1483 g 0.29 mmol) was dissolved in acetone (15 cm^3) and approx. 10 equivalents of NaI (0.448g 0.30 mmol) added with stirring. The reaction solution was stirred in the dark at room temperature for 30 min. Attempts to crystallise the product were unsuccessful so the solvent was removed *in vacuo* to yield a dark orange oil which was examined in CD_2Cl_2 by ^{31}P / ^{13}C NMR spectroscopy. The major product was characterised as $[RhI_2(COCH_2Cl)CO(PEt_3)_2]$ (**3a**). The product mixture was re-dissolved in acetone and the above reaction procedure repeated but for 16 hr followed by the same work-up / analysis. Finally the reaction of this sample with NaI / acetone was carried out for a further 12 days, then worked up and analysed by ^{31}P NMR spectroscopy as described above.

3.14.16 — *In-situ ^{31}P / ^{1}H HPVT-NMR study of the reaction of $[RhX_2(CH_2Cl)CO(PEt_3)_2]$ (2) with CO.*

A crude sample of $[RhCl_2(CH_2Cl)CO(PEt_3)_2]$ (see section 3.14.10) was dissolved in CD_2Cl_2 (0.5 cm^3) and transferred into a HP-NMR Cell. The head and gas supply tube were purged 3 times with CO (20 atm) and then the cell pressurised to 50 atm with CO. The HP-NMR cell was initially examined by ^{31}P / ^{1}H NMR spectroscopy in-situ at room temperature. The sample was then warmed in-situ to 320 K and

allowed to equilibrate for at least 10 min before examination by ^{31}P / ^{1}H NMR spectroscopy again. This procedure was repeated at a range of temperatures; 340 K (50 min), then 360 K (10 min), 370 K (70 min), 390 K (20 min). Since no significant reaction was observed, the cell was removed from the instrument, cooled to room temperature and checked to test whether initial pressurisation had occurred. The cell was observed to have been properly pressurised so was repressurised with 50 atm CO and returned to the NMR instrument. The cell was heated in-situ to 373 K for 3 hr and then examined by ^{31}P / ^{1}H NMR spectroscopy for the final time.

3.14.17 — *Synthesis of ketene by the pyrolysis of acetone.*

The experimental set up which was used is illustrated below in figure 3.14.1. The method employed was an adaptation of a method[158] first described in 1932, but adapted to take account of the more efficient modern equipment now available. The conditions described below are optimal for the experimental set-up used.

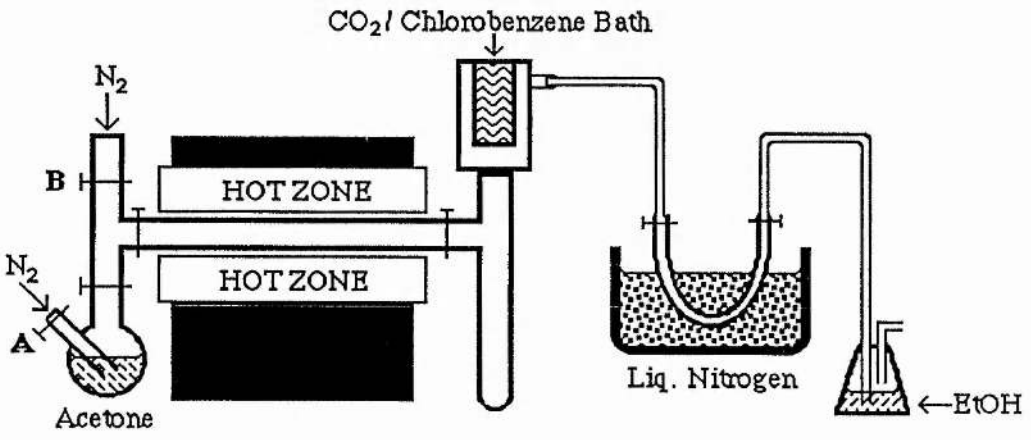

Figure 3.14.1

The whole apparatus was flushed with nitrogen (through tap B) for 10 min and then the furnace heated to 700 °C. The condenser was cooled to -45 °C using a slush of solid CO_2 and chlorobenzene and the U-tube cooled with liquid nitrogen. The temperature of the acetone reservoir was held between 0 and -5 °C by placing it in a salt/ice bath. The nitrogen flow was adjusted to be at a moderate level (this was kept consistent by comparison of the rate of the bubbles passing through the EtOH trap) and, when all the controlled temperature regions had equilibrated, the nitrogen supply was diverted to bubble through the acetone reservoir (via tap A) to carry it's vapour into the hot zone. Unreacted acetone was condensed and collected in the right-hand reservoir and ketene in the U-tube. In a typical run the acetone was transferred into

the hot zone at 0.15 cm^3 min^{-1}. Of this 50-70% is collected unreacted. It should be noted that ketene is an unstable highly toxic gas that can only be stored safely at temperatures below -80 °C.[114]

3.14.18 — *Attempted reaction of $[RhCl(I)_2CO(PEt_3)_2]$ (8c) with $AgBF_4$ / ketene / CO / BuONO.*

$AgBF_4$ (0.1100g 0.57 mmol) was dissolved in acetone (15 cm^3) and transferred to an autoclave, fitted with a magnetic stirrer, under argon and the acetone removed *in vacuo*. The autoclave was then cooled to -100 / -120°C using an EtOH / liq.N_2 bath. $[RhCl(I)_2CO(PEt_3)_2]$ (0.2232g 0.34 mmol) was dissolved in dry BuONO (12 cm^3) and transferred into the cold autoclave. This was cooled for 1 hr. Ketene (approx. 10-15 cm^3) was carefully distilled into the autoclave. The autoclave was cooled back to -120 °C (to condense the ketene) and then pressurised with CO (20 atm). The autoclave was then allowed to warm up to room temperature (as the autoclave was warmed to room temperature some of the gases were observed to leak from the autoclave which only resealed at around room temperature) and stirred at room temperature for 15 hr. The remaining gases were vented and the solution analysed by GCMS.

3.14.19 — *In-situ ^{13}C / ^1H VT-NMR study of the reaction of $[RhCl(I)_2CO(PEt_3)_2]$ (8c) with $AgBF_4$ / dimethylketene.*

$[RhCl(I_2)CO(PEt_3)_2]$ (0.0548 g 0.083 mmol) was dissolved in CD_2Cl_2 (0.6 cm^3) and cooled to 195 K. Approx. 1 equivalent of dimethylketene (7 µl) was added and the solution allow to warm slightly to allow dissolution of the dimethylketene then cooled back to 195 K. The sample was transferred to an NMR tube , sealed under nitrogen, and examined by ^{13}C / ^1H NMR spectroscopy at 193 K. After this a slurry of $AgBF_4$ (0.0592g 0.30 mmol) in CD_2Cl_2 (0.3 cm^3) was added to the sample whilst both were kept in darkness and at 195 K. The sample was returned to the NMR instrument and examined by ^{13}C / ^1H NMR spectroscopy in-situ at 193 K. The sample was warmed in-situ to 233K and allowed to equilibrate at this temperature for at least 10 min before examination by ^{31}P / ^1H NMR spectroscopy again. This procedure was repeated at 213 K and 253 K and then the sample warmed to room temperature for 16 hr and examined by ^{13}C / ^1H NMR spectroscopy for the final time. No reaction of **8b** was observed.

3.14.20 — *Synthetic scale reaction of $[RhCl(I)_2CO(PEt_3)_2]$ (8c) with $AgBF_4$ / dimethylketene.*

$[RhCl(I_2)CO(PEt_3)_2]$ (0.1621 g 0.25 mmol) was dissolved in CH_2Cl_2 (40 cm^3) and approx. 1 equivalent of $AgBF_4$ (0.0633g 0.33 mmol) and approx. 10 equivalents of dimethyl ketene (180 µl) added with stirring. The reaction solution was stirred in the dark at room temperature for 16 hr. The supernatant was filtered from the silver salts and since attempts to crystallise the product were unsuccessful the solvent was removed *in vacuo* to give a brown oil. A sample of this oil was examined by ^{31}P NMR spectroscopy and showed a forest of signals in the region δ = 35-55 ppm indicative of a breakdown of the rhodium bis-phosphine skeleton. The reaction was abandoned and no further analysis was carried out.

3.14.21 — *Synthesis of $C_6F_5OCH_2COCl$.*

$C_6F_5OCH_2CO_2H$ (1.0072 g 4.16 mmol) was dissolved in $SOCl_2$ (30 cm^3) and the mixture refluxed under dry nitrogen for 2 hr. The solution was allowed to cool to room temperature then the majority of the excess $SOCl_2$ removed by distillation at ambient pressure. When the volume was reduced to 3-4 cm^3 the sample was transferred to a short path distillation apparatus and the remainder of the $SOCl_2$ distilled off at water pump pressure. This yielded 0.5-1.0 cm^3 of clear liquid which was analysed by ^{13}C NMR spectroscopy. The product was identified by ^{13}C NMR spectroscopy as $C_6F_5OCH_2COCl$ by comparison to the ^{13}C spectrum of the original acid and the nature of the experimental conditions. ^{13}C NMR Data: 76.9 ppm (s) $\underline{C}H_2$; 137.4 ppm (m), 140.5 ppm (m), 143.8 ppm (m) F-$\underline{C}_{aryl}$; 156.7 ppm (s) O-$\underline{C}_{aryl}$; 170.0 ppm (s) $\underline{C}OCl$.

3.14.22 — *In-situ ^{31}P / ^{1}H VT-NMR study of the reaction of $[Rh(Cl)CO(PEt_3)_2]$ (1c) with $C_6F_5OCH_2COCl$.*

$[Rh(Cl)CO(PEt_3)_2]$ (0.0706g 0.18 mmol) was dissolved in CD_2Cl_2 (0.7 cm^3) and cooled to 203 K and approx. 1 equivalent of $C_6F_5OCH_2COCl$ (33 µl) added. The reaction solution was transferred to an NMR tube, sealed under nitrogen and transferred to the NMR instrument which was pre-cooled to 213 K. The sample was initially examined by ^{31}P / ^{1}H NMR spectroscopy in-situ at 213K. The sample was warmed in-situ to 233K and allowed to equilibrate for 10 min before examination again. This procedure was repeated at a range of temperatures; 253 K, 273 K and

303 K. The sample was then warmed ex-situ to 323 K and examined by ^{31}P / ^{1}H NMR spectroscopy (at room temperature) after 40 min, 7 hr then 16 hr at 323 K. During the in-situ reaction growth of signals due to just one product were observed, this was characterised by NMR spectroscopy as $[RhCl_2(COCH_2OC_6F_5)CO(PEt_3)_2]$ (**3g**). d^8-THF was added to the sample and the tube resealed under nitrogen and allowed to stand for 2 days at room temperature. No significant reaction was observed by ^{31}P NMR spectroscopy after this time.

3.14.23 — *Deuterium labelling study: Catalytic reaction carried out in 1:1 CH_3CH_2OD / toluene.*

$[Rh(I)CO(PEt_3)_2]$ (0.0253g 0.051 mmol) was dissolved in a mixture of CH_3CH_2OD (2 cm^3) and toluene (2 cm^3) and doubly distilled (MeI free) CH_2I_2 (1 cm^3) added. The sample was injected into an autoclave under a positive pressure of CO. The autoclave was charged with 40 atm CO then heated to 130 °C for 4 hr. (Refer to chapter two for details of the HP-equipment) After 4 hr the autoclave was cooled rapidly in cold water to quench the reaction. After venting the gases the contents of the autoclave were removed and CH_3CH_2OD and organic products separated from the involatile (organometallic) products and the toluene by fractional distillation. A sample of the resultant solution was examined by a range of NMR techniques to find the position of any D labels in the products. The NMR techniques employed were: $^{13}C\{^{1}H\}$ DEPT (75.4 MHz); $^{2}D\{^{1}H\}$ (46.1 MHz); and a comparison of $^{13}C\{^{1}H\}$ and $^{13}C\{^{1}H, ^{2}D\}$ spectra (125.7 MHz). The only deuterium labelled species observed were the deuterium source (CH_3CH_2OD) and $CH_2DCO_2CH_2CH_3$ (ethyl acetate) with 100% deuterium incorporation observed in the position indicated.

3.14.24 — *Use of ICH_2COR as the substrate in a catalytic reaction.*

Three reactions were carried out using standard catalytic conditions (see chapter 2, section 2.13) but where diiodomethane was replaced by the following substrates: a) ICH_2COCl (1 cm^3); b) ICH_2CO_2Et (1.5 cm^3); c) ICH_2CO_2Et (1.5 cm^3) and an equimolar amount of H_2O (230 µl). The catalytic reaction solutions were examined by GCMS and $EtOCH_2CO_2Et$ and EtI were found to be the sole organic products.

3.14.25 — *In-situ ^{31}P / ^{1}H VT-NMR study of the reaction of [Rh(Cl)CO(PEt$_3$)$_2$] (1c) with EtO$_2$CCH$_2$COCl.*

Rh(Cl)CO(PEt$_3$)$_2$] (0.0868g 0.22 mmol) was dissolved in CD_2Cl_2 (0.4 cm^3) and cooled to 213 K and approx. 0.95 equivalents of EtO_2CCH_2COCl (30 µl 0.21 mmol) added. The reaction solution was transferred to an NMR tube, sealed under nitrogen and transferred to the NMR instrument which was pre-cooled to 223 K. The sample was initially examined by ^{31}P / ^{1}H NMR spectroscopy in-situ at 223K. The sample was then warmed in-situ to 233K and allowed to equilibrate for at least 10 min before examination again. This procedure was repeated at a range of temperatures; 243 K, 263 K, and 293 K. The ^{13}C NMR spectrum was also recorded at 293 K, then the sample removed from the instrument. Ethanol (13 µl 0.22 mmol) was then added and the sample resealed under nitrogen and transferred back to the NMR instrument. The sample was again examined by ^{31}P / ^{1}H NMR spectroscopy, now at room temperature. The sample was warmed in-situ to 323 K and allowed to equilibrate for 30 min before examination by ^{31}P / ^{1}H NMR spectroscopy again. This procedure was repeated at 343 K and at 373 K the final ^{31}P / ^{1}H NMR spectra were recorded.

3.14.26 — *Synthesis of [RhCl$_2$(COCH$_2$CO$_2$Et)CO(PEt$_3$)$_2$] (7c).*

[Rh(Cl)CO(PEt$_3$)$_2$] (0.3362g 0.84 mmol) was dissolved in CH_2Cl_2 (20 cm^3) and EtO_2CCH_2COCl (160 µl 1.13 mmol) added with stirring. The reaction solution was stirred at room temperature for 20 hr then the solvent removed *in vacuo* giving a pale yellow oil. The oil was re-dissolved in a minimum volume of hot diethyl ether then cooled to 4-6 °C for 3 days to allow crystallisation to occur. The resultant white / pale yellow crystals were filtered at -5 °C and dried *in vacuo*, yield 79%. The product was identified as [$RhCl_2(COCH_2CO_2Et)CO(PEt_3)_2$] by ^{31}P / ^{13}C / ^{1}H NMR spectroscopy, IR, X-ray diffraction and microanalysis: Found; C 38.73 %, H 6.44 %. $C_{18}H_{37}Cl_2O_4P_2Rh$ requires; C 39.08 %, H 6.74 %.

3.14.27 — *The reaction of [RhCl$_2$(COCH$_2$CO$_2$Et)CO(PEt$_3$)$_2$] (7c) with EtOH.*

[$RhCl_2(COCH_2CO_2Et)CO(PEt_3)_2$] (0.1575g 0.29 mmol) was dissolved in CH_2Cl_2 (20 cm^3) and 1 equivalent of EtOH (17 µl 0.29 mmol) added with stirring. The solution was refluxed for 2 hr then cooled back to room temperature and the solvent removed *in vacuo* yielding a sticky yellow solid. The sticky solid was re-dissolved in a minimum volume of hot diethyl ether and the resulting solution cooled to -30 °C for

3 days to allow crystallisation to occur. The resultant white / pale yellow crystals were filtered at -50 °C and dried *in vacuo*. Analysis by ^{31}P NMR spectroscopy showed this to be pure starting material (**7c**). Thus the crystals, filtrate and NMR sample were recombined and re-dissolved in CH_2Cl_2 (20 cm^3) and 30 equivalents of EtOH (0.5 cm^3 8.5 mmol) added and the same procedure repeated. The result was as before but this time the filtrate was also examined by ^{31}P / ^{13}C NMR spectroscopy and GCMS and the major organometallic product (in the filtrate, not the overall reaction) observed to be $[Rh(Cl)CO(PEt_3)_2]$. The GCMS / ^{13}C NMR spectroscopy revealed the presence of diethylmalonate as the only organic product in the filtrate.

CHAPTER FOUR

Synthetic and Mechanistic Studies - Decomposition Products and Pathways

4.0 Introduction

The major limitation of the catalyst system under study is the short lifetime of the catalyst, this was demonstrated in chapter two (section 2.9). Chapter three concentrated on steps and species within the catalytic cycle. Any reaction step of a catalytic intermediate that exits the cycle, and is irreversible, constitutes a catalyst decomposition pathway. The major decomposition pathways of the $[Rh(X)CO(PEt_3)_2]$ catalysed double carbonylation of diiodomethane have been identified; the nature of these pathways and the products of such reactions are the theme of this chapter.

4.1 Loss of ketene from the metal centre

In chapter three the role of a metallo ketene intermediate in the proposed catalytic cycle was demonstrated (sections 3.6.1, 3.6.6, 3.9). The high selectivity of the catalytic reaction is presumably due to the high reactivity of such species. Unfortunately the displacement, by iodide, of ketene from the metal centre gives rise to a Rh(III) species which is not readily reduced under the reaction conditions. This pathway is illustrated in figure 4.1.1.

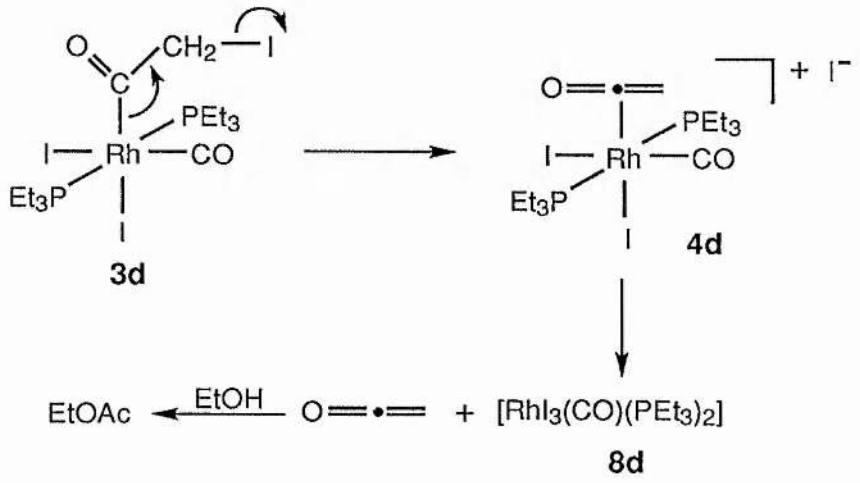

Figure 4.1.1

This irreversible reaction is thus a route to catalyst decomposition. It can be shown that it is, in fact, the major route to catalyst decomposition when the reaction is carried out under 40 atm CO, *vida infra.*

Ketene is not a stable entity under the catalytic reaction conditions, it reacts with ethanol to yield ethyl acetate[114] (in an inert solvent it dimerises to give diketene). Any free ketene present in a catalytic reaction carried out in ethanol will thus be indirectly detected as ethyl acetate at the end of the reaction. Thus, from figure 4.1.1, it can be seen that for each catalyst molecule which is irreversibly oxidised by the displacement of ketene by iodide one molecule of ethyl acetate will be present in the final reaction solution. In a standard catalytic reaction traces of MeI present in the substrate and the acetate ligands of the rhodium precursor $[Rh_2(OAc)_4]$ both act as potential sources of ethyl acetate. In order to remove these potential sources of ethyl acetate a pair of catalytic runs were carried out using pre-formed $[RhI(CO)(PEt_3)_2]$ as the catalyst and doubly distilled, ie MeI free, CH_2I_2 as substrate; the yield of ethyl acetate was quantified at the end of a 4 hour catalytic run. The results from this pair of reactions are shown in table 4.1.1.

Initial Catalyst Concentration / mM	Final Ethyl Acetate Concentration / mM
16.3 ± 1.6	9.6 ± 1.0
12.1 ± 1.2	9.9 ± 1.0

Table 4.1.1: Initial catalyst / final EtOAc concentrations in a catalytic systems under 40 atm CO and free from all sources of EtOAc except ketene formed in-situ.

These data show that ketene loss is involved in the major catalyst decomposition step. It was shown in chapter two that this decomposition pathway is disfavoured by increasing the CO pressure. Unfortunately at very highly elevated CO pressures which might be ideal for stabilising the catalytic intermediate against ketene loss, the rhodium centre appears to be susceptible to reaction with CO deactivating the catalyst by a different pathway - see chapter two, section 2.8.

4.2 The effect of bases on catalyst stability

All the previously reported catalytic systems capable of the double carbonylation of organohalides require the use of at least a stoichiometric quantity of base to remove

free hydrogen halides from the reaction. It was shown in chapter one that the catalytic system which is the subject of this thesis is unique in that it does not require a base. It might be expected that adding a base would have a beneficial effect, but it was shown in chapter two that all bases, both inorganic bases and N-centred organic bases, inhibit the formation of DEM. The study of the catalytic synthesis of α-keto esters has revealed that the choice of base and alcoholic solvent is crucial in determining the single to double carbonylation ratio of such catalytic systems (chapter one, section 1B) The present catalytic system is unusual in that when the singly carbonylated moiety (ketene) is released from the metal centre it gives rise to the decomposition of the catalyst. This explains the extremely high double / single carbonylation product ratio that is observed. With reference to the α-keto ester systems, the effect of the base / alcohol chosen is rationalised on the basis of the concentration and reactivity of the alkoxide ions in the system. Small acidic alcohols lead to low selectivity by the attack of their conjugate alkoxide upon metallo-acyl intermediates leading to singly carbonylated products. An example of this is shown in figure 4.2.1.[48, 49]

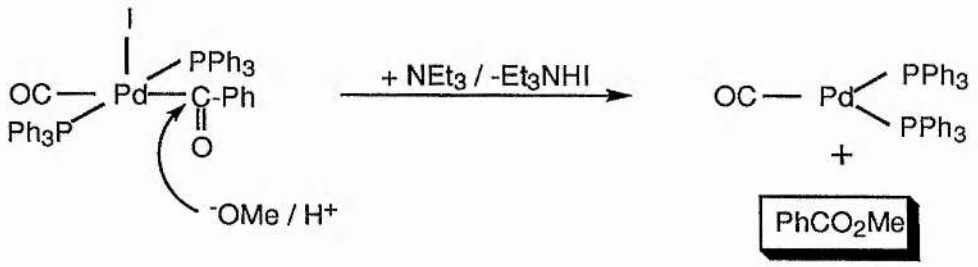

Figure 4.2.1: One pathway to singly carbonylated products in the alkoxy double carbonylation of PhI catalysed by palladium complexes.

It is likely, in the reaction under study here, that bases are observed to inhibit the reaction by increasing the ethoxide concentration. Ethoxide ions can attack the metallo ketene intermediate, releasing ethyl acetate and forming the decomposition product $[RhI_3(CO)(PEt_3)_2]$ (**8d**), thus deactivating the catalytic species, i.e. the reaction shown in figure 4.1.1. can be base catalysed.

4.3 Synthesis of $[RhCl(I)_2CO(PEt_3)_2]$ (8c) and $[RhI_3(CO)(PEt_3)_2]$ (8d)

Since species of the type $[RhX_3CO(PEt_3)_2]$ are important decomposition products of this reaction the syntheses of **8c** and **8d** were carried out by the oxidative addition of iodine to $[Rh(X)CO(PEt_3)_2]$ (X = Cl (**1c**), I (**1d**)) carried out in petrol.

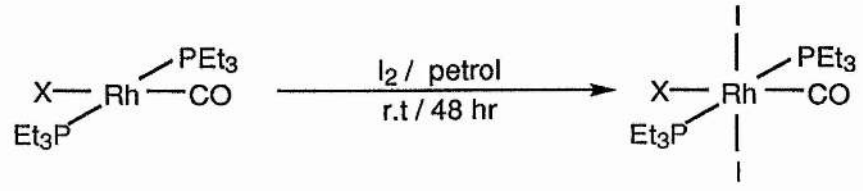

(X = Cl (**1c**), I (**1d**)) **8c/d**

Figure 4.3.1

It is important to use a non-polar solvent to achieve the clean synthesis of **8c**, to avoid halogen scrambling reactions, and also important in gaining pure **8d** for less obvious reasons.[145] The synthesis of **8d** can also be achieved in good yield by the metathesis of **8c** by NaI in acetone. The thermal stability of **8d** in d^6-acetone has been investigated and was discussed in chapter three (section 3.6.6). To summarise the work discussed there; it was found that the bis-phosphine skeleton of **8d** is not thermally stable and the species decomposes with the loss of one or more phosphine ligands. The formation of **8d** truly heralds the death of the catalyst. The formation of **8d** and the subsequent break-down of its bis-phosphine skeleton was also observed during real catalytic reactions - see chapter four, section 4.6.

4.4 The reaction of PEt_3 with CH_2I_2

In a normal catalytic run the catalyst precursors $[Rh_2(OAc)_4]$ and PEt_3 are mixed with CH_2I_2 before the reaction vessel is stirred under CO. Two equivalents of PEt_3 are required per rhodium centre to form the bis-phosphine catalyst, but it is possible that the phosphine is quaternised by the diiodomethane before the $[Rh(OAc)CO(PEt_3)_2]$ (**1a**) can form. This is highlighted by the optimal P:Rh ratio of 3:1 established in catalytic reactions (chapter 2, section 2.1). The quaternisation of PEt_3 by MeI occurs in a matter of seconds at room temperature, but the reaction with CH_2I_2 was found to occur much more slowly. Evidence for the relative rate of the quaternisation reaction comes from an investigation of the phosphorus and rhodium-phosphorus species present in a standard catalytic run at early reaction times (chapter four, section 4.6). This showed that most of the PEt_3 was bound to rhodium after a reaction time of 10 min.

The reaction of PEt_3 with CH_2I_2 was investigated by heating a 1:1 ratio of the two components, in the dark, to 70 °C in toluene. After 90 min a white precipitate was observed. After recrystallisation of this white solid from methanol the species was characterised as the expected phosphonium salt $[Et_3PCH_2I^+]I^-$.

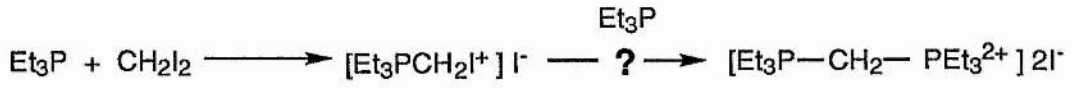

Figure 4.4.1

As CH_2I_2 is a diiodide it could potentially quaternise two phosphine molecules, thus the reaction of $[Et_3PCH_2I^+]I^-$ with a second molecule of PEt_3 was investigated. Attempts to synthesis the methylene bridged di-phosphonium salt, shown in figure 4.4.1, proved unsuccessful.

Since $[Et_3PCH_2I^+]I^-$ has the potential to be formed in the catalytic reaction, its thermal stability in ethanol was investigated. After heating $[Et_3PCH_2I^+]I^-$ to 60-70 °C in ethanol for 3 hr the product mixture was examined by ^{31}P NMR. This showed that >95 % of the phosphonium salt had remained unreacted. A small singlet (δ = 37.0 ppm) was also observed but the species responsible for this could not be characterised using ^{31}P / ^{1}H NMR.

4.5 The reaction of $[Et_3PCH_2I^+]I^-$ with $[Rh(OAc)CO(PEt_3)_2]$ (**1a**)

Having observed the potential for the formation of $[Et_3PCH_2I^+]I^-$ from PEt_3 and CH_2I_2 the reaction between the catalytically active species **1a** and the phosphonium salt was investigated. A 1:3 mixture of **1a** / phosphonium salt was stirred in THF in the dark at room temperature for 18 hr.

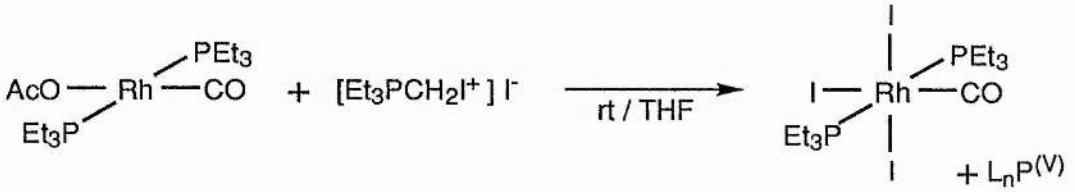

(Major) - **8d**

Figure 4.5.1: The reaction of complex **1a** with $[Et_3PCH_2I^+]I^-$.

Examination of the resultant oil by ^{31}P NMR showed the major products of the reaction to be $[RhI_3(CO)(PEt_3)_2]$ (**8d**) and a species giving a singlet at 38.2 ppm. The presence of a residual quantity of the starting materials was also observed. The species observed at 38.2 ppm was not identified but it is in the correct region of the ^{31}P spectrum to be a P(V) species, potentially $[Et_3PCH_2OEt^+]I^-$.

4.6 Time resolved NMR 'Snapshots' of the catalytic reaction

Normally the trial catalytic runs have been carried out for a duration of 4 hours. It was shown in chapter two (section 2.9) that the lifetime of the catalyst is lower than 4 hours at 120 °C. These 'Snapshot' experiments were carried out by the following method: The autoclave was set up in the conventional manner and an ethanolic solution of diiodomethane and catalyst injected into the autoclave which was then pressurised with 40 atm CO. The temperature of the stirred autoclave[159] was raised to 120 °C over 10 min, the temperature was then held at 120 °C for a fixed period of time. At the end of this time the reaction was quenched by rapid cooling of the autoclave. Once cool, the contents were removed under a nitrogen atmosphere, the solvent removed *in vacuo* and the organometallic oil re-dissolved in CD_2Cl_2 for analysis by ^{31}P / ^{1}H NMR. Small solvent shifts were observed in the NMR spectra due to the samples being dissolved in a mixture of CH_2I_2 and CD_2Cl_2, CH_2I_2 was still present due to its involatility and the method used for sample preparation.

Analogous results were observed when either pre-formed $[Rh(I)CO(PEt_3)_2]$ (**1d**) or the precursors $[Rh_2(OAc)_4]$ / 6 PEt_3 were used as the source of the catalyst. The ^{31}P NMR 'Snapshots' for 3 reactions at 10, 30 and 60 min (using **1d**) are shown in figure 4.6.1. After 10 min at 120 °C the major products were identified as $[RhH(I)_2CO(PEt_3)_2]$ (**9d**) and $[RhI_3(CO)(PEt_3)_2]$ (**8d**). Lesser amounts of $[Et_3PCH_2I^+]I^-$ and $[RhI_2(CH_2I)CO(PEt_3)_2]$ (**2d**) are observed along with signals believed to be due to mono-phosphine rhodium complexes in the 30-50 ppm spectral region. It will be shown below that the presence of **9d** does not indicate catalyst decomposition, thus the major bis-phosphine decomposition product is **8d** as earlier work had indicated (sections 4.1 & 4.5). The presence of **2d** was confirmed by ^{1}H NMR; the characterisation of the doublet at around 13.6 ppm (J_{Rh-P} = 84 Hz) as **9d** will be covered below. The ^{31}P spectral 'snapshots' of the reaction after 30 min, then 60 min show that no species with a $[RhL_n(PEt_3)_2]$ skeleton remains intact after 30 min, the predominant species is presumed to be $OPEt_3$, giving rise to a broad singlet at around 80 ppm.

$[RhH(I)_2CO(PEt_3)_2]$ (**9d**) was thought to give rise to the doublet at 13.6 ppm (J_{Rh-P} = 84 Hz), this was confirmed by both ^{1}H and partially ^{1}H coupled ^{31}P spectra. Examination of the hydride region of the ^{1}H NMR showed a doublet of triplets at -11.2 ppm where the hydride resonance is coupled to rhodium (J_{Rh-Hyd} = 16 Hz) giving a doublet and further coupled to 2 equivalent phosphorus atoms (J_{P-Hyd} = 10 Hz) which causes the further splitting into triplets.

Figure 4.6.1: ^{31}P NMR "Snapshots" of standard catalytic reactions after various times at 120 °C.

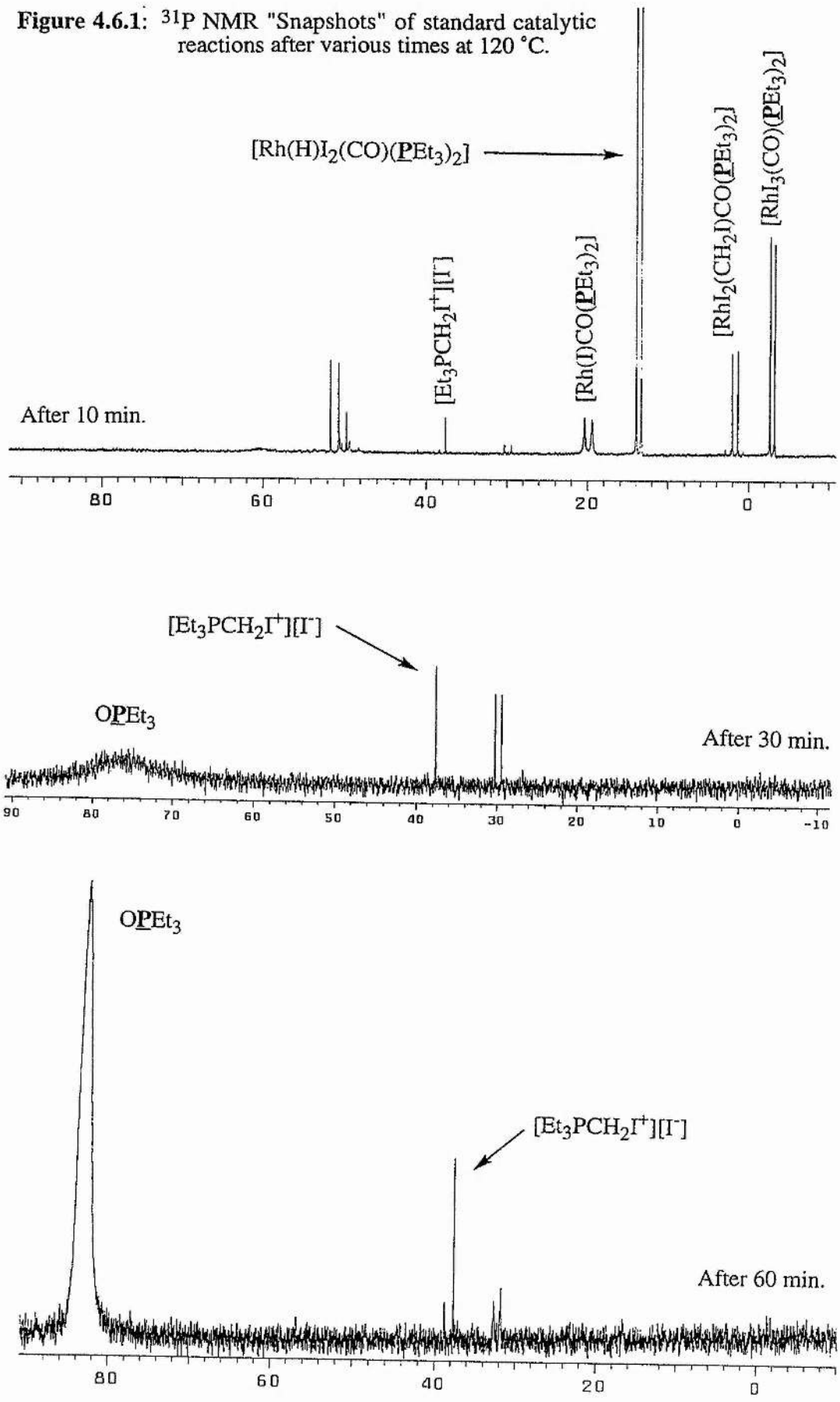

To confirm that the same species was responsible for both the ^{31}P signal at 13.6 ppm and the ^{1}H signal at -11.2 ppm a selectively ^{1}H coupled ^{31}P experiment was carried out. In this experiment the ^{1}H decoupling pulse was restricted to the region above 0 ppm thus allowing phosphorus hydride couplings to be observed. Careful examination of this ^{31}P spectrum showed all the signals to be unaffected except the doublet at 13.6 ppm which was observed to decrease in intensity and to split into a doublet of doublets. The coupling constant $J_{P\text{-}Hyd}$ was observed as 6 Hz in this ^{31}P spectrum. Simplistically one might expect the P-Hydride coupling in both the ^{1}H and ^{31}P (hydride undecoupled) spectra to be of equal magnitude, the reason why this is not observed is due to the shape of the decoupling pulse which was used. This decoupling pulse was not a simple square wave with distinct boundaries, but rather more sinusoidal in form and thus displays side-bands which do not allow for the hydride region to be fully undecoupled.

Other work from within our group has confirmed the spectroscopic assignment of **9d** by its direct synthesis (and full characterisation) from the reaction of aqueous HI with **1d** in acetone.[160] An important question to ask about $[RhH(I)_2CO(PEt_3)_2]$ (**9d**) is how readily it reductively eliminates HI in an alcoholic solution to return the catalytically active species **1d**.

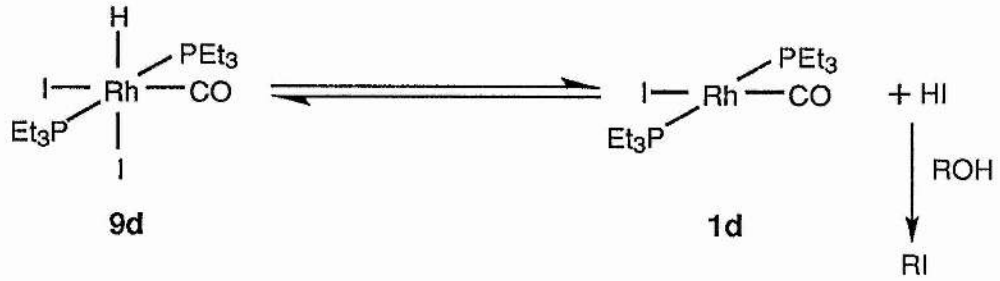

Figure 4.6.2

When **9d** is dissolved in either d^4-methanol or d^1-ethanol and allowed to stand at room temperature for 16 hours then examined by ^{31}P NMR the major species observed is $[Rh(I)CO(PEt_3)_2]$ (**1d**).[160] This complex must result from the reductive elimination of HI from the starting material. This indicates that the formation of **9d** is not a route of catalyst decomposition as the reductive elimination can occur readily in alcohols to re-form the catalytically active species **1d**. The ability of an alcohol to promote the reductive elimination of HI from **9d** is another reason why the catalytic reaction under study shows a strong dependence on an alcoholic solvent (see chapter 2, section 2.5 and chapter 3, section 3.13).

The reaction between **9d** and ethanol appears to be a special feature of this catalytic system. All the other halocarbon catalytic double carbonylation systems, which have been reported to date, require a base to remove the resultant hydrogen halide (see chapter 1). With **1d** as the catalyst, ethanol is able to play the role of the HI sink producing ethyl iodide. Complex work up procedures are required for all other reported double carbonylation systems where the product is either formed as a metal salt when inorganic bases are employed or when an amine base is used the product has to be extracted from the solid HI adduct of amine (see chapter 1). The easy separation of EtI from DEM in this catalytic system offers important practical advantages such systems.

4.7 Attempts to establish the source of $[RhH(I)_2CO(PEt_3)_2]$ (9d)

Although it has been shown independently[160] that $[RhH(I)_2CO(PEt_3)_2]$ (**9d**) can be formed by the reaction of **1d** with HI [Path A] it is also conceivable that the oxidative addition of EtI to **1d** followed by the elimination of ethene [Path B] could account for the observation of **9d** in the NMR 'Snapshots' of the catalytic reaction - see figure 4.7.1.

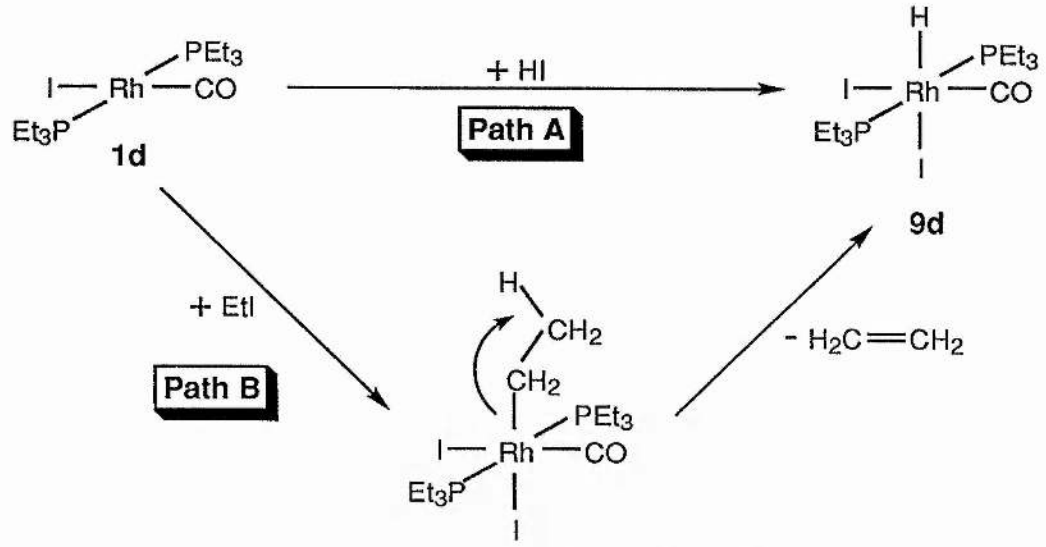

Figure 4.7.1: The two potential routes to yield complex **9d** in the catalytic reaction.

Path B was considered to be a plausible alternative route on the basis of the presumably short lifetime of free HI in the presence of EtOH and the resultant high concentration of EtI in the catalytic reaction. Three experiments were carried out to examine the possibility that Path B might account for all or some of the **9d** observed

under catalytic reaction conditions. Firstly the reaction of **1d** with one equivalent of EtI in CH_2Cl_2 was attempted under conditions designed to model the catalytic reaction: 40 atm CO, 120 °C for 10 min. After removal of the solvent the resultant oil was examined by ^{31}P NMR immediately after the reaction with no attempt made to alter the product distribution by any form of work up. The ^{31}P spectrum showed the major species to be unreacted **1d**, but a trace of **9d** (1.4% by ^{31}P peak height) was also observed.

When a NMR 'Snapshot' experiment was carried out using **1d** and diiodomethane in methanol, no hydride complexes were observed after 10 or 30 min. This could suggest that the path B is the route to **9d** as in this system there is no ethyl iodide, only methyl iodide, and thus the observation of **9d** is dependent not on the presence of HI in the system but rather on the presence of EtI. It should be noted that the absence of **9d** in the MeOH 'Snapshot' experiment could also be due to the reaction between **9d** and MeOH being much faster than between **9d** and EtOH. It was shown in section 4.6 that complex **9d** reacts readily with alcohols (ROH) to yield **1d** and RI.

The final study carried out to establish the source of **9d** was a deuterium labelling experiment which is illustrated in figure 4.7.2.

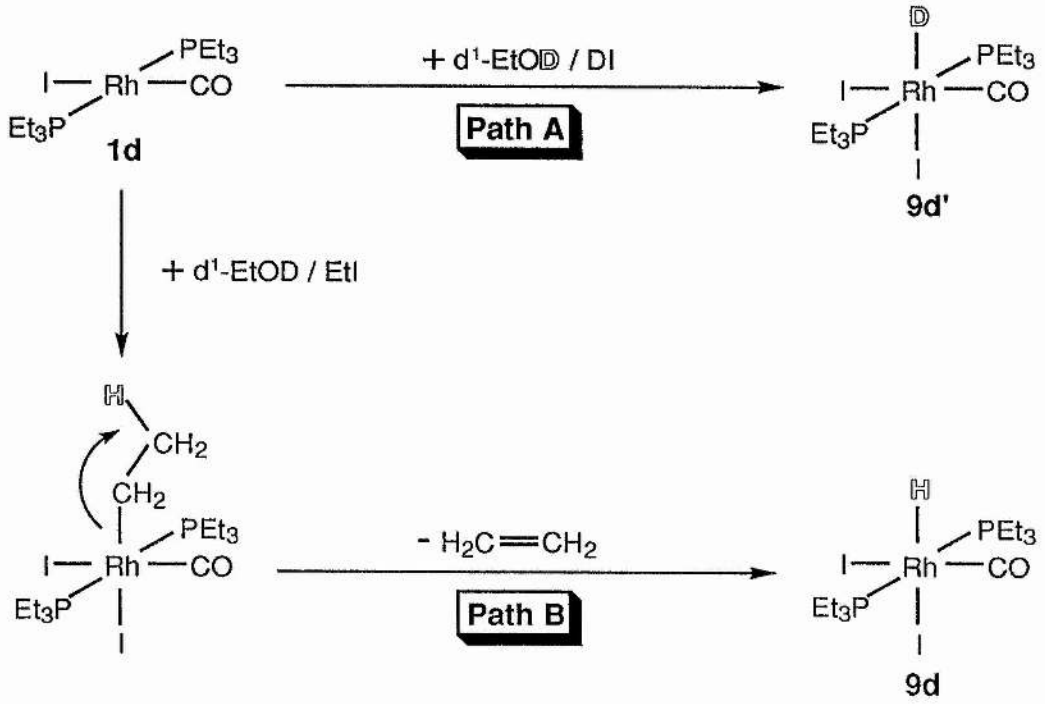

Figure 4.7.2: Deuterium labelling experiment to determine the source of complex **9d** in the catalytic reaction.

The labelling experiment shown in figure 4.7.2 was realised by carrying out an NMR 'Snapshot' experiment in 1:1 toluene / CH_3CH_2OD for 10 min at 120 °C / 40 atm CO. The products of this reaction were examined by ^{31}P and ^{1}H NMR.

The ^{31}P / ^{1}H NMR spectra are shown in figure 4.7.3. The ^{31}P spectrum clearly shows that the hydride (**9d**) / deuteride (**9d'**) species is present in significant concentration. The doublet observed at 13.5 ppm could be due to a super position of doublets from both **9d** and **9d'** due to the 1-2 Hz line width inherent to ^{31}P spectra. This line width also masks the potential phosphorus-deuteride coupling which would be expected to be only 1/7th of that observed for an analogous phosphorus-hydride coupling, ie $J_{P\text{-}D} \approx 1.4$ Hz. The ^{1}H spectrum of this product mixture shows only a weak doublet of triplets in the hydride region. The direct observation of the resonance pattern due to a potential deuteride species (**9d'**) by ^{2}D NMR did not prove possible as appropriate equipment was unavailable.

Considering all the data together it appears that $[RhH(I)_2CO(PEt_3)_2]$ (**9d**) can be formed by both Path A and Path B (see figure 4.7.1-2). The deuterium labelling experiment strongly suggests that Path A predominates as the ^{31}P spectrum shows the hydride / deuteride species to be present in high concentration and yet the ^{1}H NMR shows only a weak signal due to the hydride **9d** even after a long acquisition time. This suggests that the predominant species giving rise to $\delta_P = 13.5$ ppm is $[RhD(I)_2CO(PEt_3)_2]$ (**9d'**). Thus the reaction with HI / DI is the major route to **9d/9d'** but the reaction of **1d** with EtI and the subsequent loss of ethene could also account for a small fraction of the **9d** observed under standard catalytic reaction conditions. The HI from residual EtOH in the EtOD could also account for some or all of the **9d** observed. In addition to the examination of the product mixture by ^{2}D NMR, the potential for deuterium exchange between **9d** and EtOD should be investigated.

Figure 4.7.3: ^{31}P NMR "Snapshot" of a catalytic reaction solution (where reaction carried was out in d^1-EtOD / toluene) after 10 min at 120 °C.

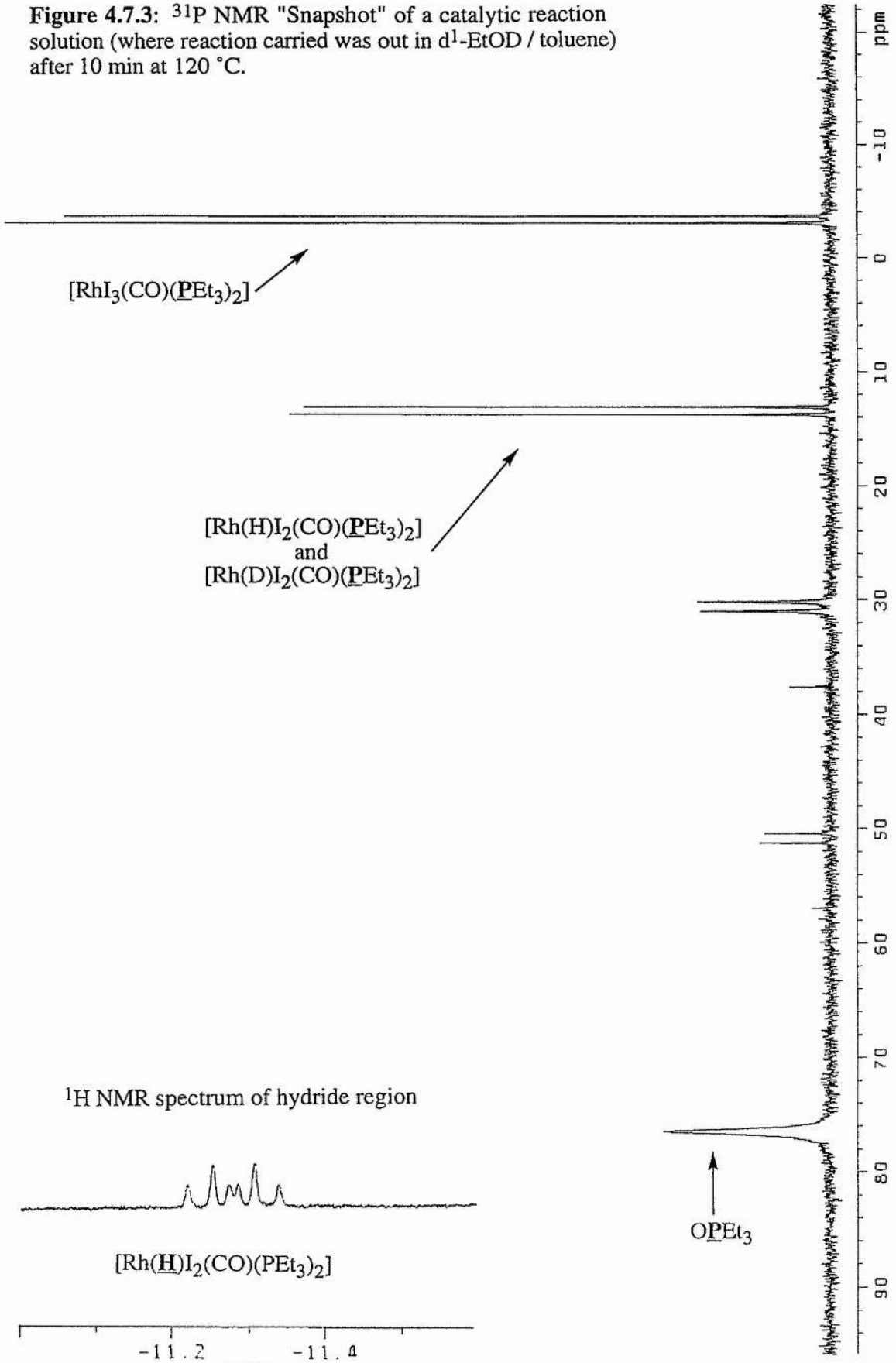

^1H NMR spectrum of hydride region

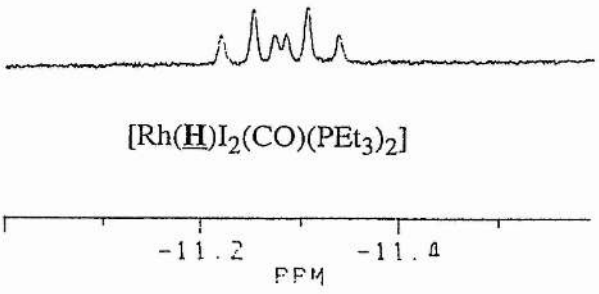

[Rh(H)I2(CO)(PEt3)2]

4.8 The reaction of $[RhCl_2(COCH_2Cl)CO(PEt_2)_3]$ (3c) with ethanol

The synthesis of **3c** was achieved by the oxidative addition of chloroacetyl chloride to **1c** (chapter 3, section 3.6.2). The reverse reaction was attempted by refluxing **3c** in ethanol.

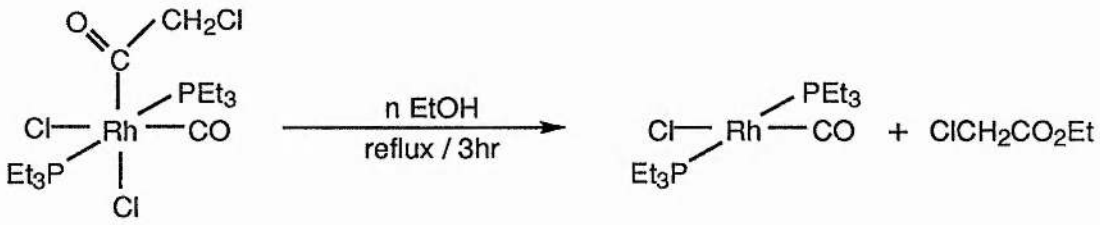

3c **1c**

Figure 4.8.1: The reaction of complex **3c** with excess ethanol under reflux.

The free energy of the reductive elimination will be more favourable at higher temperatures due to the increase in entropy in going from one species to two. Also, if an equilibrium exists between the Rh(III) and the Rh(I) species this will be pushed towards the Rh(I) species when the reaction is carried out in ethanol because any free chloroacetyl chloride will react with the ethanol thus driving the reaction according to Le Chatelier's principle.

After refluxing **3c** in ethanol for 3 hours the organic and organometallic components were separated and analysed. ^{31}P NMR analysis of the organometallic product/s showed that over 95% of **3c** had been converted into **1c**. After concentrating the organic fraction, by removing the majority of the solvents by distillation, apart from the solvent, only one product was observed. This product was characterised by GCMS and ^{13}C NMR as $ClCH_2CO_2Et$ as anticipated. The fact that this reaction occurs for this complex points to the transient nature of the intermediate of the catalytic cycle which it models (**3d**). Never in any catalytic reaction has either ICH_2CO_2Et or $EtOCH_2CO_2Et$ been observed amongst the products, these being the products one would expect from the reductive elimination of iodoacetyl iodide from **3d**. This must mean that the rearrangement of **3d** to the metallo ketene species **4d** is much more rapid than the potential reductive elimination step. Remember also that this reductive elimination would not be reversible under standard reaction conditions where ethanol is the solvent. Thus the reaction of intermediate **3d** with ethanol can be ruled out as a significant side reaction in the real catalytic system.

4.9 Carbene complexes and the loss of carbene

A potential catalyst decomposition step involving a carbene intermediate is illustrated in figure 4.9.1.

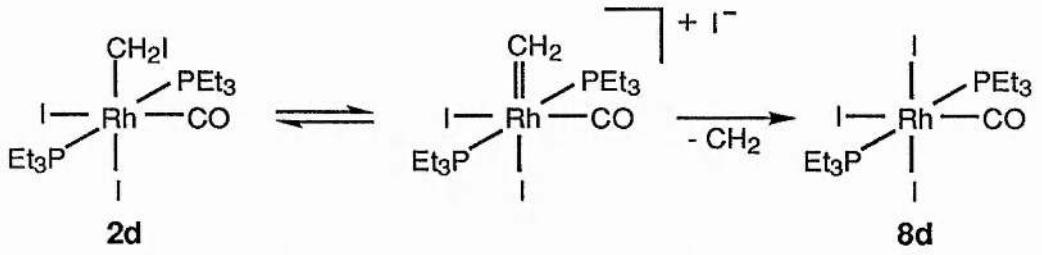

Figure 4.9.1: A potential catalyst decomposition step via a carbene complex.

To test for the potential equilibrium between **2d** and the isomeric carbene, a solution of crude **2d** (contaminated with **2e**) in THF was stirred in the dark with an excess of Z-diethyl maleate. Alkenes, particularly diethyl maleate, are known as efficient carbene traps, reacting with carbenes to form cyclopropane derivatives. Aliquots where taken from the reaction solution after 20 and 92 hours and examined by GCMS. No cyclopropyl derivative was observed, but the isomerisation of the diethyl maleate from its Z to E form appears to be catalysed by the rhodium species. This experiment gives no evidence for the iodomethyl to carbene equilibrium shown in figure 4.9.1.

To be sure that carbene complexes are not involved in the catalytic cycle or form a route to catalyst decomposition further work will need to be carried out. If free $:CH_2$ (carbene) were released in the reaction, as illustrated above, then it would probably insert into the O-H bond of the solvent (EtOH) giving MeOEt. The volatility of this species would make its detection very difficult. Two potential routes to trap the CH_2 in-situ can be envisaged. A significant quantity of diethyl maleate could be added into a standard catalyst run, replacing 25% of the ethanolic solvent for example, and the reaction products analysed for the presence of cyclopropanes. Alternatively a higher alcohol such as n-BuOH could be used as the solvent, the reaction of n-BuOH with $:CH_2$ would yield MeOBu which would be suitably involatile to be detected by GCMS / NMR at the end of the reaction.

4.10 Experimental

All the following reactions (unless specified) were carried out in dry deoxygenated solvents under a dry nitrogen atmosphere. The general experimental procedures such as the drying of solvents, the nature of the equipment used in this work and the sources of the chemicals are summarised in Appendix One. All NMR and IR data from the organorhodium species are collected in tables 3.1 - 3.4 presented in chapter three.

4.10.1 — *Quantifying the concentration of ethyl acetate formed from ketene during a catalytic reaction.*

The CH_2I_2 used for this experiment was purified by distilling twice at ambient temperature. Analysis of the purified CH_2I_2 by GCMS showed that, within the sensitivity limitations of the instrumentation, the sample contained no MeI.

[Rh(I)CO(PEt_3)$_2$] (Run 1; 0.0306 g 0.062 mmol: Run 2; 0.0403 g; 0.082 mmol) was dissolved in EtOH (4 cm^3) and (MeI free) CH_2I_2 (1 cm^3 12.4 mmol) added. The solution was injected into an autoclave and the autoclave pressurised to 40 atm with CO. (See chapter 2, section 2.14 (Runs 106-221) for details of autoclave filling and heating methods) After 4 hours at 120 °C the autoclave was cooled the contents removed, dissolved 1:1 with diethyl ether and used for analysis.

The analysis for the EtOAc concentration was carried out by GC using p-xylene as an internal standard and the following temperature program for the GC. 5 min at 25 °C followed by raising the temperature to 150 °C at 16 °C·min^{-1} (7.81 min) and then maintaining this temperature for a further 3.19 min. The concentrations of EtOAc was calculated from a calibration curve, plotted from data obtained from solutions of known concentration, also using p-xylene as the internal standard.

4.10.2 — *Synthesis of [RhCl(I)$_2$CO(PEt_3)$_2$] (8c).*

[Rh(Cl)CO(PEt_3)$_2$] (0.4900 g 1.22 mmol) was dissolved in light petroleum (40 cm^3), I_2 (0.3094g 1.22 mmol) added and the solution stirred under nitrogen in the dark for 48 hr. This gave an orange / red solution and a brown / black solid. The solution was filtered and the volume of the filtrate reduced to 15 cm^3 *in vacuo* when crystallisation was observed to have just started to occur. To this was added diethyl ether (15 cm^3)

to redissolve the crystals and the solution held at -30 °C for 48 hr to allow slow crystallisation to occur. The resultant large red / brown crystals were filtered at -40 °C, yield 83%. The product was identified as $[RhCl(I)_2CO(PEt_3)_2]$ by ^{31}P NMR spectroscopy and microanalysis: Found; C 24.7%, H 5.1%. $C_{13}H_{30}ClI_2OP_2Rh$ requires; C 23.8%, H 4.6%.

4.10.3 — *Synthesis of $[RhI_3(CO)(PEt_3)_2]$ (8d).*

This can be achieved by the method described in section 4.10.2 by substitution of starting complex **1c** by $[Rh(I)CO(PEt_3)_2]$ (**1d**) [Route A][160] or by the metathesis of $[RhCl(I)_2CO(PEt_3)_2]$ with NaI [Route B].

[Route B] - $[RhCl(I)_2CO(PEt_3)_2]$ (0.1493 g 0.23 mmol) was dissolved in acetone and approx. 5 equivalents of NaI (0.185 g 1.23 mmol) added with stirring. The reaction solution was stirred for 15 min at room temperature. The volume of the resultant orange solution was reduced to approx. 5 cm^3 then light petroleum (2 x 20 cm^3) used to extract the product. The supernatant was filtered from the sodium salts and the volume reduced *in vacuo* until crystallisation was observed to have just started to occur. To this was added diethyl ether (15 cm^3) to redissolve the crystals and the solution held at -30 °C for 48 hr to allow slow crystallisation to occur. The resultant red / brown powder was filtered at -40 °C, quantitative yield. The product was identified as $[RhI_3(CO)(PEt_3)_2]$ by ^{31}P NMR spectroscopy, IR and microanalysis: Found; C 21.28 %, H 4.20 %. $C_{13}H_{30}OP_2Rh$ requires; C 20.88 %, H 4.04 %.

4.10.4 — *The reaction of CH_2I_2 with PEt_3.*

PEt_3 (1 cm^3 6.78 mmol) was dissolved in toluene (30 cm^3) and CH_2I_2 (840 µl, 10.2 mmol) added. The reaction mixture was stirred and heated to 50-70 °C in the dark for 90 min then allowed to cool back to room temperature. The white precipitate formed was collected, washed with toluene, and dried *in vacuo*. The product was twice recrystallised from methanol (20-30 cm^3). Where possible all manipulations were carried out in the dark. The product was characterised as $[Et_3PCH_2I^+]I^-$ by ^{31}P / ^1H NMR spectroscopy and microanalysis. ^{31}P NMR δ = 39.5 ppm (s). ^1H NMR 1.5 ppm (dt) $C\underline{H}_3$, 2.6 ppm (dq) $C\underline{H}_2$, 4.0 ppm (d) $-C\underline{H}_2I$. Found; C 21.8 %, H 4.5 %. $C_7H_{17}I_2P$ requires; C 21.8 %, H 4.4 %.

4.10.5 — *The reaction of $[Et_3PCH_2I^+]I^-$ with ethanol at 60-70 °C.*

$[Et_3PCH_2I^+]\ I^-$ (0.1605 g 0.42 mmol) in ethanol (20-30 cm^3) was placed in a pressure bottle and heated to 60-70 °C for 3 hr. The solvent was removed *in vacuo* and a sample of the resultant white solid dissolved in d^4-MeOD for examination by ^{31}P NMR spectroscopy.

4.10.6 — *The reaction of $[Et_3PCH_2I^+]I^-$ with $[Rh(OAc)CO(PEt_3)_2]$.*

$[Rh(OAc)CO(PEt_3)_2]$ (0.12 g 0.28 mmol) was dissolved in THF (20-30 cm^3) and $[Et_3PCH_2I^+]\ I^-$ (0.30 g 0.78 mmol) added in THF (10 cm^3). The reaction mixture was stirred under nitrogen in the dark for 18 hr. The solvent was removed *in vacuo* and the resultant oil examined in d^6-benzene by ^{31}P NMR spectroscopy.

4.10.7 — *Time resolved NMR 'Snapshot' reactions.*

These reactions were carried out in either EtOH, MeOH or 1:1 (v/v) toluene / CH_3CH_2OD using either pre-formed $[Rh(I)CO(PEt_3)_2]$ (0.02 g 0.04 mmol) as the catalyst or the catalyst precursors $[Rh_2(OAc)_4]\cdot 2MeOH$ (0.01 g 0.02 mmol) and PEt_3 (16 µl 0.13 mmol). The autoclave was charged with a solution of the catalyst and CH_2I_2 (1cm^3) in the required solvent (4 cm^3) and the vessel pressurised to 40 atm with CO (See chapter 2, section 2.14 (Runs 106-221) for details of autoclave filling and heating methods). The autoclave was then heated for 10 min and the temperature held at 120 °C for either 10, 30 or 60 min. After the desired reaction duration the autoclave was cooled and the contents removed under a nitrogen atmosphere for analysis. The solvent was removed from the reaction solution leaving a brown product solution in the involatile residual CH_2I_2. CD_2Cl_2 (0.5 cm^3) was added to the products and the solution examined immediately by ^{31}P / ^1H NMR spectroscopy.

4.10.8 — *The Reaction of $[Rh(I)CO(PEt_3)_2]$ with EtI in EtOH.*

$[Rh(I)CO(PEt_3)_2]$ (0.1507 g 0.31 mmol) was dissolved in EtOH (5 cm^3) and 1 equivalent of EtI (25 µl 0.31 mmol) added. The solution was transferred to an autoclave and the vessel charged with 40 atm CO. The autoclave was then heated for 10 min and the temperature held at 120 °C for a further 10 min. After this time the autoclave was cooled and the contents removed under a nitrogen atmosphere for

analysis. The solvent and excess EtI were removed *in vacuo* and the resultant oil re-dissolved in CD_2Cl_2 and examined by ^{31}P NMR spectroscopy.

4.10.9 — *The reaction of $[RhCl_2(COCH_2Cl)CO(PEt_3)_2]$ (3c) with excess EtOH.*

$[RhCl_2(COCH_2Cl)CO(PEt_3)_2]$ (0.062 g 0.12 mmol) was dissolved in EtOH (5 cm^3) and refluxed for 2 hr. The reaction solution was allowed to cool and the organic and organometallic species separated by distillation at reduced pressure (0.1 mmHg). The organometallic fraction formed a yellow oil which was re-dissolved in CD_2Cl_2 and examined by ^{31}P NMR spectroscopy (>95% **1c**). The organic fraction was concentrated to 0.5-1.0 cm^3 by a careful distillation at ambient pressure. An aliquot of the concentrated organic fraction was examined by GCMS. The rest of the solution was spiked with 10% $CDCl_3$ and examined by ^{13}C NMR spectroscopy. The GCMS / ^{13}C NMR spectrum showed the sole organic product to be $ClCH_2CO_2Et$ which was identified by comparison to published spectra.

4.10.10 — *The attempted reaction of $[RhI_2(CH_2I)CO(PEt_3)_2]$ (2d) with Z-diethyl maleate in THF.*

To a solution containing trans-$[RhI_2(CH_2I)(CO)(PEt_3)_2]$ (approx. 0.12 mmol) and CH_2I_2 (approx. 12 mmol) in THF (30 cm^3) was added freshly distilled diethyl maleate (190 µl 1.2 mmol) and the mixture stirred in the dark. Simultaneously a control reaction containing CH_2I_2 (0.9 cm^3 12 mmol) and diethylmaleate (190 µl 1.2 mmol) in THF (30 cm^3) was also stirred in the dark. From each reaction an aliquot (1 µl) was taken after 20 and 92 hr and examined by GCMS.

CHAPTER FIVE

Conclusions and Further Work

The use of the catalyst precursors rhodium acetate [$Rh_2(OAc)_4$], carbon monoxide and triethyl phosphine in an alcoholic solvent forms a species capable of catalysing the double carbonylation of diiodomethane. When this reaction is carried out in ethanol, the major products are diethylmalonate (DEM) and ethyl iodide.

$$CH_2I_2 + 2CO + 2EtOH \xrightarrow{[Rh_2(OAc)_4] / PEt_3 / CO} CH_2(COOEt)_2 + 2HI$$

The ethyl iodide is formed by the reaction of EtOH with HI, presumably forming equal amounts of water. The other, minor, products of this reaction were diethoxymethane ($CH_2(OEt)_2$), ethyl propanoate ($CH_3CH_2CO_2Et$) with a trace of ethyl acetate (CH_3CO_2Et). The diethoxymethane is formed by the ethanolysis of the substrate and the ethyl propanoate may be from the carbonylation of ethyl iodide formed in situ. An attempt to use the same catalytic system to carbonylate ethyl iodide in the absence of diiodomethane proved unsuccessful.[137] The carbonylation of EtI possibly only occurs under the acidic conditions caused by the carbonylation of the diiodomethane. The source of the ethyl acetate has been shown to be ketene, a metal complex thereof being shown to be the singly carbonylated intermediate between diiodomethane and DEM. Possibly the most notable feature of this catalytic reaction is that it occurs in the absence of added base. A review of all the double carbonylation reactions reported to date (chapter one) reveals this catalytic system to be unique in this respect. It is the solvent, EtOH, which acts as the sink for HI in this system and this accounts for the high yields of EtI.

A thorough study of the mechanism of this reaction has led to the proposal of the mechanistic cycle shown overleaf in figure 5.1. The most salient feature of this mechanism is the proposal of a metallo ketene intermediate. Evidence for the involvement of a metallo ketene complex in this reaction comes from the study of the attempted synthesis of the iodoacyl intermediate **3d** described in chapter three (section 3.6.1), the results of which are summarised in figure 5.2.

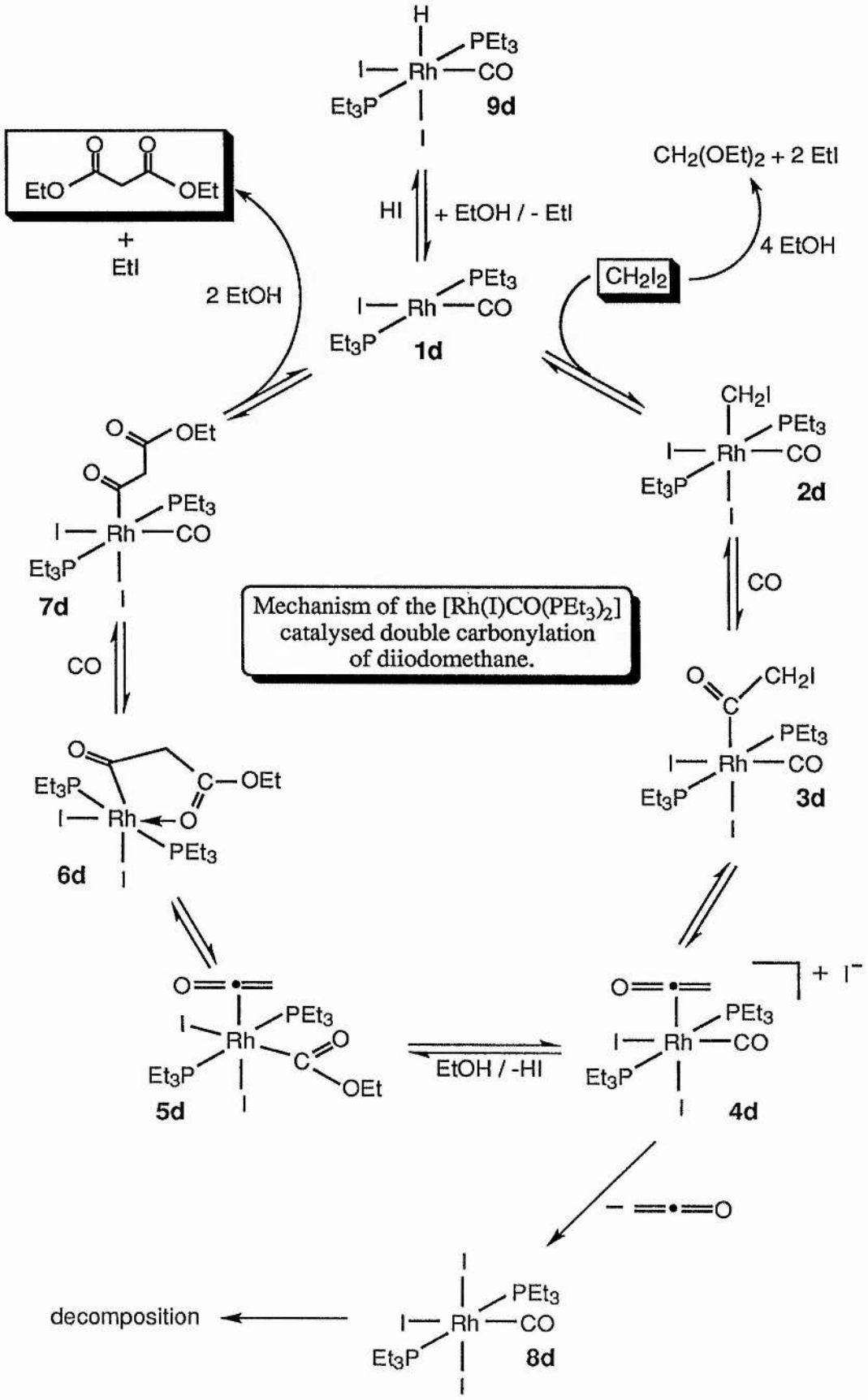
Mechanism of the [Rh(I)CO(PEt3)2] catalysed double carbonylation of diiodomethane.
9d
1d
2d
3d
4d
5d
6d
7d
8d
HI
+ EtOH / - EtI
2 EtOH
+ EtI
CH2I2
4 EtOH
CH2(OEt)2 + 2 EtI
CO
EtOH / -HI
decomposition

Figure 5.1

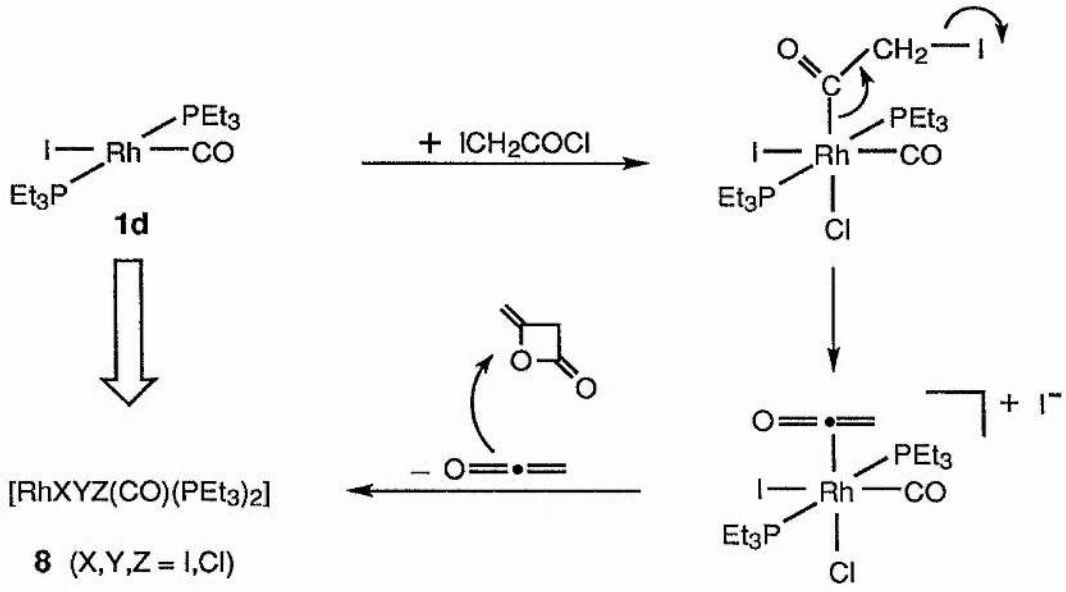

Figure 5.2

Further evidence comes from a deuterium labelling study which was carried out using d^1-EtOD. The reaction of d^1-EtOD with ketene is the only route which can explain the position of the deuterium label shown in figure 5.3.

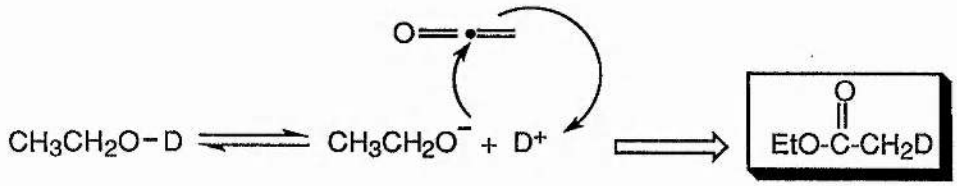

Figure 5.3

The organic products from a standard catalytic reaction carried out in 1:1 d^1-EtOD / toluene were analysed by a range of NMR techniques showing the sole deuterated product to be ethyl acetate. Further to this they showed 100% deuterium incorporation into the acetate methyl position as predicted.

Early in this project trans-[Rh(OAc)CO(PEt_3)$_2$] (**1a**) was found to be the species formed from the catalyst precursors [$Rh_2(OAc)_4$], CO and PEt_3 under standard catalytic conditions, in the absence of the substrate. The study of rhodium trans-bis-phosphine complexes which has followed on from this has highlighted the lability of the anions on both Rh(I) and Rh(III) analogues. It is for this reason that [Rh(I)CO(PEt_3)$_2$] (**1d**) rather than **1a** is highlighted as the catalyst for this reaction, with the high iodide concentration expected with CH_2I_2 as the substrate. This assumption is backed up by the time resolved NMR 'Snapshot' experiments described

in chapter four. Using the catalyst precursors $[Rh_2(OAc)_4]$, PEt_3 and CO and after a reaction time of only 10 min the only Rh(I) species observed in solution was **1d**.

The in-situ VT-NMR study of the reaction of CH_2I_2 with $[Rh(Cl)CO(PEt_3)_2]$ (**1c**) discussed in chapter three (section 3.3.1) showed that synthetic reactions with mixed halogen systems need to be carried out at low temperatures to avoid halogen scrambling and allow isolation of the desired product in good yield. The ionic nature of these halogen exchange reactions has already been established by Gash et al.[118] The work presented in chapters three and four also indicates the preferred site of halogen exchange in different species. In complexes of the type $[RhY_2(CH_2X)CO(PEt_3)_2]$ (X, Y = halogen) it is the halogen, X, which is more readily exchanged by free halide in solution, whereas with the species $[RhY_2(COCH_2X)CO(PEt_3)_2]$ halogen Y is far more readily exchanged. This shows the ready activation by the rhodium centre of organic groups close to it.

No satisfactory synthesis of $[RhCl_3(CO)(PEt_3)_2]$ (**8a**) or $[RhCl_2(I)CO(PEt_3)_2]$ (**8b**) has been reported to date,[161] the development of a suitable synthesis would be a valuable continuation to this work. The results of this project would indicate that direct reaction of $[Rh(Cl)CO(PEt_3)_2]$ (**1c**) with chlorine gas in non-polar, or low polarity, solvent at elevated temperature would be the best synthetic route. The synthesis of **8b** from **1d** and chlorine would be more challenging and would probably require a long reaction time at room temperature to give the product selectively and in good yield.

The in-situ VT-NMR study of the reaction of CH_2I_2 with **1c** mentioned above also showed that complexes of the type $[RhX_2(CH_2I)CO(PEt_3)_2]$ readily lose $:CH_2$ at around 70 °C giving Rh(III) trihalo species. The attempt to observed the equilibrium shown in figure 5.4 by using diethyl maleate as a carbene trap did not give any evidence for the formation of a carbene species.

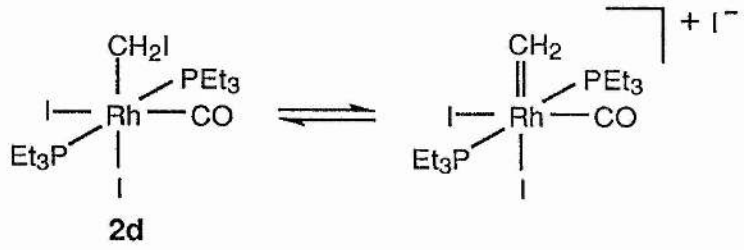

Figure 5.4

In light of the other work now carried out, this potential step linked to the catalytic cycle should be investigated again (chapter three, section 3.3.1). The initial work was carried out using only a crude sample of $[RhI_2(CH_2I)CO(PEt_3)_2]$ because of the difficulty of obtaining this species in a pure form.(chapter three, section 3.3.1) Now that the synthesis of $[RhCl(I)(CH_2I)CO(PEt_3)_2]$ (**2c**) can be readily reproduced, the attempted reaction of **2c** with diethyl maleate could be attempted. The reaction of diethyl maleate with $:CH_2$ should yield a cyclopropane derivative. The direct synthesis of a rhodium carbene complex could also be attempted by the reaction of pure **2c** with $AgSbF_6$. It was indicated in chapter four that the loss of $:CH_2$ via the formation of carbene complexes could be a minor route to catalyst decomposition. To investigate this further the use of an in-situ carbene trap in a standard catalytic run could be tried. One method would be to replace 1 cm^3 of ethanol in a standard reaction with diethyl maleate and then look for cyclopropane derivatives amongst the products. A better method would probably be to look for the reaction product of $:CH_2$ with the solvent alcohol. Unfortunately the reaction of carbene with EtOH would yield MeOEt which is too volatile to be easily detected. Thus, since the catalytic reaction is known to work in the higher alcohol n-BuOH, the examination of a catalytic reaction carried out in n-BuOH may allow for the detection of the less volatile MeOBu if free carbene were ever formed on, then released from, the metal centre.

The cornerstone of the mechanistic work of this project was understanding how the reaction between ICH_2COCl and **1d** could yield $[RhX_3(CH_2I)CO(PEt_3)_2]$ (X = halogen) and diketene. The work of Osborne[146] led us to the mechanistic pathway illustrated in figure 5.2. Preliminary mechanistic studies of the $Co_2(CO)_8$ catalysed double carbonylation of geminal dibromides had also shown the role of a metallo ketene species in this system.[162-164] In addition, further precedence for the role of ketene in such reactions based on di-iron and di-palladium species was also covered in chapter one.[112] It is the rapid β-iodide elimination of the iodoacyl species **3d** and the instability of the resultant rhodium ketene complexes **4d-5d** which confers both the high selectivity and low stability on this catalytic system. In most other double carbonylation systems a significant amount of singly carbonylated product is observed alongside the desired doubly carbonylated product (chapter one). In this rhodium based reaction it is the loss of ketene from the metal centre which yields the singly carbonylated product, EtOAc. This step has also been shown to account for the majority of catalyst decomposition. Another potential reaction of **3d** would be the reductive elimination of iodoacetyl iodide which would be promoted by the rapid reaction of the free acyl iodide with ethanol. Although the reaction of the model species **3c** with ethanol to yield **1c** and ethyl chloroacetate has been observed (chapter four) the analogous species potentially formed in a real catalytic reaction, ICH_2CO_2Et

or $EtOCH_2CO_2Et$, have never been observed. This gives further evidence of the rapid rate of β-iodide elimination of the iodoacyl species **3d**, it being faster than reductive elimination even at 120°C. The other undesired reaction of the substrate is that with the solvent to yield (in ethanol) the acetal $CH_2(OEt)_2$. Interestingly this reaction is suppressed in the presence of the catalyst as the catalytic reaction makes the solution acidic. This decreases the alkoxide ion concentration and therefore decreases the rate of the alkanolysis reaction which forms the $CH_2(OEt)_2$.

Three potential pathways from the metallo ketene complex **4d** (see figure 5.1) to return the catalytic species **1d** and yield DEM can be envisaged.

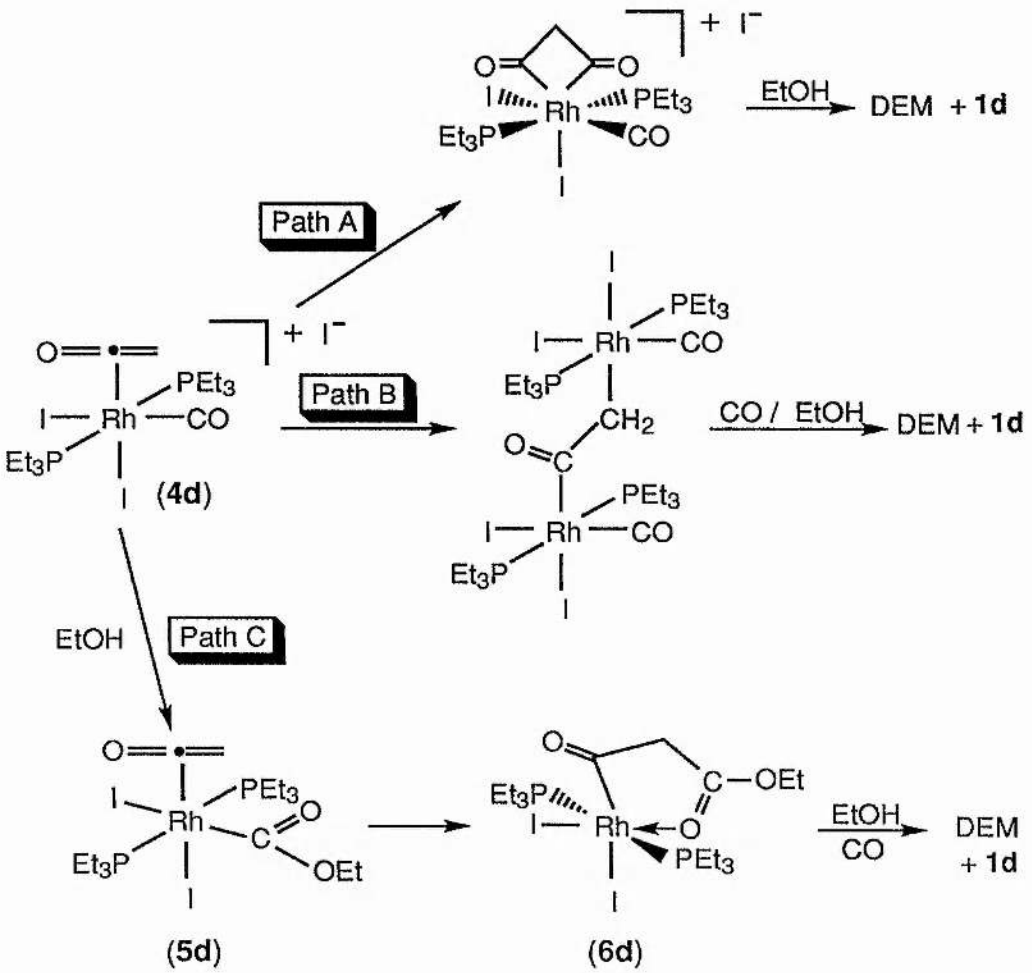

Figure 5.5: Potential pathways from **4d** to **1d** and DEM.

With Path A, a direct insertion of CO into the rhodium ketene bond would give a 7-coordinate Rh(V) species. Although Maitlis has reported two examples of rhodium(V) complexes neither resemble the species shown as an intermediate in Path A.[165,166] It is thus concluded that this pathway is very unlikely. Path B involves a

di-rhodium species with a bridging ketene ligand for which there is precedent[167-169] but the involvement of a dimetallic mechanism seems extremely unlikely given the low concentration of rhodium species in a real catalytic reaction. The attempted reaction of $[Rh(Cl)CO(PEt_3)_2]$ with $[RhCl_2(COCH_2Cl)CO(PEt_3)_2]$ was discussed in chapter three and does not yield a di-rhodium methylene bridged species as may be expected (section 3.7). The strength of the carbon chlorine bond in the chloroacyl moiety is probably the barrier to this reaction. Unfortunately any iodoacyl species of this type would be too unstable even to attempt this reaction. Path C is proposed on the basis of the work of Blake and co-workers[119] (see figure 5.14 and chapter one section 2.4). Of the three routes, we propose Path C as being the most likely. An iridium model of the intermediate **6d** has been reported[119] and the attack of nucleophiles upon CO ligands is also widely reported (see chapter one). The intramolecular attack of iodide rather the intermolecular attack of ethoxide onto the CO ligand of **4d** would be entropically favoured.

The competition reaction shown in figure 5.6 has been identified as part of the mechanistic cycle.

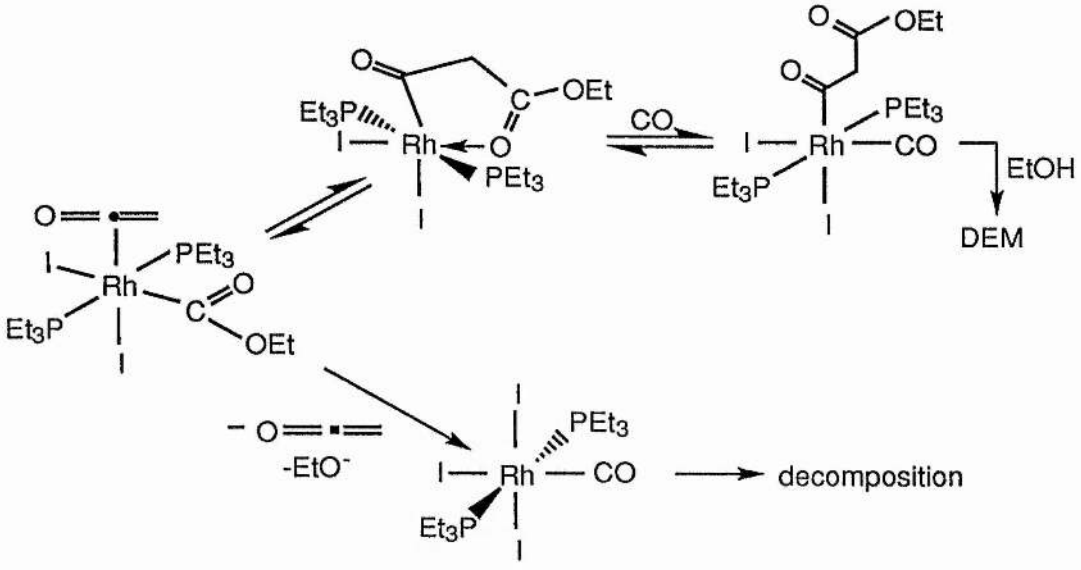

Figure 5.6

A practical consequence of the competition step shown in figure 5.6 should be the dependence of the catalyst stability (reflected by its TON) on the carbon monoxide pressure of the reaction. A first order relationship between catalyst TON and the applied CO pressure was established in chapter two.

As chapter one indicates, all other double carbonylation systems require an added base to remove excess hydrogen halide. When a very wide range of both inorganic bases and N-centred organic bases were added to the reaction all were observed to inhibit double carbonylation. The study of the catalytic synthesis of α-keto esters has revealed that the choice of base and alcoholic solvent is crucial in determining the single to double carbonylation ratio in these catalytic systems (chapter one, section 1B) These effects are rationalised on the basis of the concentration and reactivity of the alkoxide ions in the system. Small acidic alcohols lead to low selectivity by the attack of their conjugate alkoxide upon metallo-acyl intermediates leading to singly carbonylated products. In this reaction an increase in alkoxide concentration would favour the reaction of ketene with the alcoholic solvent and thus bases are observed to have a detrimental effect upon catalyst stability.

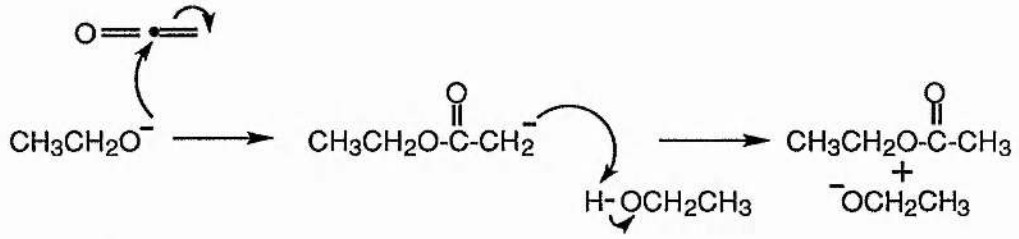

Figure 5.7

Although the proposed iodoacyl intermediate is observed to undergo a rapid β-iodide elimination to yield an unstable ketene complex (see figure 5.2) analogous chloro and bromo acyl species have been found to be stable. The species $[RhX_2(COCH_2X)CO(PR_3)_2]$ (R = Et, X = Br (**3b**), Cl (**3c**); R = Me, X = Cl) are all found to be stable at room temperature for at least 6 months. The higher lability of halides bound directly to the metal than those forming part of the haloacyl moiety prevented their conversion into ketene complexes by the proposed synthetic strategy shown in figure 5.8.

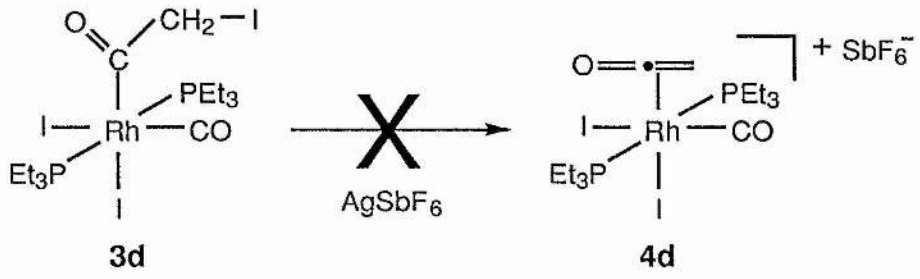

3d **4d**

Figure 5.8

The thermal rearrangement of a related species $[RhCl_2(COCH_2OC_6F_5)CO(PEt_3)_2]$ (**3g**) should be investigated further. Complex **3g** can be easily made by the reaction of $[Rh(Cl)CO(PR_3)_2]$ (**1c**) with $ClCOCH_2OC_6F_5$. The initial in-situ study of this species was carried out in CD_2Cl_2 but it this could be repeated in a more polar solvent such as d^8-THF then the ionic reaction shown in figure 5.9 may be observed in-situ.

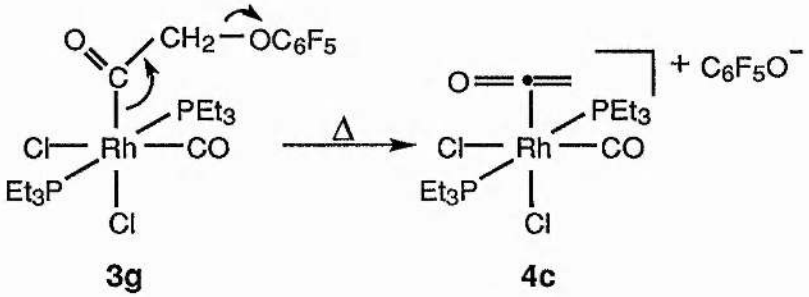

3g **4c**

Figure 5.9

The attempted in-situ observation of the insertion of CO into the [Rh]-CH_2Cl bond of **2i** proved unsuccessful but this could have been due to a number of factors. The reaction was attempted because the species which would have been the desired product (**3c**) was not only known to be stable at room temperature, but was also well characterised. The main product of this reaction was observed to be $[RhCl_3(CO)(PEt_3)_2]$ (**3a**). It may be that the initial species **2i** is unstable to loss of $:CH_2$ at elevated temperatures, giving **3a**, or that the desired species **3c** was formed but that this was unstable with respect to loss of ketene at elevated temperatures even though stable to such a reaction pathway at room temperature.

A different approach to the study of this CO insertion reaction would be to study the thermal stability of $[RhCl_2(COCH_2Cl)CO(PEt_3)_2]$ (**3c**). If complex **3c** were heated in solution then the entropically driven decarbonylation reaction may be observed. If this reaction were carried out under a CO rather than an inert atmosphere, cooling of the solution may allow for observation of the reverse, carbonylation, reaction. This transformation has already been observed for a cobalt chloroacyl species.[103] Any further reaction of either **2i** or **3c** to yield $[RhCl_3(CO)(PEt_3)_2]$ (**3a**) could also be observed, along with the organic product (ie ethene or diketene), if the reaction were studied in-situ by HPVT-NMR.

Both synthetic experiments and trial catalytic runs have shown the importance of having an alcohol as the solvent. As the catalytic reaction has been shown to be inhibited by base, one role of the alcohol is to act as a non-basic sink for HI. If this catalytic system had potential to be scaled up then the use of EtOH as the HI sink

would be a major advantage of this system over others. In other reported double carbonylation systems the product is either formed as a metal salt when inorganic bases are employed or when an amine base is used the product has to be extracted from the solid HI adduct of amine. The easy separation of EtI from DEM in this catalytic system therefore offers important practical advantages over systems where a base is used.

The model reaction of $[RhCl_2(COCH_2CO_2Et)CO(PEt_3)_2]$ **7c** with excess ethanol revealed that the reductive elimination / oxidative addition equilibrium was strongly biased towards the Rh(III) species (figure 5.10).

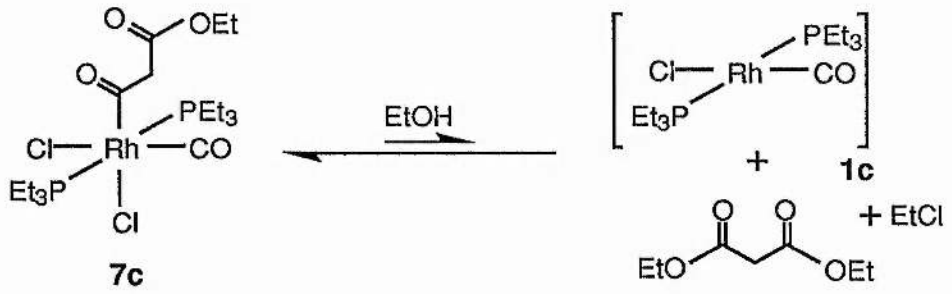

Figure 5.10

If **7c** is a good model for intermediate **7d** then this provides another reason for the this reaction to be dependent on an alcoholic solvent. If all the steps in the catalytic mechanism from **7d** back to the ketene complex **4d** are reversible then the slow reductive elimination of **7d** giving **1d** would allow time for organo-rhodium species to shuffle back through the cycle to the unstable ketene complex thus increasing their chance of being irreversibly lost from the cycle. In chapter two it was shown that decreasing the alcohol concentration by using a co-solvent had a detrimental effect on the catalyst stability. It is the ethanol that drives the equilibrium shown in figure 5.10 by reacting with the ethyl malonyl chloride formed by the reductive elimination and thus preventing the back reaction. This change in equilibrium position occurs according to Le Chatelier's principle which would also predict that any species capable of reacting with the other product (**1c**) would have also effect the equilibrium position, thus increasing the catalyst TON. The effect of increasing the initial diiodomethane concentration also increases the TON providing further validity to the predictions made on the basis of this model reaction.

The way in which EtOH plays the role of HI sink was highlighted by the NMR 'Snapshot' experiments reported in chapter four. One of the major species observed in

solution whilst the catalytic system was still active was $[RhH(I)_2(CO)(PEt_3)_2]$ (**9d**). Although $[RhI_3(CO)(PEt_3)_2]$ has been shown to be the major decomposition product, the formation of **9d** has been shown not to constitute catalyst decomposition. The complex **9d** is merely a resting state for the catalytic species as there is a ready reaction between **9d** and excess EtOH to yield the catalytically active species **1d** and EtI.

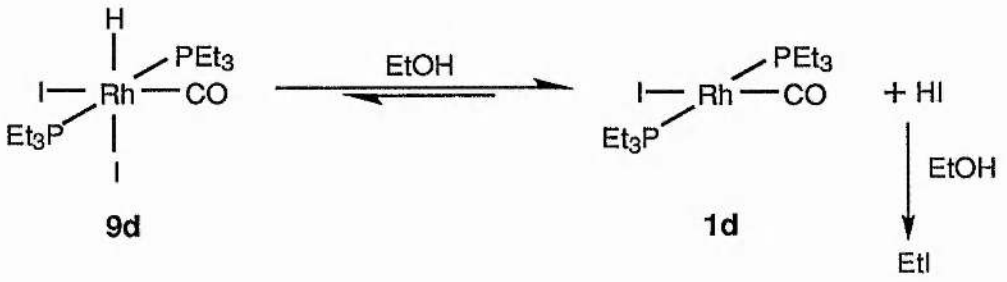

Figure 5.11

A significant fraction of this project has relied upon in-situ ^{31}P NMR experiments. These consisted of both VT-experiments between a Rh(I) species and a halocarbon and also VTHP experiments under 40-50 atm CO pressure. When studying the reaction of a rhodium-phosphine complex and an organic reagent a slight excess of the rhodium-phosphine species was used. Since the ^{31}P NMR data of the starting complex was well known this could be used as non invasive internal reference throughout the study.

Another useful technique was the NMR 'Snapshot' experiment described in chapter four. These experiments were able to show that a standard catalyst run was complete within 30 min at 120 °C and 40 atm CO. The ^{31}P NMR data after a 10 min reaction time showed the species present to be those which were predicted by the synthetic and mechanistic work. The major species present were $[RhI_3(CO)(PEt_3)_2]$ (**8d**), $[RhI_2(CH_2I)(CO)(PEt_3)_2]$ (**2d**) and $[RhH(I)_2(CO)(PEt_3)_2]$ (**9d**). Complex **2d** was proposed as the first intermediate in the catalytic cycle and **8d** was shown by separate experiments to be the predominant decomposition product of the catalytic species. The observation of **2d** in high concentration, rather than any other catalytic intermediate, suggests that the CO insertion into the carbon-rhodium bond of **2d** is the rate determining step in the catalytic cycle (see figure 5.1). The hydride complex **9d** was previously unidentified, but it was found to result via two pathways under the reaction conditions. The major pathway [Path A] was the reaction of the Rh(I) species **1d** with HI, the minor pathway [Path B] results from the reaction of **1d** with EtI followed by β-iodide abstraction and loss of ethene - these pathways are shown in figure 5.12.

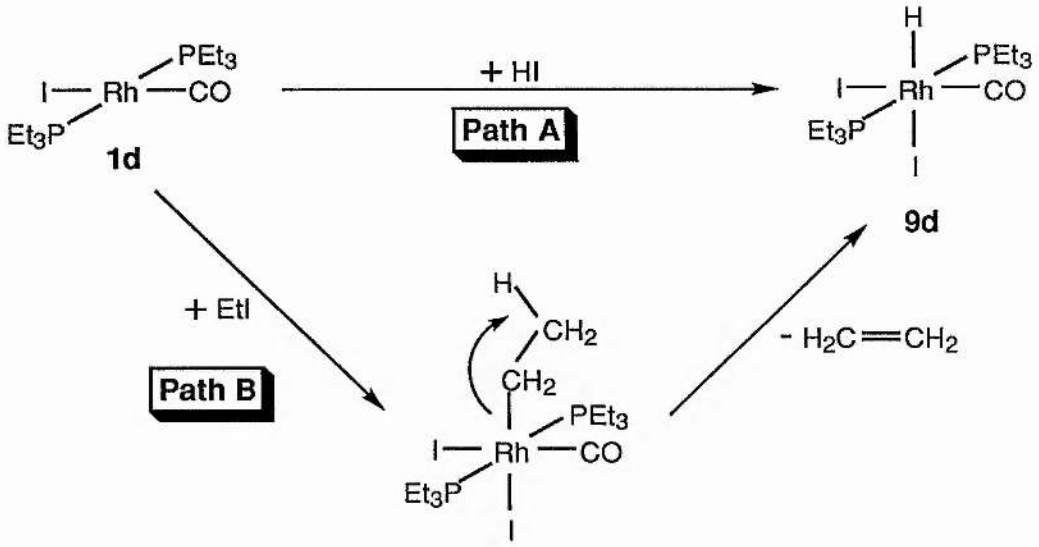

Figure 5.12

The study of solutions from longer reaction times showed that, with time, the basic trans-bis-phosphine skeleton was broken down under the reaction conditions. The mechanism of this breakdown is not known, but in a separate experiment the initial decomposition product **8d** was shown itself to decompose thermally in an analogous fashion, with the loss of PEt_3 from the metal centre. The observed phosphorus containing products were $OPEt_3$ and $[Et_3PCH_2I^+]I^-$.

The catalytic reactions carried out in Aachen at 300-350 atm CO pressure did not show the dramatic increase in catalyst TON which had been previously predicted. This could be accounted for by: i) The displacement of the phosphine ligands from the metal centre by CO given the high CO concentrations achieved at these pressures and ii) competition between CH_2I_2 and CO for co-ordination sites on the initial Rh(I) species. Examples of the second phenomenon were discussed in chapter two[67,137] but no evidence against the displacement of phosphines from the metal at elevated CO pressures has yet been obtained. Evidence for this could not be obtained by using a standard HP-NMR or HP-IR cell due to the high pressures required. However this evidence could be obtained by using the NMR 'Snapshot' technique discussed above, with the catalytic reaction being carried out with a CO pressure of 300-350 atm. If such new runs were carried out and compared to similar runs carried out at 40 atm then any acceleration of phosphine loss by increased CO pressure could be easily observed (if it occurred) by examination of the product solution by ^{31}P NMR after a short reaction time. Decreasing the reaction temperature by 20 °C could also decrease the rate of reaction and thus assist with such investigations.

There is one more intermediate in the proposed catalytic cycle (in addition to the ketene complex) which it should be possible to model, this species (**6d**) is illustrated below.

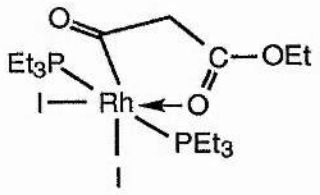

6d

Figure 5.13

The synthesis of an analogous iridium complex was reported by Blake and co-workers.[119] Their synthetic route to this species is shown in figure 5.14.

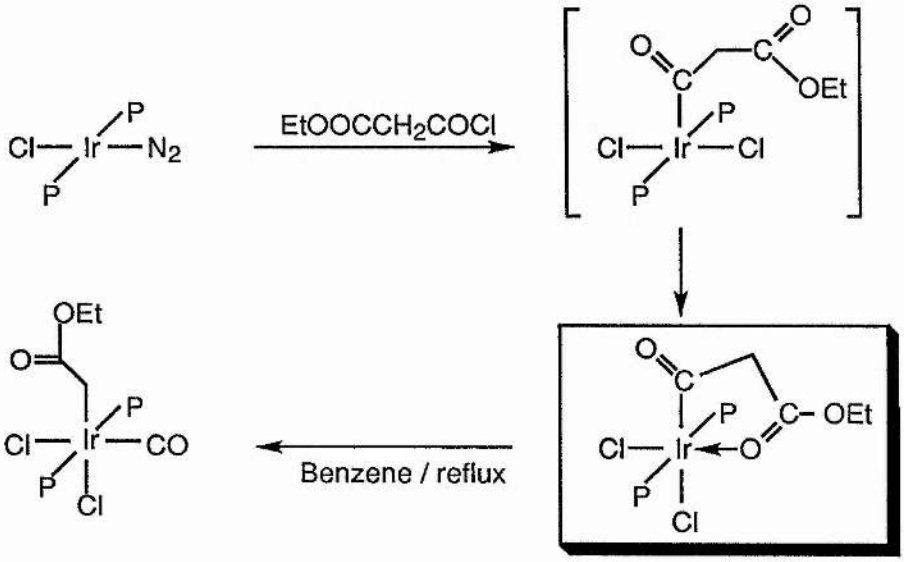

Figure 5.14

In the case of the iridium species, decarbonylation is observed when the complex is heated under an inert atmosphere, it would be interesting to know if this pathway is open to the rhodium analogue. No evidence for the participation of an analogous halo ethylacetate complex is observed in the rhodium based catalytic system, but the decarbonylation of the η^2-malonyl complex shown above would presumably be disfavoured under a positive pressure of CO.

The mechanism of the rhodium catalysed double carbonylation of diiodomethane is now well understood with comprehensive evidence for the proposed mechanism presented in chapters two to four. This work has highlighted the reasons behind the

low catalyst stability as: i) The competition between reaction of a metallo ketene complex with CO and loss of ketene, requiring a high CO pressure to achieve a high catalyst TON; ii) the loss of phosphine from the metal centre of the initial decomposition product $[RhI_3(CO)(PEt_3)_2]$ (**8d**). This second and undesirable feature of the catalytic centre could be addressed by changing from PEt_3 to a different ligand system. A neglected ligand system in carbonylation catalysis is cyclopentadienyl and its derivatives. The complex $[CpRh(CO)PMe_3]$ and similar cobalt and iridium species have been comprehensively studied both by Werner[142,144,170,171] and Graham.[172] The chemistry of this species is observed to be very similar to that of $[Rh(X)CO(PEt_3)_2]$. Cyclopentadienyl is strongly electron donating like PEt_3 but being a five electron donor it has the advantage of being much more strongly bound to the metal centre. The stability of the cyclopentadienyl-rhodium core would hopefully address the problem of ligand loss.

The requirement for a high CO concentration to stabilise the ketene intermediate could also be addressed by transfer to a rhodium-cyclopentadienyl system. A small increase in CO pressure with the present $[Rh(X)CO(PEt_3)_2]$ system is indeed advantageous (chapter two) but increasing the CO pressure still further, to 300-350 atm, causes a separate catalyst deactivation process. This process may be due to the formation of a five-co-ordinate Rh(I) species a reaction observed by HPIR by Payne[137] and illustrated in figure 5.15.

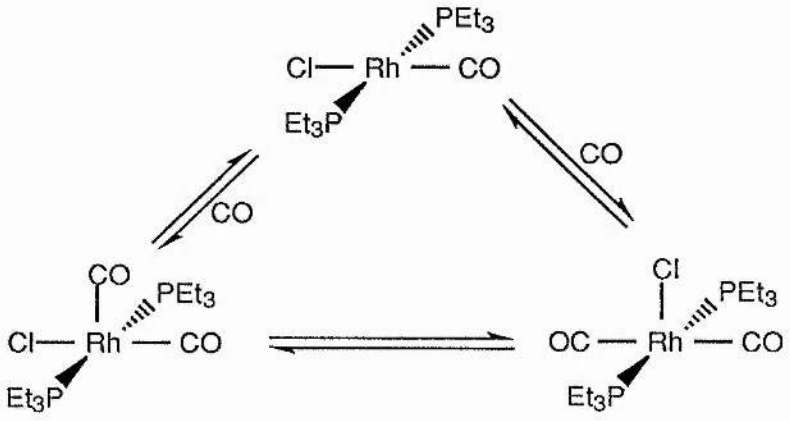

Figure 5.15

The different steric demands of the cyclopentadienyl ligand may impair the saturation of the Rh(I) co-ordination sphere by carbon monoxide and thus allow the reaction to be carried out at high CO concentrations.

The possibility for functionalisation of the cyclopentadienyl ring could also be utilised. For example, a sulphonated cyclopentadienyl ring would yield a water soluble catalyst. A more pertinent functionalisation would be the addition of perfluoro groups to the cyclopentadienyl ring which would solubilise the complex in supercritical CO_2. The solubility of CO in supercritical CO_2 is extremely high and this could be a route to the high CO concentrations required for this reaction at moderate overall pressures. Tuning of the cyclopentadienyl ring may also allow for development of more electron rich complexes capable of undergoing oxidative addition of chlorocarbon moieties and thus allow for the activation and carbonylation of more attractive substrates such as dichloromethane.

APPENDIX ONE

General Experimental Procedures

A1.1 General techniques

The work carried out with all organorhodium species and organic acid halides was carried out in gas tight (Schlenk) flasks on a standard Schlenk line (with PTFE greaseless taps and greased ball and socket compression joints), using syringe and solution transfer catheter techniques. All such work was carried out under a positive atmosphere of oxygen free nitrogen which was dried by passage though a column packed with Cr(II) adsorbed onto silica.

A1.2 Preparation of solvents

All solvents were distilled and degassed under N_2 where necessary. The drying agents for the solvents were as follows: Et_2O, THF and light petroleum (T_b = 40-60 °C) - sodium benzoate; toluene - Na wire; CH_2Cl_2 ,CH_3CN - calcium hydride; EtOH and all other alcohols - Mg; acetone - potassium carbonate. Deuterated solvents were used as supplied.

A1.3 Reagents

The following chemicals were used as supplied, without further purification: $RhCl_3 \cdot 3H_2O$ (Johnson Matthey, PGM Chemicals (South Africa) or Aldrich), Organohalides (Aldrich, Avocado, Lancaster), Silver, lithium, sodium and potassium salts (Aldrich or Fisons), acetic acid (Fisons), para-formaldehyde (Aldrich), deuterated solvents (Goss), tertiary phosphines (Strem), dmpe (Aldrich). Diiodomethane was stored over activated molecular sieves (3Å) in the absence of light, DMF and DMA were supplied anhydrous and stored under N_2 (Aldrich).

A1.4 Analytical equipment used

Most NMR spectra were recorded on either a Bruker AM300 spectrometer or a Varian Gemini 2000 spectrometer in 5 mm glass tubes (Both ^1H 300.1 MHz, ^2H 46.1 MHz, ^{31}P 121.5 MHz, ^{13}C 75.5 MHz) Additional NMR spectra were also recorded on Varian Unity Plus 500 (^1H 500.1 MHz, ^2H 76.8, ^{13}C 125.7 MHz).

IR spectra were recorded on either a Perkin Elmer 1710 FTIR or a Perkin Elmer 1330. The GCMS examination of the product mixtures from the catalytic runs was carried out using a Hewlett Packard 5890 with a Incos-50 electric quadrapole mass spectrometer. The GCMS examination of the product mixtures from the catalytic runs was carried out using a Hewlett Packard 5890 with a Incos-50 electric quadrapole mass spectrometer. CHN microanalysis was carried out on a Carlo Erba Model 1106.

A1.5 Synthesis of rhodium acetate

$[RhCl_3]\cdot 3H_2O$ (1.00 g), sodium acetate trihydrate (2.00 g) and glacial acetic acid (20 cm^3) were dissolved in ethanol (20 cm^3) and refluxed under a steady flow of N_2 for 1 hr. The initial red solution turned green and a solid precipitate was formed. This solution was cooled in the refrigerator for 80-100 hr to allow for full crystallisation. The green solid formed was filtered off and then recrystallised from methanol. The combined filtrate was reduced to two thirds of original its volume and cooled to yield a second small quantity of crystals. These were the methanol adduct, $[Rh_2(OAc)_4]\cdot 2MeOH$. This blue/green solid could be heated to 60-80 °C for 4-6 hr to remove the methanol, checked by taking an IR spectrum of the complex. The solvated adduct was used thoughout this work.

APPENDIX TWO

Crystal Structure Determinations

A2.1 Determination of the crystal structure of $[RhCl_2(COCH_2Cl)CO(PEt_3)_2]$

Pale yellow crystals of $[RhCl_2(COCH_2Cl)CO(PEt_3)_2]$ were obtained by two recrystallisations from diethyl ether. The solution was warmed to around its boiling point to aid dissolution then cooled to -30 °C for 3 days to obtain crystals. These were filtered whilst cold and dried *in vacuo*.

A yellow block crystal of $[RhCl_2(COCH_2Cl)CO(PEt_3)_2]$ having approximate dimensions of 0.50 x 0.40 x 0.25 mm was mounted on a glass fibre. Cell constants and an orientation matrix for data collection were obtained from a least-squares refinement using the setting angles of 25 carefully centred reflections in the range $24.42° < 2\vartheta < 25.04°$. All measurements were made on a Rigaku AFC7S diffractometer with graphite monochromated Mo-Kα radiation. Of the 8194 reflections which were collected, 7742 were unique, of which 5917 were used in the refinement. The data were collected at a temperature of 220±1 K using the Θ -2ϑ scan technique to a maximum 2ϑ value of 50.2°. The data were corrected for Lorentz and polarization effects.

Crystallographic Data

Formula: $C_{15}H_{32}Cl_3O_2P_2Rh$, Mw = 515.63, primitive triclinic with cell dimensions; a = 13.048(8) Å, b = 15.169(5) Å, c = 11.994(8) Å, α = 95.89(4)°, β = 95.16(6)°, γ = 103.09(4)°, V = 2284(2) Å^3, Z = 4, D_x = 1.50 gcm^{-3}.

Refinement

The structure was solved by and expanded using Fourier techniques.[173] Some non-hydrogen atoms were refined anisotropically, while the rest were refined isotropically. Hydrogen atoms were included but not refined. Neutral atom scattering factors were taken from Cromer and Waber.[174] Anomalous dispersion effects were included in Fcalc;[175] the values for δf' and δf'' were those of Creagh and McAuley.[176] The values for the mass attenuation coefficients are those of Creagh and Hubbel.[177] All calculations were performed using the teXsan crystallographic software package of Molecular Structure Corporation.

Table A2.1 - Atomic coordinates and B_{eq}

Atom	x	y	z	B_{eq}
Rh(1)	-0.0321(1)	0.2452(1)	0.6158(2)	2.16(4)
Rh(2)	0.4688(2)	0.2573(1)	1.0639(2)	2.40(4)
Cl(1)	-0.0272(6)	0.0938(5)	0.6456(6)	4.0(2)
Cl(2)	0.1453(5)	0.3065(5)	0.7335(5)	3.2(1)
Cl(3)	-0.3785(7)	0.0972(8)	0.4880(9)	6.9(3)
Cl(4)	0.5189(6)	0.3711(5)	0.9445(6)	3.8(2)
Cl(5)	0.6269(6)	0.1936(6)	1.0157(7)	4.5(2)
Cl(6)	0.1908(7)	0.3974(6)	1.0865(8)	5.3(2)
P(1)	0.0576(6)	0.2196(5)	0.4545(6)	3.3(2)
P(2)	-0.1230(5)	0.2686(4)	0.7782(5)	2.4(1)
P(3)	0.3617(6)	0.1519(5)	0.9113(5)	2.8(1)
P(4)	0.5756(6)	0.3664(5)	1.2108(5)	3.0(2)
O(1)	-0.024(2)	0.438(1)	0.582(2)	5.8(6)
O(2)	-0.209(1)	0.252(2)	0.461(2)	4.8(6)
O(3)	0.430(2)	0.109(2)	1.215(2)	6.4(7)
O(4)	0.288(2)	0.274(1)	1.184(1)	3.5(4)
C(1)	-0.028(2)	0.369(2)	0.599(2)	3.2(5)
C(2)	-0.179(2)	0.205(2)	0.524(2)	3.6(5)
C(3)	-0.240(3)	0.110(2)	0.530(3)	4.9(7)
C(4)	-0.024(3)	0.133(2)	0.346(3)	4.8(7)
C(5)	0.012(3)	0.122(3)	0.241(4)	7.0(10)
C(6)	0.099(3)	0.315(3)	0.376(4)	7.1(10)
C(7)	0.192(4)	0.387(4)	0.442(5)	10(1)
C(8)	0.172(3)	0.171(3)	0.495(3)	6.5(9)
C(9)	0.248(6)	0.139(5)	0.408(6)	14(2)
C(10)	-0.137(2)	0.177(2)	0.871(2)	3.1(5)
C(11)	-0.044(3)	0.172(3)	0.928(3)	6.3(9)
C(12)	-0.055(2)	0.372(2)	0.874(2)	3.5(5)
C(13)	-0.109(4)	0.389(3)	0.976(4)	8(1)
C(14)	-0.249(2)	0.277(2)	0.750(2)	3.0(5)
C(15)	-0.273(3)	0.366(2)	0.697(3)	5.5(8)
C(16)	0.433(3)	0.166(2)	1.167(3)	4.5(6)
C(17)	0.368(3)	0.281(3)	1.084(3)	6.5(9)
C(18)	0.279(3)	0.372(3)	1.053(3)	6.4(9)
C(19)	0.397(2)	0.042(2)	0.894(3)	4.3(6)
C(20)	0.323(3)	-0.027(2)	0.802(3)	4.6(6)
C(21)	0.362(2)	0.190(2)	0.771(2)	3.5(5)
C(22)	0.466(3)	0.189(3)	0.715(3)	6.6(9)
C(23)	0.226(2)	0.127(2)	0.925(2)	3.0(5)
C(24)	0.200(3)	0.065(2)	1.019(3)	5.8(8)
C(25)	0.519(2)	0.463(2)	1.240(2)	3.3(5)
C(26)	0.582(3)	0.538(2)	1.335(3)	5.7(8)
C(27)	0.701(3)	0.414(2)	1.171(3)	5.2(7)
C(28)	0.790(4)	0.419(4)	1.258(5)	10(1)
C(29)	0.594(2)	0.327(2)	1.349(2)	3.2(5)
C(30)	0.499(3)	0.300(3)	1.403(3)	6.0(8)
H(1)	-0.2321	0.0968	0.6046	5.7831
H(2)	-0.2158	0.0691	0.4805	5.7831
H(3)	-0.0328	0.0768	0.3757	5.7408
H(4)	-0.0890	0.1487	0.3325	5.7408
H(5)	-0.0365	0.0758	0.1937	8.2122
H(6)	0.0266	0.1769	0.2111	8.2122
H(7)	0.0789	0.1021	0.2526	8.2122

Atom	x	y	z	Beq
H(8)	0.1145	0.2940	0.3044	8.8095
H(9)	0.0361	0.3417	0.3619	8.8095
H(10)	0.2518	0.3674	0.4507	12.1260
H(11)	0.2077	0.4412	0.3952	12.1260
H(12)	0.1734	0.4141	0.5099	12.1260
H(18)	-0.1804	0.1899	0.9270	3.7612
H(19)	-0.1680	0.1210	0.8271	3.7612
H(20)	-0.0554	0.1244	0.9721	7.3401
H(21)	0.0016	0.1575	0.8706	7.3401
H(22)	-0.0097	0.2278	0.9694	7.3401
H(23)	0.0144	0.3667	0.8951	4.0415
H(24)	-0.0531	0.4223	0.8321	4.0415
H(25)	-0.0633	0.4454	1.0193	9.2247
H(26)	-0.1741	0.3960	0.9574	9.2247
H(27)	-0.1056	0.3414	1.0208	9.2247
H(28)	-0.2848	0.2264	0.6969	3.4556
H(29)	-0.2805	0.2746	0.8183	3.4556
H(30)	-0.2423	0.4185	0.7513	6.4414
H(31)	-0.2436	0.3714	0.6300	6.4414
H(32)	-0.3475	0.3593	0.6863	6.4414
H(34)	0.2571	0.3558	0.9736	7.6902
H(35)	0.3291	0.4279	1.0659	7.6902
H(36)	0.4684	0.0527	0.8753	5.1098
H(37)	0.3948	0.0184	0.9644	5.1098
H(38)	0.2510	-0.0358	0.8187	5.3686
H(39)	0.3256	-0.0027	0.7300	5.3686
H(40)	0.3421	-0.0828	0.7946	5.3686
H(41)	0.3039	0.1530	0.7250	4.1635
H(42)	0.3541	0.2520	0.7812	4.1635
H(43)	0.4740	0.1296	0.7057	7.3192
H(44)	0.4577	0.2111	0.6437	7.3192
H(45)	0.5240	0.2288	0.7613	7.3192
H(46)	0.2084	0.1833	0.9463	3.5284
H(47)	0.1894	0.0982	0.8566	3.5284
H(48)	0.1255	0.0526	1.0237	6.6533
H(49)	0.2193	0.0088	1.0006	6.6533
H(50)	0.2367	0.0940	1.0900	6.6533
H(51)	0.5125	0.4894	1.1723	4.0142
H(52)	0.4494	0.4399	1.2607	4.0142
H(53)	0.5887	0.5127	1.4041	7.0095
H(54)	0.6494	0.5637	1.3152	7.0095
H(55)	0.5439	0.5851	1.3460	7.0095
H(56)	0.7127	0.3750	1.1072	6.1459
H(57)	0.7018	0.4721	1.1495	6.1459
H(58)	0.7951	0.3648	1.2794	11.8224
H(59)	0.8560	0.4507	1.2325	11.8224
H(60)	0.7816	0.4605	1.3245	11.8224
H(61)	0.6236	0.2748	1.3385	3.6799
H(62)	0.6411	0.3738	1.3976	3.6799
H(63)	0.4692	0.3494	1.4146	6.7850
H(64)	0.4524	0.2501	1.3567	6.7850
H(65)	0.5197	0.2804	1.4734	6.7850
H(66)	0.2180	0.2131	0.5524	7.5420
H(67)	0.1439	0.1159	0.5290	7.5420
H(68)	0.3005	0.1139	0.4429	16.0459
H(69)	0.2071	0.0952	0.3474	16.0459
H(70)	0.2832	0.1913	0.3738	16.0459

Table A2.2 - Anisotropic Displacement Parameters

atom	U_{11}	U_{22}	U_{33}	U_{12}	U_{13}	U_{23}
Rh(1)	0.025(1)	0.027(1)	0.029(1)	0.0046(8)	-0.0021(8)	0.0028(8)
Rh(2)	0.034(1)	0.032(1)	0.026(1)	0.0076(9)	0.0030(8)	0.0087(8)
Cl(1)	0.059(5)	0.032(4)	0.061(5)	0.013(3)	0.003(4)	0.004(3)
Cl(2)	0.022(3)	0.056(4)	0.036(3)	0.000(3)	-0.007(3)	-0.001(3)
Cl(3)	0.037(5)	0.111(8)	0.090(7)	-0.015(5)	-0.010(4)	-0.019(6)
Cl(4)	0.066(5)	0.043(4)	0.033(4)	0.003(3)	0.009(3)	0.012(3)
Cl(5)	0.062(5)	0.062(5)	0.052(4)	0.024(4)	0.009(4)	0.011(4)
Cl(6)	0.059(5)	0.072(6)	0.077(6)	0.035(5)	-0.003(4)	-0.001(5)
P(1)	0.042(4)	0.048(4)	0.032(4)	0.012(3)	-0.002(3)	-0.006(3)
P(2)	0.029(4)	0.030(3)	0.030(3)	0.001(3)	0.005(3)	0.002(3)
P(3)	0.043(4)	0.036(4)	0.026(3)	0.008(3)	0.002(3)	0.002(3)
P(4)	0.043(4)	0.047(4)	0.023(3)	0.005(3)	0.004(3)	0.002(3)
O(1)	0.10(2)	0.03(1)	0.09(2)	0.01(1)	0.00(1)	0.02(1)
O(2)	0.03(1)	0.08(2)	0.07(2)	0.01(1)	-0.009(10)	0.00(1)
O(3)	0.12(2)	0.06(2)	0.07(2)	0.01(1)	0.01(1)	0.05(1)
O(4)	0.07(1)	0.05(1)	0.018(9)	0.02(1)	0.022(9)	-0.003(8)

Table A2.3 - Bond lengths

atom	atom	distance (Å)	atom	atom	distance (Å)
Rh(1)	Cl(1)	2.374(7)	Rh(1)	Cl(2)	2.526(6)
Rh(1)	P(1)	2.393(7)	Rh(1)	P(2)	2.406(7)
Rh(1)	C(1)	1.90(3)	Rh(1)	C(2)	2.06(3)
Rh(2)	Cl(4)	2.372(6)	Rh(2)	Cl(5)	2.555(8)
Rh(2)	P(3)	2.405(7)	Rh(2)	P(4)	2.388(7)
Rh(2)	C(16)	1.95(3)	Rh(2)	C(17)	1.47(4)
Cl(3)	C(3)	1.80(3)	Cl(6)	C(18)	1.38(4)
P(1)	C(4)	1.82(3)	P(1)	C(6)	1.82(4)
P(1)	C(8)	1.85(4)	P(2)	C(10)	1.85(3)
P(2)	C(12)	1.83(3)	P(2)	C(14)	1.69(3)
P(3)	C(19)	1.82(3)	P(3)	C(21)	1.83(3)
P(3)	C(23)	1.75(3)	P(4)	C(25)	1.80(3)
P(4)	C(27)	1.76(3)	P(4)	C(29)	1.83(3)
O(1)	C(1)	1.08(3)	O(2)	C(2)	1.20(3)
O(3)	C(16)	1.09(4)	O(4)	C(17)	1.66(4)
C(2)	C(3)	1.48(4)	C(4)	C(5)	1.38(5)
C(6)	C(7)	1.53(6)	C(8)	C(9)	1.61(8)
C(10)	C(11)	1.35(4)	C(12)	C(13)	1.50(5)
C(14)	C(15)	1.62(4)	C(17)	C(18)	2.04(6)
C(19)	C(20)	1.54(4)	C(21)	C(22)	1.57(5)
C(23)	C(24)	1.55(4)	C(25)	C(26)	1.56(4)
C(27)	C(28)	1.46(6)	C(29)	C(30)	1.45(4)
C(3)	H(1)	0.94	C(3)	H(2)	0.94
C(4)	H(3)	0.95	C(4)	H(4)	0.94
C(5)	H(5)	0.93	C(5)	H(6)	0.94
C(5)	H(7)	0.98	C(6)	H(8)	0.94
C(6)	H(9)	1.00	C(7)	H(10)	0.89
C(7)	H(11)	1.04	C(7)	H(12)	0.96
C(8)	H(66)	0.96	C(8)	H(67)	0.98
C(9)	H(68)	0.95	C(9)	H(69)	0.96

atom	atom	distance (Å)	atom	atom	distance (Å)
C(9)	H(70)	0.97	C(10)	H(18)	0.95
C(10)	H(19)	0.93	C(11)	H(20)	0.93
C(11)	H(21)	0.99	C(11)	H(22)	0.94
C(12)	H(23)	0.94	C(12)	H(24)	0.96
C(13)	H(25)	0.98	C(13)	H(26)	0.90
C(13)	H(27)	0.95	C(14)	H(28)	0.95
C(14)	H(29)	0.95	C(15)	H(30)	0.97
C(15)	H(31)	0.92	C(15)	H(32)	0.95
C(18)	H(34)	0.96	C(18)	H(35)	0.93
C(19)	H(36)	0.96	C(19)	H(37)	0.95
C(20)	H(38)	0.96	C(20)	H(39)	0.97
C(20)	H(40)	0.94	C(21)	H(41)	0.93
C(21)	H(42)	0.96	C(22)	H(43)	0.93
C(22)	H(44)	0.95	C(22)	H(45)	0.95
C(23)	H(46)	0.95	C(23)	H(47)	0.93
C(24)	H(48)	0.95	C(24)	H(49)	0.96
C(24)	H(50)	0.95	C(25)	H(51)	0.95
C(25)	H(52)	0.96	C(26)	H(53)	0.95
C(26)	H(54)	0.95	C(26)	H(55)	0.96
C(27)	H(56)	0.96	C(27)	H(57)	0.95
C(28)	H(58)	0.91	C(28)	H(59)	0.98
C(28)	H(60)	0.99	C(29)	H(61)	0.96
C(29)	H(62)	0.93	C(30)	H(63)	0.92
C(30)	H(64)	0.95	C(30)	H(65)	0.96

Table A2.3 - Bond angles

Between atoms a-b-c			angle(°)	Between atoms a-b-c			angle(°)
Cl(1)	Rh(1)	Cl(2)	90.7(2)	Cl(1)	Rh(1)	P(1)	85.7(3)
Cl(1)	Rh(1)	P(2)	93.5(2)	Cl(1)	Rh(1)	C(1)	176.3(8)
Cl(1)	Rh(1)	C(2)	93.1(8)	Cl(2)	Rh(1)	P(1)	89.3(2)
Cl(2)	Rh(1)	P(2)	90.9(2)	Cl(2)	Rh(1)	C(1)	85.6(8)
Cl(2)	Rh(1)	C(2)	175.5(8)	P(1)	Rh(1)	P(2)	179.2(2)
P(1)	Rh(1)	C(1)	94.6(8)	P(1)	Rh(1)	C(2)	93.2(8)
P(2)	Rh(1)	C(1)	86.2(8)	P(2)	Rh(1)	C(2)	86.6(8)
C(1)	Rh(1)	C(2)	90(1)	Cl(4)	Rh(2)	Cl(5)	89.0(3)
Cl(4)	Rh(2)	P(3)	92.5(2)	Cl(4)	Rh(2)	P(4)	85.3(2)
Cl(4)	Rh(2)	C(16)	177.5(10)	Cl(4)	Rh(2)	C(17)	94(1)
Cl(5)	Rh(2)	P(3)	88.6(3)	Cl(5)	Rh(2)	P(4)	91.8(3)
Cl(5)	Rh(2)	C(16)	90.2(10)	Cl(5)	Rh(2)	C(17)	171(1)
P(3)	Rh(2)	P(4)	177.8(2)	P(3)	Rh(2)	C(16)	89.8(10)
P(3)	Rh(2)	C(17)	84(1)	P(4)	Rh(2)	C(16)	92.4(10)
P(4)	Rh(2)	C(17)	95(1)	C(16)	Rh(2)	C(17)	86(1)
Rh(1)	P(1)	C(4)	112(1)	Rh(1)	P(1)	C(6)	117(1)
Rh(1)	P(1)	C(8)	109(1)	C(4)	P(1)	C(6)	101(1)
C(4)	P(1)	C(8)	103(1)	C(6)	P(1)	C(8)	110(1)
Rh(1)	P(2)	C(10)	115.3(9)	Rh(1)	P(2)	C(12)	112.6(9)
Rh(1)	P(2)	C(14)	115.3(9)	C(10)	P(2)	C(12)	103(1)
C(10)	P(2)	C(14)	102(1)	C(12)	P(2)	C(14)	106(1)
Rh(2)	P(3)	C(19)	113(1)	Rh(2)	P(3)	C(21)	116.2(9)
Rh(2)	P(3)	C(23)	113.7(9)	C(19)	P(3)	C(21)	105(1)

Between atoms a-b-c			angle(°)
C(19)	P(3)	C(23)	105(1)
Rh(2)	P(4)	C(25)	111.5(9)
Rh(2)	P(4)	C(29)	116.5(9)
C(25)	P(4)	C(29)	103(1)
Rh(1)	C(1)	O(1)	175(2)
Rh(1)	C(2)	C(3)	116(2)
Cl(3)	C(3)	C(2)	111(2)
P(1)	C(6)	C(7)	111(3)
P(2)	C(10)	C(11)	114(2)
P(2)	C(14)	C(15)	119(1)
Rh(2)	C(17)	O(4)	137(2)
O(4)	C(17)	C(18)	75(2)
P(3)	C(19)	C(20)	112(2)
P(3)	C(23)	C(24)	111(1)
P(4)	C(27)	C(28)	114(3)
Cl(3)	C(3)	H(1)	107.5
C(2)	C(3)	H(1)	109.7
H(1)	C(3)	H(2)	111.1
P(1)	C(4)	H(4)	107.1
C(5)	C(4)	H(4)	106.4
C(4)	C(5)	H(5)	110.2
C(4)	C(5)	H(7)	107.6
H(5)	C(5)	H(7)	108.3
P(1)	C(6)	H(8)	109.8
C(7)	C(6)	H(8)	111.9
H(8)	C(6)	H(9)	106.2
C(6)	C(7)	H(11)	107.2
H(10)	C(7)	H(11)	106.6
H(11)	C(7)	H(12)	101.9
P(1)	C(8)	H(67)	107.0
C(9)	C(8)	H(67)	103.8
C(8)	C(9)	H(68)	113.1
C(8)	C(9)	H(70)	109.6
H(68)	C(9)	H(70)	107.8
P(2)	C(10)	H(18)	108.0
C(11)	C(10)	H(18)	105.6
H(18)	C(10)	H(19)	110.6
C(10)	C(11)	H(21)	106.9
H(20)	C(11)	H(21)	107.9
H(21)	C(11)	H(22)	107.3
P(2)	C(12)	H(24)	107.3
C(13)	C(12)	H(24)	107.1
C(12)	C(13)	H(25)	105.6
C(12)	C(13)	H(27)	107.2
H(25)	C(13)	H(27)	106.9
P(2)	C(14)	H(28)	107.6
C(15)	C(14)	H(28)	105.4
H(28)	C(14)	H(29)	109.6
C(14)	C(15)	H(31)	109.7
H(30)	C(15)	H(31)	110.7
H(31)	C(15)	H(32)	112.2
Cl(6)	C(18)	H(35)	101.3
C(17)	C(18)	H(35)	102.9
P(3)	C(19)	H(36)	107.8
C(20)	C(19)	H(36)	109.6

Between atoms a-b-c			angle(°)
C(21)	P(3)	C(23)	101(1)
Rh(2)	P(4)	C(27)	111(1)
C(25)	P(4)	C(27)	104(1)
C(27)	P(4)	C(29)	108(1)
Rh(1)	C(2)	O(2)	121(2)
O(2)	C(2)	C(3)	121(2)
P(1)	C(4)	C(5)	118(2)
P(1)	C(8)	C(9)	124(3)
P(2)	C(12)	C(13)	114(2)
Rh(2)	C(16)	O(3)	164(3)
Rh(2)	C(17)	C(18)	143(2)
Cl(6)	C(18)	C(17)	139(2)
P(3)	C(21)	C(22)	114(2)
P(4)	C(25)	C(26)	116(2)
P(4)	C(29)	C(30)	115(2)
Cl(3)	C(3)	H(2)	107.5
C(2)	C(3)	H(2)	109.9
P(1)	C(4)	H(3)	106.4
C(5)	C(4)	H(3)	107.7
H(3)	C(4)	H(4)	110.3
C(4)	C(5)	H(6)	110.1
H(5)	C(5)	H(6)	112.6
H(6)	C(5)	H(7)	107.8
P(1)	C(6)	H(9)	106.8
C(7)	C(6)	H(9)	110.7
C(6)	C(7)	H(10)	113.9
C(6)	C(7)	H(12)	112.1
H(10)	C(7)	H(12)	113.9
P(1)	C(8)	H(66)	108.1
C(9)	C(8)	H(66)	105.3
H(66)	C(8)	H(67)	106.6
C(8)	C(9)	H(69)	110.8
H(68)	C(9)	H(69)	108.5
H(69)	C(9)	H(70)	106.8
P(2)	C(10)	H(19)	109.1
C(11)	C(10)	H(19)	109.4
C(10)	C(11)	H(20)	110.8
C(10)	C(11)	H(22)	111.3
H(20)	C(11)	H(22)	112.4
P(2)	C(12)	H(23)	108.0
C(13)	C(12)	H(23)	109.9
H(23)	C(12)	H(24)	109.6
C(12)	C(13)	H(26)	111.1
H(25)	C(13)	H(26)	111.3
H(26)	C(13)	H(27)	114.3
P(2)	C(14)	H(29)	107.3
C(15)	C(14)	H(29)	106.7
C(14)	C(15)	H(30)	107.4
C(14)	C(15)	H(32)	108.4
H(30)	C(15)	H(32)	108.3
Cl(6)	C(18)	H(34)	99.7
C(17)	C(18)	H(34)	101.4
H(34)	C(18)	H(35)	110.2
P(3)	C(19)	H(37)	108.3
C(20)	C(19)	H(37)	109.9

Between atoms a-b-c			angle(°)	Between atoms a-b-c			angle(°)
H(36)	C(19)	H(37)	108.8	C(19)	C(20)	H(38)	110.1
C(19)	C(20)	H(39)	109.9	C(19)	C(20)	H(40)	110.9
H(38)	C(20)	H(39)	107.6	H(38)	C(20)	H(40)	109.6
H(39)	C(20)	H(40)	108.7	P(3)	C(21)	H(41)	108.0
P(3)	C(21)	H(42)	106.5	C(22)	C(21)	H(41)	109.6
C(22)	C(21)	H(42)	108.2	H(41)	C(21)	H(42)	109.8
C(21)	C(22)	H(43)	108.6	C(21)	C(22)	H(44)	107.7
C(21)	C(22)	H(45)	109.0	H(43)	C(22)	H(44)	110.8
H(43)	C(22)	H(45)	111.1	H(44)	C(22)	H(45)	109.6
P(3)	C(23)	H(46)	107.4	P(3)	C(23)	H(47)	108.5
C(24)	C(23)	H(46)	108.2	C(24)	C(23)	H(47)	110.0
H(46)	C(23)	H(47)	111.1	C(23)	C(24)	H(48)	109.5
C(23)	C(24)	H(49)	109.6	C(23)	C(24)	H(50)	111.1
H(48)	C(24)	H(49)	108.5	H(48)	C(24)	H(50)	109.4
H(49)	C(24)	H(50)	108.7	P(4)	C(25)	H(51)	107.5
P(4)	C(25)	H(52)	107.2	C(26)	C(25)	H(51)	108.8
C(26)	C(25)	H(52)	108.5	H(51)	C(25)	H(52)	108.7
C(25)	C(26)	H(53)	109.8	C(25)	C(26)	H(54)	109.8
C(25)	C(26)	H(55)	109.5	H(53)	C(26)	H(54)	109.6
H(53)	C(26)	H(55)	108.8	H(54)	C(26)	H(55)	109.3
P(4)	C(27)	H(56)	108.3	P(4)	C(27)	H(57)	108.9
C(28)	C(27)	H(56)	106.0	C(28)	C(27)	H(57)	110.4
H(56)	C(27)	H(57)	109.0	C(27)	C(28)	H(58)	114.5
C(27)	C(28)	H(59)	109.8	C(27)	C(28)	H(60)	108.3
H(58)	C(28)	H(59)	110.6	H(58)	C(28)	H(60)	109.3
H(59)	C(28)	H(60)	103.8	P(4)	C(29)	H(61)	107.6
P(4)	C(29)	H(62)	108.9	C(30)	C(29)	H(61)	107.1
C(30)	C(29)	H(62)	107.4	H(61)	C(29)	H(62)	110.2
C(29)	C(30)	H(63)	109.4	C(29)	C(30)	H(64)	108.4
C(29)	C(30)	H(65)	107.1	H(63)	C(30)	H(64)	112.2
H(63)	C(30)	H(65)	111.2	H(64)	C(30)	H(65)	108.4

A2.2 Determination of the crystal structure of $[RhCl_2(COCH_2CO_2Et)CO(PEt_3)_2]$

Colourless crystals of $[RhCl_2(COCH_2CO_2Et)CO(PEt_3)_2]$ were obtained by two recrystallisations from diethyl ether. The solution was warmed to around its boiling point to aid dissolution then cooled to 5 °C for 3 days to obtain crystals. These were filtered whilst cold and dried *in vacuo*.

A yellow block crystal of $[RhCl_2(COCH_2Cl)CO(PEt_3)_2]$ having approximate dimensions of 0.20 x 0.15 x 0.10 mm was mounted on a glass fibre. Cell constants and an orientation matrix for data collection were obtained from a least-squares refinement using the setting angles of 5 carefully centred reflections in the range $7.07° < 2\vartheta < 15.56°$. All measurements were made on a Rigaku AFC7S diffractometer with graphite monochromated Mo-Kα radiation. Of the 3381 reflections which were collected, 3181 were unique, of which 2462 were used in the refinement. The data were collected at a temperature of 293±1 K using the Θ -2ϑ scan technique to a maximum 2ϑ value of 46.4°. The data were corrected for Lorentz and polarization effects.

Crystallographic Data

Formula: $C_{18}H_{37}O_4Cl_2P_2Rh$, Mw = 553.25, primitive triclinic with cell dimensions; a = 11.909(5) Å, b = 11.967(3) Å, c = 9.254(3) Å, α = 105.47(2)°, β = 95.22(3)°, γ = 91.36(3)°, V = 1264.2(7) $Å^3$, Z = 2, D_x = 1.45 gcm^{-3}.

The structure was solved by heavy-atom Patterson methods[178] and expanded using Fourier techniques[173]. Some non-hydrogen atoms were refined anisotropically, while the rest were refined isotropically. Hydrogen atoms were included but not refined. Neutral atom scattering factors were taken from Cromer and Waber.[174] Anomalous dispersion effects were included in Fcalc;[175] the values for $\delta f'$ and $\delta f''$ were those of Creagh and McAuley.[176] The values for the mass attenuation coefficients are those of Creagh and Hubbel.[177] All calculations were performed using the teXsan crystallographic software package of Molecular Structure Corporation.

Table A2.4 - Atomic coordinates and B_{eq}

Atom	x	y	z	B_{eq}
Rh(1)	0.2050(3)	0.2186(2)	0.3008(3)	3.01(7)
Cl(1)	0.1141(10)	0.1907(9)	0.053(1)	4.6(3)
Cl(2)	0.2032(10)	0.4363(8)	0.356(1)	5.3(3)
P(1)	0.382(1)	0.2317(10)	0.211(1)	5.8(3)
P(3)	0.027(1)	0.2123(9)	0.382(2)	6.3(4)
O(6)	0.203(2)	-0.219(3)	0.168(3)	5.0(7)
O(7)	0.223(2)	0.007(2)	0.386(3)	4.2(6)
O(8)	0.332(3)	-0.166(3)	0.064(4)	5.6(7)
O(9)	0.321(3)	0.259(3)	0.610(4)	7.1(9)
C(10)	0.183(3)	-0.039(3)	0.128(4)	3.4(8)
C(11)	0.471(4)	0.354(4)	0.342(5)	4.8(10)
C(13)	-0.064(3)	0.079(3)	0.278(4)	3.9(8)
C(14)	0.202(3)	0.046(3)	0.291(5)	3.9(9)
C(15)	-0.057(4)	0.333(4)	0.373(5)	4.3(9)
C(16)	0.054(4)	0.317(4)	0.709(5)	4.6(10)
C(17)	0.244(4)	-0.329(4)	0.181(6)	6(1)
C(18)	-0.092(5)	0.351(5)	0.217(6)	7(1)
C(19)	0.397(4)	0.256(4)	0.011(5)	5(1)
C(20)	0.347(4)	0.381(4)	0.010(5)	5(1)
C(21)	-0.181(3)	0.079(3)	0.288(5)	4.1(9)
C(22)	0.014(4)	0.201(4)	0.588(5)	4.2(9)
C(24)	0.337(6)	-0.305(6)	0.304(8)	10(1)
C(25)	0.584(4)	0.369(4)	0.299(5)	5(1)
C(26)	0.464(4)	0.105(4)	0.191(5)	4.6(10)
C(27)	0.260(4)	-0.150(4)	0.103(5)	4.2(9)
C(28)	0.258(4)	0.238(4)	0.503(6)	6(1)
C(29)	0.510(5)	0.070(5)	0.324(7)	8(1)
H(1)	0.1061	-0.0649	0.1084	4.1842
H(2)	0.2012	0.0032	0.0588	4.1842
H(3)	0.4357	0.4232	0.3455	5.6104
H(4)	0.4812	0.3395	0.4369	5.6104
H(5)	-0.0524	0.0644	0.1748	4.6934
H(6)	-0.0358	0.0167	0.3153	4.6934
H(7)	-0.1243	0.3239	0.4177	5.2750
H(8)	-0.0153	0.4013	0.4323	5.2750
H(9)	0.1858	-0.3738	0.2019	7.2247
H(10)	0.2715	-0.3671	0.0876	7.2247
H(11)	0.4747	0.2556	-0.0073	6.7830
H(12)	0.3563	0.1952	-0.0650	6.7830
H(13)	-0.0620	0.1824	0.5981	5.2892
H(14)	0.0604	0.1413	0.6062	5.2892
H(15)	0.4176	0.0419	0.1286	5.7761
H(16)	0.5273	0.1178	0.1411	5.7761
H(17)	0.1292	0.3379	0.6977	5.5497
H(18)	0.0059	0.3770	0.6942	5.5497
H(19)	0.0489	0.3081	0.8066	5.5497
H(20)	0.3882	0.4396	0.0864	7.1872
H(21)	0.3526	0.3940	-0.0853	7.1872
H(22)	0.2696	0.3793	0.0289	7.1872
H(23)	-0.1958	0.0942	0.3904	4.9333
H(24)	-0.2130	0.1357	0.2451	4.9333
H(25)	-0.2145	0.0040	0.2340	4.9333
H(26)	0.3661	-0.3752	0.3129	11.9066

Atom	x	y	z	B_{eq}
H(27)	0.3962	-0.2581	0.2800	11.9066
H(28)	0.3103	-0.2631	0.3948	11.9066
H(29)	0.4473	0.0495	0.3753	10.9095
H(30)	0.5525	0.0031	0.2955	10.9095
H(31)	0.5541	0.1307	0.3930	10.9095
H(32)	-0.1336	0.4179	0.2263	8.6449
H(33)	-0.0252	0.3597	0.1688	8.6449
H(34)	-0.1356	0.2848	0.1559	8.6449
H(35)	0.6271	0.3014	0.2919	6.1720
H(36)	0.5819	0.3869	0.2030	6.1720
H(37)	0.6265	0.4330	0.3720	6.1720

Table A2.5 - Anisotropic Displacement Parameters

atom	U_{11}	U_{22}	U_{33}	U_{12}	U_{13}	U_{23}
Rh(1)	0.043(2)	0.025(2)	0.036(2)	-0.002(1)	-0.011(1)	-0.005(1)
Cl(1)	0.086(9)	0.039(6)	0.036(6)	-0.002(6)	-0.023(6)	-0.001(5)
Cl(2)	0.075(9)	0.024(5)	0.084(9)	0.003(5)	-0.017(7)	-0.012(5)
P(1)	0.09(1)	0.034(7)	0.067(9)	0.000(6)	-0.051(8)	-0.017(6)
P(3)	0.09(1)	0.028(6)	0.083(10)	0.005(6)	-0.061(8)	-0.021(6)

Table A2.6 - Bond lengths

atom	atom	distance (Å)	atom	atom	distance (Å)
Rh(1)	Cl(1)	2.384(10)	Rh(1)	Cl(2)	2.518(10)
Rh(1)	P(1)	2.35(2)	Rh(1)	P(3)	2.32(2)
Rh(1)	C(14)	2.05(4)	Rh(1)	C(28)	1.87(5)
P(1)	C(11)	1.86(4)	P(1)	C(19)	1.97(5)
P(1)	C(26)	1.79(4)	P(3)	C(13)	1.88(4)
P(3)	C(15)	1.79(4)	P(3)	C(22)	1.97(4)
O(6)	C(17)	1.44(5)	O(6)	C(27)	1.35(5)
O(7)	C(14)	1.11(4)	O(8)	C(27)	0.96(5)
O(9)	C(28)	1.15(5)	C(10)	C(14)	1.57(5)
C(10)	C(27)	1.61(5)	C(11)	C(25)	1.46(6)
C(13)	C(21)	1.41(5)	C(15)	C(18)	1.54(6)
C(16)	C(22)	1.56(5)	C(17)	C(24)	1.49(7)
C(19)	C(20)	1.62(6)	C(26)	C(29)	1.47(7)
C(10)	H(1)	0.94	C(10)	H(2)	0.95
C(11)	H(3)	0.93	C(11)	H(4)	0.94
C(13)	H(5)	0.95	C(13)	H(6)	0.96
C(15)	H(7)	0.95	C(15)	H(8)	0.95
C(16)	H(17)	0.95	C(16)	H(18)	0.95
C(16)	H(19)	0.95	C(17)	H(9)	0.93
C(17)	H(10)	0.96	C(18)	H(32)	0.94
C(18)	H(33)	0.96	C(18)	H(34)	0.95
C(19)	H(11)	0.95	C(19)	H(12)	0.95
C(20)	H(20)	0.94	C(20)	H(21)	0.95
C(20)	H(22)	0.96	C(21)	H(23)	0.95
C(21)	H(24)	0.94	C(21)	H(25)	0.95
C(22)	H(13)	0.95	C(22)	H(14)	0.95

atom	atom	distance (Å)	atom	atom	distance (Å)
C(24)	H(26)	0.94	C(24)	H(27)	0.96
C(24)	H(28)	0.94	C(25)	H(35)	0.96
C(25)	H(36)	0.97	C(25)	H(37)	0.97
C(26)	H(15)	0.95	C(26)	H(16)	0.95
C(29)	H(29)	0.98	C(29)	H(30)	0.94
C(29)	H(31)	0.94			

Table A2.7 - Bond angles

Between atoms a-b-c			angle(°)	Between atoms a-b-c			angle(°)
Cl(1)	Rh(1)	Cl(2)	92.6(4)	Cl(1)	Rh(1)	P(1)	90.3(4)
Cl(1)	Rh(1)	P(3)	87.6(4)	Cl(1)	Rh(1)	C(14)	94(1)
Cl(1)	Rh(1)	C(28)	172(1)	Cl(2)	Rh(1)	P(1)	87.5(4)
Cl(2)	Rh(1)	P(3)	90.4(4)	Cl(2)	Rh(1)	C(14)	170(1)
Cl(2)	Rh(1)	C(28)	88(1)	P(1)	Rh(1)	P(3)	176.9(5)
P(1)	Rh(1)	C(14)	97(1)	P(1)	Rh(1)	C(28)	97(1)
P(3)	Rh(1)	C(14)	84(1)	P(3)	Rh(1)	C(28)	85(1)
C(14)	Rh(1)	C(28)	83(1)	Rh(1)	P(1)	C(11)	109(1)
Rh(1)	P(1)	C(19)	122(1)	Rh(1)	P(1)	C(26)	115(1)
C(11)	P(1)	C(19)	103(2)	C(11)	P(1)	C(26)	106(1)
C(19)	P(1)	C(26)	97(2)	Rh(1)	P(3)	C(13)	114(1)
Rh(1)	P(3)	C(15)	115(1)	Rh(1)	P(3)	C(22)	118(1)
C(13)	P(3)	C(15)	105(1)	C(13)	P(3)	C(22)	98(1)
C(15)	P(3)	C(22)	102(1)	C(17)	O(6)	C(27)	121(3)
C(14)	C(10)	C(27)	113(3)	P(1)	C(11)	C(25)	114(3)
P(3)	C(13)	C(21)	119(2)	Rh(1)	C(14)	O(7)	126(3)
Rh(1)	C(14)	C(10)	115(2)	O(7)	C(14)	C(10)	117(3)
P(3)	C(15)	C(18)	118(3)	O(6)	C(17)	C(24)	108(4)
P(1)	C(19)	C(20)	107(3)	P(3)	C(22)	C(16)	111(2)
P(1)	C(26)	C(29)	121(3)	O(6)	C(27)	O(8)	125(4)
O(6)	C(27)	C(10)	101(3)	O(8)	C(27)	C(10)	133(5)
Rh(1)	C(28)	O(9)	158(4)				
C(14)	C(10)	H(1)	108.6	C(14)	C(10)	H(2)	108.0
C(27)	C(10)	H(1)	109.1	C(27)	C(10)	H(2)	107.4
H(1)	C(10)	H(2)	109.9	P(1)	C(11)	H(3)	109.3
P(1)	C(11)	H(4)	108.9	C(25)	C(11)	H(3)	106.2
C(25)	C(11)	H(4)	105.5	H(3)	C(11)	H(4)	112.2
P(3)	C(13)	H(5)	107.2	P(3)	C(13)	H(6)	106.7
C(21)	C(13)	H(5)	107.2	C(21)	C(13)	H(6)	107.0
H(5)	C(13)	H(6)	109.2	P(3)	C(15)	H(7)	107.2
P(3)	C(15)	H(8)	107.3	C(18)	C(15)	H(7)	107.2
C(18)	C(15)	H(8)	107.8	H(7)	C(15)	H(8)	109.0
C(22)	C(16)	H(17)	109.6	C(22)	C(16)	H(18)	109.2
C(22)	C(16)	H(19)	109.6	H(17)	C(16)	H(18)	109.3
H(17)	C(16)	H(19)	109.9	H(18)	C(16)	H(19)	109.3
O(6)	C(17)	H(9)	110.5	O(6)	C(17)	H(10)	107.9
C(24)	C(17)	H(9)	110.5	C(24)	C(17)	H(10)	109.5
H(9)	C(17)	H(10)	110.4	C(15)	C(18)	H(32)	110.4
C(15)	C(18)	H(33)	108.8	C(15)	C(18)	H(34)	109.7
H(32)	C(18)	H(33)	109.2	H(32)	C(18)	H(34)	110.5
H(33)	C(18)	H(34)	108.3	P(1)	C(19)	H(11)	109.9

Between atoms a-b-c			angle(°)	Between atoms a-b-c			angle(°)
P(1)	C(19)	H(12)	109.6	C(20)	C(19)	H(11)	110.1
C(20)	C(19)	H(12)	110.5	H(11)	C(19)	H(12)	109.0
C(19)	C(20)	H(20)	109.6	C(19)	C(20)	H(21)	109.3
C(19)	C(20)	H(22)	108.8	H(20)	C(20)	H(21)	110.5
H(20)	C(20)	H(22)	109.6	H(21)	C(20)	H(22)	109.1
C(13)	C(21)	H(23)	109.6	C(13)	C(21)	H(24)	109.7
C(13)	C(21)	H(25)	109.3	H(23)	C(21)	H(24)	109.8
H(23)	C(21)	H(25)	108.8	H(24)	C(21)	H(25)	109.6
P(3)	C(22)	H(13)	108.9	P(3)	C(22)	H(14)	108.9
C(16)	C(22)	H(13)	109.0	C(16)	C(22)	H(14)	108.7
H(13)	C(22)	H(14)	109.5	C(17)	C(24)	H(26)	109.3
C(17)	C(24)	H(27)	109.0	C(17)	C(24)	H(28)	109.0
H(26)	C(24)	H(27)	109.5	H(26)	C(24)	H(28)	111.2
H(27)	C(24)	H(28)	108.9	C(11)	C(25)	H(35)	112.7
C(11)	C(25)	H(36)	111.8	C(11)	C(25)	H(37)	111.3
H(35)	C(25)	H(36)	107.2	H(35)	C(25)	H(37)	107.1
H(36)	C(25)	H(37)	106.4	P(1)	C(26)	H(15)	106.7
P(1)	C(26)	H(16)	106.7	C(29)	C(26)	H(15)	107.3
C(29)	C(26)	H(16)	105.4	H(15)	C(26)	H(16)	109.4
C(26)	C(29)	H(29)	108.6	C(26)	C(29)	H(30)	111.3
C(26)	C(29)	H(31)	111.4	H(29)	C(29)	H(30)	107.3
H(29)	C(29)	H(31)	107.3	H(30)	C(29)	H(31)	110.7

REFERENCES

1. R. Perron. *French Pat.*, 1975, 29459-00533; *Chem. Abstr.* 86:55171n.
2. R. Perron. *French Pat.*, 1976, 2,297,200; *Chem. Abstr.* 86:55171n.
3. M. Tanaka, T. Kobayashi and T. Sakakura. *J. Chem. Soc., Chem. Commun.*, 1985, 837.
4. M. Tanaka, T.-A. Kobayashi, H. Yamashita and T. Sakakura. *J. Mol. Catal.*, 1987, **41**, 379.
5. Dynamit Nobel A.G. *Belgian Pat.*, 1979, 877,229; *Chem. Abstr.* 92:128578m.
6. R. Perron and J. Gauthier-Lafaye. *European Pat.*, 1984, 108,698; *Chem. Abstr.* 101:130413b.
7. M. El-Chahawi. *German Pat.*, 1980, 28,28,041; *Chem. Abstr.* 92:128578m.
8. M. El-Chahawi. *British Pat.*, 1980, 2,026,478A; *Chem. Abstr.* 92:128578m.
9. R. Perron, P. Coste, M. Baudoin and P. Leconte. 1988, *French Pat.*, 2,629,816; *Chem. Abstr.* 112:216449g
10. K. Hirai and T. Fuchigami. *Japanese Pat.*, 1987, 62,116,541; *Chem. Abstr.* 108:74989z.
11. H. des Abbayes and A. Buloup. *J. Chem. Soc., Chem. Commun.*, 1978, 1090.
12. H. Alper and H. des Abbayes. *J. Organomet. Chem.*, 1977, **134**, C11.
13. M. Foà, A. Moro, A. Gardano and L. Cassar. *US Pat.*, 1982, 4,351,952; *Chem. Abstr.* 97:215770q.
14. R. Perron. US Pat., 1979, 4,152,352; *Chem. Abstr.* 86:55171n.
15. M. Tanaka and K. Otsuka. *Japanese Pat.*, 1988, 63,48,244; *Chem. Abstr.* 101:28111q.
16. R. Perron. *German Pat.*, 1976, 26,00,541; *Chem. Abstr.* 86:55171n.
17. M. Foà, F. Francalanci. *J. Mol. Catal.*, 1987, **41**, 89 and references therein.
18. B. Fell, W. Kohl and H. Chrobaczek. *Chem. Zeitung*, 1985, **109**, 167.
19. A. Mortreux, E. Monflier and F. Petit. *Appl. Cat. A Gen.*, 1993, **102**, 53.
20. L. Cassar. *Ann. N.Y. Acad. Sci.*, 1980, **333**, 208.

21. M. Foà, F. Francalanci, A. Gardano, L. Abis and T. Morani. *J. Organomet. Chem.*, 1983, **243**, 87.

22. H. des Abbayes, A. Buloup and G. Tanguy. *Organometallics*, 1983, **2**, 1730.

23. M. Foà, F. Francalanci, F. Bencini, A. Gardano and M. Vincenti. *J. Organomet. Chem.*, 1986, **301**, C27.

24. M. Miura, K. Itoh and M. Nomura. *Bull. Chem. Soc. Jpn.*, 1988, **61**, 4151.

25. T. Kashimura, K. Kudo, S. Mori and N. Sugita. *Chem. Lett.*, 1986, 483.

26. M. Miura, F. Akase and M. Nomura. *J. Org. Chem.*, 1987, **52**, 2623.

27. B. Fell and H. Chrobaczek. *Chem. Zeitung*, 1984, **108**, 291.

28. J.W. Wolfram and J.Y. Lee. *US Pat.*, 1985, 4,492,798; *Chem. Abstr.* 102:78371.

29. D.F. Shriver, F. Correa, R. Nakamura, R.E. Stimson and R.L. Burwell. *J. Am. Chem. Soc.*, 1980, **102**, 5114.

30. D.F. Shriver, S.B. Butts, S.H. Strauss, E.M. Holt, R.E. Stimson and N.W. Alcock. *J. Am. Chem. Soc.*, 1979, **101**, 5864.

31. D.F. Shriver, S.B. Butts, S.H. Strauss, E.M. Holt, R.E. Stimson and N.W. Alcock. *J. Am. Chem. Soc.*, 1980, **102**, 5093.

32. M. Miura, F. Akase, M. Shinohara and M. Nomura. *J. Chem. Soc., Perkin Trans. I*, 1987, 1021.

33. M. Foà and F. Francalanci. *J. Organomet. Chem.*, 1982, **232**, 59.

34. M. Foà, F. Francalanci and A. Gardano. *Europeen Pat.*, 1983, 076,721; *Chem. Abstr.* 99:104978k.

35. B. Fell and W. Kohl. *Chem. Zeitung*, 1986, **110**, 401.

36. B. Fell and W. Kohl. *Chem. Zeitung*, 1987, **111**, 171.

37. J.W. Wolfram. *Europeen Pat. Appl.*, 1985, 142,571; *Chem. Abstr.* 103:214871d.

38. J.W. Wolfram. *US Pat.*, 1985, 4,544,505; *Chem. Abstr.* 104:148321s.

39. a) J.Y. Lee and T.J. Walter. *European Pat. Appl.*, 1985, 141,876; Chem. Abs. 103, 214898t.

b) J.Y. Lee and T.J. Walter. *US Pat.*, 1984, 4,473,706; *Chem. Abstr.* 102:24173j

40. J.W. Wolfram and J.Y. Lee. *Int. Pat. Appl.*, 1984, 84,02,699; Chem. Abs. 102, 78371r.

41. A. Mortreux and E. Monflier. *J. Mol. Catal.*, 1994, **88**, 295.

42. H. Alper and S. Gambarotta. *J. Organomet. Chem.*, 1981, **212**, C23.

43. A. Sen and J.-T. Chen. *J. Am. Chem. Soc.*, 1984, **106**, 1506.

44. A. Yamamoto, F. Ozawa, T. Sugimoto, Y. Yuasa, M. Santra and T. Yamamoto. *Organometallics*, 1984, **3**, 683.

45. A. Yamamoto, F. Ozawa, T. Sugimoto and T. Yamamoto. *Organometallics*, 1984, **3**, 692.

46. M. Tanaka, T. Kobayashi and T. Sakakura. *Tet. Lett.*, 1987, **28**, 2721.

47. M. Tanaka, T.-A. Kobayashi, T. Sakakura, H. Itatani, S. Danno and K. Zushi. *J. Mol. Catal.*, 1985, **32**, 115.

48. A. Yamamoto, F. Ozawa, N. Kawasaki, H. Okamoto and T. Yamamoto. *Organometallics*, 1987, **6**, 1640.

49. M. Tanaka, T. Sakakura, H. Yamashita, T. Kobayashi and T. Hayashi. *J. Org. Chem.*, 1987, **52**, 5733.

50. A. Yamamoto, F. Ozawa, N. Kawasaki and T. Yamamoto. *Chem. Lett.*, 1985, 567.

51. A. Mortreux, F. Petit and Y. Castanet. *J. Mol. Catal.*, 1990, **63**, 313.

52. A. Yamamoto, T. Yamamoto and F. Ozawa. *Pure. Appl. Chem.*, 1985, **57**, 1799.

53. F. Hugues, B. Morin, A. Hirschauer, D. Commereuc and Y. Chauvin. *J. Mol. Catal.*, 1986, **34**, 317.

54. C.A. Tolman. *Chem. Rev.*, 1977, **77**, 313.

55. A. Mortreux, J.F. Carpentier, Y. Castanet and F. Petit. *J. Organomet. Chem.*, 1994, **482**, 31.

56. D. Milstein. *J. Chem. Soc., Chem. Commun.*, 1986, 817.

57. M. Tanaka, H. Yamashita, T. Sakakura and T.-A. Kobayashi. *J. Mol. Catal.*, 1988, **48**, 69.

58. R.J. Angelici and E.D. Dobrzynski. *Inorg. Chem.*, 1975, **14**, 59.

59. A. Yamamoto, F. Ozawa, K. Osakada, L. Huang, T. Son, N. Kawasaski and M.-K. Doh. *Pure. Appl. Chem.*, 1991, **63**, 687.

60. A. Sen, J.-T. Chen, W.M. Vetter and R.R. Whittle. *J. Am. Chem. Soc.*, 1987, **109**, 148.

61. H. des Abbayes, S. Sabo-Etienne and A.M. Larsonneur. *Abst. Papers Amer. Chem. Soc.*, 1990, **199**, 632.

62. H. des Abbayes, S. Sabo-Etienne and A.M. Larsonneur. *J. Chem. Soc., Chem. Commun.*, 1989, 1671.

63. G.L. Geoffroy, J.B. Sheridan, J.R. Johnson and B.M. Handwerker. *Organometallics*, 1988, **7**, 2404.

64. G.L. Geoffroy, J.B. Sheridan and S.-H. Han. *J. Am. Chem. Soc.*, 1987, **109**, 8097.

65. M. Tanaka and T. Kobayashi. *J. Organomet. Chem.*, 1982, **233**, C64.

66. A. Yamamoto, F. Ozawa, H. Soyama and T. Yamamoto. *Tet. Lett.*, 1982, **23**, 3383.

67. A. Yamamoto, F. Ozawa, H. Soyama, H. Yanagihara, I. Aoyama, H. Takino, K. Izawa and T. Yamamoto. *J. Am. Chem. Soc.*, 1985, **107**, 3235.

68. A. Yamamoto, F. Ozawa and H. Yanagihara. *J. Org. Chem.*, 1986, **51**, 415.

69. Z. Feng, B. Chen and H. Liu. *J. Macromol. Sci. Chem.*, 1987, **A23**, 289.

70. A. Yamamoto, T. Son, H. Yanagihara and F. Ozawa. *Bull. Chem. Soc. Jpn.*, 1988, **61**, 1251.

71. T. Fuchikami, H. Urata and Y. Ishii. *Tet. Lett.*, 1989, **30**, 4407.

72. J.M. Basset, R. Mutin, C. Lucas, J. Thivolle-Cazet, V. Dufaud and F. Dany. *J. Chem. Soc., Chem. Commun.*, 1988, 896.

73. A. Yamamoto, N. Kawasaki, K. Masuzoe and F. Ozawa. *Bull. Chem. Soc. Jpn.*, 1989, **68**, 433.

74. J.-T. Chen, T.M. Huang, G.-H. Lee and Y. Wang. *Organometallics*, 1991, **10**, 175.

75. C.P. Casey, C.A. Bunnell and J.C. Calabrese. *J. Am. Chem. Soc.*, 1976, **98**, 1166.

76. H. des Abbayes, P. Laurent, J.-Y. Salaün and G.L. Gall. *J. Organomet. Chem.*, 1994, **466**, 175.

77. W. Beck and B. Purucker. *J. Organomet. Chem.*, 1976, **112**, 361.

78. R.J. Angelici and C.R. Green. *Inorg. Chem.*, 1972, **11**, 2097.

79. R.J. Angelici. *Acc. Chem. Res.*, 1972, **5**, 335.

80. A. Yamamoto, F. Ozawa and L. Huang. *J. Organomet. Chem.*, 1987, **334**, C9.

81. A. Yamamoto, F. Ozawa and L. Huang. *Organometallics*, 1990, **9**, 2603.

82. A. Yamamoto, F. Ozawa, L. Huang and K. Osakada. *J. Organomet. Chem.*, 1990, **383**, 587.

83. A. Yamamoto, F. Ozawa and L. Huang. *Organometallics*, 1990, **9**, 2612.

84. M. A. Bennett and A. Rokicki. *Organometallics*, 1985, **4**, 180.

85. A. Yamamoto, F. Ozawa, S. Chikaoka and X.-Z. Cao. *J. Organomet. Chem.*, 1992, **424**, 173.

86. B. Morinphelippeau and A. Fafrefafet. *J. Mol. Catal.*, 1989, **51**, 145.

87. J.P. Collman and L.S. Hegedus. in "Principles and Applications of Organotransition Metal Chemistry", Ed. A. Kelly, University Science Books, Mill Valley, California, 1980, p622.

88. H. Alper and G. Vasapollo. *Tet. Lett.*, 1989, **30**, 2617.

89. I. Amer, K. Younis and H. Alper. *Abst. Papers Amer. Chem. Soc.*, 1991, **202**, 117.

90. I. Amer and K. Younis. *Organometallics*, 1994, **13**, 3120.

91. A. Mortreux, F. Petit, E. Monflier and S. Pellegrini. *Tet. Lett.*, 1991, **32**, 4703.

92. M. Uchiyama, T. Suzuki and Y. Yamazaki. *Chem. Lett.*, 1983, **8**, 1201.

93. J.I. Kim, N.J. Kim and C.M. Ryu. *Bull. Korean Chem. Soc.*, 1988, **9**, 30.

94. R.J. Eisenberg, K.W. Kramarz, T.E. Eisenschmid and D.A. Deutsch. *J. Am. Chem. Soc.*, 1991, **113**, 5090.

95. R. Eisenberg and K.W. Kramarz. *Organometallics*, 1992, **11**, 1997.

96. J.-T. Chen, Y.-S. Yeh, C.-S. Yang, F.-S. Tsai, G.-L. Huang, B.-C. Shu, T.-M. Huang, Y.-S. Chen, G.-H. Lee, M.-C. Cheng, C.-C. Wang and Y-Wang. *Organometallics*, 1994, **13**, 4804.

97. A. Yamamoto and F. Ozawa. *Chem. Lett.*, 1981, 289.

98. A. Miyashita, T. Kihara, K. Nomura and H. Nohira. *Chem. Lett.*, 1986, 1607.

99. A. Miyashita. *Tet. Lett.*, 1991, **32**, 781.

100. A. Miyashita, K. Nomura, S. Kaji and H. Nohira. *Chem. Lett.*, 1989, 1983.

101. A. Miyashita, H. Shitara and H. Nohira. *J. Chem. Soc., Chem. Commun.*, 1985, 850.

102. A. Miyashita, H. Shitara and H. Nohira. *Organometallics*, 1985, **4**, 1463.

103. G. Pályi, V. Galamb, R. Boese and G. Schmid. *Organometallics*, 1987, **6**, 861.

104. I. Kato, M. Takakura, T. Ogawa and M. Michio. *Japanese Pat.*, JP53-7613A; *Chem. Abs.* 88:136148d.

105. H. Yagita, H. Kuwahara, K. Omata and K. Fujimoto. *Chem. Lett.*, 1990, 335.

106. T. Suzuki, T. Matsuki, K. Kudo and N. Sugita. *Nippon Kagaku Kaishi*, 1983, **10**, 1482; *Chem. Abstr.* 100:33956.

107. A. Mortreux, P. Suisse, S. Pellegrini, Y. Castanet and S. Lecolier. *J. Chem. Soc., Chem. Commun.*, 1995, 847.

108. S. Noburu, T. Hiroshi, H. Akira and H. Hideo. *Japanese Pat.*, 1979, 7955,516.

109. K.K. Mayer and W.A. Herrmann. *J. Organomet. Chem.*, 1979, **182**, 361.

110. M.C. Baird and S. Singh. *J. Organomet. Chem.*, 1988, **338**, 255.

111. M. Hidai, Y. Ishii, Y. Kobayashi and M. Iwasaki. *J. Organomet. Chem.*, 1991, **405**, 133.

112. H. Rudler, B. Denise, D. Navarre and J.C. Daran. *J. Organomet. Chem.*, 1989, **375**, 273.

113. W. Keim, M. Röper and H. Strutz. *J. Organomet. Chem.*, 1981, **219**, C5.

114. "The Chemistry of Ketenes, Allenes and Related Compounds", Ed. S. Patai, Wiley, New York, 1980, Vol.1.

115. A.R. Cutler and C.C. Tso. *Organometallics*, 1986, **5**, 1834.

116. D.J. Cole-Hamilton, W.S. Weston and R.C. Gash. *J. Chem. Soc., Chem. Commun.*, 1994, 745.

117. U. Romano and F. Rivetti. *British Pat.*, 1978, 1,574,113; *Chem. Abstr.* 90:88305v.

118. D.J. Cole-Hamilton, M.C. Simpson and R.C. Gash. *J. Chem. Soc., Dalton Trans.*, 1993, 1963.

119. D.M. Blake, A. Vinson and R. Dye. *J. Organomet. Chem.*, 1981, **204**, 257.

120. M. Foà, F. Francalanci, E. Bencini and A. Gardano. *J. Organomet. Chem.*, 1985, **285**, 293.

121. T. Kashimura, N. Sugita, K. Kudo and S. Mori. *Chem. Lett.*, 1986, 299.

122. D. Milstein, Y. Ben-David and M. Portnoy. *J. Am. Chem. Soc.*, 1989, **111**, 8742.

123. Y. Sugi, Y. Kubota, T. Hanaoka and K. Takeuchi. *Synlett*, 1994, 515.

124. Y. Sugi, K. Takeuchi, T. Hanaoka, T. Matsuzaki, S. Takagi and S. Doi. *Sekiya Gakkaishi*, 1994, **37**, 70.

125. Y. Sugi, T. Hanaoka, K. Takeuchi, K. Teranishi, M. Okuno and T. Sato. *Cat. Lett.*, 1994, **28**, 337.

126. R.J. Perry and B.D. Wilson. *Macromol.*, 1993, **26**, 1503.

127. Y. Imai. *Polym. Prep. (Am. Chem. Soc. Div. Polym. Chem.)*, 1991, **32**, 331 and references therein. *Chem. Abstr.* 115:208755.

128. Y. Sugi, Y. Kubota, T. Hanaoka and K. Takeuchi. *Bull. Chem. Soc. Jpn.*, 1994, **67**, 563.

129. R.J. Perry, S.R. Turner and R.W. Blevins. *Macromol.*, 1993, **26**, 1509.

130. M. Imai, M. Yoneyama T. Kakimoto and M Kakimoto. *Macromol. Chem. Rapid. Commun.*, 1990, **11**, 381.

131. E. Negishi and J.M. Tour. *J. Am. Chem. Soc.*, 1985, **107**, 8289.

132. E. Negishi, J.M. Tour and G. Wu. *Tet. Lett.*, 1988, **29**, 6745.

133. R.C. Gash. "Metal Haloalkyl Complxes in Catalysis", Ph.D Thesis, University of St. Andrews, 1992.

134. R.S. Dickson. "The Organometallic Chemistry of Rhodium and Iridium", Academic Press, London, 1983.

135. D.J. Cole-Hamilton, J. Rankin and S. Duncan. *Unpublished results.*

136. J. Rankin. "The rhodium phosphine catalysed carbonylation of methanol", Second Year Report, University of St. Andrews, 1996.

137. M.J. Payne. Ph.D Thesis, "The Carbonylation of Allylic and Benzylic Halides", University of St. Andrews, 1996.

138. Private communication with A. Poole, BP Chemicals (Hull, England).

139. Daicel Industries Ltd (Japan). *British Pat.*, 1985, 2 146 637 A.

140. J Houben and T Weyl. "Methoden der Organischem", 1958.

141. L.S. Frankel, K.S. McCallum and L. Collier. *Environ. Sci. Technol.*, 1974, **8**, 356.

142. H. Werner, L. Hofmann and W. Paul. *J. Organomet. Chem.*, 1982, **236**, C65.

143. J. Chatt and B.L. Shaw. *J. Chem. Soc., (A)*, 1966, 1437.

144. H. Werner. *Angew. Chem. Int. Ed. Eng.*, 1983, **22**, 927.

145. Work carried out in collaboration with M. Simpson. (BP Chemicals, Hull, England) and also reported in reference 118.

146. J.A. Osborne, M. Huser and M.-T. Youinou. *Angew. Chem. Int. Ed. Eng.*, 1989, **28**, 1386.

147. L.D. Field, S.E. Boyd, T.W. Hambley and M.G. Partridge. *Organometallics*, 1993, **12**, 1720.

148. A.S. Goldman, S.B. Duckett and R. Eisenberg. *J. Chem. Soc., Chem. Commun.*, 1993, 1185.

149. H. Itagaki, H. Murayama and Y. Saito. *Bull. Chem. Soc. Jpn.*, 1994, **67**, 1254.

150. A.S. Goldman and K. Shih. *Organometallics*, 1993, **12**, 3390.

151. W.E. Hanford, J.C. Sauer. "Organic Reactions", 1946, Vol 3, p108.

152. T. Tidwell. *Acc. Chem. Res.*, 1990, **23**, 273.

153. Ube Industries. *European Pat.*, 0 077 542; *Chem. Abstr.* 99:87654g

154. Ube Industries. *European Pat.*, 1981, 0006 611; *Chem. Abstr.* 93:45987p.

155. Ube Industries. 1984, *Japanese Pat.*, 59-67, 243; *Chem. Abstr.* 101:110373k.

156. Ube Industries. 1984, *Japanese Pat.*, 59-67, 243 [84, 67, 243]; *Chem. Abstr.* 101:110373k.

157. B.E. Mann, C. Masters and B.L. Shaw. *J. Chem. Soc. (A)*, 1971, 1104.

158. S. Andreades and H.D. Carlson. *Org. Synth.*, 1932, **45**, 50.

159. N. Pondicherry. "Polycarboxylic acids via catalytic hydrocarboxylation of polybutadienes", Ph.D Thesis, Univ. of St. Andrews, 1991.

160. Private communication with J. Rankin (Univ. of St. Andrews).

161. G.M. Intille. *Inorg. Chem.*, 1972, **11**, 695.

162. A. Miyashita, T. Kihara, K. Nomura and H. Nohira. *Chem. Lett.*, 1986, 1607.

163. A. Miyashita, K. Nomura, S. Kaji and H. Nohira. *Chem. Lett.*, 1989, 1983.

164. A. Miyashita, T. Kawashima, S. Kaji, K. Noruma and H. Nohira. *Tet. Lett.*, 1991, **32**, 781.

165. P. Maitlis, M-J. Fernandez, P.M.Bailey, P.O.Bentz, J.S. Ricci and T.F. Koetzle *J. Am. Chem. Soc.*, 1984, **106**, 5458.

166. P. Maitlis, M. Gomez, J.M. Kesenyi and G.J. Sunley. *J. Organomet. Chem.*, 1985, **296**, 197.

167. A.L. Rheingold, J.M. O'Connor, R. Uhrhammer, R.K. Chadra and B. Tsuie. *J. Organomet. Chem.*, 1993, **455**, 143.

168. J.A. Gladysz, P.C. Heah and A.T. Palton. *J. Am. Chem. Soc.*, 1986, **108**, 1185.

169. K. Seppelt, W. Schultz and H. Hartl. *Angew. Chem. Int. Ed. Eng.*, 1986, **25**, 185.

170. H. Werner, R. Feser, W. Paul and L. Hofmann. *J. Organomet. Chem.*, 1981, **219**, C29.

171. H. Werner and A. Spencer. *J. Organomet. Chem.*, 1979, **171**, 219.

172. W.A.G. Graham and A.J. Hart-Davis. *Inorg. Chem.*, 1970, **9**, 2658.

173. P.T. Beurskens, G. Admiraal, G. Beurskens, W.P. Bosman, R.d. Gelder, R. Israel and R.M.M. Smits. "The DIRDIF-94 program system, Technical Report of the Crystallography Laboratory, University of Nijmegen, The Netherlands", Univ. of Nijmegen, The Netherlands, 1994.

174. D.T. Cromer and J.T. Waber. in "International Tables for X-ray Crystallography", 1974 The Kynoch Press, Birmingham, England.

175. J.A. Ibers and W.C. Hamilton. *Acta Crystallogr.*, 1964, **17**, 781.

176. D.C. Creagh and W.J. McAuley. in "International Tables for Crystallography", Kluwer Academic Publishers, Boston, 1992, p219.

177. D.C. Creagh and J.H. Hubbell. in "International Tables for Crystallography", Kluwer Academic Publishers, Boston, 1992, p200.

178. P.T. Beurskens, G. Admiraal, G. Beurskens, W.P. Bosman, S. Garcia-Granda, R.O. Gould, J.M.M. J M M Smits and C. Smykalla. "The DIRDIF program system, Technical Report of the Crystallography Laboratory, University of Nijmegen, The Netherlands.", Univ. of Nijmegen, The Netherlands, 1992.